

**INVESTIGATIONS INTO Pt-C MULTIPLE BONDS WITH SPECTATOR SCORPIONATE LIGANDS**

Katherine D. Lavoie

A dissertation submitted to the faculty of the University of North Carolina at Chapel Hill in  
partial fulfillment of the requirements for the degree of Doctor of Philosophy in the  
Department of Chemistry.

Chapel Hill  
2016

Approved by:

Joseph L. Templeton

Alexander J. M. Miller

Maurice S. Brookhart

Cindy Schauer

Matthew R. Lockett

© 2016  
Katherine D. Lavoie  
ALL RIGHTS RESERVED

## ABSTRACT

Katherine D Lavoie: Investigations into Pt-C Multiple Bonds With Spectator Scorpionate Ligands

(Under the direction of Joseph L. Templeton)

After an overview of Pt organometallic chemistry with an emphasis on Pt(IV) complexes formed through C-H activation, the introduction discusses platinum-carbene complexes. The platinum complexes described here are anchored by scorpionate ligands. Previous investigations into  $Tp'PtL_nX_m$  complexes [ $Tp'$  = hydridotris(3,5-dimethylpyrazolyl)borate] revealed the importance of hemilability as the  $Tp'$  ligand facilitates Pt(II/IV) interconversions. In this thesis the synthesis and metalation of a series of asymmetric scorpionate ligands bearing two pyrazolyl rings and one triazolyl ring are presented. A comparison of octahedral structures of Pt(IV) complexes with P=O and C-H and B-H caps at the pole of the facial tridentate umbrella is included. A series of Pt(IV) carbene complexes of the form  $[(Tp')Pt(=C(X)(Y))(Me)_2]^+$  was synthesized. Methylating Pt-carboxamido precursors allowed isolation of  $[(Tp')Pt(=C(OMe)NHR)Me_2][OTf]$ . The method for generating these rare Pt(IV) carbenes was extended to synthesize a methoxy stabilized Pt carbene complex,  $[Tp'Pt(=C(OCH_3)CH_3)Me_2][OTf]$ . Low temperature protonation of a Pt-vinyl complex,  $(Tp')Pt(CH=CH_2)(Me)_2$ , generated a small amount of an ethylidene Pt complex. Definitive  $^{13}C$  labeling studies revealed the carbene carbon signal at 500 ppm, a dramatic downfield chemical shift. A Pt(IV)-acetylide was prepared as a potential

precursor to a Pt-vinylidene complex. The isolation of a Pt(IV) acetylide complex,  $(Tp')PtMe_2(C\equiv CPh)$  followed by protonation of the acetylide moiety resulted in the observation of a cation Pt-vinylidene complex,  $[Tp'Pt(=C=C(H)(Ph))(Me)_2][B(Ar^F)_4]$ . The carbon alpha to the platinum center appears at 526 ppm in the C-13 NMR spectrum. Using a heteroscorpionate ligand bound to platinum allowed oxidation of a dimethylPt(II) neutral species with electrophilic reagents, simple acids and acid chlorides, and leads to isomers. The binding properties of the various donor arms dictate the stereochemistry of the products. Investigations into the reactivity of heteroscorpionate tridentate ligands bound to platinum(II) led to C-Cl activation reactions with methylene chloride and 1,2-dichloroethane. Isolation of a dinuclear platinum complex bridged by an ethylene unit produced an unusual proton NMR AA'XX' pattern in the  $^1H$  NMR spectrum due to chirality at each platinum center.

## **ACKNOWLEDGEMENTS**

The moment I met Joe I knew I wanted to work in his lab. I have tremendous respect for Joe, both as a chemist and as a person. He always prioritized his graduate students, no matter how busy his jobs on campus kept him. He didn't just want us to be good chemists but rather good people, ready to handle whatever the world will throw at us. I'm so grateful for the time spent in his lab and getting to know Joe throughout my time at UNC. His character and priorities were displayed throughout our lab—leaving it to be a welcoming environment, where we developed friendships inside and out of lab.

I would like to thank professors Maurice Brookhart and Alex Miller for all their help throughout the last five years. Whenever I had a question, their doors were always open and they would send me away with insight, and normally a list of seven new experiments to try. Their helpfulness extended to their labs—sharing glassware, chemicals, and most importantly, knowledge. Jill Dempsey's was a great source for personal help. Whenever I had a problem, Jill was there to talk to and help me through it. I would like to acknowledge Cindy Schauer, Matt Lockett, and David Lawrence for serving on my committee at various times throughout the five years. Finally, I would like to thank Peter White and Marc ter Horst for their assistance and guidance with crystallography and nuclear magnetic spectroscopy, respectively.

Graduate school wouldn't have been the same without the people that surrounded me. Thank you to all the friends who turned UNC from a school into a home.

Last, but certainly not least, I want to thank my family. Words cannot explain how much I appreciate their constant and unwavering support. Their emphasis on education as a child helped develop my desire to learn, which is what has led me to where I am today.

*Dedicated to  
K-J and Jay Lavoie and Diana Page*

## TABLE OF CONTENTS

<b>LIST OF TABLES.....</b>	<b>xxii</b>
<b>LIST OF FIGURES.....</b>	<b>xxiv</b>
<b>LIST OF SCHEMES.....</b>	<b>xxvi</b>
<b>LIST OF ABBREVIATIONS AND SYMBOLS.....</b>	<b>xxvii</b>

### **CHAPTER 1            INTRODUCTION TO ORGANOMETALLIC PLATINUM CHEMISTRY**

1.1     Introduction .....	1
1.2     Isolation and Investigations of Pt(IV) complexes .....	3
1.3     Pt-Carbene Complexes .....	8
1.4     References .....	12

### **CHAPTER 2            INVESTIGATIONS INTO A BISPYRAZOLYL MONOTRIAZOLYL HETEROSCORPIONATE PLATINUM(IV) SYSTEM**

2.1     Introduction .....	16
2.2     Results and discussion .....	19
2.3     Conclusion .....	31
2.4     Experimental Section.....	31
2.5     References .....	43

## **CHAPTER 3 CATIONIC Pt(IV) Tp' CARBENES**

3.1	Introduction .....	54
3.2	Results and Discussion .....	57
3.3	Conclusions .....	80
3.4	Experimental Section .....	80
3.5	References .....	89

## **CHAPTER 4 INVESTIGATIONS OF Tp'Pt VINYLEDENE COMPLEXES**

4.1	Introduction .....	103
4.2	Results and Discussion .....	106
4.3	Conclusion.....	114
4.4	Experimental Section.....	114
4.5	References .....	118

## **CHAPTER 5 SYNTHESSES OF CATIONIC PLATINUM(IV) COMPLEXES INCLUDING AN UNUSUAL Pt-CH<sub>2</sub>CH<sub>2</sub>-Pt BRIDGE**

5.1	Introduction .....	120
5.2	Results and Discussion .....	123
5.2.1	Electrophilic Addition: Isomer Preferences for d <sup>8</sup> Pt(II) and d <sup>6</sup> Pt(IV) .....	123
5.2.2	Pt(II) Reactions with Alkyl Chloride Solvents .....	123
5.3	Conclusion.....	136
5.4	Experimental Section.....	137
5.5	References .....	144

Appendix 2-1 Representative NMR Data for Ch 2 .....	154
Appendix 2-2 Atomic coordinates and isotropic displacement parameters for [bpztz <sup>Cy</sup> PtMe <sub>3</sub> ][I] ( <b>5-L2</b> ) .....	190
Appendix 2-3 Atomic coordinates and isotropic displacement parameters for [bpztz <sup>C6F5</sup> PtMe <sub>3</sub> ][I] ( <b>5-L3</b> ) .....	193
Appendix 2-4 Atomic coordinates and isotropic displacement parameters for [POPz <sub>3</sub> PtMe <sub>3</sub> ][OTf] ( <b>7</b> ) .....	196
Appendix 2-5 Atomic coordinates and isotropic displacement parameters for [Tp <sup>m</sup> PtMe <sub>3</sub> ][OTf] ( <b>8</b> ) .....	200
Appendix 3-1 Representative NMR Data for Ch 3 .....	207
Appendix 3-2 Atomic coordinates and isotropic displacement parameters for [Tp'Pt(=C(OMe)NHCH <sub>2</sub> Ph)(CH <sub>3</sub> ) <sub>2</sub> ][OTf] ( <b>4d</b> ) .....	232
Appendix 3-3 Atomic coordinates and isotropic displacement parameters for [Tp'Pt(=C(OMe)CH <sub>3</sub> )(Me) <sub>2</sub> ][OTf] ( <b>6</b> ) .....	236
Appendix 3-4 Atomic coordinates and isotropic displacement parameters for Tp'Pt(C(OCH <sub>3</sub> )=CH <sub>2</sub> )(Me) <sub>2</sub> ( <b>7</b> ) .....	239
Appendix 3-5 Atomic coordinates and isotropic displacement parameters for Tp'Pt(CH=CH <sub>2</sub> )(Me) <sub>2</sub> ( <b>9</b> ) .....	242
Appendix 3-6 Atomic coordinates and isotropic displacement parameters for [ $\kappa^2$ (Tp' <sup>(NH)</sup> )Pt( $\eta^2$ CH <sub>2</sub> =CHCH <sub>3</sub> )(Me)][B(Ar <sup>F</sup> ) <sub>4</sub> ] ( <b>10</b> ) .....	245
Appendix 3-7 Atomic coordinates and isotropic displacement parameters for [ $\kappa^2$ (Tp' <sup>(NH)</sup> )Pt(O=C(H)(CH <sub>3</sub> ))(Me)][B(Ar <sup>F</sup> ) <sub>4</sub> ] ( <b>12</b> ) .....	252
Appendix 4-1 Representative NMR Data for Ch 4 .....	259
Appendix 5-1 Representative NMR Data for Ch 5 .....	265
Appendix 5-2 Atomic coordinates and isotropic displacement parameters for [bpztz <sup>Ph</sup> PtMe <sub>2</sub> C(O)CH <sub>3</sub> ][OTf] ( <b>2</b> ) .....	280
Appendix 5-3 Atomic coordinates and isotropic displacement parameters for [Tp <sup>m</sup> PtMe <sub>2</sub> C(O)CH <sub>3</sub> ][OTf] ( <b>3</b> ) .....	283
Appendix 5-4 Atomic coordinates and isotropic displacement parameters	

for [bpztz <sup>Ph</sup> PtMe <sub>2</sub> CH <sub>2</sub> Cl][BF <sub>4</sub> ] ( <b>4</b> ) .....	287
Appendix 5-5 Atomic coordinates and isotropic displacement parameters for [TpmPtMe <sub>2</sub> CH <sub>2</sub> Cl][Cl] ( <b>5</b> ) .....	292

## LIST OF TABLES

Table 2-1	Selected bond lengths and angles for complex <b>5-L2</b> .....	23
Table 2-2	Selected bond lengths and angles for complex <b>5-L3</b> .....	25
Table 2-3	Selected bond lengths and angles for complex <b>7</b> .....	28
Table 2-4	Selected bond lengths and angles for complex <b>8</b> .....	30
Table 2-5	Crystal data and structural refinement parameters for complex [bpztz <sup>Cy</sup> PtMe <sub>3</sub> ][I] ( <b>5-L2</b> ) .....	46
Table 2-6	Crystal data and structural refinement parameters for complex [bpztz <sup>C6F<sub>5</sub></sup> PtMe <sub>3</sub> ][I] ( <b>5-L3</b> ).....	48
Table 2-7	Crystal data and structural refinement parameters for complex [POPz <sub>3</sub> PtMe <sub>3</sub> ][OTf] ( <b>7</b> ) .....	50
Table 2-8	Crystal data and structural refinement parameters for complex [TpmpPtMe <sub>3</sub> ][OTf] ( <b>8</b> ) .....	52
Table 3-1	Selected bond distances and angles for complex <b>4d</b> .....	59
Table 3-2	Selected bond distances and angles for complex <b>6</b> .....	64
Table 3-3	Selected bond distances and angles for complex <b>7</b> .....	66
Table 3-4	Selected bond distances and angles for complex <b>9</b> .....	70
Table 3-5	Selected bond distances and angles for complex <b>10</b> .....	72
Table 3-6	Selected bond distances and angles for complex <b>12</b> .....	79
Table 3-7	Crystal data and structural refinement parameters for complex [Tp'Pt(=C(OMe)NHCH <sub>2</sub> Ph)(CH <sub>3</sub> ) <sub>2</sub> ][OTf] ( <b>4d</b> ).....	91
Table 3-8	Crystal data and structural refinement parameters for complex [Tp'Pt(=C(OMe)CH <sub>3</sub> )(Me) <sub>2</sub> ][OTf] ( <b>6</b> ) .....	93
Table 3-9	Crystal data and structural refinement parameters for complex [Tp'Pt(C(OCH <sub>3</sub> )=CH <sub>2</sub> )(Me) <sub>2</sub> ] ( <b>7</b> ).....	95
Table 3-10	Crystal data and structural refinement parameters for complex [Tp'Pt(CH=CH <sub>2</sub> )(Me) <sub>2</sub> ] ( <b>9</b> ) .....	97

Table 3-11	Crystal data and structural refinement parameters for complex [ $\kappa^2$ (Tp <sup>(NH)</sup> )Pt( $\eta^2$ CH <sub>2</sub> =CHCH <sub>3</sub> )(Me)][B(Ar <sup>F</sup> ) <sub>4</sub> ] ( <b>10</b> ) .....	99
Table 3-12	Crystal data and structural refinement parameters for complex [ $\kappa^2$ (Tp <sup>(NH)</sup> )Pt(O=C(H)(CH <sub>3</sub> ))(Me)][B(Ar <sup>F</sup> ) <sub>4</sub> ] ( <b>12</b> ) .....	101
Table 5-1	Selected bond distances and angles for one monomer of complex 2 .....	126
Table 5-2	Selected bond distances and angles for complex 3 .....	128
Table 5-3	Selected bond distances and angles for complex 4 .....	130
Table 5-4	Selected bond distances and angles for complex 5 .....	132
Table 5-5	Crystal data and structural refinement parameters for complex [bpztz <sup>Ph</sup> PtMe <sub>2</sub> C(O)CH <sub>3</sub> ][OTf] ( <b>2</b> ) .....	146
Table 5-6	Crystal data and structural refinement parameters for complex [TpmPtMe <sub>2</sub> C(O)CH <sub>3</sub> ][OTf] ( <b>3</b> ) .....	148
Table 5-7	Crystal data and structural refinement parameters for complex [bpztz <sup>Ph</sup> PtMe <sub>2</sub> CH <sub>2</sub> Cl][BF <sub>4</sub> ] ( <b>4</b> ) .....	150
Table 5-8	Crystal data and structural refinement parameters for complex [TpmPtMe <sub>2</sub> CH <sub>2</sub> Cl][BF <sub>4</sub> ] ( <b>5</b> ) .....	152

## LIST OF FIGURES

Figure 1-1	Isolation and reactivity of five-coordinate Pt(IV) complexes .....	5
Figure 1-2	The products in two attempts at isolating five-coordiante Pt(IV) complexes demonstrating the importance of steric hinderance.....	5
Figure 1-3	Different classifications of carbene ligands in organometallic chemistry.....	9
Figure 2-1	Hemilabile representations in bidentate (a) and tridentate (b) ligands .....	16
Figure 2-2	Homo and heteroscorpionate ligands .....	22
Figure 2-3	X-ray structure of [bpztz <sup>Cy</sup> PtMe <sub>3</sub> ][I] <b>5-L2</b> .....	23
Figure 2-4	X-ray structure of [bpztz <sup>C6F5</sup> PtMe <sub>3</sub> ][I] <b>5-L3</b> .....	25
Figure 2-5	X-ray structure of [POPz <sub>3</sub> PtMe <sub>3</sub> ][OTf] <b>7</b> .....	28
Figure 2-6	X-ray structure of [Tp'mPtMe <sub>3</sub> ][OTf] <b>8</b> .....	30
Figure 3-1	X-ray structure of [Tp'Pt(=C(OMe)NHCH <sub>2</sub> Ph)(Me) <sub>2</sub> ][OTf] <b>4d</b> .....	59
Figure 3-2	Variable temperature <sup>1</sup> H NMR of the methoxy methyl signal in complex <b>6</b> .....	62
Figure 3-3	X-ray structure of [Tp'Pt(=C(OCH <sub>3</sub> )CH <sub>3</sub> )Me <sub>2</sub> ][OTf] <b>6</b> .....	63
Figure 3-4	X-ray structure of Tp'Pt(C(OCH <sub>3</sub> )=CH <sub>2</sub> )Me <sub>2</sub> <b>7</b> .....	66
Figure 3-5	<sup>1</sup> H NMR spectrum for [Tp'Pt(C*(OCH <sub>3</sub> )(H)CH <sub>3</sub> )Me <sub>2</sub> ], complex <b>8</b> , in CD <sub>2</sub> Cl <sub>2</sub> .....	68
Figure 3-6	X-ray structure of Tp'Pt(CH=CH <sub>2</sub> )Me <sub>2</sub> <b>9</b> .....	69
Figure 3-7	X-ray structure of [ $\kappa^2$ (Tp' <sup>(NH)</sup> Pt( $\eta^2$ CH <sub>2</sub> =CHCH <sub>3</sub> )(Me)][B(Ar <sup>F</sup> ) <sub>4</sub> ] <b>10</b> .....	71
Figure 3-8	X-ray structure of [ $\kappa^2$ (Tp' <sup>(NH)</sup> Pt(O=C(H)(CH <sub>3</sub> ))(Me)][B(Ar <sup>F</sup> ) <sub>4</sub> ] <b>12</b> .....	79
Figure 4-1	Proposed mechanism for formation of complex <b>3</b> .....	108
Figure 5-1	X-ray structure of [bpztz <sup>Ph</sup> PtMe <sub>2</sub> C(O)CH <sub>3</sub> ][OTf] <b>2</b> .....	126
Figure 5-2	X-ray structure of [Tp'mPtMe <sub>2</sub> C(O)CH <sub>3</sub> ][OTf] <b>3</b> .....	127

Figure 5-3	X-ray structure of [bpztz <sup>Ph</sup> PtMe <sub>2</sub> (CH <sub>2</sub> Cl)][BF <sub>4</sub> ] <b>4</b>	130
Figure 5-4	X-ray structure of [TpmPtMe <sub>2</sub> (CH <sub>2</sub> Cl)][Cl] <b>5</b>	132
Figure 5-5	Observed and simulated spectra of the bridging ligand for complex <b>7</b>	135

## LIST OF SCHEMES

Scheme 1-1	Shilov methanol production system .....	3
Scheme 1-2	Reactivity accessible from $\text{Tp}'\text{PtMe}_2\text{H}$ .....	7
Scheme 3-1	Various synthetic methods toward Pt(IV) carbenes .....	56
Scheme 3-2	Proposed mechanistic pathways for formation of <b>10</b> .....	74
Scheme 3-3	Proposed mechanism for formation of <b>12</b> .....	78
Scheme 4-1	Mechanism for the isomerization of M-acetylene to M-vinylidene complexes .....	104
Scheme 4-2	Proposed mechanistic pathways after formation of <b>6</b> .....	114
Scheme 5-1	Mechanisms for electrophiles adding to $d^8$ platinum centers .....	121
Scheme 5-2	Oxidative ligation with a bidentate and tridentate nitrogen donor ligands .....	122

## LIST OF ABBREVIATIONS AND SYMBOLS

°	degree(s)
$\alpha$	Greek alpha: crystallographic angle
$\beta$	Greek beta: crystallographic angle
$\gamma$	Greek gamma: crystallographic angle
$\delta$	Greek delta: denotes chemical shift reference scale
$\eta$	Greek eta: ligand hapticity
$\kappa$	Greek kappa: denotes coordination to metal by x atoms
$\nu$	Greek mu: IR absorption band frequency
$\pi$	Greek pi: denotes bond
$\theta$	Greek theta: general angle
$\sigma$	Greek sigma: denotes coordination to a metal via a single atom
$\nu_{XY}$	Greek nu: denotes infrared absorbance band corresponding to the stretching of the bond between atoms X and Y
$\Delta$	Greek capital delta: denotes separation between values or applied heat
$\mu\text{L}$	microliter
a,b,c	crystallographic unit cell parameters
$\text{\AA}$	angstrom(s)

ACN	acetonitrile
Ar	general aromatic
ax	axial
$B(Ar^F)_4$	tetrakis(3,5-trifluoromethylphenyl)borate
br	broad
C	Celsius
C-C	carbon-carbon bond
$\text{cm}^{-1}$	wavenumber
COSY	correlation spectroscopy
d	doublet
$\Delta G^\circ$	standard Gibbs energy
$\Delta G^\ddagger$	Gibbs energy of activation
eq	equatorial (NMR data)
eq	equation
eq	equivalents
ESI	ElectroSpray Ionization
Et	ethyl, $-\text{CH}_2\text{CH}_3$

EXSY	exchange spectroscopy
G	Gibbs Free Energy
h	hour(s)
HMQC	Heteronuclear Multiple Quantum Coherence
HRMS	high resolution mass spectroscopy
Hz	Hertz
IR	infrared
$^xJ_{YZ}$	magnetic coupling between atoms X and Y through a distance of x bonds
K	Kelvin
kcal	kilocalorie
L	general ligand, usually 2 e <sup>-</sup> donor
M	general metal atom
m	multiplet
<i>m</i>	meta
Me	methyl, -CH <sub>3</sub>
mg	milligram
min	minute(s)

ml	milliliter
mmol	millimole
mol	mole
MS	mass spectroscopy
<i>n</i> Bu	<i>n</i> -butyl, -C <sub>4</sub> H <sub>9</sub>
NHC	N-heterocyclic carbenes
NMR	nuclear magnetic resonance
<i>o</i>	ortho
ORTEP	Oak Ridge Thermal Ellipsoid Plot
OTf	triflate, trifluoromethane sulfonate: CF <sub>3</sub> SO <sub>3</sub> <sup>-</sup>
<i>p</i>	para
Ph	phenyl, -C <sub>6</sub> H <sub>5</sub>
ppm	parts per million
py	pyridine
q	quartet
R	general alkyl group
R, R <sub>W</sub>	crystallographic refinement quality indicators

rt	room temperature
s	singlet (NMR data)
s	second
t	triplet
<sup>1</sup> Bu	tertiary butyl, -C(CH <sub>3</sub> ) <sub>3</sub>
THF	tetrahydrofuran
TMS	trimethylsilyl, -Si(CH <sub>3</sub> ) <sub>3</sub>
Tp	hydridotrispyrazolylborate
Tpm	tris(3,5-dimethylpyrazolyl)methane
Tp'	hydridotris(3,5-dimethylpyrazolyl)borate
X	general halogen atom
<sup>1</sup> H NMR	proton nuclear magnetic resonance spectroscopy
2-D NMR	two-dimensional nuclear magnetic resonance
<sup>13</sup> C NMR	carbon nuclear magnetic resonance spectroscopy

# CHAPTER ONE

## Introduction to Organometallic Platinum Chemistry

### 1.1 Introduction

Platinum was first discovered and named in 1736 in present day Colombia, making it the eighth identified metal.<sup>1</sup> Due to its high melting point and brittle nature, it was a challenge to work with platinum. Finding ways to isolate and purify platinum required forcing conditions, including boiling in strong acid and then dissolving in aqua regia.<sup>2</sup> This process proved worthwhile, and platinum has become an integral part of various aspects of our life today since it is found in catalytic converters for cars, electronics, dentistry, and jewellery.

In addition to every day life, platinum has been widely used in chemistry. Platinum crucibles helped lay the foundations of classical analytical chemistry.<sup>1</sup> Initial investigations into incandescent lamps and thermionic valves utilized platinum before switching to cheaper metals.<sup>3</sup> To date, 10% of the platinum produced annually is used to catalyze hydrogenation and dehydrogenation reactions.<sup>4</sup>

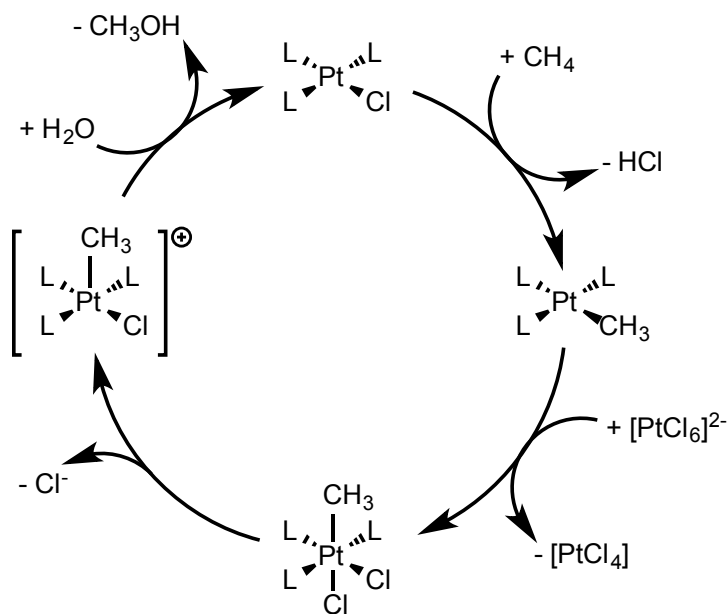
In 1913, Alfred Werner was awarded the Nobel Prize in chemistry.<sup>5</sup> Among many topics, Werner studied the coordination of nitrogen atoms to metals, particularly platinum. He expanded upon the insight he gained into the realm of inorganic molecules, proposing that a single metal atom acts as a central nuclei and around this central atom the other molecules arrange in definitive geometric patterns. The Nobel Prize, classified as

inorganic chemistry in this instance, was awarded for the insight between bonding in atoms and molecules, opening up the field of inorganic chemistry and pointing toward organometallic chemistry. It was not until the 1950s that organometallic chemistry became recognized as an independent field. Henry Taube reported on substitution reactions and the distinction between inner and outer sphere electron transfer reactions, studying complexes from the both p- and d-block metals.<sup>6</sup> The discovery and identification of ferrocene by Wilkinson and Woodward pushed the field of organometallic chemistry to the forefront, leading to many sandwich structures.<sup>7</sup>

With the field of organometallic chemistry expanding, the “golden age” of catalysis developed.<sup>3</sup> Metal clusters, fluxional complexes, and metal carbon double bonds were all reported in the 1960s. Catalysis blossomed as evident in olefin metathesis,<sup>8,9</sup> enantioselective hydrogenation,<sup>10</sup> and epoxidation of alcohols<sup>11</sup> that produced chemicals on an industrial scale. The following decades led to improved catalysis and new transformations were targeted. Catalytic systems and improvements are continually being introduced including C-H bond activation<sup>12,13</sup> and polymerization.<sup>14</sup> Currently, organometallic complexes catalyze 10 of the top 30 reactions being implemented on an industrial scale.<sup>3</sup>

New catalysts for alternative energy are needed due to the depletion of fossil fuels. Platinum is a promising option, and it is currently used in fuel cells for the reduction of oxygen.<sup>15</sup> Methanol production is another attractive energy source. Catalyzing conversion of methane to methanol is desirable since methane is abundant and accessible.<sup>16,17</sup> The homogeneous Shilov system was the first reported organometallic transformation of methane to methanol.<sup>18</sup> Using Pt(II) in acidic solutions, a C-H bond of methane is

activated, forming a Pt-methyl complex. Oxidation to form a d<sup>6</sup> platinum complex followed by ligand dissociation gives a highly reactive five-coordinate Pt(IV) species that reductively eliminates methanol and re-establishes the d<sup>8</sup> starting material. While the Shilov system shows the promise of converting methane to methanol, it is not plausible on an industrial scale since it uses a stoichiometric amount of Pt(IV) as a sacrificial oxidant (scheme 1). Despite this fatal flaw, the process highlights the potential for Group 10 metals to help mediate important catalytic cycles.<sup>19-23</sup>



**Scheme 1** Shilov methanol production system

## 1.2 Isolation and Investigation of Pt(IV) complexes

The reactivity of platinum complexes extends beyond this example of methane C-H activation. Platinum is known for its chemical behaviour, namely its high catalytic activity, which is often easy to probe due to its chemical robustness. More specifically, platinum is able to cycle between three different oxidation states, Pt(0)/Pt(II)/Pt(IV),

allowing it to catalyze a wide variety of transformations, often involving C-H activation. Bercaw et al. reported the KIE associated with C-H activation using platinum as a way to better understand the mechanism by which the reaction occurs.<sup>24</sup> A surprisingly large KIE was reported, believed to be due to quantum tunnelling, alternatively an inverse KIE is indicative of protonation of a Pt-C bond to go from Pt(II) to Pt(IV). The insight gained can be used to make more reactive catalysts. Goldberg has published work on O<sub>2</sub> insertion into Pt-C bonds, since oxygen is a cheap and readily available oxidizing source, forming Pt(IV) peroxides and facilitating metal-ligand cooperation.<sup>25</sup> Puddephatt and coworkers have explored oxidation of Pt(II) to Pt(IV) to better probe proton coupled electron transfer and activate C-H bonds at high oxidation state platinum centers.<sup>26</sup> Our group has been particularly interested in high oxidation state, d<sup>6</sup> Pt complexes formed from C-H activation.

It was believed that reductive elimination from Pt(IV) is promoted by dissociation of a ligand from the Pt(IV) state generating a highly reactive, five-coordinate intermediate. However, few examples of these five-coordinate intermediate Pt(IV) complexes exist due to their propensity to reductively eliminate and generate a more energetically favorable Pt(II) square planner complex. Goldberg et al. isolated a sterically hindered five-coordinate Pt(IV)Me<sub>3</sub> complex (Figure 1).<sup>27</sup> They were able to observe reductive elimination and subsequent C-H activation from the isopropyl group of the bidentate ligand to generate a second five-coordinate Pt(IV) complex. From there, reduction of methane resulted in an equilibrium between two Pt(II) complexes. A few years later, the Wang group reported the influence of sterically encumbered N,N-

chelating ligands which controlled the ability to isolate a five-coordinate Pt(IV) rather than an octahedral d<sup>6</sup> Pt (Figure 2).<sup>28</sup>

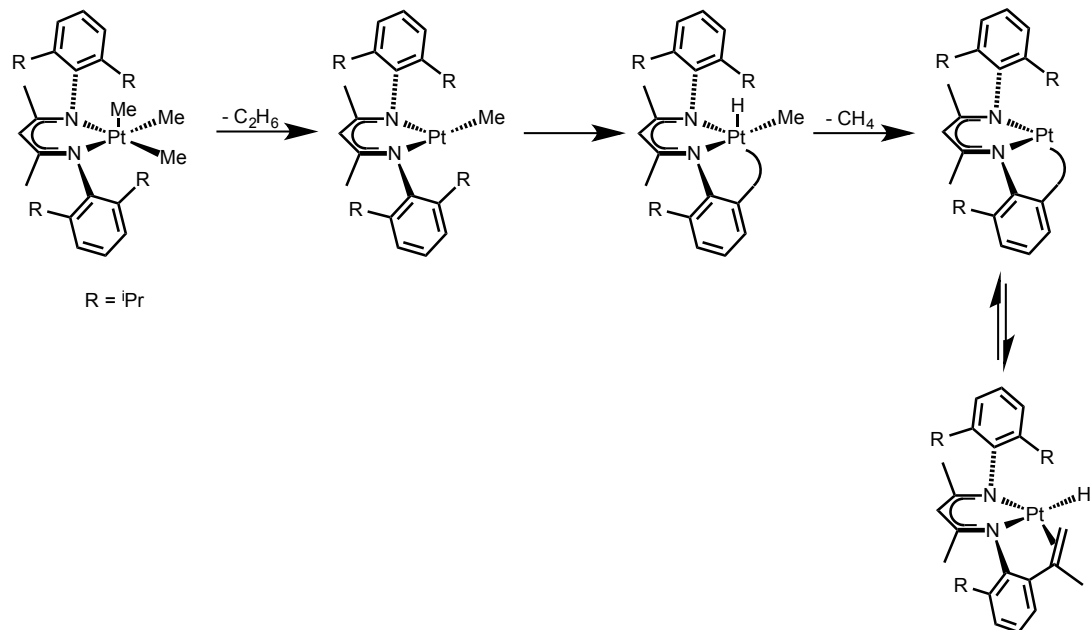


**Figure 1** Isolation and reactivity of five-coordinate Pt(IV) complexes

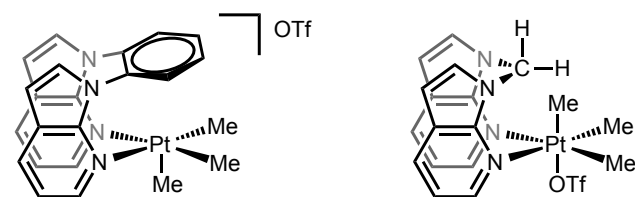
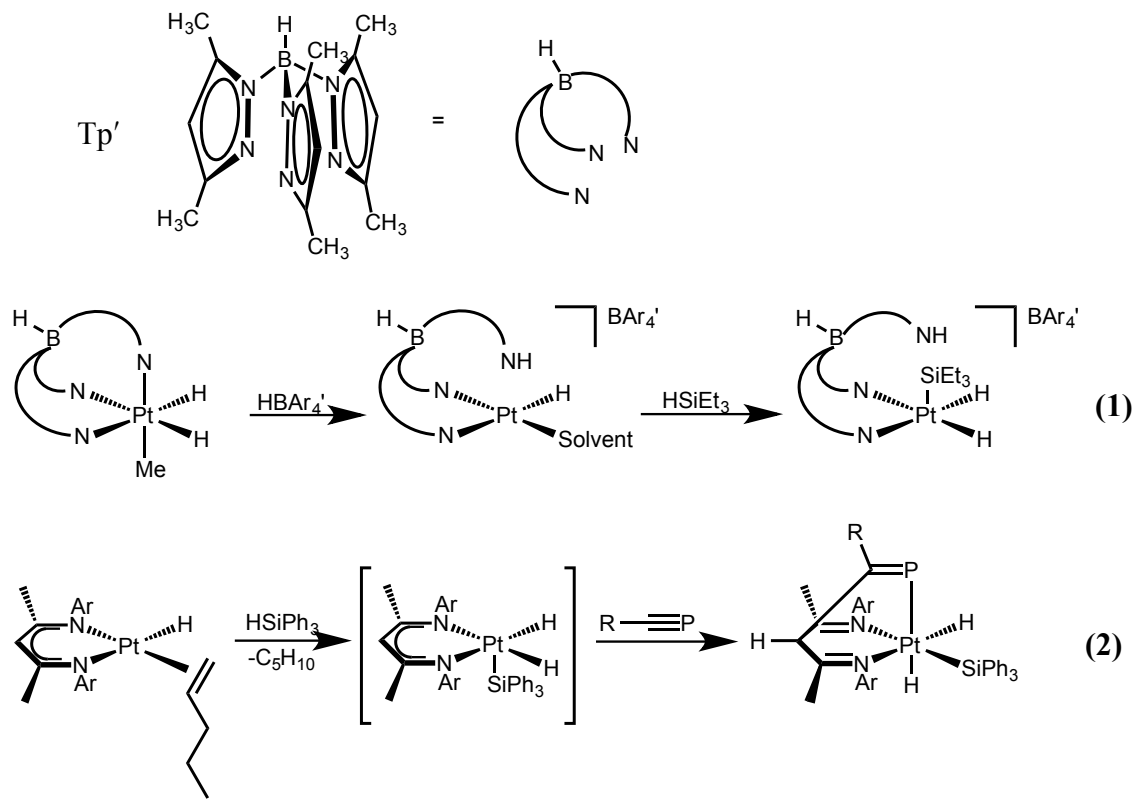


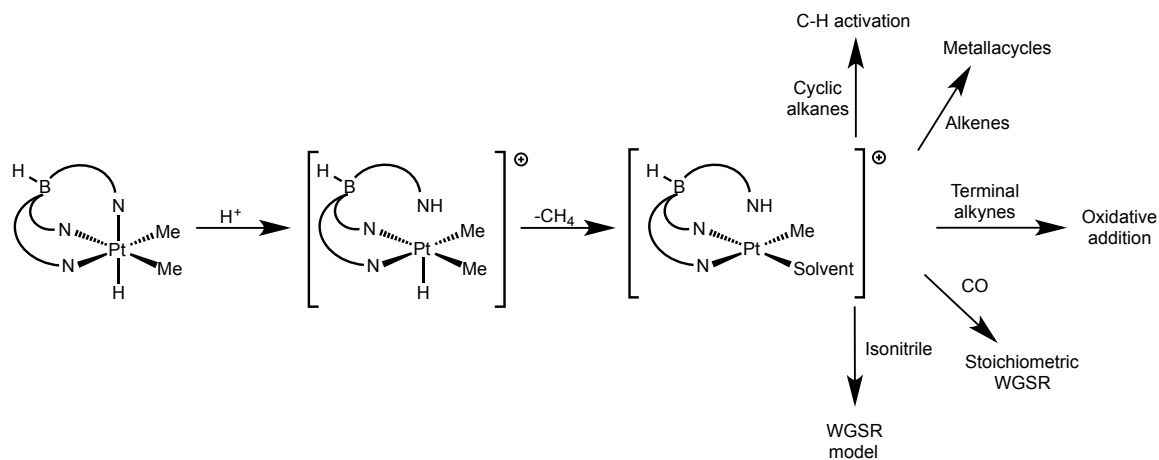
**Figure 2** The products in two attempts at isolating five-coordinate Pt(IV) complexes demonstrating the importance of steric hinderance

In the past few decades the use of tridentate ligands for investigations into organometallic transformations has increased. Tridentate ligands help stabilize Pt(IV) complexes by minimizing the formation of five-coordinate species that result in reductive elimination. With a myriad of meridionally and facially coordinating ligands available, chemists are able to control oxidative addition and reductive elimination through strategic

ligand design. Since 1960 when Trofimenko first reported the synthesis of Tp ( $\text{Tp} =$  hydridotrispyrazolyl borate), scorpionate ligands have grown in popularity.<sup>29-32</sup> Scorpionate ligands typically contain three strongly donating nitrogen arms and allow a wide variety of steric and electronic tunability. These ligands allow isolation of five- and six-coordinate Pt(IV) complexes and also provide a platform for investigations into Pt(II)/Pt(IV) transformations. Our group found we could isolate a five-coordinate  $d^6$  Pt complex which was stabilized by a tridentate ligand (eq 1).<sup>33</sup> Repeating similar chemistry with a bidentate ligand resulted in a less stable five-coordinate intermediate seen at low temperatures. In the presence of phosphalkynes, the five-coordinate Pt complex facilitates C-C bond formation and generates a new tridentate ligand (eq 2).



In 1996 our lab reported the synthesis of the first stable Pt(IV) alkyl hydride complex,  $\text{Tp}'\text{PtMe}_2\text{H}$  ( $\text{Tp}'$  = hydridotris(3,5-dimethylpyrazolyl)borate), which has served as a starting point for extensive additional studies thereafter (Scheme 2).<sup>34</sup> We found we could induce methane reductive elimination either with the addition of an acid or by thermolysis. Both pathways follow a similar mechanism; one arm of the scorpionate ligand dissociates to form a five-coordinate intermediate, which promotes reductive elimination to form a d<sup>8</sup> Pt complex. The newly formed Pt(II) complex has demonstrated a multitude of reactivity patterns.<sup>35-42</sup> Most of the research reported to date has focused on C-H oxidative activations leading to neutral Pt(IV) complexes.



**Scheme 2** Reactivity accessible from  $\text{Tp}'\text{PtMe}_2\text{H}$

While our lab primarily focused on  $\text{Tp}'\text{Pt}$  complexes, we recently reported a system utilizing tris(1-R-1H-1,2,3-triazol-4-yl)- phosphine oxide ( $\text{Tt}^{\text{R}}$ , R = cyclohexyl, phenyl).<sup>43,44</sup> To mimic chemistry observed with the  $\text{Tp}'$  ligand,  $[\text{Tt}^{\text{R}}\text{PtMe}_2\text{H}]^+$  was synthesized and heated in the presence of CO to release methane and form  $[\text{Tt}^{\text{R}}\text{PtMe}(\text{CO})]^+$ . However, while  $\text{Tp}'\text{PtMe}(\text{CO})$  allowed the addition of a nucleophile to

the C group of the Pt-CO ligand, attempting the same reactivity with  $[Tt^R\text{PtMe}(\text{CO})]^+$  resulted in loss of the tridentate ligand and led to formation of Pt black. We hypothesized that forming a heteroscorpionate ligand consisting of two tightly binding pyrazolyl groups and a more weakly binding triazolyl arm would allow for easier Pt(II) oxidation to Pt(IV) without complete ligand loss from the metal center. Chapter 2 discusses the synthesis of a new ligand series and metalation to generate Pt(IV) complexes while Chapter 5 focuses on the oxidative addition of various substrates with scorpionate ligands bound to Pt(II) and subsequent addition of an electrophile.

### 1.3 Pt-Carbene Complexes

Since the first carbene complex was discovered in the 1960s by E.O. Fischer, investigations into carbenes in catalytic and organometallic chemistry have grown exponentially.<sup>45</sup> Carbenes can be categorized into five classes: Fischer, Schrock, vinylidene, carbenoid, and N-Heterocyclic (NHCs) (Figure 3). Fischer and Schrock carbenes are the two most common classifications, as they refer to early descriptions of the classic M-C double bond moiety.<sup>8,45</sup> Vinylidenes are heterocumulene structures with a metal bound at one end. The singlet state of free vinylidenes is 42 kcal/mol more stable than the triplet state, causing it to react in ways similar to reactivity displayed by a Fischer carbene.<sup>46</sup> Carbenoid complexes, also referred to as acceptor substituted carbenes, contain a carbonyl moiety bound to the carbene carbon. While this subcategory is seldomly isolated, carbenoid complexes are proposed as important intermediates in many catalytic cycles.<sup>47-49</sup> The fifth group, NHCs, tend to be the least reactive of the carbene complexes discussed. As ligands, NHCs bind as strong  $\sigma$ -donors to the metal center and

weak  $\pi$ -acceptors. The NHC moiety consists of two nitrogens bound to the carbene carbon and these donate electron density from their lone pairs to help stabilize the central carbon.<sup>50</sup> NHCs are sufficiently stable to withstand numerous reagents unscathed while promoting reactivity at ancillary ligands bound to the metal center.<sup>51</sup>

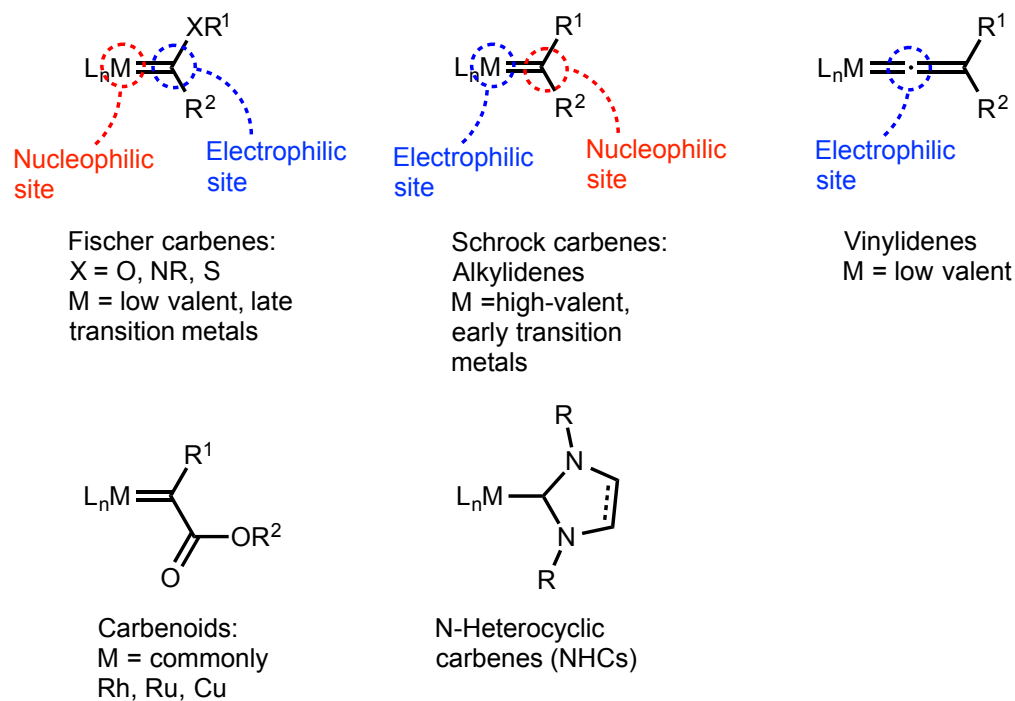


**Figure 3** Different classifications of carbene ligands in organometallic chemistry

While Fischer and Schrock carbenes both exhibit M-C double bond and are the ends of a continuum of reactivity. Fischer carbenes are often bound to a low oxidation state, late transition metal.<sup>4</sup> The carbene carbons are considered singlet donors, the carbon is bound as a  $\sigma$ -donor to an empty metal d-orbital and the metal is  $\pi$ -backbonding. Another common characteristic of Fischer carbenes is the presence of a heteroatom bound to the carbene carbon such as an alkoxy or alkylated amino group. Schrock

carbenes are typically bound to high oxidation state metals in early transition metal complexes. The bonding can be pictured as between a triplet carbene carbon and triplet state metal electrons and orbitals. Since the carbene carbon is bound to hydrogen or alkyl substituents, these complexes are often called alkylidenes.

The difference in binding of carbene complexes brings up the importance of electron counting. Schrock carbenes, binding in the triplet state, are often considered doubly anionic ligands when counted in the ionic formalism. Alternatively, Fischer carbenes are considered neutral, 2 e- donor ligands. While we will count carbenes in this thesis using the neutral 2 e- donor formalisms, it is important to remember that the oxidation state assigned to the metal center is a strict formalism. To quote Puddephatt “there is no obligatory association between formal oxidation state and electron density at the metal center”.<sup>52</sup>

The differences in the electrophilic atom in Fischer and Schrock carbenes controls the chemistry that is observed. Fischer carbenes have an electrophilic carbon; these complexes often react with nucleophiles to displace substituents on the carbene carbon<sup>53,54</sup> or insert and form cyclopropene complexes.<sup>55-57</sup> Schrock carbenes, with electrophilic metal centers, are known intermediates for olefin metathesis, which is a process that breaks C-C bonds, shuffles them, and generates new C-C bonds.<sup>58,59</sup> We were interested in exploring reactivity patterns as we attempted to generate Pt(IV) carbene complexes.

Changing the substituents on the carbene carbon would allow us to systematically go from Fischer-type reactivity (nucleophilic metal center, heteroatom substituents) towards Schrock-like (alkylidenes with electrophilic metal centers). In chapter 3 we

report our findings on the synthesis and reactivity on cationic Pt(IV) carbene complexes. These complexes vary from classic Fischer carbenes, with a nitrogen and oxygen moiety bound to the carbene carbon, to a Pt(IV) alkylidene. In chapter 4 we report our attempts to synthesize a cationic Pt(IV) vinylidene complex.

## REFERENCES

- (1) Greenwood, N. N.; Earnshaw, A. *Chemistry of the Elements*, 2nd ed.; Elsevier Ltd: Oxford, 2005; pp 1144–1172.
- (2) Normandeau, G. *Technical Aspects of Platinum Refining*; 2006; p 38.
- (3) Rayner-Canham, G.; Overton, T. *Descriptive Inorganic Chemistry*, 4 ed.; Craig Bleyer: New York, 2006.
- (4) Crabtree, R. H. *The Organometallic Chemistry of the Transition Metals*, 2nd ed.; Wiley: New York, 1994.
- (5) Werner, A. *The Nobel Foundation*. Amersterdam.
- (6) Taube, H. *Chem. Rev.* **1952**, *50*, 69.
- (7) Wilkinson, G.; Rosenblum, M.; Whiting, M. C. *J. Am. Chem. Soc.* **1952**, *74*, 2125.
- (8) Schrock, R. R. *J. Am. Chem. Soc.* **1974**, *96*, 6796.
- (9) Schrock, R. R. *Acc. Chem. Res.* **1986**, *19*, 342.
- (10) Kellie, A. E.; Smith, E. R. *Nature* **1956**, *178*, 323.
- (11) Henbest, H. B.; Wilson, R. *J. Chem. Soc.* **1957**, 1958.
- (12) Chatt, J.; Davidson, J. M. *J. Chem. Soc.* **1965**, 843.
- (13) Fujiwara, Y.; Noritani, I.; Danno, S.; Asano, R. *J. Am. Chem. Soc.* **1969**, *91*, 7166.
- (14) DuPont. *Patent US 178,184 A*. 1974.
- (15) Larminie, J.; Dicks, A. *Fuel Cell Systems Explained*, Second. John Wiley & Sons: West Sussex, 2005; pp 1–433.
- (16) Olah, G. A. *Angew. Chem. Int. Ed.* **2005**, *44*, 2636.
- (17) Huber, G. W.; Iborra, S.; Corma, A. *Chem. Rev.* **2006**, *106*, 4044.
- (18) Goldshle, N. F.; Shteinma, A. A.; Shilov, A. E.; Eskova, V. V. *Russian Journal of Physical Chemistry, Ussr* **1972**, *46*, 785.
- (19) Jia, C.; Kitamura, T.; Fujiwara, Y. *Acc. Chem. Res.* **2001**, *34*, 633.

- (20) Dyker, G. *Angew. Chem. Int. Ed.* **1999**, *38*, 1699.
- (21) Stahl, S. S.; Labinger, J. A.; Bercaw, J. E. *Angew. Chem. Int. Ed.* **1998**, *37*, 2181.
- (22) Periana, R. A.; Taube, D. J.; Gamble, S.; Taube, H.; Satoh, T.; Fujii, H. *Science* **1998**, *280*, 560.
- (23) Periana, R. A.; Mironov, O.; Taube, D.; Bhalla, G.; Jones, C. J. *Science* **2003**, *301*, 814.
- (24) Bercaw, J. E.; Chen, G. S.; Labinger, J. A.; Lin, B.-L. *J. Am. Chem. Soc.* **2008**, *130*, 17654.
- (25) Scheuermann, M. L.; Goldberg, K. I. *Chem. Eur. J.* **2014**, *20*, 14556.
- (26) Moustafa, M. E.; Boyle, P. D.; Puddephatt, R. J. *Chem. Commun.* **2015**, *51*, 10334.
- (27) Luedtke, A. T.; Goldberg, K. I. *Inorg. Chem.* **2007**, *46*, 8496.
- (28) Zhao, S.-B.; Wu, G.; Wang, S. *Organometallics* **2008**, *27*, 1030.
- (29) Trofimenko, S. *J. Am. Chem. Soc.* **1966**, *88*, 1842.
- (30) Trofimenko, S. *J. Am. Chem. Soc.* **1967**, *89*, 3170.
- (31) Trofimenko, S. *J. Am. Chem. Soc.* **1967**, *89*, 6288.
- (32) Trofimenko, S. *J. Am. Chem. Soc.* **1970**, *92*, 5118.
- (33) Reinartz, S.; White, P. S.; Brookhart, M.; Templeton, J. L. *J. Am. Chem. Soc.* **2001**, *123*, 6425.
- (34) O'Reilly, S. A.; White, P. S.; Templeton, J. L. *J. Am. Chem. Soc.* **1996**, *118*, 5684.
- (35) MacDonald, M. G.; Kostelansky, C. N.; White, P. S.; Templeton, J. L. *Organometallics* **2006**, *25*, 4560.
- (36) Engelman, K. L.; White, P. S.; Templeton, J. L. *Organometallics* **2010**, *29*, 4943.
- (37) Reinartz, S.; White, P. S.; Brookhart, M.; Templeton, J. L. *Organometallics* **2000**, *19*, 3854.
- (38) Reinartz, S.; Brookhart, M.; Templeton, J. L. *Organometallics* **2001**, *21*, 247.

- (39) Reinartz, S.; Baik, M. H.; White, P. S.; Brookhart, M. *Inorg. Chem.* **2001**, *40*, 4726.
- (40) West, N. M.; Reinartz, S.; White, P. S.; Templeton, J. L. *J. Am. Chem. Soc.* **2006**, *128*, 2059.
- (41) Frauhiger, B. E.; Ondisco, M. T.; White, P. S.; Templeton, J. L. *J. Am. Chem. Soc.* **2012**, *134*, 8902.
- (42) West, N. M.; Templeton, J. L. *Can. J. Chem.* **2009**, *87*, 288.
- (43) Frauhiger, B. E.; White, P. S.; Templeton, J. L. *Organometallics* **2011**, *31*, 225.
- (44) Frauhiger, B. E.; Templeton, J. L. *Organometallics* **2012**, *31*, 2770.
- (45) Fischer, E. O.; Maasböl, A. *Angew. Chem. Int. Ed. Engl.* **1964**, *3*, 580.
- (46) Bruce, M. I. *Chem. Rev.* **1991**, *91*, 197.
- (47) Doyle, M. P. *Chem. Rev.* **1986**, *86*, 919.
- (48) Doyle, M. P.; Forbes, D. C. *Chem. Rev.* **1998**, *98*, 911.
- (49) Davies, H. M. L.; Beckwith, R. E. J. *Chem. Rev.* **2003**, *103* (8), 2861.
- (50) Arduengo, A. J.; Krafczyk, R.; Schmutzler, R.; Craig, H. A.; Goerlich, J. R.; Marshall, W. J.; Unverzagt, M. *Tetrahedron* **1999**, *55*, 14523.
- (51) Canac, Y.; Soleilhavoup, M.; Conejero, S.; Bertrand, G. *J. Organomet. Chem.* **2004**, *689*, 3857.
- (52) Rendina, L. M.; Puddephatt, R. J. *Chem. Rev.* **1997**, *97*, 1735.
- (53) de Meijere, A.; Schirmer, H.; Duetsch, M. *Angew. Chem.* **2000**, *112*, 4124.
- (54) Barluenga, J.; Fernández-Rodríguez, M. A.; Aguilar, E. *J. Organomet. Chem.* **2005**, *690*, 539.
- (55) Brookhart, M.; Studabaker, W. B. *Chem. Rev.* **1987**, *87*, 411.
- (56) Merino, I.; Hegedus, L. S. *Organometallics* **1995**, *14*, 2522.
- (57) Harvey, D. F.; Lund, K. P. *J. Am. Chem. Soc.* **1991**, *113*, 8916.
- (58) Schrock, R. R.; Hoveyda, A. H. *Angew. Chem. Int. Ed.* **2003**, *42*, 4592.

- (59) Rocklage, S. M.; Schrock, R. R.; Churchill, M. R. *Organometallics* **1982**, *1*, 1332.

## CHAPTER TWO

### Investigations into a Bispyrazolyl Monotriazolyl Heteroscorpionate Platinum(IV) System<sup>1</sup>

#### 2.1 Introduction

Hemilabile ligands containing both strong and weak donor arms have been employed in a wide range of metal-mediated processes.<sup>1,2</sup> Such ligands provide the benefit of opening a coordination site on the metal while preventing complete ligand loss. Bidentate and tridentate hemilabile representations are sketched in Figure 1, where a strong donor ligand (X) remains bound to the metal center while a weaker donor (Y) can bind reversibly, thus creating a vacant coordination site.

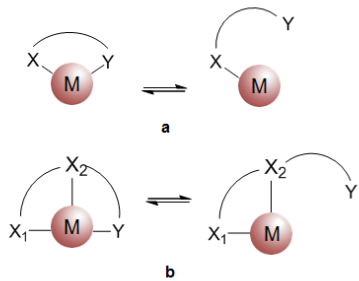


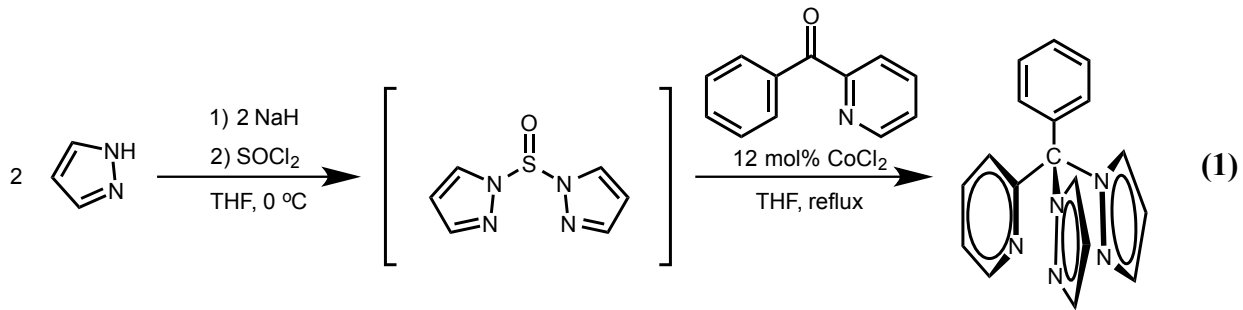
**Figure 1** Hemilabile representations in bidentate (a) and tridentate (b) ligands

A plethora of metal-ligand systems have been developed that display reversible binding of one arm, and pincer ligands are an important class of hemilabile ligands. Milstein and co-workers have reported a Ru PNN pincer system that converts alcohols to

<sup>1</sup> Reproduced with permission from Lavoie, K. D., Frauhiger, B. E., White, P.S., Templeton, J. L., DOI: 10.1016/j.molcata.2016.07.002

esters, and the mechanism is believed to involve reversible coordination of a tethered amine.<sup>3</sup> Goldberg et al. have synthesized a PCO tridentate ligand that can adopt  $\kappa^1$ ,  $\kappa^2$ , and  $\kappa^3$  coordination modes.<sup>4</sup> Van der Vlugt and co-workers have reported a simple synthetic route that generates PNN chelates that reversibly bind to Rh and Ir metal centers.<sup>5</sup> A hemilabile bidentate ligand with an oxygen donor arm bound to Rh(I) developed by Dunbar has been utilized for the reversible uptake of small molecules.<sup>6,7</sup> A hemilabile Ru(II) system reported by Wolf displays reversible uptake of SMe<sub>2</sub>, DMSO, and acetonitrile.<sup>8</sup> Recently, Miller has synthesized a NCP pincer-crown ether complex that can reversibly bind oxygen from the crown ether to help stabilize the metal center.<sup>9</sup>

The past decade has seen significant progress in the development of asymmetrical hemilabile tridentate facial chelates, including contributions from Rominger<sup>10</sup> (NCO, PCO), Zargarian<sup>11</sup> (PCN), Szabó<sup>12</sup> (PCS), and Song<sup>13</sup> (PCP). The initial syntheses of asymmetric facially-coordinating ligands suffered from poor yields, especially for tris(3,5-dimethylpyrazolyl)methane (Tpm) derivatives.<sup>14-17</sup> Carty and co-workers developed a significantly improved synthetic route to asymmetrical Tpm-derived heteroscorpionates containing two pyrazolyl rings and a third, unique donor arm using a cobalt-catalyzed condensation.<sup>18-23</sup> Deprotonation of free pyrazole followed by the addition of phosgene results in a bispyrazolyl ketone intermediate. Reger et al. advanced relevant synthetic methodology by using a bispyrazolyl sulfoxide intermediate that was prepared by employing thionyl chloride in place of phosgene, noteworthy since the thionyl chloride is both safer and easier to handle than phosgene (eq 1).<sup>24-27</sup>

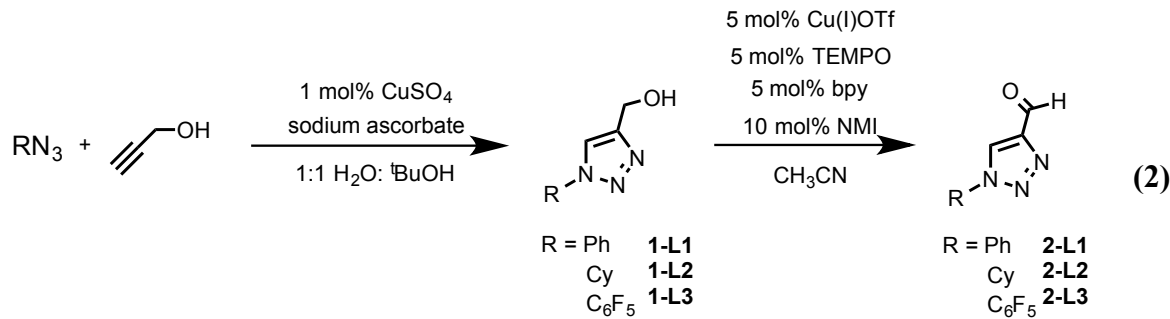


With a goal of facilitating interconversions between Pt(II) and Pt(IV), our lab published the synthesis and reactivity of tris(1-R-1H-1,2,3-triazol-4-yl)phosphine oxide ( $R = \text{phenyl, cyclohexyl}$ ) ( $Tt^R$ ).<sup>28,29</sup> The  $Tt^R$  ligand was completely displaced from the Pt(II) center when nucleophilic reagents were introduced to the solution in attempts to attack the carbonyl ligand in the Pt-CO unit at the carbon atom. The inability to add nucleophilic reagents to ligands, like CO, without displacing the chelate ligand motivated us to synthesize a mixed pyrazolyl/triazolyl ligand. As observed with the  $Tp'Pt$  system ( $Tp'$  = hydridotris(3,5-dimethylpyrazolyl)borate), strong donation from the pyrazolyl nitrogen donors keeps the ligand bound while still allowing the  $\kappa^2/\kappa^3$  interconversion.<sup>30-32</sup>

Utilizing Reger's improved method for generating mixed donor ligands, we prepared similar heteroscorpionates with a C-H backbone that incorporates the triazolyl functionality. We hypothesized that a mixed pyrazolyl/triazolyl donor ligand would tolerate the introduction of nucleophilic reagents for attack on the carbon of a platinum carbonyl, without causing complete ligand loss. Herein, we report the synthesis and metalation of ligands that contain two pyrazolyl rings and one triazolyl ring as well as investigations into their reactivity. Structural data from four monomeric platinum d<sup>6</sup> complexes that exhibit octahedral geometries are included here.

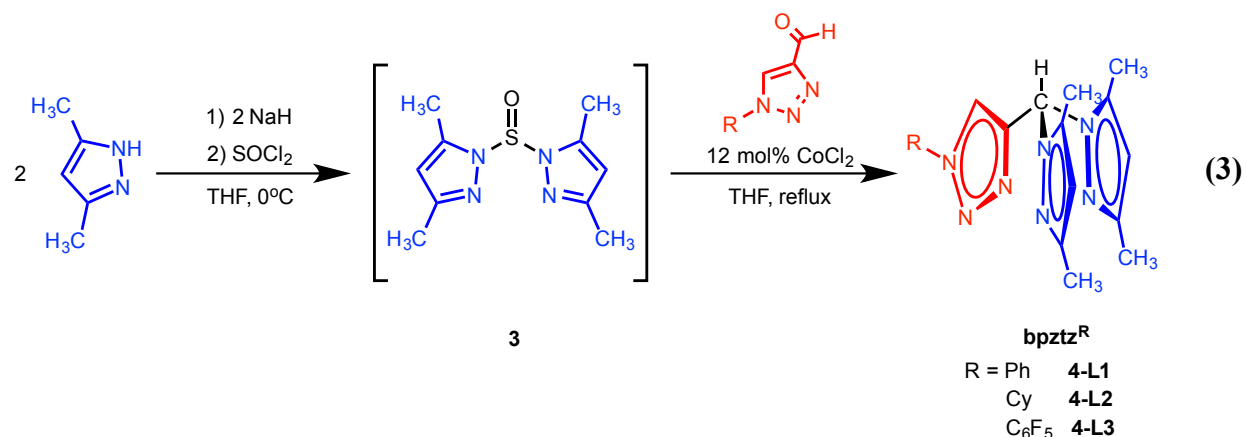
## 2.2 Results and Discussion

In the synthetic route to heteroscorpionate ligands reported by Reger,<sup>24</sup> the final condensation step requires a carbonyl functionality attached to the heterocycle that will ultimately be the unique donor arm of the heteroscorpionate. We synthesized a 1,2,3-triazole with an aldehyde at the 4-position. Employing the same conditions as for the copper-catalyzed azide-alkyne cycloaddition “click” reaction that was used to generate Tt<sup>R</sup>,<sup>29,33,34</sup> phenyl azide and propargyl alcohol were combined to produce (1-phenyl-1*H*-1,2,3-triazol-4-yl)methanol **1-L1** in 66% yield (step 1 in eq 2). The analogous cyclohexyl (cy) derivative (**1-L2**) was generated in 69% yield using cyclohexyl azide. Stahl et al. recently reported selective oxidation of primary alcohols to the corresponding aldehyde using an aerobic Cu(I) triflate/TEMPO system.<sup>35</sup> Applying similar conditions to **1-L1** produced 1-phenyl-1*H*-1,2,3-triazole-4-carbaldehyde **2-L1** in 72% yield (69% yield for **2-L2**).



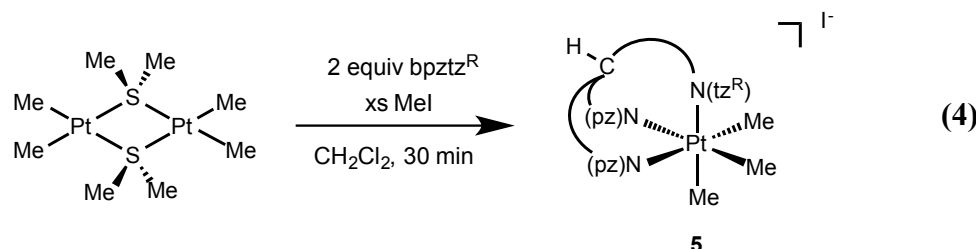
With the aldehyde compounds in hand, a heteroscorpionate ligand containing two 3,5-dimethyl pyrazolyl donors and a 1,2,3-triazole ring was targeted. Treating a THF solution of 3,5-dimethyl pyrazole with sodium hydride resulted in deprotonation of the pyrazole NH and evolution of hydrogen gas. The addition of thionyl chloride presumably

generated the bispyrazolyl sulfonyl intermediate, **3**. Treating **3** with 1,2,3-triazole aldehyde **2-L1** and a catalytic amount of cobalt chloride while refluxing overnight produced 4-(bis(3,5-dimethyl-1*H*-pyrazol-1-yl)methyl)-1-phenyl-1*H*-1,2,3-triazole **4-L1** in 87% yield, which we will abbreviate as bp<sub>tz</sub><sup>Ph</sup> (eq 3). The analogous bp<sub>tz</sub><sup>Cy</sup> ligand **4-L2** was produced in 56% yield. Discussion of the fluorinated ligand **4-L3** is included later in this section.

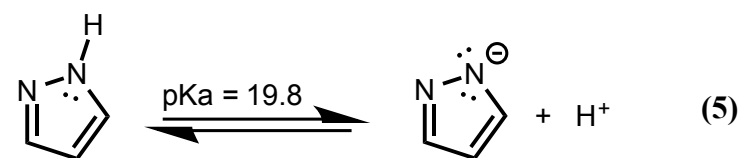


Metalation of the bp<sub>tz</sub><sup>R</sup> ligands was achieved by sequentially treating two equiv of **4** with one equiv of [PtMe<sub>2</sub>(SMe<sub>2</sub>)<sub>2</sub>] and then an excess of methyl iodide was added in dichloromethane and the solution was stirred at room temperature for 30 min (eq 4). Removal of the solvent and triturating with pentane produced the air- and moisture-stable Pt(IV) cation [bp<sub>tz</sub><sup>R</sup>PtMe<sub>3</sub>][I] **5** as a pale yellow solid in quantitative yield (eq 4). In the <sup>1</sup>H NMR spectrum of **5-L1**, two Pt-Me resonances appear in a 2:1 ratio at 1.4 and 1.3 ppm (<sup>2</sup>J<sub>Pt-H</sub> = 71 Hz and 73 Hz), respectively, reflecting the presence of a mirror plane and C<sub>s</sub> symmetry. The chemical shift values and coupling constants for these Pt-Me signals are compatible with other reported Pt(IV)-Me complexes.<sup>36-39</sup> The triazolyl proton in **5-L1** shifts significantly downfield (to 10.7 ppm) when the triazole ring binds to the metal center. Although the chemical shift for this proton usually moves downfield in <sup>1</sup>H

NMR spectra of  $\text{Pt}^{\text{R}}$  platinum complexes,<sup>29,33</sup> the triazolyl signal in **5-L1** moves over 2 ppm, an unusually large shift. In the C-13 NMR spectrum, the one-bond platinum carbon coupling values for the two Pt-Me resonances are 688 Hz (trans to pyrazole) and 701 Hz (trans to triazole) for **5-L1**. These one-bond coupling constants are not good indicators of bond strength; that correlation works well when hydrogen is involved, but for other NMR active nuclei the correlation is far more complex. Coupling constants for Pt-C bonds in **5-L2** are comparable.



As a point of departure before looking at Pt-N bond lengths we note that the  $\text{pK}_a$  for pyrazole is 19.8 whereas the triazole proton is far more acidic with a  $\text{pK}_a$  of 13.9 in DMSO.<sup>40</sup> While binding to the metal center in fact occurs at an alternative nitrogen, it's reasonable to keep the proton dissociation properties of pyrazoles and triazoles in mind as we look at structures of Pt(IV) compounds.



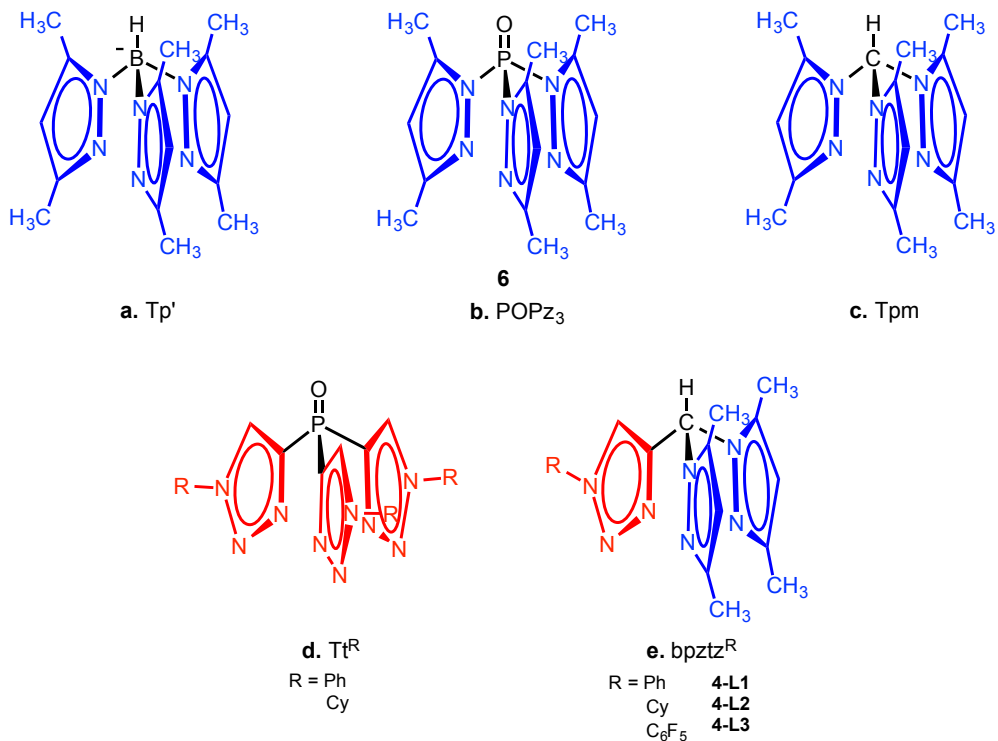


**Figure 2** **a.** hydridotris(3,5-dimethylpyrazolyl)borate. **b.** tris(3,5-dimethylpyrazolyl)phosphine oxide. **c.** tris(3,5-dimethylpyrazolyl)methane. **d.** tris(1-R-1H-1,2,3-triazol-4-yl) phosphine oxide (R = phenyl, cyclohexyl). **e.** 4-(bis(3,5-dimethyl-1H-pyrazol-1-yl)methyl)-1-R-1H-1,2,3-triazole (R = phenyl, cyclohexyl, pentafluorophenyl).

Slow diffusion of hexanes into a dichloromethane solution of **5-L2** produced clear, orange-red hexagonal crystals that were suitable for X-ray crystallography. Figure 3 shows the x-ray structure of **5-L2** and selected bond distances and angles are presented in Table 1. As in the related symmetric  $[\text{Tt}^{\text{R}}\text{PtMe}_3]^+$  complex,<sup>29</sup> the metal center adopts an octahedral geometry with a  $\kappa^3$  coordination mode for the chelating ligand. The Pt-N bond distance to the triazolyl donor (2.135 Å) is the shortest of the three Pt-N bond lengths. The two pyrazolyl donors, with Pt-N distances of 2.18 and 2.19 Å, appear to be weaker donors to the Pt(IV) than the triazole ring. The PtMe<sub>3</sub> unit assures that identical trans

influences will impact the three Pt-N bond lengths. The contrast between the pK<sub>a</sub> indicators and the observed Pt-N bond distances is striking.

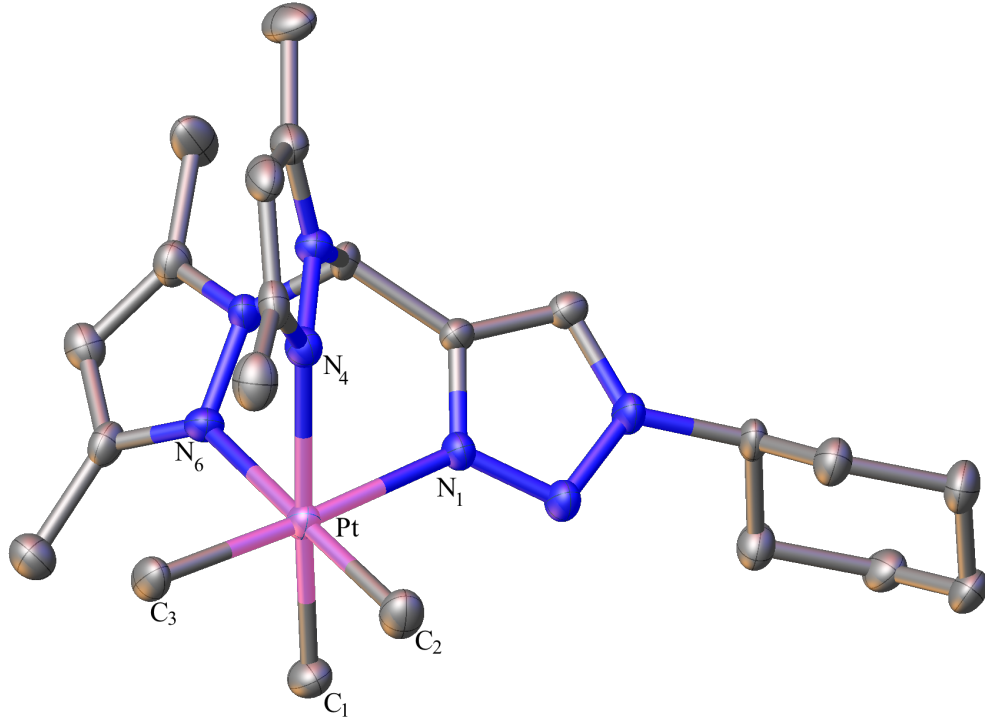


**Figure 3** X-ray structure of [bpztz<sup>Cy</sup>PtMe<sub>3</sub>][I] **5-L2**. Ellipsoids are drawn at the 50% probability level. Hydrogen atoms and counterion are omitted for clarity.

**Table 1** Selected bond lengths (Å) and angles (deg) for complex **5-L2**.

<u>Bond Lengths</u>			
Pt-N1	2.135(4)	Pt-C1	2.061(5)
Pt-N4	2.178(4)	Pt-C2	2.042(5)
Pt-N6	2.193(4)	Pt-C3	2.054(4)
<u>Bond Angles</u>			
N1-Pt-N4	84.85(14)	C2-Pt-C1	84.8(2)
C1-Pt-N1	93.54(17)		

Comparing the new mixed ligand to the Tt<sup>R</sup> ligand, it's conceivable that the difference in binding strength of the triazole arm arises from differences in tips of the

umbrella skeletons. The average Pt-N bond length for the Tt<sup>R</sup> ligand in Tt<sup>R</sup>PtMe<sub>3</sub> was 2.18 Å, similar to the bound pyrazole arms in our new bpztz<sup>R</sup>PtMe<sub>3</sub><sup>+</sup> complexes.<sup>29</sup> It seemed reasonable that the electron withdrawing backbone in the Tt<sup>R</sup> ligands (P=O) played an important role in modulating the donor strength of the triazolyl nitrogen. We hypothesized that the synthesis of a bpztz derivative containing an electron-withdrawing group as a substituent on the triazolyl ring would make the triazolyl bind less tightly. Repeating the ligand synthesis using pentafluorophenyl azide produced the pentafluorophenyl derivative bpztz<sup>C6F<sub>5</sub></sup> **4-L3** (eq 3). Using the same conditions for the generation of **5-L1** and **5-L2**, [bpztz<sup>C6F<sub>5</sub></sup>PtMe<sub>3</sub>][I] (**5-L3**) was produced in quantitative conversion as observed by <sup>1</sup>H NMR spectroscopy. Like **5-L1** and **5-L2**, complex **5-L3** also displays C<sub>s</sub> symmetry with a 2:1 ratio evident in Pt-Me signals (<sup>2</sup>J<sub>Pt-H</sub> = 72 Hz for each). The F-19 NMR spectrum exhibits the expected doublet and two triplets for the *ortho* and *meta/para* fluorine atoms. The one-bond platinum-carbon coupling values of the two Pt-Me resonances are 685 Hz (trans to pyrazole) and 706 Hz (trans to triazole), similar to **5-L1** and **5-L2**.

Slow diffusion of hexanes into a dichloromethane solution of **5-L3** produced clear, orange/red hexagonal crystals that were suitable for X-ray crystallography. Figure 4 shows the x-ray structure of **5-L2** and selected bond distances and angles are presented in Table 2. The Pt-N(triazole) bond distance of 2.138 Å is again shorter than the two Pt-N(pyrazole) distances, both 2.19 Å, reflecting stronger binding from the triazolyl ring compared to the two pyrazoles. Comparing the Pt-N(triazole) distance to the analogous [bpztz<sup>Cy</sup>PtMe<sub>3</sub>]<sup>+</sup> structure reveals that the addition of the pentafluorophenyl substituent did not have a noticeable impact on the donor strength of the triazolyl ring as determined

by bond distance measurements. The bond angles about platinum (84-95°) hover near the ideal 90°, with the three nitrogens of the tridentate ligand slightly pinched, similar to the angles in **5-L2**.

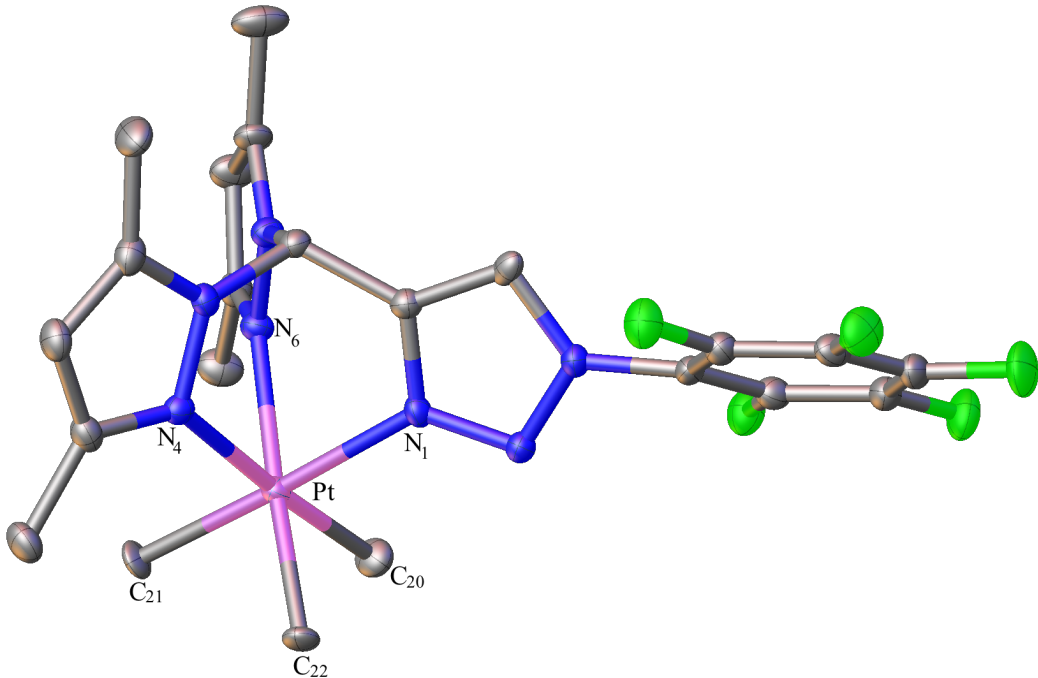
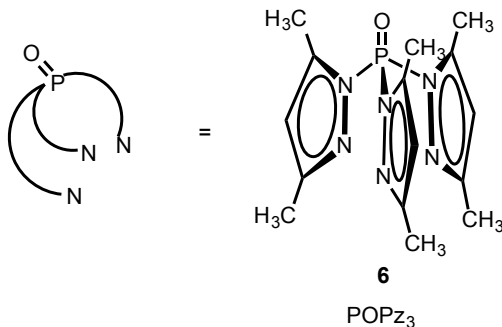


**Figure 4** X-ray structure of  $[bpztc_6F_5PtMe_3][I]$  **5-L3**. Ellipsoids are drawn at the 50% probability level. Hydrogen atoms and the iodide counterion are omitted for clarity.

**Table 2.** Selected bond lengths (Å) and angles (deg) for complex **5-L3**.

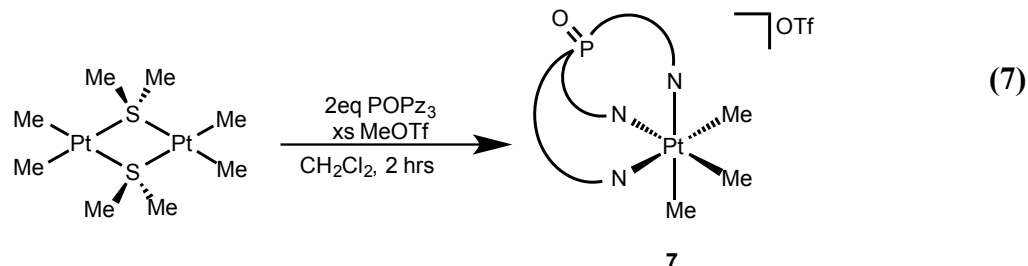
<u>Bond Lengths</u>			
Pt-N1	2.138(3)	Pt-C20	2.042(4)
Pt-N4	2.188(3)	Pt-C21	2.050(4)
Pt-N6	2.188(3)	Pt-C22	2.058(4)
<u>Bond Angles</u>			
N1-Pt-N4	84.95(12)	C20-Pt-C21	89.67(18)
C20-Pt-N1	91.61(15)		



While the two  $\text{bpztz}^{\text{R}}\text{PtMe}_3^+$  structures were in good agreement with one another, the triazole to platinum bond distances were shorter than in the analogous  $\text{Tt}^{\text{R}}$  complex with three triazole arms for the scorpionate ligand. The average Pt-N bond length for the  $\text{Tt}^{\text{R}}$  ligand in the  $\text{Tt}^{\text{R}}\text{PtMe}_3^+$  comp complex<sup>29</sup> was 2.18 Å, longer than the Pt-N bond to the triazole in **5-L2** and **5-L3**.

Since the pentafluorophenyl group on the triazolyl arm had no significant impact on the Pt-N bond length, we turned to an investigation of the influence of the phosphine oxide spine in the  $\text{Tt}^{\text{R}}$  system. Comparing the new mixed ligand to the triazole based  $\text{Tt}^{\text{R}}$  ligand with a P=O spine, it's conceivable that the difference in the binding strength of the triazole arm arises from differences in the spine of the umbrella skeletons. Deprotonation of 3,5-dimethylpyrazole with sodium hydride followed by addition of phosphoryl chloride resulted in the desired tris(3,5-dimethylpyrazolyl)phosphine oxide (POPz<sub>3</sub>) **6**, in 96% yield. Conditions used for the preparation of complex **5-L1** proved insufficient to push the metalation of **6** to completion. Switching from MeI to a stronger methylating reagent, methyl trifluoromethansulfonate (MeOTf), and extending reaction times allowed for generation and isolation of the desired cationic Pt(IV) complex,  $[\text{POPz}_3\text{PtMe}_3][\text{OTf}]$ , **7**, in quantitative yields (eq 7). Complex **7** displayed  $C_{3v}$  symmetry in the <sup>1</sup>H NMR spectrum as evident by a single Pt-CH<sub>3</sub> peak. The pyrazolyl proton showed a small

coupling to phosphorus (1 Hz) while the P-31 NMR signal at -18.26 ppm exhibited 3-bond coupling to platinum (9 Hz).



Slow diffusion of benzene into a solution of **7** in dichloromethane produced clear crystals suitable for X-ray crystallography. Figure 5 shows the x-ray structure of **7** and selected bond distances and angles are presented in Table 3. Complex **7** crystallized in a chiral space group. The three pyrazolyl Pt-N bond distances of ca. 2.20 Å are slightly elongated from those of the analogous trimethylPt(IV)Tp' complex, which are near 2.19 Å.<sup>41</sup> The Pt-N distances for these pyrazolyl donors are also close to the bond lengths observed for the triazole based Tt<sup>R</sup> ligand (2.17-2.19 Å).<sup>29</sup>

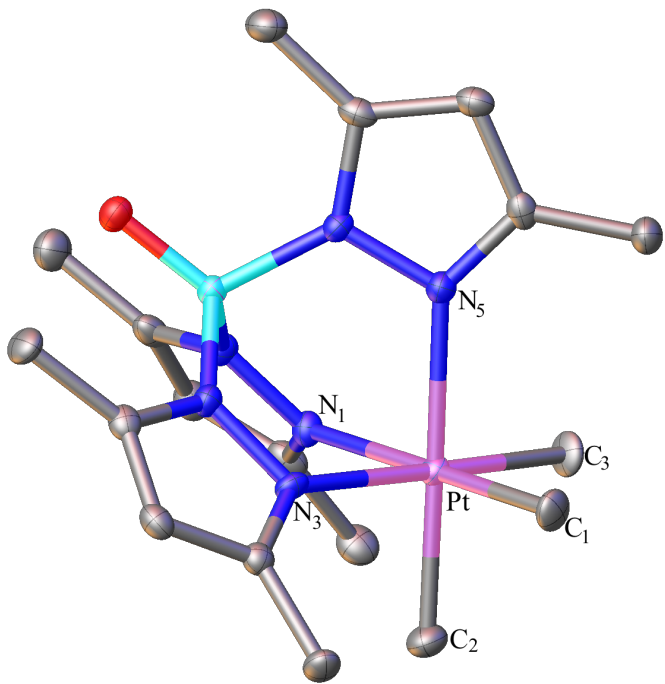
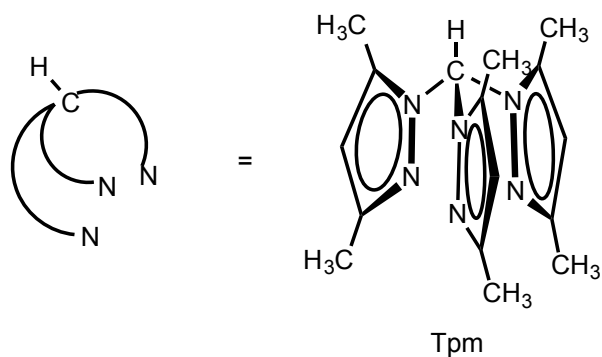


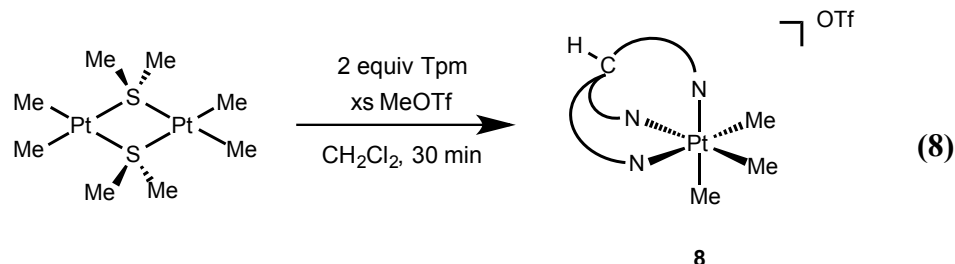
**Figure 5** X-ray structure of  $[\text{POPz}_3\text{PtMe}_3]\text{[OTf]}$  7. Ellipsoids are drawn at the 50% probability level. Hydrogen atoms, trifluoromethansulfonate counterion, and benzene molecule are omitted for clarity.

**Table 3** Selected bond lengths ( $\text{\AA}$ ) and angles (deg) for complex 7.

<u>Bond Lengths</u>			
Pt-N1	2.201(4)	Pt-C1	2.041(6)
Pt-N3	2.199(4)	Pt-C2	2.047(5)
Pt-N5	2.185(5)	Pt-C3	2.052(4)
<u>Bond Angles</u>			
N1-Pt-N3	88.2(2)	C2-Pt-C1	89.0(2)
C1-Pt-N3	91.6(3)		



The phosphine oxide backbone did not significantly change the Pt-N bond length so we turned to the C-H backbone in the well-known Tpm ligand, just as the C-H moiety is present in the mixed bp<sub>2</sub>tz<sup>R</sup> set of ligands. Employing Tpm<sup>24</sup> under the same conditions as for the preparation of POPz<sub>3</sub> complex **7** generated the desired cationic Pt(IV) complex, [TpmPtMe<sub>3</sub>][OTf], **8**, eq 8.



Slow diffusion of pentane into a solution of **8** in dichloromethane produced clear crystals suitable for X-ray crystallography. Complex **8** crystallized with three independent molecules in the unit cell. Figure 6 shows the x-ray structure of one of the three independent molecules and selected bond distances and angles are presented in Table 4. Complex **8** shows nearly octahedral geometry, with bond angles around platinum between 84-93° with the three nitrogens slightly pinched together, generating a slightly opened N-Pt-C angle. The Pt-N bond distances in this Tpm complex average 2.18 Å, slightly shorter than those observed in trimethyl Pt(IV) complexes with the other neutral ligands, namely Tt<sup>R</sup> and POPz<sub>3</sub>, presumably due to the more electron donating C-H backbone. The anionic Tp' ligand leads to a neutral Pt(IV) complex while all the other complexes reported here are cationic Pt(IV) compounds. Despite the slightly shorter bond lengths of the TpmPt complex compared to the mixed ligand system, the Pt-N bonds found in Tpm complex **8** were about 0.02 Å longer than the Pt-N distances for the triazole arm in the bp<sub>2</sub>tz<sup>R</sup> hybrid ligand system.

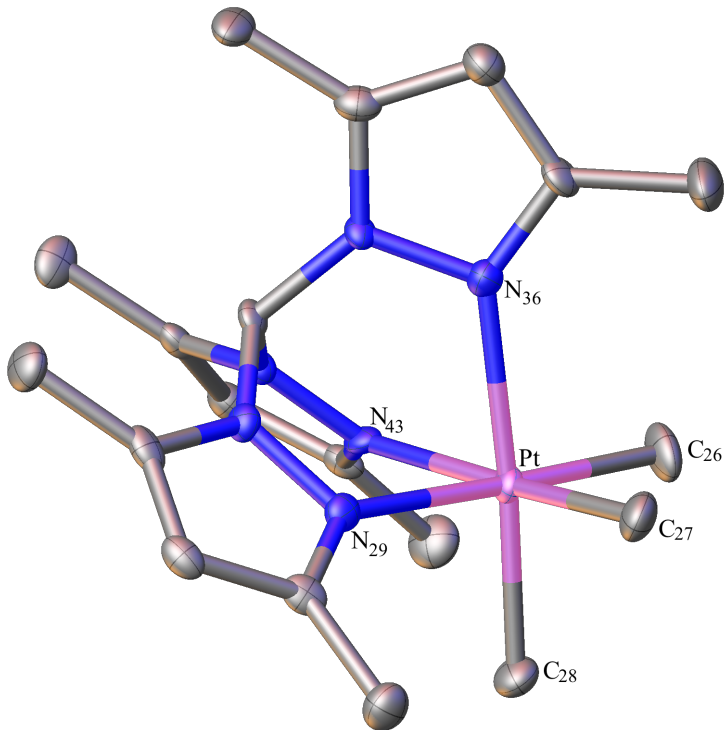


**Figure 6** X-ray structure of  $[\text{TpmPtMe}_3]\text{[OTf]}$  **8**. Ellipsoids are drawn at the 50% probability level. Hydrogen atoms and trifluoromethansulfonate counterion are omitted for clarity.

**Table 4** Selected bond lengths ( $\text{\AA}$ ) and angles (deg) for one of the three independent molecules of complex **8**.

<u>Bond Lengths</u>			
Pt-N29	2.187(6)	Pt-C26	2.044(7)
Pt-N36	2.189(6)	Pt-C27	2.072(8)
Pt-N43	2.162(6)	Pt-C28	2.049(8)
<u>Bond Angles</u>			
N29-Pt-N36	83.0(2)	C26-Pt-C27	88.4(3)
C26-Pt-N26	93.3(3)		

### **2.3 Conclusion**

A series of asymmetrical scorpionate ligands bearing two pyrazolyl rings and one triazolyl ring has been synthesized using a cobalt-catalyzed condensation reaction. Metalation of these ligands to generate neutral Pt(II) complexes followed by subsequent methylation results in stable Pt(IV) cations. Solid-state structural data reveal that the platinum-nitrogen distance to the triazolyl moiety is shorter than the two platinum-nitrogen pyrazolyl distances, indicating that the triazolyl ring is a stronger donor to Pt(IV). The addition of an electron withdrawing substituent on the triazole arm does not influence the ligand donor strength as assessed by Pt-N distances. While the backbone of the scorpionate ligand plays an integral part in binding to platinum, there is no evidence for why the triazole arm of the heteroscorpionate ligand binds more tightly to the Pt center.

### **2.4 Experimental Section**

**Materials and Methods.** All reactions were performed under an atmosphere of dry nitrogen using standard Schlenk and drybox techniques. Nitrogen was purified by passage through columns of BASF R3-11 catalyst and 4 Å molecule sieves. Dichloromethane, dimethyl ether, tetrahydrofuran (THF), and pentane were purified under an argon atmosphere and passed through a column packed with activated alumina. All other chemicals were used as received without further purification. Silica column chromatography was conducted with 230-400 mesh silica gel and alumina column chromatography was conducted with 80-200 mesh alumina.

<sup>1</sup>H, <sup>19</sup>F, <sup>31</sup>P, and <sup>13</sup>C NMR spectra were recorded on Bruker DRX400, AVANCE500, or ULTRA SHIELD CRYOQNP600 spectrometers. <sup>1</sup>H NMR and <sup>13</sup>C NMR chemical shifts were referenced to residual <sup>1</sup>H and <sup>13</sup>C signals of the deuterated solvents. Elemental analyses were performed by Robertson Microlit Laboratories of Madison, NJ. High-resolution mass spectra were recorded on a Bruker BioTOF II ESI-TOF mass spectrometer. Mass spectral data are reported for the most abundant platinum isotope.

**(1-phenyl-1*H*-1,2,3-triazol-4-yl)methanol 1-L1.** To a 250-mL Schlenk flask was added phenyl azide (7.8 g, 65.5 mmol) and propargylic alcohol (3.78 mL, 68.0 mmol). The flask was purged with nitrogen and 60 mL of a 1:1 mixture of *tert*-butanol and water was added through the septum. The solution was treated with 3.9 mL (3.9 mmol) of a 1 M aqueous sodium ascorbate solution and 1.54 mL (0.58 mmol) of a 0.37 M aqueous copper sulfate solution. The cloudy yellow solution was allowed to stir for 2 d at room temperature at which point the solution had become clear. The product was extracted into CH<sub>2</sub>Cl<sub>2</sub> and dried over MgSO<sub>4</sub>. The mixture was then passed through a Celite plug, the solvent was evaporated, and the resulting oil was triturated with pentane to produce 7.5 g (43.5 mmol) of **1-L1** in 66% yield. <sup>1</sup>H NMR ( $\delta$ , CD<sub>2</sub>Cl<sub>2</sub>, 298 K): 7.74 (s, 1H, tz), 7.72 (d, 2H, *o*-Ph), 7.53 (t, 2H, *m*-Ph), 7.45 (t, 1H, *p*-Ph), 4.84 (s, 2H, CH<sub>2</sub>), 3.13 (br s, 1H, OH). <sup>13</sup>C NMR ( $\delta$ , CD<sub>2</sub>Cl<sub>2</sub>, 298 K): 148.9 (tz 4-position), 137.5 (*ipso*-Ph), 130.1 (*o*-Ph), 129.1 (*p*-Ph), 120.9 (*m*-Ph), 120.5 (tz 5-position), 56.6 (CH<sub>2</sub>). Anal Calcd for C<sub>9</sub>H<sub>9</sub>N<sub>3</sub>O: C, 61.70; H, 5.18; N, 23.99. Found: C, 61.71; H, 5.46; N, 23.94.

**(1-cyclohexyl-1*H*-1,2,3-triazol-4-yl)methanol 1-L2.** To a 250-mL Schlenk flask was added cyclohexyl azide (7.15 g, 57.7 mmol) and propargylic alcohol (3.31 mL, 59.6

mmol). The flask was purged with nitrogen and a 1:1 mixture (60 mL) of *tert*-butanol and water was added through the septum. The solution was treated with 4.3 mL (4.3 mmol) of a 1 M aqueous sodium ascorbate solution and 2.15 mL (0.80 mmol) of a 0.37 M aqueous copper sulfate solution. The cloudy yellow mixture was allowed to stir for 2 d at room temperature at which point the solution became clear. The product was extracted with CH<sub>2</sub>Cl<sub>2</sub> and dried over MgSO<sub>4</sub>. The mixture was then passed through a Celite plug, the solvent was evaporated, and the resulting solid was triturated with pentane to produce 7.06 g (39.7 mmol) of **1-L2** in 69% yield. <sup>1</sup>H NMR ( $\delta$ , CD<sub>2</sub>Cl<sub>2</sub>, 298 K): 7.60 (s, 1H, tz), 4.69 (s, 2H, CH<sub>2</sub>), 4.40 (tt, 1H, C<sub>A</sub>-H), 4.31 (s, 1H, OH), 2.17-1.21 (m, 11 H, cyclohexyl). <sup>13</sup>C NMR ( $\delta$ , CD<sub>2</sub>Cl<sub>2</sub>, 298 K): 147.9 (tz 4-position), 120.1 (tz 5-position), 60.4 (C<sub>A</sub>), 56.2 (CH<sub>2</sub>), 33.8 (C<sub>B</sub>), 25.5 (C<sub>C</sub>), 25.4 (C<sub>D</sub>). Anal Calcd for C<sub>9</sub>H<sub>15</sub>N<sub>3</sub>O: C, 59.64; H, 8.34; N, 23.19. Found: C, 59.78; H, 8.13; N, 23.18.

**(1-pentafluorophenyl-1*H*-1,2,3-triazol-4-yl)methanol 1-L3.** To a 250-mL Schlenk flask was added pentafluorophenyl azide (1.18 g, 5.65 mmol) and propargylic alcohol (0.32 mL, 5.62 mmol). The flask was purged with nitrogen and a 1:1 mixture (60 mL) of *tert*-butanol and water was added through the septum. The solution was treated with 0.33 mL (0.33 mmol) of a 1 M aqueous sodium ascorbate solution and 0.20 mL (0.07 mmol) of a 0.37 M aqueous copper sulfate solution. The cloudy yellow mixture was allowed to stir overnight at room temperature. The product was extracted with CH<sub>2</sub>Cl<sub>2</sub> and dried over MgSO<sub>4</sub>. The mixture was then passed through a Celite plug, the solvent was evaporated, and the resulting solid was triturated with pentane to produce 1.02 g (3.84 mmol) of **1-L3** in 68% yield. <sup>1</sup>H NMR ( $\delta$ , CD<sub>2</sub>Cl<sub>2</sub>, 298 K): 7.85 (s, 1H, tz), 4.88 (s, 2H, CH<sub>2</sub>), 3.21 (s, 1H, OH). <sup>19</sup>F NMR ( $\delta$ , CD<sub>2</sub>Cl<sub>2</sub>, 298 K): -145.7 (d, *o*-F), -

149.9 (t, *p*-F), -159.5 (t, *m*-F).  $^{13}\text{C}$  NMR ( $\delta$ , CD<sub>2</sub>Cl<sub>2</sub>, 298 K): 148.2 (tz 4-position), 142.4 (m, *o*-ArF and *p*-ArF,  $^1\text{J}_{\text{C},\text{F}} = 264$  Hz), 138.0 (m, *m*-ArF,  $^1\text{J}_{\text{C},\text{F}} = 261$  Hz), 124.4 (tz 5-position), 112.8 (m, *ipso*-ArF). Anal Calcd for C<sub>9</sub>H<sub>4</sub>N<sub>3</sub>OF<sub>5</sub>: C, 40.77; H, 1.52; N, 15.85. Found: C, 40.98; H, 1.57; N, 15.50.

**1-phenyl-1*H*-1,2,3-triazole-4-carbaldehyde 2-L1.** A modified version of Stahl's procedure was performed.<sup>35</sup> A 250-mL Schlenk flask was charged with 7.5 g (43.4 mmol) of **1-L1**. Acetonitrile (100 mL) was added and the mixture was stirred until all of **1-L1** dissolved. The solution was treated with tetrakisacetonitrile copper(I) triflate (0.780 g, 2.07 mmol), bipyridine (0.331 g, 2.12 mmol), TEMPO (0.331 g, 2.12 mmol), and N-methyl imidazole (0.31 mL, 4.14 mmol) and the resulting dark red solution was stirred open to air overnight at which point it became emerald green. Diethyl ether (40 mL) and pentane (40 mL) were added and the solution was filtered through a silica plug. The solvent was removed by rotary evaporation and pentane (50 mL) was added to remove excess TEMPO. The pink supernatant was decanted off to afford 5.38 g (31.5 mmol) of **1-L2** as a white crystalline solid in 72% yield.  $^1\text{H}$  NMR ( $\delta$ , CD<sub>2</sub>Cl<sub>2</sub>, 298 K): 10.19 (s, 1H, C(O)H), 8.57 (s, 1H, tz), 7.79 (d, 2H, *o*-Ph), 7.60 (t, 2H, *m*-Ph), 7.55 (t, 1H, *p*-Ph).  $^{13}\text{C}$  NMR ( $\delta$ , CD<sub>2</sub>Cl<sub>2</sub>, 298 K): 184.8 (C(O)H), 148.1 (tz 4-position), 136.2 (*ipso*-Ph), 130.0 (*o*-Ph), 129.7 (*p*-Ph), 123.9 (tz 5-position), 120.9 (*m*-Ph). IR(CH<sub>2</sub>Cl<sub>2</sub>):  $\nu_{\text{C=O}} = 1703$  cm<sup>-1</sup>. Anal Calcd for C<sub>9</sub>H<sub>7</sub>N<sub>3</sub>O: C, 62.42; H, 4.07; N, 24.27. Found: C, 62.65; H, 3.93; N, 24.22.

**1-cyclohexyl-1*H*-1,2,3-triazole-4-carbaldehyde 2-L2.** A 250-mL Schlenk flask was charged with 6.29 g (35.3 mmol) of **1-L2**. Acetonitrile (100 mL) was added and the mixture was stirred until all of **1-L2** dissolved. The solution was treated with

tetrakisacetonitrile copper(I) triflate (0.658 g, 1.74 mmol), bipyridine (0.280 g, 1.67 mmol), TEMPO (0.280 g, 1.67 mmol), and N-methyl imidazole (0.28 g, 3.27 mmol) and the dark red solution was stirred open to air overnight at which point it became emerald green. Diethyl ether (40 mL) and pentane (40 mL) were added and the solution was filtered through a silica plug. The solvent was removed by rotary evaporation and pentane (50 mL) was added to remove excess TEMPO. The pink supernatant was decanted off to afford 4.27 g (24.3 mmol) of **2-L2** as a white crystalline solid in 69% yield.  $^1\text{H}$  NMR ( $\delta$ , CD<sub>2</sub>Cl<sub>2</sub>, 298 K): 10.08 (s, 1H, C(O)H), 8.14 (s, 1H, tz), 4.51 (tt, 1H, C<sub>A</sub>-H), 2.25-1.28 (m, 11 H, cyclohexyl).  $^{13}\text{C}$  NMR ( $\delta$ , CD<sub>2</sub>Cl<sub>2</sub>, 298 K): 185.3 (C(O)H), 147.7 (tz 4-position), 123.6 (tz 5-position), 60.9 (C<sub>A</sub>), 33.7 (C<sub>B</sub>), 25.3 (C<sub>C</sub>), 25.3 (C<sub>D</sub>). IR(CH<sub>2</sub>Cl<sub>2</sub>):  $\nu_{\text{C=O}} = 1698 \text{ cm}^{-1}$ . Anal Calcd for C<sub>9</sub>H<sub>13</sub>N<sub>3</sub>O: C, 60.32; H, 7.31; N, 23.45. Found: C, 60.26; H, 7.35; N, 23.31.

**1-pentafluorophenyl-1*H*-1,2,3-triazole-4-carbaldehyde **2-L3**.** A 250-mL Schlenk flask was charged with 1.25 g (4.72 mmol) of **1-L3**. Acetonitrile (30 mL) was added and the mixture was stirred until all of **1-L3** dissolved. The solution was treated with tetrakisacetonitrile copper(I) triflate (0.087 g, 0.23 mmol), bipyridine (0.036 g, 0.24 mmol), TEMPO (0.036 g, 0.24 mmol), and N-methyl imidazole (0.037 g, 0.48 mmol) and the dark red solution was stirred open for 2 d at which point it became emerald green. Diethyl ether (40 mL) and pentane (40 mL) were added and the solution was filtered through a silica plug. The solvent was removed by rotary evaporation and pentane (50 mL) was added to remove excess TEMPO. The pink supernatant was decanted off to afford 0.80 g (3.04 mmol) of **2-L3** as a white crystalline solid in 64% yield.  $^1\text{H}$  NMR ( $\delta$ , CD<sub>2</sub>Cl<sub>2</sub>, 298 K): 10.20 (s, 1H, C(O)H), 8.50 (s, 1H, tz).  $^{19}\text{F}$  NMR ( $\delta$ , CD<sub>2</sub>Cl<sub>2</sub>, 298 K): -

145.9 (d, *o*-F), -149.3 (t, *p*-F), -159.6 (t, *m*-F).  $^{13}\text{C}$  NMR ( $\delta$ , CD<sub>2</sub>Cl<sub>2</sub>, 298 K): 184.1 (C(O)H), 147.8 (tz 4-position), 143.0 (m, *p*-ArF,  $^1\text{J}_{\text{C},\text{F}} = 260$  Hz), 142.5 (m, *o*-ArF,  $^1\text{J}_{\text{C},\text{F}} = 261$  Hz), 138.4 (m, *m*-ArF,  $^1\text{J}_{\text{C},\text{F}} = 258$  Hz), 129.0 (tz 5-position), 112.3 (m, *ipso*-ArF). IR(CH<sub>2</sub>Cl<sub>2</sub>):  $\nu_{\text{C}=\text{O}} = 1709$  cm<sup>-1</sup>. Anal Calcd for C<sub>9</sub>H<sub>3</sub>N<sub>3</sub>OF<sub>5</sub>: C, 41.08; H, 0.77; N, 15.97. Found: C, 41.46; H, 0.77; N, 15.94.

#### **4-(bis(3,5-dimethyl-1*H*-pyrazol-1-yl)methyl)-1-phenyl-1*H*-1,2,3-triazole**

**(bpztz<sup>Ph</sup>) 4-L1.** A modified version of Reger's procedure was performed.<sup>24</sup> A 250-mL Schlenk flask was charged with 0.278 g (11.58 mmol) of sodium hydride. THF (40 mL) was added through the septum and the cloudy white solution was cooled to 0°C in an ice bath. 3,5-dimethyl pyrazole (1.098 g, 11.55 mmol) was slowly added to the mixture and hydrogen gas evolved. The solution was stirred for 30 min at 0°C and became clear and colorless. Thionyl chloride (0.42 mL, 5.78 mmol) was added through the septum and the solution was stirred at 0°C. After 45 min, **2-L1** (0.500 g, 2.92 mmol) and a catalytic amount of CoCl<sub>2</sub> (0.018 g, 0.14 mmol) were added. The sea green solution was refluxed overnight then cooled to room temperature. Diethyl ether (40 mL) and water (40 mL) were added and stirred for 30 min to quench the cobalt catalyst. The organic layer was extracted and dried over MgSO<sub>4</sub>. After filtration, the solvent was removed by rotary evaporation and the yellow oil was triturated three times with pentane to afford 0.880 g (2.53 mmol) of **4-L1** as a yellow solid in 87% yield.  $^1\text{H}$  NMR ( $\delta$ , CD<sub>2</sub>Cl<sub>2</sub>, 298 K): 8.32 (s, 1H, tz H), 7.78 (d, 2H, *o*-Ph), 7.69 (s, 1H, HC(pz)<sub>2</sub>(tz)), 7.55 (t, 2H, *m*-Ph), 7.47 (t, 1H, *p*-Ph), 5.88 (s, 2H, pz H), 2.32, 2.19 (s, 3H each, pz CH<sub>3</sub>).  $^{13}\text{C}$  NMR ( $\delta$ , CD<sub>2</sub>Cl<sub>2</sub>, 298 K): 149.0, 140.6 (pz C-CH<sub>3</sub>), 144.7 (tz 4-position), 137.3 (*ipso*-Ph), 130.0, (*m*-Ph), 129.2 (*p*-Ph), 123.6 (tz 5-position), 120.9 (*o*-Ph), 107.1 (pz CH), 67.1 (HC(pz)<sub>2</sub>(tz)), 13.7, 11.5 (pz

$\text{CH}_3$ ). Anal Calcd for  $\text{C}_{19}\text{H}_{21}\text{N}_7$ : C, 65.69; H, 6.09; N, 28.22. Found: C, 65.55; H, 5.86; N, 27.57.

**4-(bis(3,5-dimethyl-1*H*-pyrazol-1-yl)methyl)-1-cyclohexyl-1*H*-1,2,3-triazole**

**(bpztz<sup>Cy</sup>) 4-L2.** A 250-mL Schlenk flask was charged with 0.556 g (23.2 mmol) of sodium hydride. THF (40 mL) was added through the septum and the cloudy white solution was cooled to 0°C in an ice bath. 3,5-dimethyl pyrazole (2.196 g, 23.1 mmol) was slowly added to the mixture and hydrogen gas evolved. The solution was stirred for 30 min at 0°C and became clear and colorless. Thionyl chloride (0.84 mL, 11.6 mmol) was added through the septum and the solution was stirred at 0°C. After 45 min, **2-L2** (1.03 g, 5.85 mmol) and a catalytic amount of  $\text{CoCl}_2$  (0.036 g, 0.28 mmol) were added. The sea green solution was refluxed overnight then cooled to room temperature. Diethyl ether (40 mL) and water (40 mL) were added and stirred for 30 min to quench the cobalt catalyst. The organic layer was extracted and dried over  $\text{MgSO}_4$ . After filtration, the solvent was removed by rotary evaporation and the yellow oil was triturated five times with pentane to afford 1.15 g (3.26 mmol) of **4-L2** as an orange solid in 56% yield. <sup>1</sup>H NMR ( $\delta$ ,  $\text{CD}_2\text{Cl}_2$ , 298 K): 7.91 (s, 1H, tz H), 7.68 ( $\text{HC}(\text{pz})_2(\text{tz})$ ), 5.89 (s, 2H, pz H), 4.47 (tt, 1H,  $\text{C}_A$ -H), 2.33, 2.23 (s, 3H each, pz  $\text{CH}_3$ ), 2.33-1.32 (11H, cyclohexyl). <sup>13</sup>C NMR ( $\delta$ ,  $\text{CD}_2\text{Cl}_2$ , 298 K): 148.6, 140.4 (pz C- $\text{CH}_3$ ), 143.4 (tz 4-position), 123.0 (tz 5-position), 106.1 (pz CH), 67.4 ( $\text{HC}(\text{pz})_2(\text{tz})$ ), 60.6 ( $\text{C}_A$ ), 33.7 ( $\text{C}_B$ ), 25.4 ( $\text{C}_C$  and  $\text{C}_D$ ), 13.6, 11.4 (pz  $\text{CH}_3$ ). Anal Calcd for  $\text{C}_{19}\text{H}_{26}\text{N}_7$ : C, 64.56; H, 7.70; N, 27.74. Found: C, 64.31; H, 7.77; N, 27.22.

**4-(bis(3,5-dimethyl-1*H*-pyrazol-1-yl)methyl)-1-pentafluorophenyl-1*H*-1,2,3-triazole (bpztz<sup>C6F5</sup>) 4-L3.** A 250-mL Schlenk flask was charged with 0.294 g (12.3

mmol) of sodium hydride. THF (40 mL) was added through the septum and the cloudy white solution was cooled to 0°C in an ice bath. 3,5-dimethyl pyrazole (1.16 g, 16.3 mmol) was slowly added to the mixture and hydrogen gas evolved. The solution was stirred for 30 min at 0°C and became clear and colorless. Thionyl chloride (0.45 mL, 6.21 mmol) was added through the septum and the solution was stirred at 0°C. After 45 min, **2-L3** (0.80 g, 3.04 mmol) and a catalytic amount of CoCl<sub>2</sub> (0.019 g, 0.15 mmol) were added. The sea green solution was refluxed overnight then cooled to room temperature. Diethyl ether (40 mL) and water (40 mL) were added and stirred for 30 min to quench the cobalt catalyst. The organic layer was extracted and dried over MgSO<sub>4</sub>. After filtration, the solvent was removed by rotary evaporation and the yellow oil was triturated five times with pentane to afford 0.85 g (2.19 mmol) of **4-L3** as an orange solid in 72% yield. <sup>1</sup>H NMR ( $\delta$ , CD<sub>2</sub>Cl<sub>2</sub>, 298 K): 8.28 (s, 1H, tz H), 7.71 (HC(pz)<sub>2</sub>(tz)), 5.87 (s, 2H, pz H), 2.32, 2.18 (s, 3H each, pz CH<sub>3</sub>). <sup>19</sup>F NMR ( $\delta$ , CD<sub>2</sub>Cl<sub>2</sub>, 298 K): -146.1 (d, *o*-F), -150.7 (t, *p*-F), -160.4 (m, *m*-F). <sup>13</sup>C NMR ( $\delta$ , CD<sub>2</sub>Cl<sub>2</sub>, 298 K): 149.2, 140.7 (pz C-CH<sub>3</sub>), 144.7 (tz 4-position), 142.8 (m, *o*-ArF and *p*-ArF, <sup>1</sup>J<sub>C,F</sub> = 249 Hz), 138.5 (m, *m*-ArF, <sup>1</sup>J<sub>C,F</sub> = 255 Hz), 128.3 (tz 5-position), 113.2 (m, *ipso*-ArF), 107.2 (pz CH), 67.0 (HC(pz)<sub>2</sub>(tz)), 13.7, 11.4 (pz CH<sub>3</sub>). Anal Calcd for C<sub>19</sub>H<sub>21</sub>N<sub>7</sub>F<sub>5</sub>: C, 52.18; H, 3.69; N, 22.42. Found: C, 52.13; H, 3.60; N, 22.16.

**[bpztz<sup>Ph</sup>PtMe<sub>3</sub>]**I** 5-L1.** A 50-mL Schlenk was charged with 0.030 g (0.05 mmol) of [PtMe<sub>2</sub>(SMe<sub>2</sub>)<sub>2</sub>] and 0.036 g (0.10 mmol) of **4-L1**. The flask was purged with nitrogen and CH<sub>2</sub>Cl<sub>2</sub> (10 mL) was added through the septum. The yellow solution was treated with 20 uL (0.30 mmol) of methyl iodide and stirred for 30 min at room temperature. The solvent was removed via rotary evaporation and the resulting oil was

triturated with pentane to afford **5-L1** as a pale yellow solid in quantitative yield. <sup>1</sup>H NMR ( $\delta$ , CD<sub>2</sub>Cl<sub>2</sub>, 298 K): 10.67 (s, 1H, tz H), 8.85 (s, 1H, HC(pz)<sub>2</sub>(tz)), 7.84 (d, 2H, *o*-Ph), 7.55 (m, 3H, *m*-Ph and *p*-Ph), 6.00 (s, 2H, pz H), 2.83, 2.32 (s, 3H each, pz CH<sub>3</sub>), 1.42 (s, 6H, <sup>2</sup>*J*<sub>Pt-H</sub> = 71 Hz, Pt-CH<sub>3</sub>), 1.32 (s, 3H, <sup>2</sup>*J*<sub>Pt-H</sub> = 73 Hz, Pt-CH<sub>3</sub>). <sup>13</sup>C NMR ( $\delta$ , CD<sub>2</sub>Cl<sub>2</sub>, 298 K): 152.8, 142.8 (pz C-CH<sub>3</sub>), 139.4 (tz 4-position), 136.4 (ipso-Ph), 130.5, (p-Ph), 130.4 (*m*-Ph), 126.2 (tz 5-position), 121.1 (*o*-Ph), 108.8 (pz CH), 61.4 (HC(pz)<sub>2</sub>(tz)), 13.2, 13.1 (pz CH<sub>3</sub>), -8.0 (<sup>1</sup>*J*<sub>Pt-C</sub> = 688 Hz, Pt-CH<sub>3</sub>), -10.7 (<sup>1</sup>*J*<sub>Pt-C</sub> = 701 Hz, Pt-CH<sub>3</sub>). Anal Calcd for C<sub>22</sub>H<sub>30</sub>N<sub>7</sub>IPt: C, 36.82; H, 4.23; N, 13.72. Found: C, 35.97; H, 4.50; N, 13.39.

**[bpztz<sup>Cy</sup>PtMe<sub>3</sub>][I] 5-L2.** A 50-mL Schlenk was charged with 0.030 g (0.05 mmol) of [PtMe<sub>2</sub>(SMe<sub>2</sub>)<sub>2</sub>] and 0.037 g (0.10 mmol) of **4-L2**. The flask was purged with nitrogen and CH<sub>2</sub>Cl<sub>2</sub> (10 mL) was added through the septum. The yellow solution was treated with 20  $\mu$ L (0.30 mmol) of methyl iodide and stirred for 30 min at room temperature. The solvent was removed via rotary evaporation and the resulting oil was triturated with pentane to afford **5-L1** as a pale yellow solid in quantitative yield. <sup>1</sup>H NMR ( $\delta$ , CD<sub>2</sub>Cl<sub>2</sub>, 298 K): 10.10 (s, 1H, tz H), 8.73 (HC(pz)<sub>2</sub>(tz)), 5.98 (s, 2H, pz H), 4.50 (tt, 1H, C<sub>A</sub>-H), 2.83, 2.29 (s, 3H each, pz CH<sub>3</sub>), 2.33-1.25 (11H, cyclohexyl), 1.34 (s, 6H, <sup>2</sup>*J*<sub>Pt-H</sub> = 72 Hz, Pt-CH<sub>3</sub>), 1.25 (s, 3H, <sup>2</sup>*J*<sub>Pt-H</sub> = 70 Hz, Pt-CH<sub>3</sub>). <sup>13</sup>C NMR ( $\delta$ , CD<sub>2</sub>Cl<sub>2</sub>, 298 K): 152.7, 142.6 (pz C-CH<sub>3</sub>), 138.6 (tz 4-position), 126.2 (tz 5-position), 108.7 (pz CH), 62.6 (C<sub>A</sub>), 61.7 (HC(pz)<sub>2</sub>(tz)), 33.4 (C<sub>B</sub>), 25.2 (C<sub>C</sub> and C<sub>D</sub>), 13.4, 13.2 (pz CH<sub>3</sub>), -8.3 (<sup>1</sup>*J*<sub>Pt-C</sub> = 690 Hz, Pt-CH<sub>3</sub>), -11.1 (<sup>1</sup>*J*<sub>Pt-C</sub> = 703 Hz, Pt-CH<sub>3</sub>). Anal Calcd for C<sub>22</sub>H<sub>35</sub>N<sub>7</sub>IPt: C, 36.67; H, 5.04; N, 13.61. Found: C, 36.39; H, 4.91; N, 13.39.

**[bpztz<sup>C6F<sub>5</sub></sup>PtMe<sub>3</sub>][I] 5-L3.** A 50-mL Schlenk was charged with 0.030 g (0.05 mmol) of [PtMe<sub>2</sub>(SMe<sub>2</sub>)<sub>2</sub>] and 0.041 g (0.10 mmol) of **4-L3**. The flask was purged with nitrogen and CH<sub>2</sub>Cl<sub>2</sub> (10 mL) was added through the septum. The yellow solution was treated with 20 μL (0.30 mmol) of methyl iodide and stirred for 30 min at room temperature. The solvent was removed via rotary evaporation and the resulting oil was triturated with pentane to afford **5-L3** as a pale yellow solid in quantitative yield. <sup>1</sup>H NMR ( $\delta$ , CD<sub>2</sub>Cl<sub>2</sub>, 298 K): 10.65 (s, 1H, tz H), 8.99 (HC(pz)<sub>2</sub>(tz)), 6.03 (s, 2H, pz H), 2.88, 2.32 (s, 3H each, pz CH<sub>3</sub>), 1.38 (s, 6H, <sup>2</sup>J<sub>Pt-H</sub> = 72 Hz, Pt-CH<sub>3</sub>), 1.36 (s, 3H, <sup>2</sup>J<sub>Pt-H</sub> = 72 Hz, Pt-CH<sub>3</sub>). <sup>19</sup>F NMR ( $\delta$ , CD<sub>2</sub>Cl<sub>2</sub>, 298 K): -145.0 (d, *o*-F), -147.7 (t, *p*-F), -158.9 (t, *m*-F). <sup>13</sup>C NMR ( $\delta$ , CD<sub>2</sub>Cl<sub>2</sub>, 298 K): 153.2, 143.2 (pz C-CH<sub>3</sub>), 140.3 (tz 4-position), 131.0 (tz 5-position), 109.1 (pz CH), 61.4 (HC(pz)<sub>2</sub>(tz)), 13.7, 13.3 (pz CH<sub>3</sub>), -7.9 (<sup>1</sup>J<sub>Pt-C</sub> = 685 Hz, Pt-CH<sub>3</sub>), -10.2 (<sup>1</sup>J<sub>Pt-C</sub> = 706 Hz, Pt-CH<sub>3</sub>). Anal Calcd for C<sub>22</sub>H<sub>30</sub>N<sub>7</sub>F<sub>5</sub>IPt: C, 32.64; H, 3.74; N, 12.11. Found: C, 32.01; H, 3.60; N, 12.21.

**tris(3,5-dimethylpyrazolyl)phosphine oxide (POPz<sub>3</sub>) 6.** A 250-mL Schlenk flask was charged with 0.857 g (35.72 mmol) of sodium hydride. THF (60 mL) was added through the septum and the cloudy white solution was cooled to 0°C in an ice bath. 3,5-dimethyl pyrazole (3.417 g, 35.55 mmol) was slowly added to the mixture and hydrogen gas evolved. The solution was stirred for 30 min at 0°C and became clear and colorless. Phosphoryl chloride (1.01 mL, 10.9 mmol) was added through the septum and the solution was stirred at room temperature for 45 minutes. The solvent was removed under reduced pressure and the resulting oil was triturated with pentane to afford **6** as a white solid in 96% yield (3.4 g). <sup>1</sup>H NMR ( $\delta$ , CD<sub>2</sub>Cl<sub>2</sub>, 298 K): 6.05 (d, 3H, <sup>4</sup>J<sub>P-H</sub> = 5 Hz, pz H), 2.25, 2.18 (s, 9H each, pz CH<sub>3</sub>). <sup>13</sup>C NMR ( $\delta$ , CD<sub>2</sub>Cl<sub>2</sub>, 298 K): 155.1, 148.6 (<sup>2</sup>J<sub>P-C</sub>

= 11 Hz, pz C-CH<sub>3</sub>), 111.2 (<sup>3</sup>J<sub>P-C</sub> = 9 Hz, pz CH), 13.8, 12.3 (pz CH<sub>3</sub>). <sup>31</sup>P NMR (externally referenced to 85% H<sub>3</sub>PO<sub>4</sub>) -11.42. Anal Calcd for C<sub>15</sub>H<sub>21</sub>N<sub>6</sub>PO: C, 54.21; H, 6.37; N, 25.29. Found: C, 54.10; H, 6.32; N, 25.20.

**[POPz<sub>3</sub>PtMe<sub>3</sub>][OTf] 7.** A 50-mL Schlenk was charged with 0.030 g (0.05 mmol) of [PtMe<sub>2</sub>(SMe<sub>2</sub>)]<sub>2</sub> and 0.035 g (0.10 mmol) of tris(3,5-dimethylpyrazolyl)phosphine oxide. The flask was purged with argon and CH<sub>2</sub>Cl<sub>2</sub> (10 mL) was added through the septum. The yellow solution was treated with 34 μL (0.30 mmol) of methyl trifluoromethansulfonate and stirred for 30 min at room temperature. The solvent was removed under reduced pressure and the resulting oil was triturated with pentane to afford **7** as a white solid in quantitative yield. <sup>1</sup>H NMR (δ, CD<sub>2</sub>Cl<sub>2</sub>, 298 K): 6.31 (d, 3H, <sup>4</sup>J<sub>P-H</sub> = 5 Hz, pz H), 2.67, 2.44 (s, 9H each, pz CH<sub>3</sub>), 1.51 (s, 9H, <sup>2</sup>J<sub>Pt-H</sub> = 71 Hz, Pt-CH<sub>3</sub>), 1.25 (s, 3H, <sup>2</sup>J<sub>Pt-H</sub> = 70 Hz, Pt-CH<sub>3</sub>). <sup>13</sup>C NMR (δ, CD<sub>2</sub>Cl<sub>2</sub>, 298 K): 159.9, 151.9 (<sup>2</sup>J<sub>P-C</sub> = 11 Hz, pz C-CH<sub>3</sub>), 114.0 (<sup>3</sup>J<sub>P-C</sub> = 10 Hz, pz CH), 14.1, 13.7 (pz CH<sub>3</sub>), -6.3 (<sup>1</sup>J<sub>Pt-C</sub> = 693 Hz, Pt-CH<sub>3</sub>). <sup>31</sup>P NMR (externally referenced to 85% H<sub>3</sub>PO<sub>4</sub>) -18.26 (<sup>3</sup>J<sub>Pt-P</sub> = 9 Hz). Anal Calcd for C<sub>19</sub>H<sub>30</sub>N<sub>6</sub>PtF<sub>3</sub>SO<sub>3</sub>: C, 33.83; H, 4.48; N, 12.46. Found: C, 33.01; H, 4.50; N, 12.92.

**[TpmpPtMe<sub>3</sub>][OTf] 8.** A 50-mL Schlenk was charged with 0.030 g (0.05 mmol) of [PtMe<sub>2</sub>(SMe<sub>2</sub>)]<sub>2</sub> and 0.031 g (0.10 mmol) of tris(3,5-dimethylpyrazolyl)methane. The flask was purged with argon and CH<sub>2</sub>Cl<sub>2</sub> (10 mL) was added through the septum. The yellow solution was treated with 34 μL (0.30 mmol) of methyl trifluoromethansulfonate and stirred for 30 min at room temperature. The solvent was removed under reduced pressure and the resulting oil was triturated with pentane to afford **8** as a white solid in quantitative yield. <sup>1</sup>H NMR (δ, CD<sub>2</sub>Cl<sub>2</sub>, 298 K): 7.90 (s, 1H, HC(pz)<sub>3</sub>), 6.14 (s, 3H, Pz H),

2.62, 2.35 (s, 9H each, pz  $CH_3$ ), 1.42 (s, 9H,  $^2J_{\text{Pt-H}} = 70$  Hz, Pt- $CH_3$ ).  $^{13}\text{C}$  NMR ( $\delta$ , CD<sub>2</sub>Cl<sub>2</sub>, 298 K): 153.7, 141.6 (pz C- $CH_3$ ), 110.0 (pz CH), 70.0 (HC(pz)<sub>3</sub>), 13.2, 11.5 (pz CH<sub>3</sub>), -8.8 ( $^1J_{\text{Pt-C}} = 693$  Hz, Pt- $CH_3$ ). Anal Calcd for C<sub>20</sub>H<sub>31</sub>N<sub>6</sub>F<sub>3</sub>SPt: C, 34.93; H, 4.54; N, 12.22. Found: C, 35.01; H, 4.52; N, 12.74.

## REFERENCES

- (1) Braunstein, P.; Naud, F. *Angew. Chem. Int. Ed.* **2001**, *40*, 680.
- (2) Slone, C. S.; Weinberger, D. A.; Mirkin, C. A. *Progress in Inorganic Chemistry*, Vol 48 **1999**, *48*, 233.
- (3) Zhang, J.; Leitus, G.; Ben-David, Y.; Milstein, D. *J. Am. Chem. Soc.* **2005**, *127*, 10840.
- (4) Fulmer, G. R.; Kaminsky, W.; Kemp, R. A.; Goldberg, K. I. *Organometallics* **2011**, *30*, 1627.
- (5) Lindner, R.; van den Bosch, B.; Lutz, M.; Reek, J.; van der Vlugt, J. I. *Organometallics* **2011**, *30*, 499.
- (6) Dulebohn, J. I.; Haefner, S. C.; Berglund, K. A.; Dunbar, K. R. *Chemistry of Materials* **1992**, *4*, 506.
- (7) Dunbar, K. R.; Haefner, S. C. *Inorg. Chem.* **1992**, *31*, 3676.
- (8) Rogers, C. W.; Wolf, M. O. *Chem. Commun.* **1999**, 2297.
- (9) Kita, M. R.; Miller, A. J. M. *J. Am. Chem. Soc.* **2014**, *136*, 14519.
- (10) Ebeling, G.; Meneghetti, M. R.; Rominger, F. *Organometallics* **2002**, *21*, 3221.
- (11) Spasyuk, D. M.; Zargarian, D.; van der Est, A. *Organometallics* **2009**, *28*, 6531.
- (12) Gagliardo, M.; Selander, N.; Mehendale, N. C.; van Koten, G.; Gebbink, R. J. M. K.; Szabó, K. J. *Chem. Eur. J.* **2008**, *14*, 4800.
- (13) Niu, J. L.; Chen, Q. T.; Hao, X. Q.; Zhao, Q. X.; Gong, J. F.; Song, M. P. *Organometallics* **2010**, *29*, 2148.
- (14) De Angelis, F.; Gambacorta, A.; Nicoletti, R. *Synthesis* **1976**, 798.
- (15) Jameson, D. L.; Castellano, R. K.; Reger, D. L.; Collins, J. E.; Tolman, W. B.; Tokar, C. J. *Inorganic Syntheses*; John Wiley & Sons, Inc.: Hoboken, NJ, USA, 1998; *32*, 51–63.
- (16) Juliá, S.; del Mazo, J. M.; Avila, L. *Organic Preparations and Procedures Int.* **1984**, *5*, 299.
- (17) Reger, D. L.; Collins, J. E.; Jameson, D. L. *Inorganic Syntheses*; John Wiley & Sons, Inc.: Hoboken, NJ, USA, 1998; *32*.

- (18) Byers, P. K.; Canty, A. J. *Organometallics* **1990**, *9*, 210.
- (19) Byers, P. K.; Canty, A. J.; Honeyman, R. T. *J. Organomet. Chem.* **1990**, *385*, 417.
- (20) Byers, P. K.; Canty, A. J.; Honeyman, R. T. *Inorganic Syntheses*; John Wiley & Sons, Inc.: Hoboken, NJ, USA, 2004; 34.
- (21) Canty, A. J.; Honeyman, R. T. *J. Organomet. Chem.* **1990**, *387*, 247.
- (22) Canty, A. J.; Honeyman, R. T.; Skelton, B. W.; White, A. H. *J. Organomet. Chem.* **1990**, *389*, 277.
- (23) Canty, A. J.; Honeyman, R. T.; Skelton, B. W. *J. Chem. Soc. Dalton Trans.* **1992**, 2663.
- (24) Reger, D. L.; Grattan, T. C.; Brown, K. J.; Little, C. A.; Lamba, J.; Rheingold, A. L.; Sommer, R. D. *J. Organomet. Chem.* **2000**, *607*, 120.
- (25) Peterson, L. K.; Kiehlmann, E. *Can. J. Chem.* **1974**, *52*, 2367.
- (26) The, K. I.; Peterson, L. K. *Can. J. Chem.* **1973**, *51*, 422.
- (27) Peterson, L. K.; Kiehlmann, E. *Can. J. Chem.* **1973**, *51*, 2448.
- (28) Rostovtsev, V. V.; Green, L. G.; Fokin, V. V.; Sharpless, K. B. *Angew. Chem. Int. Ed.* **2002**, *41*, 2596.
- (29) Frauhiger, B. E.; White, P. S.; Templeton, J. L. *Organometallics* **2011**, *31*, 225.
- (30) West, N. M.; Reinartz, S.; White, P. S.; Templeton, J. L. *J. Am. Chem. Soc.* **2006**, *128*, 2059.
- (31) MacDonald, M. G.; Kostelansky, C. N.; White, P. S.; Templeton, J. L. *Organometallics* **2006**, *25*, 4560.
- (32) Jensen, M. P.; Wick, D. D.; Reinartz, S.; White, P. S.; Templeton, J. L.; Goldberg, K. I. *J. Am. Chem. Soc.* **2003**, *125*, 8614.
- (33) Frauhiger, B. E.; Templeton, J. L. *Organometallics* **2012**, *31*, 2770.
- (34) van Assema, S. G. A.; Tazelaar, C. G. J.; de Jong, G. B.; van Maarseveen, J. H.; Schakel, M.; Lutz, M.; Spek, A. L.; Slootweg, J. C.; Lammertsma, K. *Organometallics* **2008**, *27*, 3210.
- (35) Hoover, J. M.; Stahl, S. S. *J. Am. Chem. Soc.* **2011**, *133*, 16901.

- (36) Abo-Amer, A.; Puddephatt, R. J. *Inorganic Chemistry Communications* **2011**, *14*, 111.
- (37) Engelman, K. L.; White, P. S.; Templeton, J. L. *Organometallics* **2010**, *29*, 4943.
- (38) Reinartz, S.; Brookhart, M.; Templeton, J. L. *Organometallics* **2001**, *21*, 247.
- (39) Scollard, J. D.; Day, M.; Labinger, J. A.; Bercaw, J. E. *Helvetica Chimica Acta* **2001**, *84*, 3247.
- (40) Bordwell, F. G. *Acc. Chem. Res.* **1988**, *21*, 456.
- (41) Fekl, U.; van Eldik, R.; Lovell, S.; Goldberg, K. I. *Organometallics* **2000**, *19*, 3535.

**Table 5** Crystal data and structural refinement parameters for complex [bpztz<sup>Cy</sup>PtMe<sub>3</sub>][I] (**5-L2**).

---

<b>Empirical formula</b>	C <sub>22</sub> H <sub>36</sub> IN <sub>7</sub> Pt
<b>Formula weight</b>	720.57
<b>Temperature/K</b>	100
<b>Crystal system</b>	triclinic
<b>Space group</b>	P-1
<b>a/Å</b>	10.0223(4)
<b>b/Å</b>	10.4114(4)
<b>c/Å</b>	13.6904(5)
<b>α/°</b>	94.156(2)
<b>β/°</b>	109.859(2)
<b>γ/°</b>	107.026(2)
<b>Volume/Å<sup>3</sup></b>	1261.00(8)
<b>Z</b>	2
<b>ρ<sub>calc</sub>mg/mm<sup>3</sup></b>	1.898
<b>m/mm<sup>-1</sup></b>	20.192
<b>F(000)</b>	696.0
<b>Crystal size/mm<sup>3</sup></b>	0.194 × 0.153 × 0.112
<b>2Θ range for data collection</b>	7 to 133.64°
<b>Index ranges</b>	-11 ≤ h ≤ 11, -12 ≤ k ≤ 11, -16 ≤ l ≤ 16
<b>Reflections collected</b>	21695

<b>Independent reflections</b>	4338[R(int) = 0.0471]
<b>Data/restraints/parameters</b>	4338/0/287
<b>Goodness-of-fit on <math>F^2</math></b>	1.043
<b>Final R indexes [<math>I \geq 2\sigma(I)</math>]</b>	$R_1 = 0.0286, wR_2 = 0.0708$
<b>Final R indexes [all data]</b>	$R_1 = 0.0313, wR_2 = 0.0721$
<b>Largest diff. peak/hole / e Å<sup>-3</sup></b>	1.12/-0.64

**Table 6** Crystal data and structural refinement parameters for complex [bpztz<sup>C6F5</sup>PtMe<sub>3</sub>][I] (**5-L3**).

---

<b>Empirical formula</b>	C <sub>22</sub> H <sub>25</sub> F <sub>5</sub> IN <sub>7</sub> Pt
<b>Formula weight</b>	804.48
<b>Temperature/K</b>	100
<b>Crystal system</b>	monoclinic
<b>Space group</b>	P2 <sub>1</sub> /c
<b>a/Å</b>	15.1356(5)
<b>b/Å</b>	12.7423(5)
<b>c/Å</b>	13.9156(6)
<b>α/°</b>	90.00
<b>β/°</b>	108.392(2)
<b>γ/°</b>	90.00
<b>Volume/Å<sup>3</sup></b>	2546.71(17)
<b>Z</b>	4
<b>ρ<sub>calc</sub>mg/mm<sup>3</sup></b>	2.098
<b>m/mm<sup>-1</sup></b>	20.386
<b>F(000)</b>	1528.0
<b>Crystal size/mm<sup>3</sup></b>	0.335 × 0.135 × 0.092
<b>2Θ range for data collection</b>	6.16 to 139.44°
<b>Index ranges</b>	-18 ≤ h ≤ 18, -15 ≤ k ≤ 15, -16 ≤ l ≤ 12
<b>Reflections collected</b>	28097

<b>Independent reflections</b>	4714[R(int) = 0.0316]
<b>Data/restraints/parameters</b>	4714/0/332
<b>Goodness-of-fit on <math>F^2</math></b>	1.117
<b>Final R indexes [<math>I \geq 2\sigma(I)</math>]</b>	$R_1 = 0.0257, wR_2 = 0.0652$
<b>Final R indexes [all data]</b>	$R_1 = 0.0268, wR_2 = 0.0658$
<b>Largest diff. peak/hole / e Å<sup>-3</sup></b>	1.28/-0.92

**Table 7** Crystal data and structural refinement parameters for complex [POPz<sub>3</sub>PtMe<sub>3</sub>][OTf] (7).

---

<b>Empirical formula</b>	C <sub>31</sub> H <sub>42</sub> N <sub>6</sub> O <sub>4</sub> F <sub>3</sub> PSPt
<b>Formula weight</b>	877.82
<b>Temperature/K</b>	100
<b>Crystal system</b>	orthorhombic
<b>Space group</b>	P2 <sub>1</sub> 2 <sub>1</sub> 2 <sub>1</sub>
<b>a/Å</b>	9.9490(4)
<b>b/Å</b>	17.1179(7)
<b>c/Å</b>	19.9506(8)
<b>α/°</b>	90
<b>β/°</b>	90
<b>γ/°</b>	90
<b>Volume/Å<sup>3</sup></b>	3397.7(2)
<b>Z</b>	4
<b>ρ<sub>calc</sub>g/cm<sup>3</sup></b>	1.716
<b>μ/mm<sup>-1</sup></b>	9.278
<b>F(000)</b>	1752.0
<b>Crystal size/mm<sup>3</sup></b>	0.22 × 0.071 × 0.061
<b>Radiation</b>	CuKα ( $\lambda = 1.54178$ )
<b>2Θ range for data collection/°</b>	6.804 to 148.884
<b>Index ranges</b>	-10 ≤ h ≤ 12, -21 ≤ k ≤ 20, -23 ≤ l ≤ 24

<b>Reflections collected</b>	31914
<b>Independent reflections</b>	6861 [ $R_{\text{int}} = 0.0456$ , $R_{\text{sigma}} = 0.0406$ ]
<b>Data/restraints/parameters</b>	6861/0/433
<b>Goodness-of-fit on <math>F^2</math></b>	1.019
<b>Final R indexes [<math>I &gt;= 2\sigma(I)</math>]</b>	$R_1 = 0.0241$ , $wR_2 = 0.0531$
<b>Final R indexes [all data]</b>	$R_1 = 0.0262$ , $wR_2 = 0.0538$
<b>Largest diff. peak/hole / e Å<sup>-3</sup></b>	0.92/-0.47

**Table 8** Crystal data and structural refinement parameters for complex [TpmPtMe<sub>3</sub>][OTf] (**8**).

---

<b>Empirical formula</b>	C <sub>20</sub> H <sub>31</sub> F <sub>3</sub> N <sub>6</sub> O <sub>3</sub> PtS
<b>Formula weight</b>	687.66
<b>Temperature/K</b>	100
<b>Crystal system</b>	monoclinic
<b>Space group</b>	P2 <sub>1</sub> /n
<b>a/Å</b>	13.6758(9)
<b>b/Å</b>	24.0130(17)
<b>c/Å</b>	23.3289(16)
<b>α/°</b>	90
<b>β/°</b>	98.766(3)
<b>γ/°</b>	90
<b>Volume/Å<sup>3</sup></b>	7571.6(9)
<b>Z</b>	12
<b>ρ<sub>calc</sub>g/cm<sup>3</sup></b>	1.810
<b>μ/mm<sup>-1</sup></b>	11.670
<b>F(000)</b>	4056.0
<b>Crystal size/mm<sup>3</sup></b>	0.231 × 0.196 × 0.1
<b>Radiation</b>	CuKα ( $\lambda = 1.54178$ )
<b>2Θ range for data collection/°</b>	5.314 to 133.56
<b>Index ranges</b>	-16 ≤ h ≤ 16, -29 ≤ k ≤ 26, -26 ≤ l ≤ 28

<b>Reflections collected</b>	141398
<b>Independent reflections</b>	13514 [ $R_{\text{int}} = 0.0312$ , $R_{\text{sigma}} = 0.0143$ ]
<b>Data/restraints/parameters</b>	13514/0/947
<b>Goodness-of-fit on <math>F^2</math></b>	1.081
<b>Final R indexes [<math>I \geq 2\sigma(I)</math>]</b>	$R_1 = 0.0480$ , $wR_2 = 0.1150$
<b>Final R indexes [all data]</b>	$R_1 = 0.0501$ , $wR_2 = 0.1165$
<b>Largest diff. peak/hole / e Å<sup>-3</sup></b>	7.39/-3.91

## CHAPTER THREE

### Cationic Pt(IV) Tp' Carbene<sup>1</sup>

#### 3.1 Introduction

Transition-metal carbene complexes play a crucial role in many stoichiometric and catalytic reactions. A plethora of Pt(0) and Pt(II) carbene compounds have been reported and characterized,<sup>1-11</sup> but despite these numerous examples isolation of Pt(IV) carbenes remains rare.<sup>1,12-24</sup> Such high oxidation state species have been postulated as intermediates in insertion reactions of diazo compounds and in elimination processes from platinumcycloalkanes.<sup>25,26</sup> Additionally, it has been noted that cationic Pt(IV) carbenes represent an unusual subset of carbenes that in some ways lie between traditional Fischer-type complexes of low-oxidation-state late transition metals and Schrock-type carbenes of high-oxidation-state early transition metals.<sup>1</sup>

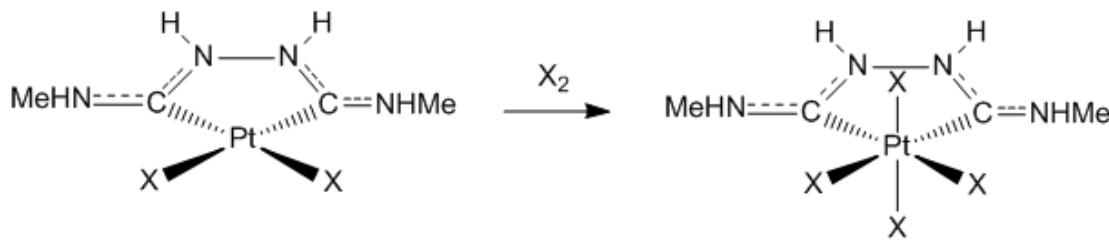
A variety of synthetic strategies and tactics have been employed to access Pt(IV) carbene species. Some of the earliest reports utilized oxidation of Pt(II) carbene complexes using MeX or X<sub>2</sub> reagents to promote oxidative addition and form the corresponding Pt(IV) species (Scheme 1, a). This method has been successful for both simple Pt(II) carbenes<sup>12-14</sup> and for platinum carbene complexes containing ancillary N-heterocyclic carbene ligands.<sup>23,24</sup> Alternatively, the carbene ligand can sometimes be installed during the oxidative addition step by using organic carbene reagents.<sup>1,15,16</sup> For example, Puddephatt and co-workers demonstrated that the addition of chloroiminium

---

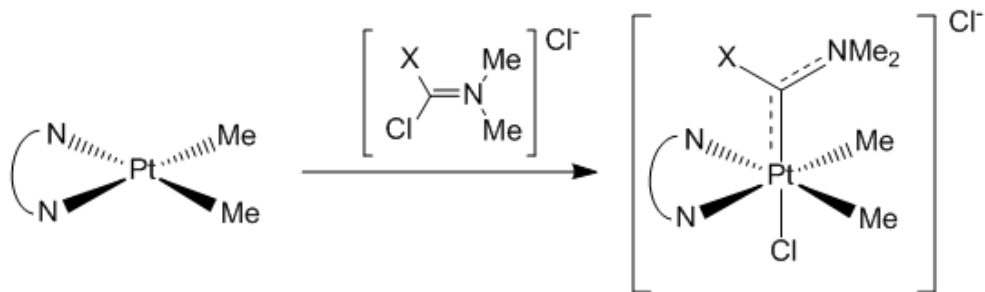
<sup>1</sup> Reproduced with permission from Lavoie, K. D., Frauhiger, B. E., White, P.S., Templeton, J. L., J. of Organomet. Chem. 2015, 793, 182. Copyright 2015 Elsevier B. V.

salts, such as  $[\text{ClXC}=\text{NMe}_2]\text{Cl}$  ( $\text{X} = \text{H}$  or  $\text{Cl}$ ), to  $\text{PtMe}_2(^t\text{Bu}_2\text{bpy})$  generates Pt(IV) carbenes of the type  $(^t\text{Bu}_2\text{bpy})\text{PtClMe}_2(=\text{CXNMe}_2)$  in good yield (Scheme 1, b).<sup>1</sup> Clark et al. have reported the generation of a Pt(IV) carbene through rearrangement of  $\pi$ -alkynol species.<sup>17-19</sup> Intramolecular nucleophilic attack on the alkyne carbon by the pendant alcohol initiates a cyclization and hydride migration sequence that leads to a cationic Pt(IV) alkoxy carbene (Scheme 1, c).<sup>17-19</sup> More recently, Steinborn and co-workers have reported the synthesis of trimethyl Pt(IV) NHC carbene complexes through the substitution of labile acetone ligands.<sup>24</sup>

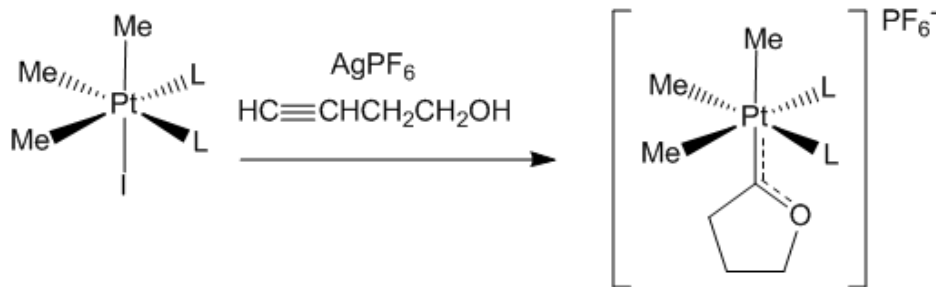
**a. Oxidation of Pt(II) Carbenes**



**b. Oxidative Addition of Organic Carbenes**



**c. Intramolecular Rearrangement of Pt(IV) π-Alkynes**



**Scheme 1** Various synthetic methods toward Pt(IV) carbenes

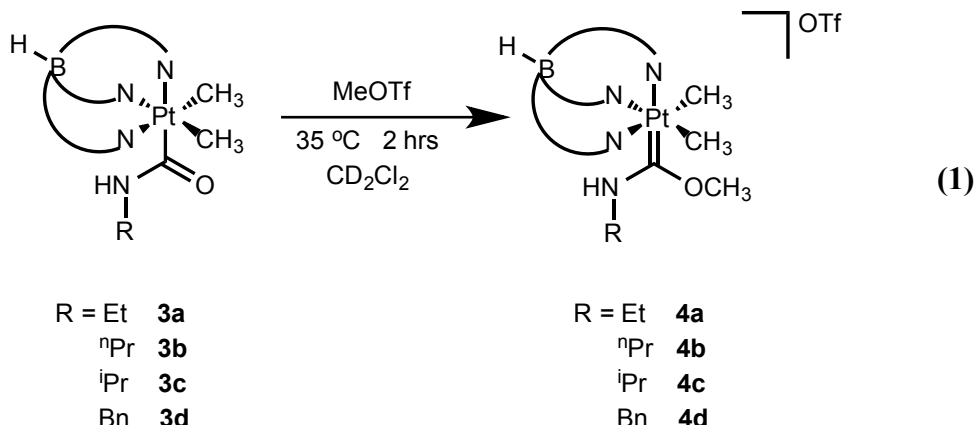
Takahashi and co-workers have reported the synthesis of cationic Pt(IV) aminocarbenes via the addition of nucleophiles to bis(carbene)Pt(II) precursors. We have reported addition of methyl lithium to the isonitrile ligand in  $\text{Tp}'\text{PtMe}(\text{C}\equiv\text{N}-\text{Ar})$  followed by methylation at platinum by methyl iodide to form the Pt(IV) iminoacyl complex  $[\text{Tp}'\text{Pt}(\text{C}(\text{CH}_3)=\text{NAr})\text{Me}_2]^+$  **1** ( $\text{Tp}'$  = hydridotris(3,5-dimethylpyrazolyl)borate).<sup>20</sup>

Subsequent protonation of iminoacyl **1** at nitrogen generates the corresponding resonance-stabilized aminocarbene,  $[Tp'Pt(=C(CH_3)NHR)Me_2]^{+2}$  **2**.

In a study designed to probe mechanistic pathways relevant to a platinum-mediated Water-Gas Shift Reaction, we reported a series of Pt(IV) carboxamido complexes of the type  $Tp'Pt(C(O)NHR)Me_2$  ( $R = Et$  **3a**,  $nPr$  **3b**,  $iPr$  **3c**,  $Bn$  **3d**).<sup>27</sup> Recognizing the structural similarity of these complexes to the iminoacyl species **1**, we sought to access Pt(IV) carbenes by electrophilic addition at the  $\beta$ -heteroatom as utilized by Fischer in the first preparation of isolable metal carbene complexes. Here we report our findings.

### 3.2 Results and Discussion

Paralleling our previous work we sought to mimic chemistry accessible to the iminoacyl ligand using methylating reagents. Treating a solution of ethyl carboxamido complex **3a** with methyl triflate under gentle heating resulted in quantitative conversion to the oxygen-methylated cationic carbene complex  $[Tp'Pt(=C(OMe)NHR)Me_2][OTf]$  **4a** without the need for further purification (eq 1). The 2:1 ratio of  $Tp'$ -H signals in  $^1H$  NMR spectrum is indicative of a  $C_s$  symmetric complex. The methoxy methyl signal resonates as a sharp singlet at 3.1 ppm. In the  $^{13}C$  NMR spectrum, the platinum-bound carbene carbon moves downfield from 150 ppm in the neutral reagent **3a** to 175 ppm in the cationic product **4a** with nearly a 100 Hz increase in one-bond platinum-carbon coupling ( $^1J_{Pt-C}$  goes from 1100 Hz to 1193 Hz). Using the same reaction conditions as above for reagents **3b**, **3c**, and **3d** resulted in formation of the corresponding platinum carbene derivatives.



Slow diffusion of hexanes into a methylene chloride solution of benzyl complex

**4d** at 0 °C resulted in clear, colorless crystals suitable for x-ray crystallography. The x-ray data revealed two rotamers in the crystal lattice, reflecting different orientations of the benzyl group. One rotamer is shown in Figure 1 and selected bond angles and distances are presented in Table 1. The structure of benzyl complex **4d** displays a slightly distorted octahedral geometry at platinum, with typical angles about the metal center (86-96°). The Pt-C<sub>carbene</sub> distance is 2.00 Å and the C<sub>carbene</sub>-N distance is 1.30 Å, decreases of 0.03 Å and 0.06 Å, respectively, from the corresponding values in the solid-state structure of the neutral benzyl carboxamido precursor **3d**.<sup>27</sup> Conversely, the C-O bond to the carbene carbon lengthens by 0.11 Å to 1.33 Å in the methylated product as the C=O is converted to C-O-CH<sub>3</sub>.

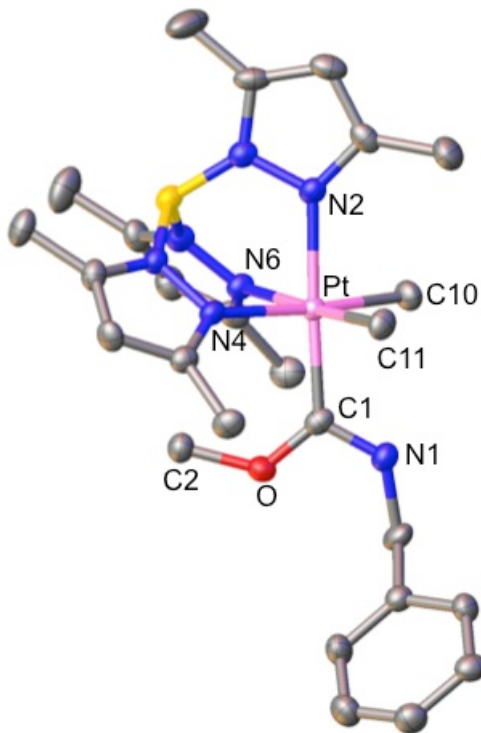


**Figure 1** X-ray structure of  $[Tp'\text{Pt}(=\text{C}(\text{OMe})\text{NHCH}_2\text{Ph})(\text{Me})_2]\text{[OTf]} \mathbf{4d}$ . Ellipsoids are drawn at the 50% probability level. Hydrogen atoms and the triflate counterion are omitted for clarity.

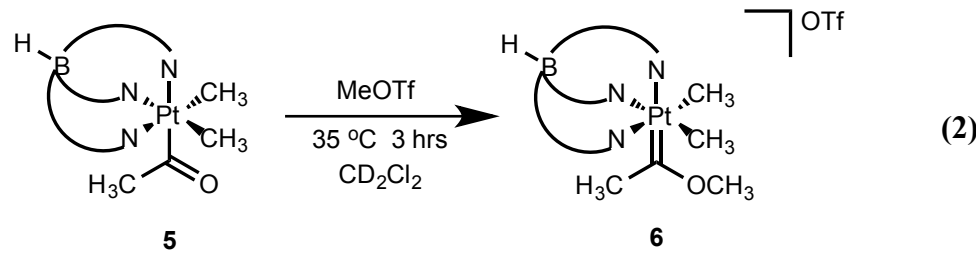
**Table 1** Selected bond distances ( $\text{\AA}$ ) and angles (deg) for complex **4d**.

<u>Bond Lengths</u>			
Pt-C1	1.997(4)	Pt-N2	2.090(3)
Pt-C10	2.081(4)	Pt-N4	2.168(3)
Pt-C11	2.069(4)	Pt-N6	2.175(4)
C1-O	1.327(5)	C1-N1	1.301(5)
<u>Bond Angles</u>			
C1-Pt-C10	88.49(18)	N2-Pt-N4	85.94(13)
Pt-C1-O	127.6(13)	N4-Pt-C1	95.87(16)
O-C1-N1	111.3(4)	Pt-C1-N1	121.1(3)
N6-Pt-C1-O	47.5		

The shortening of both the Pt-C and C-N bonds reflects a resonance-stabilized carbene complex with significant double bond character to both the metal and the

nitrogen. Even after lengthening upon methylation, the bond length of the original C-O linkage is shorter than typical single bonds, suggesting that the carbene is also stabilized by donation from one of the lone pairs on the oxygen. The “CNO” plane of the carbene bisects the two adjacent methyl ligands and the two equatorial pyrazolyl rings with a N6-Pt-C1-O1 torsional angle of 47.5°.

Examining geometrical parameters for complex **4d** showed similarities to parameters for other cationic Pt(IV) carbene complexes.<sup>1,28</sup> The Pt-C<sub>carbene</sub> bond distance of 2.00 Å is significantly shorter than the Pt-C<sub>methyl</sub> distances of 2.08 and 2.07 Å as anticipated for the shift from sp<sup>2</sup> to sp<sup>3</sup> carbons bound to the metal. The Pt-N bond lengths trans to the methyl groups are similar in length (2.17 and 2.18 Å) while the apical Pt-N bond is contracted (2.09 Å) due to the weaker trans influence of the electron deficient platinum carbene bond. Similar bond length variations were observed in the solid state structure of a cationic Pt(IV) carbene complex,



Given the ease with which the carboxamido compounds underwent methylation at oxygen, we turned our attention to the acyl ligand in the dimethyl Pt(IV) acyl complex  $\text{Tp}'\text{Pt}(\text{C(O)Me})\text{Me}_2$  **5**.<sup>29</sup> Methylation of acyl complex **5** under similar conditions to those

used for methylation of complexes **3a-d** proceeded cleanly, but slowly, requiring 24 hours to go to completion. The addition of excess methyl triflate (10 equiv.) assisted in driving the reaction to completion at 35 °C after three hours (eq. 2). As is true for **4a-d**, the carbene product,  $[\text{Tp}'\text{Pt}(=\text{C}(\text{OCH}_3)\text{CH}_3)\text{Me}_2][\text{OTf}]$  **6**, displays a 2:1 ratio for the  $\text{Tp}'\text{-H}$  NMR signals, indicative of a  $C_s$  symmetric complex. The  $^{13}\text{C}$  NMR spectrum showed a significant downfield shift for the carbene carbon relative to the doubly heteroatom stabilized carbene complexes **4a-d**. For the methoxy methyl carbene, the carbene carbon signal resonates at 264 ppm, about 90 ppm further downfield than the aminocarbene complexes. The platinum-carbon coupling constant is 1093 Hz.

In the  $^1\text{H}$  NMR spectrum of **6**, the methoxy methyl signal resonates at 4.8 ppm with four-bond Pt-H coupling of 8 Hz while the carbene methyl signal at 2.9 ppm is noticeably broad at room temperature. The broad signal suggested that a dynamic process was occurring at room temperature and, indeed, as the solution was cooled to 235 K, both the carbene methoxy signal (Figure 2) and the carbene methyl resonance decoalesced into two separate signals in a 3:2 ratio, reflecting the presence of two species in solution. As expected, the low-temperature EXSY spectrum at 220 K displays crosspeaks indicating slow exchange between the two isomers. Presumably two rotamers are present due to hindered rotation around either the Pt-C<sub>carbene</sub> or the O-C<sub>carbene</sub> bond. The activation energy was found to be 13 kcal/mol to interconvert the two isomers on the basis of variable temperature NMR in CD<sub>2</sub>Cl<sub>2</sub> ( $T_c = 263$  K). The relatively large chemical shift difference between the two carbene methyl signals at 220 K (ca. 0.5 ppm) points toward hindered rotation about the Pt-C<sub>carbene</sub> bond since such a rotation would place the methyl group in significantly different environments as a result of proximity to

either the Pt methyl groups or the aromatic pyrazole rings. Unlike **4a-d**, the lack of lone pair donation to the carbene carbon from nitrogen results in greater donation from the platinum center, thus increasing the double bond character of the Pt-C bond and giving rise to a higher energy barrier for rotation. As expected, increasing the temperature resulted in coalescence to produce sharp carbene methoxy methyl and methyl signals that display platinum couplings of 8 and 10.5 Hz, respectively.

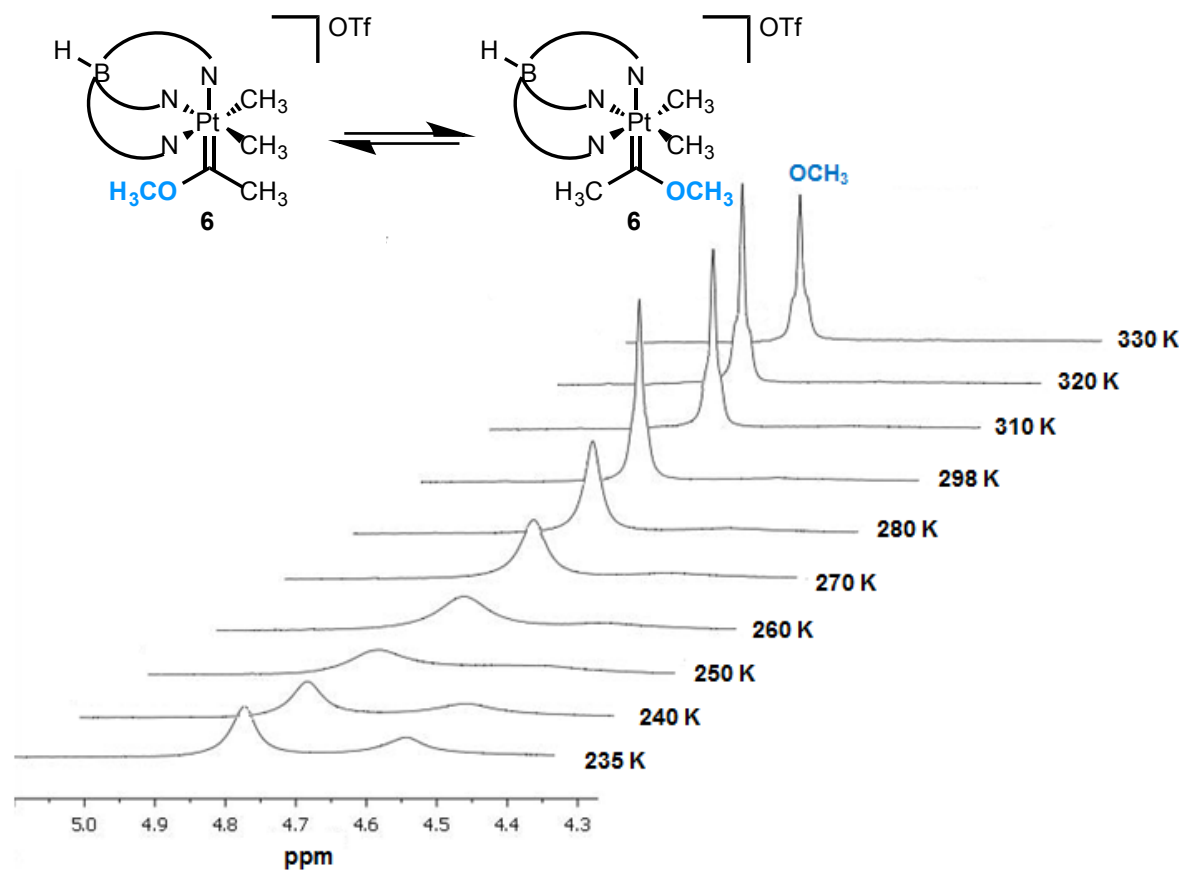


**Figure 2** Variable temperature  $^1\text{H}$  NMR of the methoxy methyl signal in complex **6**.

Diffusion of hexanes into a methylene chloride solution of **6** at 0 °C produced colorless crystals suitable for x-ray crystallography. The solid-state structure of **6** is shown in Figure 3, and selected distances and angles are presented in Table 2. Similar to the solid-state structure of aminocarbene **4d**, methyl methoxy carbene **6** displays the expected slightly distorted octahedral geometry about the metal center. The absence of the resonance stabilizing nitrogen atom in complex **6** has resulted in a shortening of both the O-C<sub>carbene</sub> and Pt-C<sub>carbene</sub> bonds by ca. 0.04 Å relative to the analogous distances in aminocarbene **4d**. The electron-deficient carbene ligand again has a weaker trans-influence than the methyl ligands, with the Pt-N distance trans to the carbene (Pt-N1) being the shortest of the three Pt-N bonds.

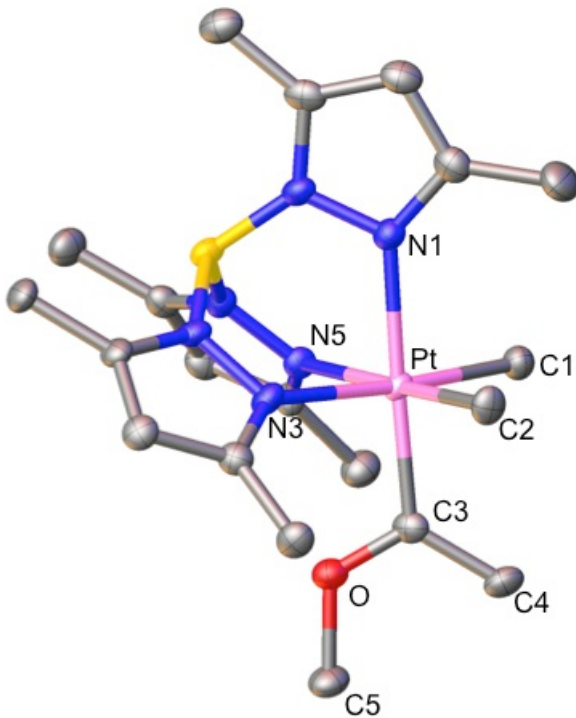
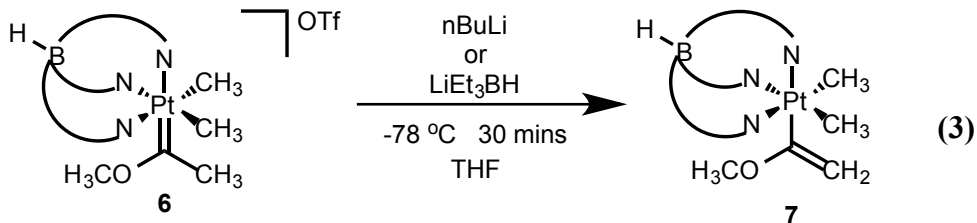


**Figure 3** X-ray structure of  $[\text{Tp}'\text{Pt}(=\text{C}(\text{OCH}_3)\text{CH}_3)\text{Me}_2]\text{[OTf]}$  **6**. Ellipsoids are drawn at the 50% probability level. Hydrogen atoms and the triflate counterion are omitted for clarity.

**Table 2** Selected bond distances ( $\text{\AA}$ ) and angles (deg) for complex **6**.

<u>Bond Lengths</u>			
Pt-C1	2.073(6)	Pt-N1	2.111(4)
Pt-C2	2.070(6)	Pt-N3	2.178(5)
Pt-C3	1.957(5)	Pt-N5	2.165(5)
C3-O1	1.282(7)	C3-C4	1.469(5)
C5-O1	1.477(7)		
<u>Bond Angles</u>			
C1-Pt-C3	89.2(2)	N3-Pt-N5	87.23(17)
Pt-C3-C4	125.2(4)	N5-Pt-C3	94.2(2)
Pt-C3-O1	115.9(4)	C3-O1-C5	121.4(5)
N5-Pt-C3-O	48.2		

Having successfully isolated cationic platinum carbene complexes with two and one heteroatom-stabilizing elements substituents on the carbene carbon, we turned our attention to synthesizing an alkylidene carbene with -H and -CH<sub>3</sub> substituents. In attempts to parallel our previous work, we sought to add an electrophile to the atom beta to the metal center. We hypothesized that the addition of a hydride to the cationic methyl methoxy carbene complex, **6**, would generate a chiral methoxy substituted ethyl ligand. From there, loss of methanol would afford a platinum-vinyl moiety suitable for attempting protonation to form the desired alkylidene. To attempt the synthetic route, a solution of **6** in tetrahydrofuran was cooled to -78 °C and allowed to react with lithium triethylborohydride (LiEt<sub>3</sub>BH). The reaction proceeded cleanly but LiEt<sub>3</sub>BH acted as a base rather than a nucleophile. Deprotonation of the carbene methyl group generated a methoxy substituted vinyl group, **7**, (eq. 3). The behavior of LiEt<sub>3</sub>BH as a base was confirmed when addition of butyl lithium to complex **6** generated the same neutral deprotonated complex.



The  $^1\text{H}$  NMR spectra for **7** shows doublets at 4.32 ppm ( $^2J_{\text{H-H}} = 1.8$  Hz) and 3.57 ppm ( $^2J_{\text{H-H}} = 1.8$  Hz) with  $^3J_{\text{Pt-H}} = 108$  Hz and 43 Hz, respectively, for the vinyl CH<sub>2</sub> group which is consistent with an sp<sup>2</sup> carbon. Vapor diffusion of pentane into a methylene chloride solution of **7** resulted in light yellow crystals suitable for x-ray crystallography, and the geometry of the complex is presented in Figure 4 with important bond lengths and angles listed in Table 3. The structure shows the O-C<sub>methyl</sub> bond of 1.38 Å and the Pt-C<sub>(sp<sup>2</sup>)</sub> bond is 2.00 Å. As anticipated, both of these bonds are elongated from the cationic Pt carbene complex **6**, the precursor to neutral methoxy substituted vinyl complex **7**.

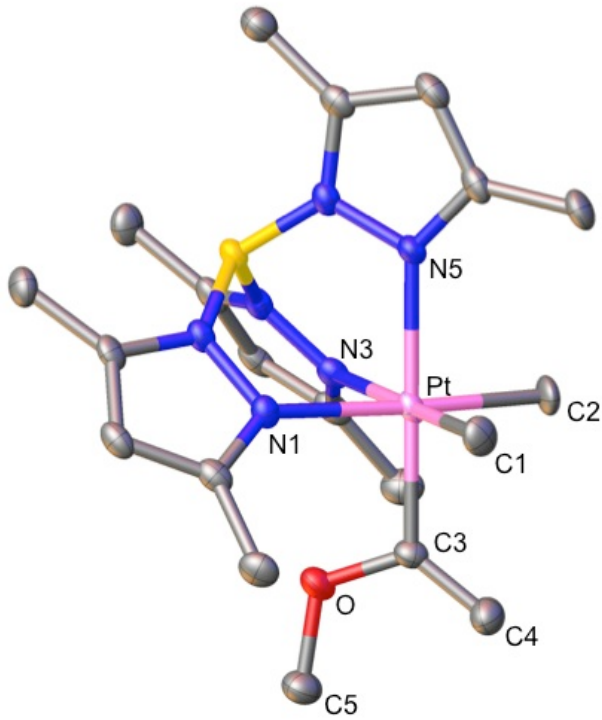


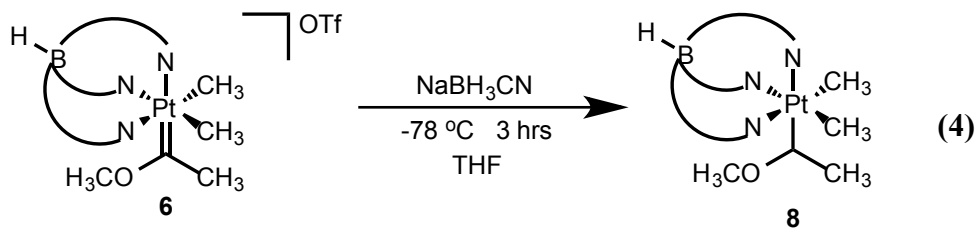
**Figure 4** X-ray structure of  $\text{Tp}'\text{Pt}(\text{C}(\text{OCH}_3)=\text{CH}_2)\text{Me}_2$  **7**. Ellipsoids are drawn at the 50% probability level. Hydrogen atoms are omitted for clarity.

**Table 3** Selected bond distances ( $\text{\AA}$ ) and angles (deg) for complex **7**.

<u>Bond Lengths</u>			
Pt-C1	2.056(6)	Pt-N1	2.165(4)
Pt-C2	2.065(5)	Pt-N3	2.170(5)
Pt-C3	1.998(4)	Pt-N5	2.153(4)
C3-O	1.379(6)	C3-C4	1.329(9)
C5-O	1.417(6)		
<u>Bond Angles</u>			
C1-Pt-C3	88.6(2)	N3-Pt-N5	88.03(15)
Pt-C3-C4	126.6(4)	N3-Pt-C3	92.95(16)
Pt-C3-O	110.0(4)	N5-Pt-C3	178.88(18)
C3-O-C5	117.2(5)	N5-Pt-C3-	106(10)

In order to avoid deprotonation, the methoxy methyl carbene complex **6** was combined with a weaker hydride transfer reagent, sodium cyanoborohydride [Na(BH<sub>3</sub>CN)]. This reaction afforded a mixture of deprotonated product **7** and the desired

hydride addition product,  $[Tp'Pt(C(OCH_3)(H)CH_3)Me_2]$  complex **8**, containing a chiral methoxy substituted ethyl ligand. Performing the reaction at -78 °C gave full conversion to the desired addition product, complex **8** (eq. 4). As expected, hydride addition results in a chiral center at carbon, thus descending to  $C_1$  symmetry as strikingly evident in the  $^1\text{H}$  NMR spectrum of **8** (Figure 5), which displays 3 signals for the aromatic pyrazolyl hydrogens of  $Tp'$  and separate signals for the two diastereotopic methyl groups bound to platinum. At room temperature the  $-OCH_3$  signal appears at 2.89 ppm as a broad singlet. Warming to 313 K results in sharpening of this methoxy methyl resonance. The methyl group bound to the chiral carbon appears as a doublet at 1.01 ppm with  $^3J_{H-H} = 5.5$  Hz and with Pt satellites separated by 35 Hz. The alpha proton is a quartet at 4.73 ppm with  $^3J_{H-H} = 5.5$  Hz and  $^2J_{Pt-H} = 69$  Hz.



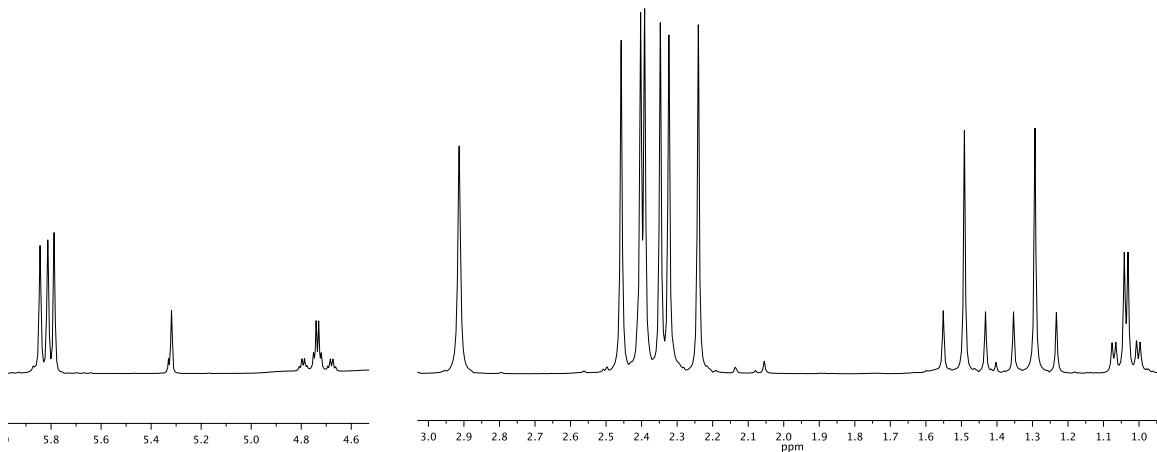
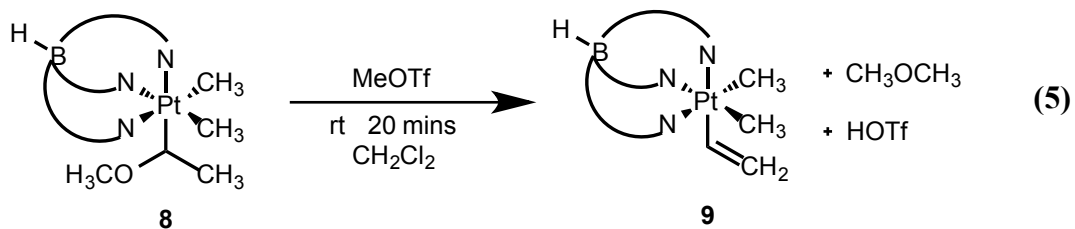


**Figure 5**  $^1\text{H}$  NMR spectrum for  $[\text{Tp}'\text{Pt}(\text{C}^*(\text{OCH}_3)(\text{H})\text{CH}_3)\text{Me}_2]$ , complex **8**, in  $\text{CD}_2\text{Cl}_2$

With the neutral methyl methoxy alkyl group bound to platinum we were able to realize methanol elimination to form the parent vinyl complex. Addition of excess methyl triflate to a solution of **8** results in the formation of  $[\text{Tp}'\text{Pt}(\text{CH}=\text{CH}_2)\text{Me}_2]$ , complex **9**, (eq. 5). Following the reaction via NMR showed the release of dimethyl ether as a byproduct of forming the Pt-vinyl ligand, thus the methoxy group is lost independent of the terminal proton.  $C_s$  symmetry is reestablished, as the chiral center is destroyed, and the plane of the vinyl ligand effectively bisects the two methyl ligands and two equatorial pyrazole ligands on the NMR time scale, as is evident in the  $^1\text{H}$  NMR spectrum by the 2:1 ratio for  $\text{Tp}'\text{-H}$  signals. A classic pattern for the vinyl  $\text{CH}=\text{CH}_2 \text{ H}_A\text{H}_M\text{H}_X$  spin system was observed as three distinct doublets of doublets.



Colorless crystals suitable for x-ray crystallography were obtained by vapor diffusion of hexanes into a methylene chloride solution of **9** at room temperature. The vinyl group had partial occupancy at three different positions due to disorder in the crystal. The predominant vinyl occupancy is presented in Figure 6 and selected bond angles and distances are shown in Table 4.

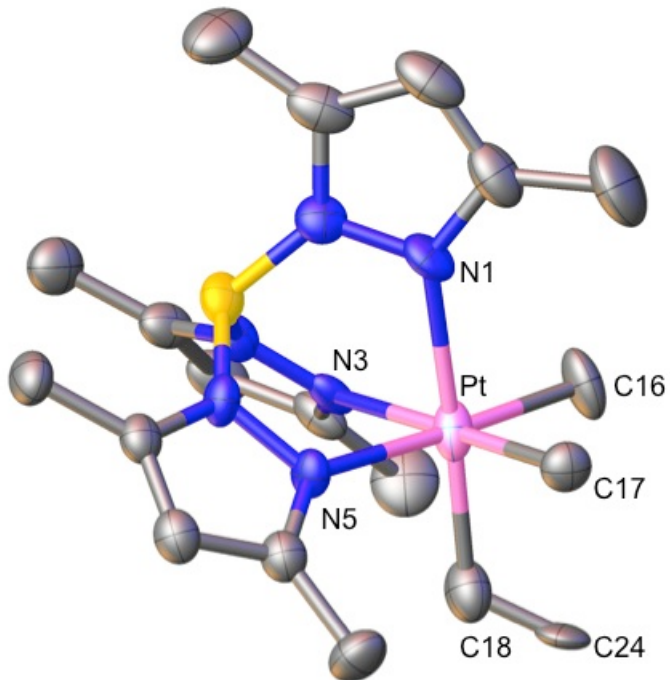


**Figure 6** X-ray structure of  $\text{Tp}'\text{Pt}(\text{CH}=\text{CH}_2)\text{Me}_2$  **9**. Ellipsoids are drawn at the 50% probability level. Hydrogen atoms are omitted for clarity.

**Table 4** Selected bond distances ( $\text{\AA}$ ) and angles (deg) for complex **9**.

<u>Bond Lengths</u>			
Pt-C16	2.047(12)	Pt-N1	2.194(9)
Pt-C17	2.058(12)	Pt-N3	2.172(8)
Pt-C18	2.031(13)	Pt-N5	2.161(8)
C18-C24	1.25(3)		
<u>Bond Angles</u>			
C16-Pt-C18	89.6(5)	N3-Pt-N5	86.5(3)
C17-Pt-C18	89.2(5)	N3-Pt-C18	90.5(4)
Pt-C18-C24	120.2(13)	N5-Pt-C18	92.2(4)
N1-Pt-C18-C24	178(10)		

The double bond to the terminal carbon of the vinyl ligand from complex **9** suggested protonation at the  $\beta$ -site might lead to formation of a  $\text{Pt}=\text{CH}(\text{CH}_3)$  moiety. Addition of  $\text{HB}(\text{Ar}^F)_4 \bullet (\text{Et}_2\text{O})_2$  to a solution of **9** at low temperatures ultimately results in protonation of the  $\text{Tp}'$  ligand at one of the nitrogens along with C-C bond formation to form  $[\kappa^2(\text{Tp}'^{(\text{NH})})\text{Pt}(\text{CH}_3)(\eta^2\text{-CH}_2=\text{CHCH}_3)][\text{B}(\text{Ar}^F)_4]$ , complex **10**. The  $^1\text{H}$  NMR spectrum of cationic Pt(II) propylene complex **10** shows 6 singlets for the aromatic  $\text{Tp}'\text{-H}$  signals, and these arise from two isomers that are present in a 3:2 ratio. The isomers reflect different orientations of the propylene methyl group in the platinum coordination sphere. A barrier of 9 kcal/mol was calculated for propylene rotation on the basis of variable temperature NMR studies in 80%  $\text{D}_{10}$ -ether 20%  $\text{CD}_2\text{Cl}_2$  ( $T_c = 183$  K). We believe the four isomers evident at the lowest temperatures we can access with this NMR solvent mixture reflect the four potential locations of the propene methyl substituent. When olefin rotation is rapid the methyl location in the SW and NE quadrants are exchanged as are the SE and NW quadrant environments, thus producing the “two

isomers" observed at intermediate temperatures. Variable temperature NMR allows us to probe the system further, changing the ratio of different isomers since the ratio is temperature dependent. A Von't Hoff plot allows for the calculation of  $\Delta H^{\circ} = 1.4$  kcal/mol and a  $\Delta S^{\circ} = 7.1$  cal/mol.

Vapor diffusion of hexanes into a methylene chloride solution of **10** at room temperature resulted in colorless crystals suitable for x-ray crystallography. The crystal lattice confirmed that the two isomers were due to different orientations of the propylene methyl group. The predominant rotamer is shown in Figure 7 with selected bond lengths and angles listed in Table 5.

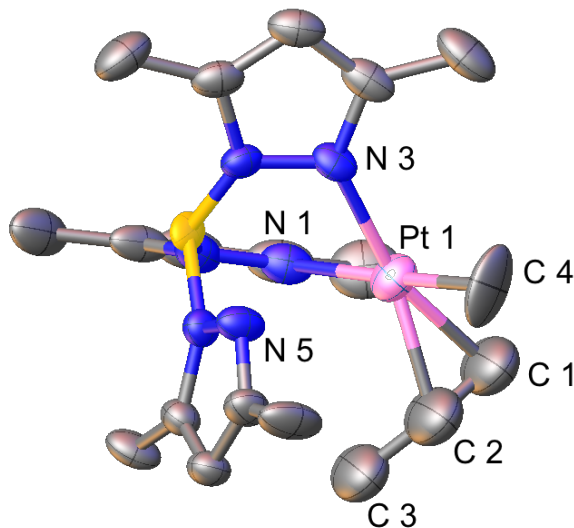
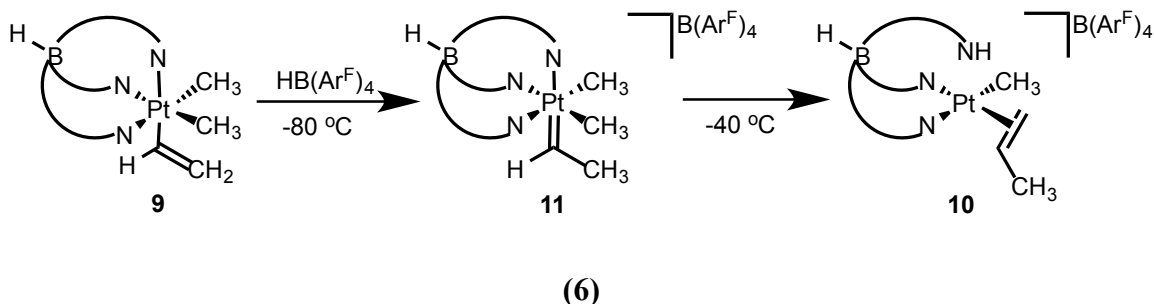


**Figure 7** X-ray structure of  $[\kappa^2(\text{Tp}'^{(\text{NH})})\text{Pt}(\eta^2 \text{CH}_2=\text{CHCH}_3)(\text{Me})][\text{B}(\text{Ar}^{\text{F}})_4]$  **10**. Ellipsoids are drawn at the 50% probability level. Hydrogen atoms and  $\text{B}(\text{Ar}^{\text{F}})_4$  anion are omitted for clarity.

**Table 5** Selected bond distances ( $\text{\AA}$ ) and angles (deg) for complex **10**.

<u>Bond Lengths</u>			
Pt-C1	2.148(10)	Pt-N1	2.124(9)
Pt-C2	2.12(2)	Pt-N3	2.070(5)
Pt-C4	2.071(13)	C2-C3	1.50(4)
C1-C2	1.30(3)		
<u>Bond Angles</u>			
C1-Pt-C4	83.2(6)	N3-Pt-N1	84.1(3)
C2-Pt-C4	82.7(8)	N3-Pt-C1	161.4(5)
C1-Pt-C2	35.5(7)	N1-Pt-C1	102.7(5)
N3-Pt-C1-C2	158.8(15)	C1-C2-C3	122(2)

As shown in equation 6, the beta carbon of the vinyl ligand is protonated by  $\text{HB}(\text{Ar}^F)_4$ , resulting in a cationic Pt(IV) ethylidene complex. This short-lived intermediate can be seen by NMR at temperatures below 233 K. The methyl carbene proton signal appears as a doublet at 2.7 ppm with  ${}^3\text{J}_{\text{H-H}} = 5$  Hz and with  ${}^3\text{J}_{\text{Pt-H}} = 82$  Hz. The methyl methoxy carbene **6** displays a similar shift for the methyl carbene resonance at 2.9 ppm. Direct observation of the carbene proton is challenging by conventional  ${}^1\text{H}$  NMR but in a 1-dimensional COSY spectrum, the carbene methyl doublet at 2.7 ppm couples to a quartet at 6.3 ppm. This small quartet corresponds to the proton directly bound to the carbene carbon.



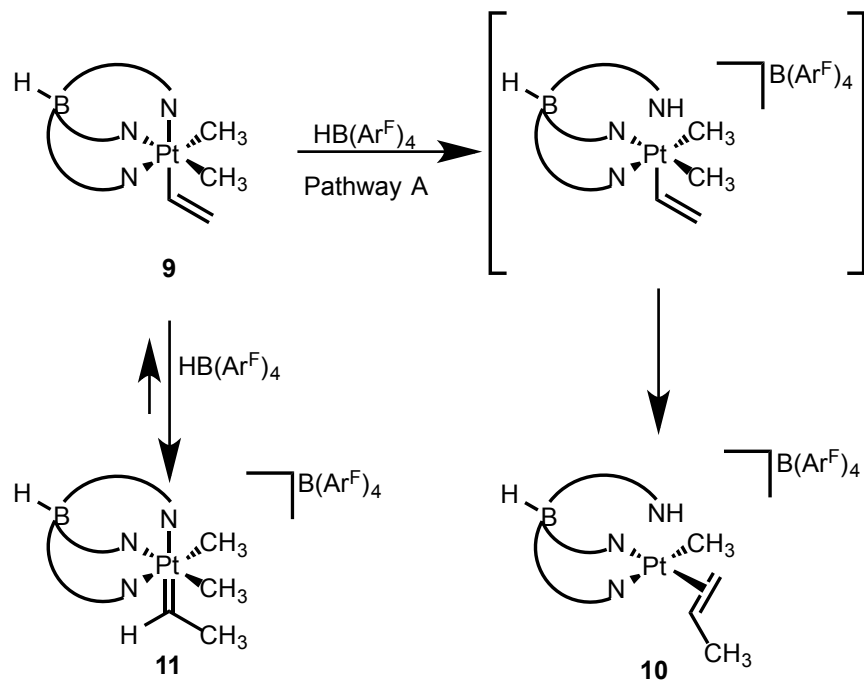
To gain more insight into the ethyldene carbene,  $^{13}\text{C}$  labeling was utilized.

Starting with  $^{13}\text{CO}$  gas allowed us to enrich the  $\alpha$ -carbon of the acyl complex **5** and then sequentially track the  $^{13}\text{C}$  signal of **6**, **8**, and **9**. Looking at complex **9**, the alpha carbon of the vinyl ligand was labeled. Monitoring protonation of the  $^{13}\text{C}$  labeled vinyl group with  $^1\text{H}$  NMR showed the methyl carbene signal appeared as a triplet at 2.7 with  $^3J_{\text{Pt-H}} = 83$  Hz. Literature values for two bond carbon hydrogen coupling constants often fall between 4 and 6 Hz.<sup>30,31</sup> We concluded that the observed signal results from an overlapping doublet of doublets from the splitting to both the proton bound directly to the carbene and the enriched  $^{13}\text{C}_{\text{carbene}}$  carbon. A 1-dimensional COSY spectrum shows the methyl signal is coupled to a doublet (C-13) of quartets ( $J_{\text{H-H}}$ ) assigned to the carbene hydrogen centered at 6.3 ppm with  $^1J_{\text{C-H}} = 165$  Hz, consistent with typical  $\text{sp}^2$   $^1J_{\text{C-H}}$  couplings.<sup>30,32</sup>

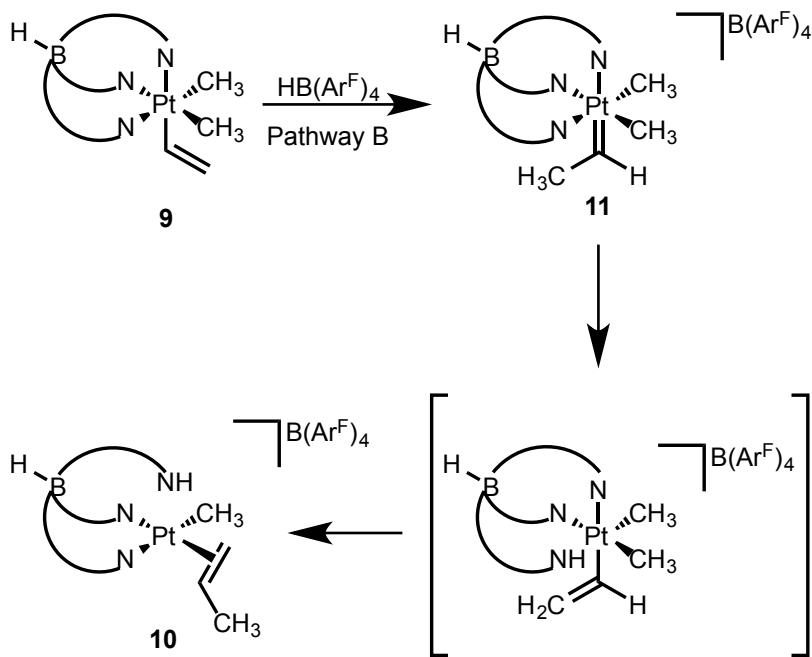
$^{13}\text{C}$  NMR reveals the carbene carbon at 500 ppm, a striking chemical shift value and the most downfield carbene carbon C-13 chemical shift value we have seen. Other metal carbenes have been reported as far downfield as 431 ppm when substituted with electron rich silicon groups.<sup>33</sup> The downfield shift of over 240 ppm from the methyl methoxy carbene (complex **6**) at 264 ppm to the ethyldene Pt(IV) (complex **11**) at 500 ppm implies the Pt(IV) carbene carbon has significant cationic character and the platinum center is weakly back-bonding to the carbene. Note that we are counting the carbene as a neutral, 2-electron donor ligand. Alternatively, the carbene could be considered a doubly anionic carbene which would then result in a formal Pt(VI) oxidation state. The electrophilic and the cationic character of the carbene carbon are compatible with either oxidation state formalism, but we favor the neutral counting formalism for consistency with the  $=\text{C}(\text{X})(\text{Y})$  fragments containing heteroatom donors.

**Scheme 2** Proposed mechanistic pathways for formation of **10**.

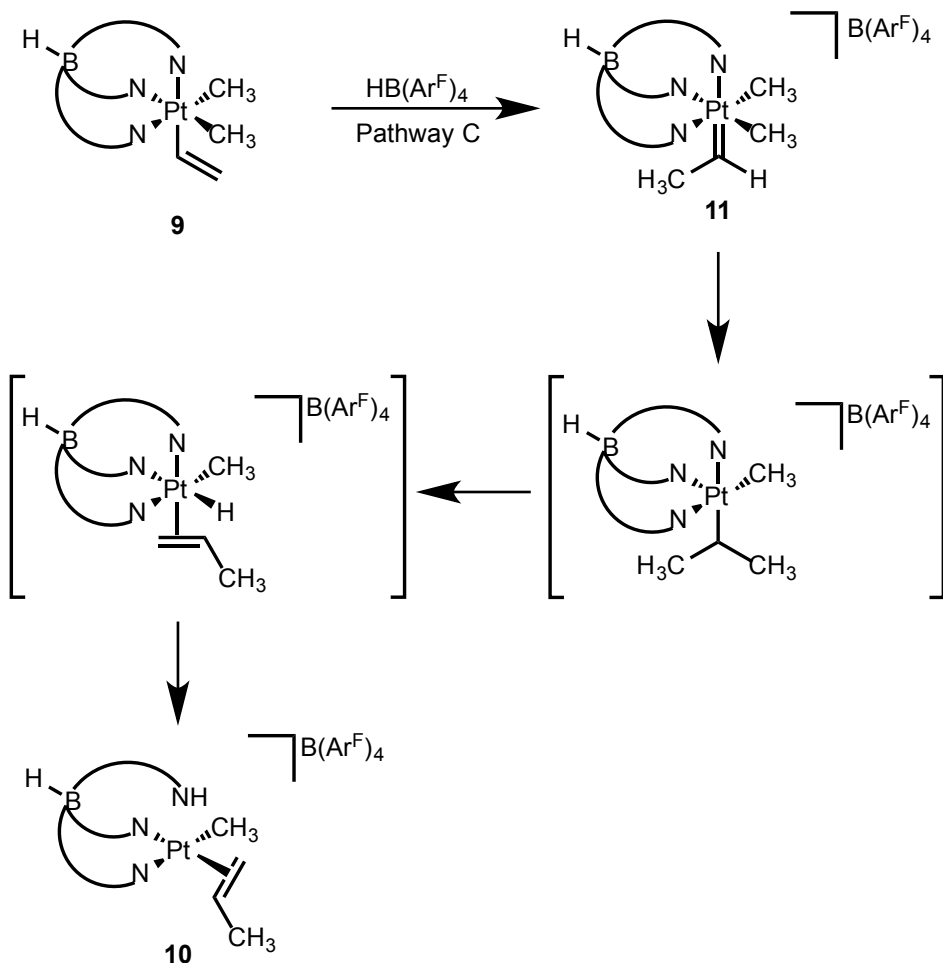
a. Direct Protonation of Pyrazole Arm



**b. Carbene Protonation of Pyrazole Arm**



c. Carbene Migratory Insertion



We have no evidence that the Pt(IV) ethylidene is on the path leading to reductive elimination. There are several plausible reactivity options for the Pt(IV) carbene. One, the protonation reaction could be reversible and regenerate the neutral starting material, scheme 2, a. The cationic carbene complex, once formed, is highly electrophilic and thus the protons on the terminal methyl group are acidic. Once the neutral reagent is reformed, a proton could bind to a pyrazole arm, generating a 5-coordinate Pt(IV) cation poised for reductive elimination and going on to form complex **10**. Alternatively, after formation of

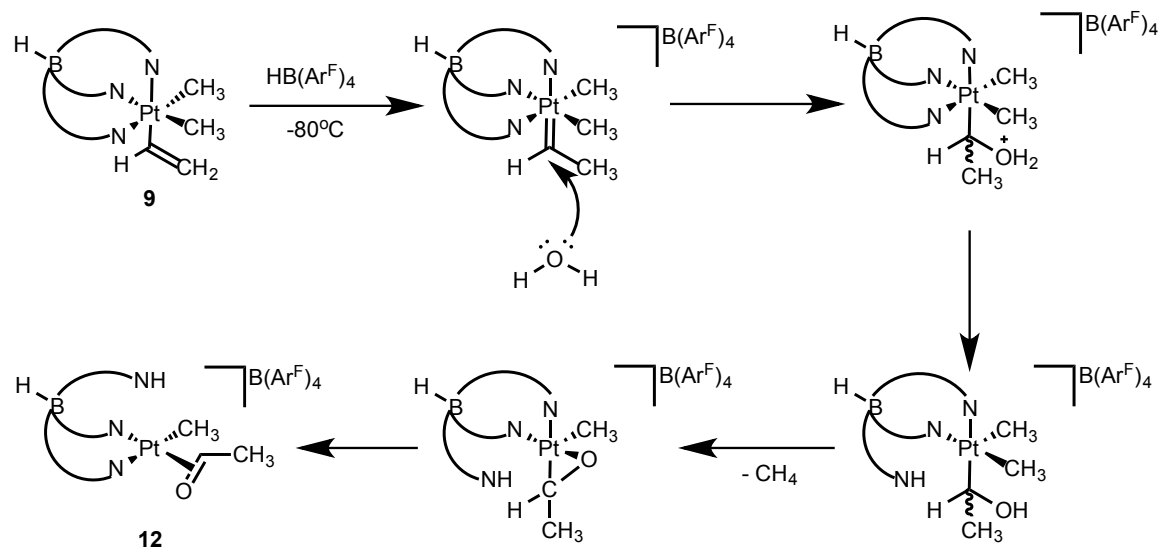
the ethylidene carbene, one of the acidic protons on the terminal carbon could protonate the proximal pyrazole arm directly (scheme 2, b). It would then follow the same reductive coupling path to establish a C-C bond from the vinyl group to an adjacent methyl ligand. Finally, it is conceivable that the propylene forms through the same pathway as the Schrock  $\text{Cp}_2\text{Ta}(\text{CHMe})(\text{Me})$  complex proceeds.<sup>34</sup> It is believed that the ethylidene is inserted into the Pt-Me bond to synthesize an isopropyl ligand. In the Schrock system, beta-hydride elimination generates the propylene ligand. In our system it is conceivable that beta-hydride elimination generates the propylene ligand, then the newly formed hydride reductively eliminates with a pyrazole arm to generate the final product, **10** (scheme 2, c).

Additionally, we studied protonation of the chiral methoxy substituted ethyl complex **8** at low temperatures with  $\text{HB}(\text{Ar}^{\text{F}})_4$ . This resulted in the same propylene adduct, complex **10**. We hypothesize that the  $-\text{OCH}_3$  ligand is protonated, releasing methanol to again form the Pt(IV) carbene. The reaction can then follow any of the mechanisms proposed above to form complex **10** in 68% yield. We believe the protonation of a pyrazole arm followed by reductive elimination, pathway a, is most likely since similar reactivity has been previously reported for Pt(IV) systems.<sup>35</sup>

For completeness, we are reporting the protonation of the vinyl complex **9** at low temperatures, which occurred in several instances under conditions that we later discovered were not dry or air free. Protonation in the presence of water and oxygen resulted in what is proposed to be  $[\kappa^2(\text{Tp}'^{(\text{NH})})\text{Pt}(\eta^2 \text{O}=\text{C}(\text{H})(\text{CH}_3))(\text{Me})][\text{B}(\text{Ar}^{\text{F}})_4]$  complex **12**.  $^1\text{H}$  NMR showed a complex multiplet at 3.8 with 93 Hz coupling. We attribute this to the proton bound to the alpha carbon, coupling to both the methyl group,

which is complicated by free rotation of the aldehyde ligand. Proton corollary shows this peak at 3.8 ppm also correlates to a doublet at 1.19 ppm, consistent with a methyl group.

A proposed mechanism for the formation is shown in Scheme 3. We believe that after the carbene is formed, water attacks the carbon alpha to the metal. The proton on the alcohol ligand would protonate a nitrogen arm, which would generate a 5-coordinate intermediate. Release of methane from a methyl arm would yield a 3-membered ring which would rearrange to generate a cationic Pt(II) aldehyde complex. Further investigations into the formation of this compound were not carried out.



Scheme 3. Proposed mechanism for formation of **12**.

The slow evaporation of a solution of **12** in methylene chloride resulted in clear crystals, suitable for x-ray crystallography. The structure is shown in Figure 8 with selected bond lengths and angles listed in Table 6. The Pt-O distance is 2.17 Å, a reasonable distance for the oxygen to be donating to the platinum center.

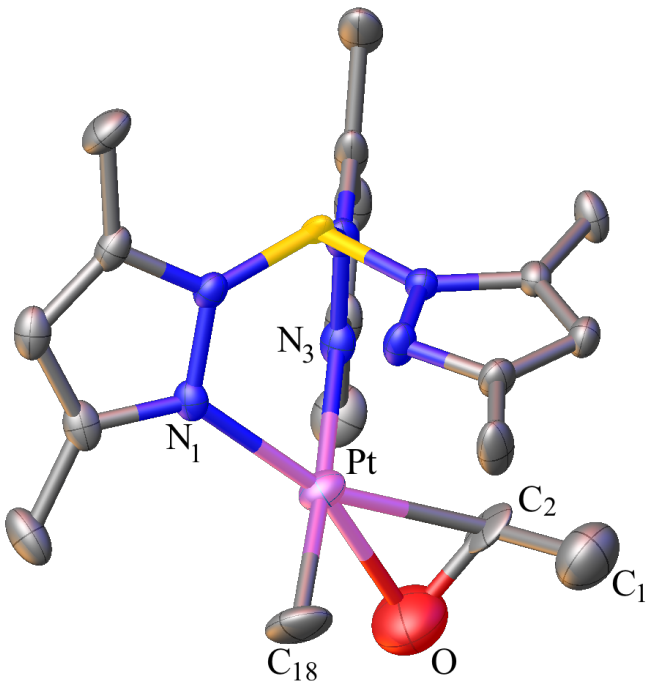


**Figure 8** X-ray structure of  $[\kappa^2(\text{Tp}'^{(\text{NH})})\text{Pt}(\eta^2 \text{O}=\text{C}(\text{H})(\text{CH}_3))(\text{Me})][\text{B}(\text{Ar}^{\text{F}})_4]$  **12**. Ellipsoids are drawn at the 40% probability level. Hydrogen atoms and  $\text{B}(\text{Ar}^{\text{F}})_4$  anion are omitted for clarity.

**Table 6** Selected bond distances ( $\text{\AA}$ ) and angles (deg) for complex **12**.

<u>Bond Lengths</u>			
Pt-C18	2.148(10)	Pt-N1	2.072(4)
Pt-C2	2.071(13)	Pt-N3	2.118(5)
Pt-O	2.174(8)	C1-C2	1.50(4)
O-C2	1.441(10)		
<u>Bond Angles</u>			
C18-Pt-C2	102.7(7)	N1-Pt-N3	84.35(17)
O-Pt-C2	38.6(3)	C18-Pt-N3	175.0(3)
O-C2-C1	115.0(2)	C18-Pt-N1	90.9(3)
C1-C2-Pt	109.0(16)		

## 2.3 Conclusion

In summary, we have prepared a series of cationic Pt(IV) carbenes via electrophilic addition to the beta atom relative to the metal of the Pt(IV) acyl complex. Methylation of the oxygen atom results in a resonance-stabilized carbene. In the methyl methoxy carbene, the absence of the nitrogen atom results in greater Pt-C<sub>carbene</sub> double-bond character, which is reflected by a large rotational barrier. We observed a non-heteroatom stabilized Pt(IV) carbene formed via the protonation of a platinum vinyl group, with <sup>1</sup>H and <sup>13</sup>C NMR. The platinum-vinyl protonation results in C-C bond formation via reductive coupling with an adjacent methyl group at low temperatures.

## 2.4 Experimental Method

All reactions were performed under an atmosphere of dry argon using standard Schlenk and drybox techniques. Argon was purified by passage through columns of BASF R3-11 catalyst and 4 Å molecule sieves. Methylene chloride, hexanes, and pentane were purified under an argon atmosphere and passed through a column packed with activated alumina. All other chemicals were used as received without further purification.

<sup>1</sup>H and <sup>13</sup>C NMR spectra were recorded on Bruker cryoprobe B600 or AV3500 spectrometers. <sup>1</sup>H NMR and <sup>13</sup>C NMR chemical shifts were referenced to residual <sup>1</sup>H and <sup>13</sup>C signals of the deuterated solvents. Elemental analyses were performed by Robertson Microlit Laboratories of Madison, NJ. High-resolution mass spectra were recorded on a Bruker BioTOF II ESI-TOF mass spectrometer. Mass spectral data are reported for the most abundant platinum isotope. Carboxamido complexes **3a-e**<sup>27</sup> and Tp'PtMe<sub>2</sub>(C(O)Me)**5**<sup>29</sup> were prepared following literature procedures.

**General Procedure 4.** A Schlenk flask was charged with the appropriate carboxamido complex **3** (0.05 mmol) and purged with nitrogen. Methylene chloride (10 mL) was added through the septum and the solution was cooled to -78°C. Methyl triflate (1.5 equiv, 0.075 mmol) was added and the reaction was allowed to warm to 35°C and stirred for 2 hrs. The solvent was removed and the resulting oil was triturated with pentane to afford the methylated carbene product **4** as a light yellow powder in quantitative yield.

**[Tp'Pt(=C(OMe)NHCH<sub>2</sub>CH<sub>3</sub>)(CH<sub>3</sub>)<sub>2</sub>] [OTf] (4a).** The general method above was employed using 30 mg (0.05 mmol) of ethyl carboxamido **3a** and 8.5 μL of methyl triflate. <sup>1</sup>H NMR ( $\delta$ , CD<sub>2</sub>Cl<sub>2</sub>, 298 K): 8.93 (bt, 1H, NH), 5.95 (s, 2H, Tp'CH), 5.91 (s, 1H, Tp'CH), 3.65 (q, 2H, NCH<sub>2</sub>CH<sub>3</sub>), 3.09 (s, 3H, OMe), 2.43, 2.09 (s, 6H each, Tp'CH<sub>3</sub>), 2.39, 2.37 (s, 3H each, Tp'CH<sub>3</sub>), 1.79 (s, 6H, Pt-Me,  $^2J_{\text{Pt,H}} = 65$  Hz), 1.28 (t, 3H, NCH<sub>2</sub>CH<sub>3</sub>). <sup>13</sup>C NMR ( $\delta$ , CD<sub>2</sub>Cl<sub>2</sub>, 298 K): 175.4 (Pt=C,  $^1J_{\text{Pt,C}} = 1193$  Hz), 151.3, 150.0, 146.1, 145.4 (Tp'CCH<sub>3</sub>), 121.0 (OTf), 109.5, 108.5 (Tp'CH), 61.3 (OMe,  $^3J_{\text{Pt,C}} = 18$  Hz), 40.4 (NCH<sub>2</sub>CH<sub>3</sub>,  $^3J_{\text{Pt,C}} = 33$  Hz), 13.9 (NCH<sub>2</sub>CH<sub>3</sub>), 13.8, 13.4, 13.0, 12.8 (Tp'CH<sub>3</sub>), -2.7 (Pt-CH<sub>3</sub>,  $^1J_{\text{Pt,C}} = 568$  Hz). IR(CH<sub>2</sub>Cl<sub>2</sub> solution):  $\nu_{\text{B-H}} = 2561$  cm<sup>-1</sup>. HRMS (ESI) *m/z* Calc.: 609.2800 (M<sup>+</sup>). Found: 609.2792. Anal Calcd for C<sub>22</sub>H<sub>37</sub>BF<sub>3</sub>N<sub>7</sub>O<sub>4</sub>PtS: C, 34.84; H, 4.92; N, 12.93. Found: C, 34.60; H, 4.75; N, 12.67.

**[Tp'Pt(=C(OMe)NHCH<sub>2</sub>CH<sub>2</sub>CH<sub>3</sub>)(CH<sub>3</sub>)<sub>2</sub>] [OTf] (4b).** The general method above was employed using 30 mg (0.05 mmol) of *n*-propyl carboxamido **3b** and 8.5 μL of methyl triflate. <sup>1</sup>H NMR ( $\delta$ , CD<sub>2</sub>Cl<sub>2</sub>, 298 K): 8.87 (bt, 1H, NH), 5.96 (s, 2H, Tp'CH), 5.90 (s, 1H, Tp'CH), 3.55 (q, 2H, NCH<sub>2</sub>CH<sub>2</sub>CH<sub>3</sub>), 3.08 (s, 3H, OMe), 2.42, 2.08 (s, 6H each, Tp'CH<sub>3</sub>), 2.38, 2.37 (s, 3H each, Tp'CH<sub>3</sub>), 1.79 (s, 6H, Pt-Me,  $^2J_{\text{Pt,H}} = 65$  Hz), 1.70

(m, 2H, NCH<sub>2</sub>CH<sub>2</sub>CH<sub>3</sub>), 1.00 (t, 3H, NCH<sub>2</sub>CH<sub>2</sub>CH<sub>3</sub>). <sup>13</sup>C NMR ( $\delta$ , CD<sub>2</sub>Cl<sub>2</sub>, 298 K): 175.6 (Pt=C, <sup>1</sup>J<sub>Pt,C</sub> = 1201 Hz), 151.3, 149.9, 146.0, 145.3 (Tp'CCH<sub>3</sub>), 121.0 (OTf), 109.5, 108.4 (Tp'CH), 61.3 (OMe, <sup>3</sup>J<sub>Pt,C</sub> = 18 Hz), 46.9 (NCH<sub>2</sub>CH<sub>2</sub>CH<sub>3</sub>, <sup>3</sup>J<sub>Pt,C</sub> = 33 Hz), 22.2 (NCH<sub>2</sub>CH<sub>2</sub>CH<sub>3</sub>), 13.7, 13.4, 13.0, 12.8 (Tp'CH<sub>3</sub>), 11.4 (NCH<sub>2</sub>CH<sub>2</sub>CH<sub>3</sub>), -2.8 (Pt-CH<sub>3</sub>, <sup>1</sup>J<sub>Pt,C</sub> = 566 Hz). IR(CH<sub>2</sub>Cl<sub>2</sub> solution):  $\nu_{B-H}$  = 2561 cm<sup>-1</sup>. HRMS (ESI) *m/z* Calc.: 623.2957 (M<sup>+</sup>). Found: 623.2948. Anal Calcd for C<sub>23</sub>H<sub>39</sub>BF<sub>3</sub>N<sub>7</sub>O<sub>4</sub>PtS: C, 35.76; H, 5.09; N, 12.69. Found: C, 35.57; H, 4.82; N, 12.67.

**[Tp'Pt(=C(OMe)NHCH(CH<sub>3</sub>)<sub>2</sub>)(CH<sub>3</sub>)<sub>2</sub>][OTf] (4c).** The general method above was employed using 30 mg (0.05 mmol) of isopropyl carboxamido **3c** and 8.5  $\mu$ L of methyl triflate. <sup>1</sup>H NMR ( $\delta$ , CD<sub>2</sub>Cl<sub>2</sub>, 298 K): 8.06 (bd, 1H, NH), 5.95 (s, 2H, Tp'CH), 5.91 (s, 1H, Tp'CH), 4.43 (m, 1H, NCH(CH<sub>3</sub>)<sub>2</sub>), 3.09 (s, 3H, OMe), 2.42, 2.08 (s, 6H each, Tp'CH<sub>3</sub>), 2.38, 2.37 (s, 3H each, Tp'CH<sub>3</sub>), 1.77 (s, 6H, Pt-Me, <sup>2</sup>J<sub>Pt,H</sub> = 64 Hz), 1.36 (m, 6H, NCH(CH<sub>3</sub>)<sub>2</sub>). <sup>13</sup>C NMR ( $\delta$ , CD<sub>2</sub>Cl<sub>2</sub>, 298 K): 175.2 (Pt=C, <sup>1</sup>J<sub>Pt,C</sub> = 1188 Hz), 151.5, 149.8, 146.1, 145.4 (Tp'CCH<sub>3</sub>), 121.0 (OTf), 109.6, 108.5 (Tp'CH), 61.6 (OMe, <sup>3</sup>J<sub>Pt,C</sub> = 18 Hz), 48.1 (NCH(CH<sub>3</sub>)<sub>2</sub>, <sup>3</sup>J<sub>Pt,C</sub> = 32 Hz), 21.2 (NCH(CH<sub>3</sub>)<sub>2</sub>), 13.7, 13.3, 13.0, 12.8 (Tp'CH<sub>3</sub>), -2.5 (Pt-CH<sub>3</sub>, <sup>1</sup>J<sub>Pt,C</sub> = 566 Hz). IR(CH<sub>2</sub>Cl<sub>2</sub> solution):  $\nu_{B-H}$  = 2561 cm<sup>-1</sup>. HRMS (ESI) *m/z* Calc.: 623.2956 (M<sup>+</sup>). Found: 623.2935. Anal Calcd for C<sub>23</sub>H<sub>39</sub>BF<sub>3</sub>N<sub>7</sub>O<sub>4</sub>PtS: C, 35.76; H, 5.09; N, 12.69. Found: C, 35.41; H, 4.65; N, 12.45.

**[Tp'Pt(=C(OMe)NHCH<sub>2</sub>Ph)(CH<sub>3</sub>)<sub>2</sub>][OTf] (4d).** The general method above was employed using 33 mg (0.05 mmol) of benzyl carboxamido **3e** and 8.5  $\mu$ L of methyl triflate. <sup>1</sup>H NMR ( $\delta$ , CD<sub>2</sub>Cl<sub>2</sub>, 298 K): 9.59 (bt, 1H, NH), 7.47, 7.34, 7.29 (m, 5H, Ph), 5.89 (s, 2H, Tp'CH), 5.84 (s, 1H, Tp'CH), 4.65 (d, 2H, CH<sub>2</sub>Ph, <sup>3</sup>J<sub>Pt,H</sub> = 6 Hz), 2.98 (s, 3H, OMe), 2.37, 1.68 (s, 6H each, Tp'CH<sub>3</sub>), 2.35, 2.35 (s, 3H each, Tp'CH<sub>3</sub>), 1.75 (s, 6H, Pt-

Me,  $^2J_{\text{Pt,H}} = 65$  Hz).  $^{13}\text{C}$  NMR ( $\delta$ , CD<sub>2</sub>Cl<sub>2</sub>, 298 K): 176.1 (Pt=C,  $^1J_{\text{Pt,C}} = 1198$  Hz), 151.2, 149.9, 145.9, 145.3 (Tp'CH<sub>3</sub>), 136.4 (*ipso*-Ph), 129.3, 128.9, 128.2 (Ph), 121.0 (OTf), 109.4, 108.2 (Tp'CH), 61.1 (OMe,  $^3J_{\text{Pt,C}} = 18$  Hz), 48.7 (NCH<sub>2</sub>Ph,  $^3J_{\text{Pt,C}} = 36$  Hz), 13.3, 13.1, 12.9, 12.8 (Tp'CH<sub>3</sub>), -2.8 (Pt-CH<sub>3</sub>,  $^1J_{\text{Pt,C}} = 564$  Hz). IR(CH<sub>2</sub>Cl<sub>2</sub> solution):  $\nu_{\text{B-H}} = 2561$  cm<sup>-1</sup>. HRMS (ESI) *m/z* Calc.: 671.2597 (M<sup>+</sup>). Found: 671.2927. Anal Calcd for C<sub>27</sub>H<sub>39</sub>BF<sub>3</sub>N<sub>7</sub>O<sub>4</sub>PtS: C, 39.52; H, 4.79; N, 11.95. Found: C, 39.35; H, 4.87; N, 11.56.

**[Tp'Pt(=C(OMe)CH<sub>3</sub>)(Me)<sub>2</sub>][OTf] (6).** An NMR tube was charged with 30 mg (0.05 mmol) of acyl complex **5** in a glove box. Dry CD<sub>2</sub>Cl<sub>2</sub> (0.5 mL) was added to the tube and a septum was placed on top. Methyl triflate (60  $\mu$ L, 0.50 mmol) was syringed through the septum. The tube was placed in a 35°C bath for 3 hours. Methoxy methyl carbene complex, **6**, was produced in near quantitative conversion by  $^1\text{H}$  NMR. Drying by rotovaporation resulted in 36 mg of a white powder (93.0% yield).  $^1\text{H}$  NMR ( $\delta$ , CD<sub>2</sub>Cl<sub>2</sub>, 298 K): 5.96 (s, 2H, Tp'CH), 5.91 (s, 1H, Tp'CH), 4.88 (s, 3H, OCH<sub>3</sub>,  $^4J_{\text{Pt,H}} = 8$  Hz), 2.90 (s, 3H, carbene CH<sub>3</sub>), 2.43, 1.97 (s, 6H each, Tp'CH<sub>3</sub>), 2.40, 2.38 (s, 3H each, Tp'CH<sub>3</sub>), 1.66 (s, 6H, Pt-Me,  $^2J_{\text{Pt,H}} = 67$  Hz).  $^{13}\text{C}$  NMR ( $\delta$ , CD<sub>2</sub>Cl<sub>2</sub>, 298 K): 264.9 (Pt=C), 151.7, 148.8, 146.0, 145.7 (Tp'CH<sub>3</sub>), 109.8, 108.4 (Tp'CH), 70.1 (OMe), 38.8 (carbene CH<sub>3</sub>), 14.5, 13.6, 13.0, 12.8 (Tp'CH<sub>3</sub>), -2.2 (Pt-CH<sub>3</sub>,  $^1J_{\text{Pt,C}} = 588$  Hz). Anal Calcd for C<sub>22</sub>H<sub>34</sub>BF<sub>3</sub>N<sub>6</sub>O<sub>4</sub>PtS: C, 34.58; H, 4.70; N, 11.52. Found: C, 34.82; H, 4.42; N, 11.86.

**[Tp'Pt(C(OCH<sub>3</sub>)=CH<sub>2</sub>)(Me)<sub>2</sub>] (7).** 0.040g (0.055mmol) of carbene complex **6** was placed in 100ml Schlenk flask under argon. THF (25mL) was added through the septum and the mixture was cooled to -78°C. n-Butyl lithium (0.07mL 0.11mmol) was added through the septum at low temperature and the mixture was allowed to warm to

room temperature. After 20 minutes the reaction was quenched with saturated NH<sub>4</sub>Cl in water and extracted with CH<sub>2</sub>Cl<sub>2</sub>. Drying the organic layer with MgSO<sub>4</sub> followed by filtrating off the solid and removal of the solvent afforded a yellow oil which was chromatographed on alumina with methylene chloride as the elutant. After collection of the elutant and drying by rotovaporation, 23 mg of a white powder were collected (73% yield). <sup>1</sup>H NMR (CD<sub>2</sub>Cl<sub>2</sub>, 298 K, δ) 5.82 (s, 1H, Tp'CH), 5.79 (s, 2H, Tp'CH), 4.32 (d, 1H, C=CH<sub>2</sub>, <sup>2</sup>J<sub>H-H</sub> = 1.8 Hz, <sup>3</sup>J<sub>Pt-H</sub> = 108 Hz), 3.57 (d, 1H, C=CH<sub>2</sub>, <sup>2</sup>J<sub>H-H</sub> = 1.8 Hz, <sup>3</sup>J<sub>Pt-H</sub> = 43 Hz), 3.44 (s, 3H, OCH<sub>3</sub>), 2.38 (s, 3H, Tp'CH<sub>3</sub>), 2.37 (s, 6H, Tp'CH<sub>3</sub>), 2.29 (s, 3H, Tp'CH<sub>3</sub>), 2.14 (s, 6H, Tp'CH<sub>3</sub>), 1.44 (s, 6H, Pt-CH<sub>3</sub>, <sup>2</sup>J<sub>Pt-H</sub> = 74.4 Hz). <sup>13</sup>C NMR (CD<sub>2</sub>Cl<sub>2</sub>, 298 K, δ), 149.8, 149.7, 143.7, 143.3 (Tp'CCH<sub>3</sub>), 149.2 (PtC=CH<sub>2</sub>), 107.8, 106.7 (Tp'CH), 85.4 (C=CH<sub>2</sub>, <sup>2</sup>J<sub>Pt-C</sub> = 97 Hz), 54.8 (OCH<sub>3</sub>, <sup>3</sup>J<sub>Pt-C</sub> = 9 Hz), 12.8, 12.6 (Tp'CH<sub>3</sub>), -6.64 (Pt-C, <sup>1</sup>J<sub>Pt-C</sub> = 659 Hz). Anal Calcd for C<sub>20</sub>H<sub>33</sub>BN<sub>6</sub>OPt: C, 41.46; H, 5.74; N, 14.51. Found: C, 41.21; H, 5.45; N, 14.28.

**[Tp'Pt(C(OCH<sub>3</sub>)(H)CH<sub>3</sub>)(Me)<sub>2</sub>] (8).** 0.040g (0.055mmol) of carbene complex **6** and sodium cyanoborohydride (0.044g, 0.70mmol) were placed in 100ml Schlenk flask under nitrogen, sealed with a septum and cooled to -78°C. Dry THF (25mL) was cooled to -78°C in a separate Schlenk flask and cannula transferred into the original Schlenk tube. The mixture stirred at -78°C for 3 hours. Removal of the solvent through rotary evaporation produced a cloudy white oil. The oil was chromatographed on alumina with methylene chloride as the elutant. After collection of the elutant, solvent was removed and the resulting oil was triturated with pentane to afford a white powder. Yield: 13.9 mg (44%). <sup>1</sup>H NMR (CD<sub>2</sub>Cl<sub>2</sub>, 298 K, δ) 5.85, 5.82, 5.80 (s, 3H each, Tp'CH), 4.75 (q, 1H, PtC-H, <sup>3</sup>J<sub>H-H</sub> = 5.5 Hz, <sup>2</sup>J<sub>Pt-H</sub> = 68.4 Hz), 2.93 (s, 3H, OCH<sub>3</sub>), 2.47, 2.41, 2.40, 2.36, 2.34,

2.25 (s, 3H each, Tp'CH<sub>3</sub>), 1.51 (s, 3H, Pt-CH<sub>3</sub>, <sup>2</sup>J<sub>Pt-H</sub> = 71.2 Hz), 1.32 (s, 3H, Pt-CH<sub>3</sub>, <sup>2</sup>J<sub>Pt-H</sub> = 80.4 Hz), 1.05 (d, 3H, CCH<sub>3</sub>, <sup>3</sup>J<sub>H-H</sub> = 5.5 Hz, <sup>3</sup>J<sub>Pt-H</sub> = 41.2 Hz). <sup>13</sup>C NMR (CD<sub>2</sub>Cl<sub>2</sub>, 298 K, δ), 149.6 149.3, 149.2, 143.8, 143.6, 143.5 (Tp'CCH<sub>3</sub>), 107.7, 107.7, 107.2 (Tp'CH), 59.6 (PtCHCH<sub>3</sub>, <sup>1</sup>J<sub>Pt-C</sub> = 785 Hz), 57.5 (OCH<sub>3</sub>, <sup>3</sup>J<sub>Pt-C</sub> = 6 Hz), 23.2 (PtCHCH<sub>3</sub>), 13.7, 13.4, 12.8, 12.8, 12.5 (Tp'CH<sub>3</sub>), -6.4 (Pt-CH<sub>3</sub>, <sup>1</sup>J<sub>Pt-C</sub> = 745 Hz), -8.3 (Pt-CH<sub>3</sub>, <sup>1</sup>J<sub>Pt-C</sub> = 740 Hz). Anal Calcd for C<sub>20</sub>H<sub>35</sub>BN<sub>6</sub>OPt: C, 41.32; H, 6.07; N, 14.46. Found: C, 41.59; H, 6.04; N, 14.18.

**[Tp'Pt(CH=CH<sub>2</sub>)(Me)<sub>2</sub>] (9).** An NMR tube was charged with 0.100 g (0.17mmol) of complex **8** in a glove box. Dry CD<sub>2</sub>Cl<sub>2</sub> (0.5 mL) and methyl triflate (0.15mL, 1.37mmol) were added to the tube and a septa was placed on top. The reaction sat for 20 minutes. The mixture was chromatographed on alumina with methylene chloride as the elutant. Collection of the elutant resulted in 47 mg of a white powder (50% yield). <sup>1</sup>H NMR (CD<sub>2</sub>Cl<sub>2</sub>, 298 K, δ) 7.00 (dd, 1H, Pt-CH, <sup>3</sup>J<sub>H-Htrans</sub> = 17 Hz, <sup>3</sup>J<sub>H-Hcis</sub> = 9 Hz, <sup>2</sup>J<sub>Pt-H</sub> = 35 Hz), 5.86 (s, 1H, Tp'CH), 5.84 (s, 2H, Tp'CH), 5.47 (dd, 1H vinyl H, <sup>2</sup>J<sub>H-Hgeminal</sub> = 1 Hz, <sup>3</sup>J<sub>H-H</sub> = 9 Hz, <sup>3</sup>J<sub>Pt-H</sub> = 130 Hz), 4.83 (dd, 1H, <sup>3</sup>J<sub>H-H</sub> = 17 Hz, <sup>3</sup>J<sub>Pt-H</sub> = 66 Hz), 2.50 (s, 3H, Tp'CH<sub>3</sub>), 2.42 (s, 6H, Tp'CH<sub>3</sub>), 2.35 (s, 3H, Tp'CH<sub>3</sub>), 2.26 (s, 6H, Tp'CH<sub>3</sub>), 1.40 (s, 6H, Pt-CH<sub>3</sub>, <sup>2</sup>J<sub>Pt-H</sub> = 66 Hz). <sup>13</sup>C NMR (CD<sub>2</sub>Cl<sub>2</sub>, 298 K, δ), 149.9 (1C, Tp'CCH<sub>3</sub>), 149.6 (2C, Tp'CCH<sub>3</sub>), 144.1 (1C, Tp'CCH<sub>3</sub>), 144.0 (2C, Tp'CCH<sub>3</sub>), 126.8 (1C, PtC=C, <sup>1</sup>J<sub>Pt-C</sub> = 870 Hz), 117.8 (1C, PtC=C, <sup>2</sup>J<sub>Pt-C</sub> = 13.5 Hz), 107.6 (1C, Tp'CH), 107.1 (2C, Tp'CH), 12.7 (1C, Tp'CH<sub>3</sub>), 12.4 (2C, Tp'CH<sub>3</sub>), -8.0 (2C, Pt-CH<sub>3</sub>, <sup>1</sup>J<sub>Pt-C</sub> = 676.5) Anal Calcd for C<sub>19</sub>H<sub>31</sub>BN<sub>6</sub>Pt: C, 41.54; H, 5.69; N, 15.30. Found: C, 41.26; H, 5.39; N, 15.03.

**[κ<sup>2</sup>(Tp'<sup>(NH)</sup>)Pt(η<sup>2</sup> CH<sub>2</sub>=CHCH<sub>3</sub>)(Me)][B(Ar<sup>F</sup>)<sub>4</sub>] (10).** An NMR tube was charged with 0.092g (0.09mmol) of HB(Ar<sup>F</sup>)<sub>4</sub> in a glove box. Dry CD<sub>2</sub>Cl<sub>2</sub> (0.3 mL) was added and the tube was sealed. The NMR tube was cooled to -80 °C and a solution of 10mg (0.018mmol) of **9** in 0.3mL of CD<sub>2</sub>Cl<sub>2</sub> was slowly added. The mixture was mixed for 1 min using a thin copper wire. The sample was transported cold (-78 °C) to an NMR probe cooled to -80 °C. After slowly warming to room temperature, the mixture was chromatographed on silica with methylene chloride as the elutant. Collection of the elutant followed by removal of solvent resulted in a light yellow powder. Yield: 10.4mg, 40%. At room temperature, two isomers are observed in a 3:2 ratio. <sup>1</sup>H NMR (CD<sub>2</sub>Cl<sub>2</sub>, 298 K, δ) Major: 10.26 (br s, 1H, Tp'NH), 7.71 (br s, 24H, B(Ar<sup>F</sup>)<sub>4</sub>), 7.56 (s, 12H, B(Ar<sup>F</sup>)<sub>4</sub>), 6.30 (s, 1H, Tp'CH), 6.10 (s, 1H, Tp'CH), 5.92 (s, 1H, Tp'CH), 4.60 (m, 1H, H<sub>2</sub>C=CHCH<sub>3</sub>), 3.93(d, 1H, H<sub>2</sub>C=CHCH<sub>3</sub>, <sup>3</sup>J<sub>H-H</sub> = 14 Hz), 3.67 (d, 1H, H<sub>2</sub>C=CHCH<sub>3</sub>, <sup>3</sup>J<sub>H-H</sub> = 7 Hz), 2.37, 2.36, 2.36, 2.35, 2.32, 2.13 (s, 3H each, Tp'CH<sub>3</sub>), 1.11 (d, 3H, H<sub>2</sub>C=CHCH<sub>3</sub>, <sup>3</sup>J<sub>H-H</sub> = 7 Hz), 0.35 (s, 3H, Pt-CH<sub>3</sub>, <sup>2</sup>J<sub>Pt-H</sub> = 71 Hz). Minor: 10.07 (br s, 1H, Tp' NH), 7.71 (br s, 24H, B(Ar<sup>F</sup>)<sub>4</sub>), 7.56 (s, 12H, B(Ar<sup>F</sup>)<sub>4</sub>), 6.32 (s, 1H, Tp'CH), 6.11 (s, 1H, Tp'CH), 5.93 (s, 1H, Tp'CH), 4.79 (d, 1H, H<sub>2</sub>C=CHCH<sub>3</sub>, <sup>3</sup>J<sub>H-H</sub> = 7 Hz), 4.48 (m, 1H, H<sub>2</sub>C=CHCH<sub>3</sub>), 3.72 (d, 1H, H<sub>2</sub>C=CHCH<sub>3</sub>, <sup>3</sup>J<sub>H-H</sub> = 14 Hz), 2.37, 2.36, 2.35, 2.35, 2.32, 2.12 (s, 3H each, Tp'CH<sub>3</sub>), 1.12 (d, 3H, H<sub>2</sub>C=CHCH<sub>3</sub>, <sup>3</sup>J<sub>H-H</sub> = 7 Hz), 0.35 (s, 3H, Pt-CH<sub>3</sub>, <sup>2</sup>J<sub>Pt-H</sub> = 71 Hz). <sup>13</sup>C NMR (δ, CD<sub>2</sub>Cl<sub>2</sub>, 298 K) Major: 162.2, 161.9, 161.5, 161.2 (B(Ar<sup>F</sup>)<sub>4</sub>), 152.7, 151.2, 149.8, 149.1, 148.5, 148.5 (Tp'CCH<sub>3</sub>), 134.8, 129.2, 129.2, 129.1, 129.1, 129.0, 129.0, 128.9, 128.9, 128.9, 128.8, 128.7, 128.7, 128.7, 128.6, 128.5, 128.5, 128.5, 128.4, 127.3, 125.5, 123.7, 121.9 (B(Ar<sup>F</sup>)<sub>4</sub>), 109.7, 108.9, 108.8 (Tp'CH), 89.9 (CH<sub>2</sub>=CHCH<sub>3</sub>), 68.4 (CH<sub>2</sub>=CHCH<sub>3</sub>), 19.1 (CH<sub>2</sub>=CHCH<sub>3</sub>), 14.7, 14.3, 13.2, 12.9, 12.0,

11.0 ( $\text{Tp}'\text{CH}_3$ ), -14.2 (Pt- $\text{CH}_3$ ).  $^{13}\text{C}$  NMR ( $\delta$ ,  $\text{CD}_2\text{Cl}_2$ , 298 K) Minor: 162.2, 161.9, 161.5, 161.2 ( $\text{B}(\text{Ar}^F)_4$ ), 152.4, 151.6, 150.0, 148.5, 148.0, 147.9 ( $\text{Tp}'\text{CCH}_3$ ), 134.8, 129.2, 129.2, 129.1, 129.1, 129.0, 129.0, 128.9, 128.9, 128.9, 128.8, 128.7, 128.7, 128.7, 128.6, 128.5, 128.5, 128.5, 128.4, 127.3, 125.5, 123.7, 121.9 ( $\text{B}(\text{Ar}^F)_4$ ), 110.3, 109.1, 109.0 ( $\text{Tp}'\text{CH}$ ), 86.2 ( $\text{CH}_2=\text{CHCH}_3$ ), 70.3 ( $\text{CH}_2=\text{CHCH}_3$ ), 18.7( $\text{CH}_2=\text{CHCH}_3$ ), 14.4, 13.1, 13.0, 11.4, 10.9, 10.7 ( $\text{Tp}'\text{CH}_3$ ), -15.6 (Pt- $\text{CH}_3$ ). Anal Calcd for  $\text{C}_{51}\text{H}_{44}\text{B}_2\text{N}_6\text{F}_{24}\text{Pt}$ : C, 43.33; H, 3.14; N, 5.95. Found: C, 43.09; H, 2.87; N, 6.16.

**[ $\text{Tp}'\text{Pt}=\text{CHCH}_3(\text{Me})_2\text{][B}(\text{Ar}^F)_4$ ] (11).** An NMR tube was charged with 0.092g (0.09 mmol) of  $\text{HB}(\text{Ar}^F)_4$  in a glove box. Dry  $\text{CD}_2\text{Cl}_2$  (0.3 mL) was added and the tube was sealed. The NMR tube was cooled to -80 °C and a solution of 0.010g (0.018 mmol) of **9** in 0.3mL of  $\text{CD}_2\text{Cl}_2$  was slowly added. The mixture was mixed for 1 min using a thin copper wire. The sample was transported cold (-78 °C) to an NMR probe cooled to -80 °C and slowly warmed to -45°C. Complex **11** was only formed in situ, roughly 10% yield, with the rest of the metal present as reagent, complex **9**, and product, complex **10**.  $^1\text{H}$  NMR ( $\text{CD}_2\text{Cl}_2$ , 228 K,  $\delta$ ), 2.71 (d, 3H, Pt=CHCH<sub>3</sub>,  $^3J_{\text{H-H}} = 5$  Hz,  $^3J_{\text{Pt-H}} = 82$  Hz) or 2.70 (br, 3H, Pt=<sup>13</sup>CHCH<sub>3</sub>). 1-dimensional COSY, ( $\text{CD}_2\text{Cl}_2$ , 228 K,  $\delta$ ): 6.3 (q, 1H, Pt=CHCH<sub>3</sub>,  $^3J_{\text{H-H}} = 5$  Hz), 2.71 (d, 3H, Pt=CHCH<sub>3</sub>,  $^3J_{\text{H-H}} = 5$  Hz) or 6.3 (dq, 1H, Pt=<sup>13</sup>CHCH<sub>3</sub>,  $^3J_{\text{H-H}} = 5$  Hz,  $^1J_{\text{C-H}} = 164$  Hz), 2.71 (br, 3H, Pt=<sup>13</sup>CHCH<sub>3</sub>).  $^{13}\text{C}$  NMR ( $\text{CD}_2\text{Cl}_2$ , 228 K,  $\delta$ ), 499.8 (1C, Pt=<sup>13</sup>C).

**[ $\kappa^2(\text{Tp}'^{(\text{NH})})\text{Pt}(\text{O=C(H)(CH}_3)(\text{Me})\text{)][B}(\text{Ar}^F)_4$ ] (12).** Complex **12** was synthesized in the same fashion as complex **10** but not under air free conditions. An NMR tube was charged with  $\text{HB}(\text{Ar}^F)_4$  in a glove box. Dry  $\text{CD}_2\text{Cl}_2$  was added and the tube was sealed. The NMR tube was cooled to -80 °C and a solution of **9** in  $\text{CD}_2\text{Cl}_2$  was slowly added.

The mixture was mixed for 1 min using a thin copper wire. The sample was transported cold (-78 °C) to an NMR probe cooled to -80 °C. After slowly warming to room temperature, the mixture was chromatographed on silica with methylene chloride as the elutant. Collection of the elutant followed by removal of solvent resulted in a light yellow powder.  $^1\text{H}$  NMR ( $\text{CD}_2\text{Cl}_2$ , 253 K,  $\delta$ ) 7.71 (br s, 24H,  $\text{B}(\text{Ar}^{\text{F}})_4$ ), 7.56 (s, 12H,  $\text{B}(\text{Ar}^{\text{F}})_4$ ), 5.88 (s, 1H,  $\text{Tp}'\text{CH}$ ), 5.86 (s, 1H,  $\text{Tp}'\text{CH}$ ), 5.60 (s, 1H,  $\text{Tp}'\text{CH}$ ), 3.81 (m, 1H,  $\text{O}=\text{C}(H)(\text{CH}_3)$ ,  $^2J_{\text{Pt-H}} = 90$  Hz), 2.35, 2.34, 2.31, 2.24, 2.21, 2.12 (s, 3H each,  $\text{Tp}'\text{CH}_3$ ), 1.20 (d, 3H,  $\text{O}=\text{C}(H)(\text{CH}_3)$ ,  $^3J_{\text{Pt-H}} = 60$  Hz), 0.37 (s, 3H,  $\text{Pt-CH}_3$ ,  $^2J_{\text{Pt-H}} = 71$  Hz).

## REFERENCES

- (1) Rendina, L. M.; Vittal, J. J.; Puddephatt, R. J. *Organometallics* **1995**, *14*, 1030.
- (2) Silbestri, G. F.; Flores, J. C.; de Jesús, E. *Organometallics* **2012**, *31*, 3355.
- (3) Adhikary, Das, S.; Samanta, T.; Roymahapatra, G.; Loiseau, F.; Jouvenot, D.; Giri, S.; Chattaraj, P. K.; Dinda, J. *New J. Chem.* **2010**, *34*, 1974.
- (4) Chen, C.; Qiu, H.; Chen, W.; Wang, D. *J. Organomet. Chem.* **2008**, *693*, 3273.
- (5) Brissy, D.; Skander, M.; Retailleau, P.; Marinetti, A. *Organometallics* **2007**, *26*, 5782.
- (6) De Bo, G.; Berthon-Gelloz, G.; Tinant, B.; Markó, I. E. *Organometallics* **2006**, *25*, 1881.
- (7) Duin, M. A.; Clement, N. D.; Cavell, K. *J. Chem. Comm.* **2003**, *3*, 400.
- (8) Markó, I. E.; Stérin, S.; Buisine, O.; Mignani, G.; Branlard, P.; Tinant, B.; Declercq, J.-P. *Science* **2002**, *298*, 204.
- (9) Cucciolito, M. E.; Panunzi, A.; Ruffo, F.; Albano, V. G.; Monari, M. *Organometallics* **1999**, *18*, 3482.
- (10) Zhang, S. W.; Motoori, F.; Takahashi, S. *J. Organomet. Chem.* **1999**, *574*, 163.
- (11) Cave, G.; Hallett, A. J.; Errington, W.; Rourke, J. P. *Angew. Chem. Int. Ed.* **1998**, *37*, 3270.
- (12) Balch, A. L. *J. Organomet. Chem.* **1972**, *37*, 19.
- (13) Muir, K. W.; Walker, R.; Chatt, J.; Richards, R. L. *J. Organomet. Chem.* **1973**, *56*, 30.
- (14) Chatt, J.; Richards, R. L.; Royston, G. H. D. *Dalton Trans.* **1976**, *7*, 599.
- (15) Hartshorn, A. J.; Lappert, M. F.; Turner, K. *Dalton Trans.* **1978**, 348.
- (16) Cetinkaya, B.; Lappert, M. F.; Turner, K. *J. Chem. Soc., Chem. Commun.* **1972**, *14*, 851.
- (17) Clark, H. C.; Manzer, L. E. *Inorg. Chem.* **1973**, *12*, 362.
- (18) Chisholm, M. H.; Clark, H. C.; Johns, W. S.; Ward, J. *Inorg. Chem.* **1975**, *14*,

900.

- (19) Chisholm, M. H.; Clark, H. C. *J. Chem. Soc. D* **1971**, *22*, 1484.
- (20) Engelman, K. L.; White, P. S.; Templeton, J. L. *Organometallics* **2010**, *29*, 4943.
- (21) Zhang, S.-W.; Takahashi, S. *Organometallics* **1998**, *17*, 4757.
- (22) Walker, R.; Muir, K. W. *Dalton Trans.* **1975**, *3*, 272.
- (23) Prokopchuk, E. M.; Puddephatt, R. J. *Organometallics* **2002**, *22*, 563.
- (24) Lindner, R.; Wagner, C.; Steinborn, D. *J. Am. Chem. Soc.* **2009**, *131*, 8861.
- (25) McCrindle, R.; McAlees, A. J. *Organometallics* **1993**, *12*, 2445.
- (26) Jennings, P. W.; Johnson, L. L. *Chem. Rev.* **1994**, *94*, 2241.
- (27) Frauhiger, B. E.; Ondisco, M. T.; White, P. S.; Templeton, J. L. *J. Am. Chem. Soc.* **2012**, *134*, 8902.
- (28) Engelman, K. L.; White, P. S.; Templeton, J. L. *Organometallics* **2010**, *29*, 4943.
- (29) Reinartz, S.; Brookhart, M.; Templeton, J. L. *Organometallics* **2001**, *21*, 247.
- (30) Pedersoli, S.; Tormena, C. F.; Santos, dos, F. P.; Contreras, R. H.; Rittner, R. *Journal of Molecular Structure* **2008**, *891*, 508.
- (31) Nyberg, N. T.; Duus, J. Ø.; Sørensen, O. W. *J. Am. Chem. Soc.* **2005**, *127*, 6154.
- (32) Yu, B.; van Ingen, H.; Vivekanandan, S.; Rademacher, C.; Norris, S. E.; Freedberg, D. I. *Journal of Magnetic Resonance* **2012**, *215*, 10.
- (33) Fischer, E. O.; Hollfelder, H.; Friedrich, P.; Kreißl, F. R.; Huttner, G. *Chem. Ber.* **1977**, *110*, 3467.
- (34) Sharp, P. R.; Schrock, R. R. *J. Organomet. Chem.* **1979**, *171*, 43.
- (35) Reinartz, S.; White, P. S.; Brookhart, M.; Templeton, J. L. *Organometallics* **2000**, *19*, 3854.

**Table 7** Crystal data and structural refinement parameters for complex [Tp'Pt(=C(OMe)NHCH<sub>2</sub>Ph)(Me)<sub>2</sub>][OTf] (**4d**).

---

<b>Empirical formula</b>	C <sub>27</sub> H <sub>39</sub> BF <sub>3</sub> N <sub>7</sub> O <sub>4</sub> PtS
<b>Formula weight</b>	820.61
<b>Temperature/K</b>	100
<b>Crystal system</b>	monoclinic
<b>Space group</b>	P2 <sub>1</sub> /n
<b>a/Å</b>	11.5528(3)
<b>b/Å</b>	12.9321(4)
<b>c/Å</b>	21.6844(6)
<b>α/°</b>	90.00
<b>β/°</b>	102.983(2)
<b>γ/°</b>	90.00
<b>Volume/Å<sup>3</sup></b>	3156.87(15)
<b>Z</b>	4
<b>ρ<sub>calc</sub>g/cm<sup>3</sup></b>	1.727
<b>μ/mm<sup>-1</sup></b>	9.476
<b>F(000)</b>	1632
<b>Crystal size/mm<sup>3</sup></b>	0.182 × 0.115 × 0.072
<b>2Θ range for data collection/°</b>	8.02 to 140.04
<b>Index ranges</b>	-13 ≤ h ≤ 14, -15 ≤ k ≤ 13, -26 ≤ l ≤ 22
<b>Reflections collected</b>	17016
<b>Independent reflections</b>	5746[R(int) = 0.0303]

<b>Data/restraints/parameters</b>	5746/31/449
<b>Goodness-of-fit on <math>F^2</math></b>	1.045
<b>Final R indexes [<math>I \geq 2\sigma(I)</math>]</b>	$R_1 = 0.0323, wR_2 = 0.0811$
<b>Final R indexes [all data]</b>	$R_1 = 0.0375, wR_2 = 0.0841$
<b>Largest diff. peak/hole / e Å<sup>-3</sup></b>	2.281/-0.582

**Table 8** Crystal data and structural refinement parameters for complex  $[\text{Tp}'\text{Pt}(\text{=C(OMe)CH}_3)(\text{Me})_2]\text{[OTf]} \textbf{(6)}$ .

---

<b>Empirical formula</b>	C <sub>21</sub> H <sub>34</sub> BF <sub>3</sub> N <sub>6</sub> O <sub>4</sub> PtS
<b>Formula weight</b>	729.50
<b>Temperature/K</b>	100
<b>Crystal system</b>	triclinic
<b>Space group</b>	P-1
<b>a/Å</b>	10.2122(2)
<b>b/Å</b>	11.1220(3)
<b>c/Å</b>	11.9615(3)
<b><math>\alpha/^\circ</math></b>	80.657(2)
<b><math>\beta/^\circ</math></b>	82.450(2)
<b><math>\gamma/^\circ</math></b>	88.041(2)
<b>Volume/Å<sup>3</sup></b>	1328.83(6)
<b>Z</b>	2
<b><math>\rho_{\text{calc}}/\text{g/cm}^3</math></b>	1.823
<b><math>\mu/\text{mm}^{-1}</math></b>	11.148
<b>F(000)</b>	720.0
<b>Crystal size/mm<sup>3</sup></b>	0.161 × 0.066 × 0.056
<b>2Θ range for data collection/°</b>	7.56 to 133.12
<b>Index ranges</b>	-12 ≤ h ≤ 12, -13 ≤ k ≤ 12, -14 ≤ l ≤ 12
<b>Reflections collected</b>	9369
<b>Independent reflections</b>	4437[R(int) = 0.0398]
<b>Data/restraints/parameters</b>	4437/0/344

<b>Goodness-of-fit on <math>F^2</math></b>	1.029
<b>Final R indexes [<math>I \geq 2\sigma(I)</math>]</b>	$R_1 = 0.0349, wR_2 = 0.0833$
<b>Final R indexes [all data]</b>	$R_1 = 0.0405, wR_2 = 0.0863$
<b>Largest diff. peak/hole / e Å<sup>-3</sup></b>	2.42/-0.86

**Table 9** Crystal data and structural refinement parameters for complex [Tp'Pt(C(OCH<sub>3</sub>)=CH<sub>2</sub>)(Me)<sub>2</sub>] (**7**).

---

<b>Empirical formula</b>	C <sub>20</sub> H <sub>33</sub> BN <sub>6</sub> OPt
<b>Formula weight</b>	579.42
<b>Temperature/K</b>	100
<b>Crystal system</b>	monoclinic
<b>Space group</b>	P2 <sub>1</sub> /c
<b>a/Å</b>	10.3548(3)
<b>b/Å</b>	23.6906(7)
<b>c/Å</b>	10.2238(3)
<b>α/°</b>	90
<b>β/°</b>	115.5668(13)
<b>γ/°</b>	90
<b>Volume/Å<sup>3</sup></b>	2262.44(12)
<b>Z</b>	4
<b>ρ<sub>calc</sub>g/cm<sup>3</sup></b>	1.701
<b>μ/mm<sup>-1</sup></b>	11.775
<b>F(000)</b>	1144.0
<b>Crystal size/mm<sup>3</sup></b>	0.177 × 0.165 × 0.05
<b>Radiation</b>	CuKα (λ = 1.54178)
<b>2Θ range for data collection/°</b>	7.462 to 140.27
<b>Index ranges</b>	-12 ≤ h ≤ 12, -28 ≤ k ≤ 28, -12 ≤ l ≤ 12
<b>Reflections collected</b>	22936
<b>Independent reflections</b>	4313[R(int) = 0.0400]

<b>Data/restraints/parameters</b>	4313/0/271
<b>Goodness-of-fit on <math>F^2</math></b>	1.194
<b>Final R indexes [<math>I \geq 2\sigma(I)</math>]</b>	$R_1 = 0.0313, wR_2 = 0.0649$
<b>Final R indexes [all data]</b>	$R_1 = 0.0331, wR_2 = 0.0657$
<b>Largest diff. peak/hole / e Å<sup>-3</sup></b>	2.67/-1.39

**Table 10** Crystal data and structural refinement parameters for complex  $[\text{Tp}'\text{Pt}(\text{CH}=\text{CH}_2)(\text{Me})_2]$  (9).

---

<b>Empirical formula</b>	$\text{C}_{19}\text{H}_{31}\text{BN}_6\text{Pt}$
<b>Formula weight</b>	549.40
<b>Temperature/K</b>	100
<b>Crystal system</b>	monoclinic
<b>Space group</b>	$\text{P}2_1/\text{n}$
<b>a/Å</b>	8.0746(2)
<b>b/Å</b>	13.9475(5)
<b>c/Å</b>	19.2322(6)
<b><math>\alpha/^\circ</math></b>	90
<b><math>\beta/^\circ</math></b>	100.1258(17)
<b><math>\gamma/^\circ</math></b>	90
<b>Volume/Å<sup>3</sup></b>	2132.20(11)
<b>Z</b>	4
<b><math>\rho_{\text{calc}}\text{g/cm}^3</math></b>	1.711
<b><math>\mu/\text{mm}^{-1}</math></b>	12.421
<b>F(000)</b>	1080.0
<b>Crystal size/mm<sup>3</sup></b>	0.25 × 0.25 × 0.1
<b>Radiation</b>	$\text{CuK}\alpha (\lambda = 1.54178)$
<b>2Θ range for data collection/°</b>	4.66 to 140.26
<b>Index ranges</b>	-9 ≤ h ≤ 9, -16 ≤ k ≤ 17, -22 ≤ l ≤ 23
<b>Reflections collected</b>	22936
<b>Independent reflections</b>	4018 [ $\text{R}_{\text{int}} = 0.0481$ , $\text{R}_{\text{sigma}} = 0.0342$ ]

<b>Data/restraints/parameters</b>	4018/20/274
<b>Goodness-of-fit on <math>F^2</math></b>	1.344
<b>Final R indexes [<math>I \geq 2\sigma(I)</math>]</b>	$R_1 = 0.0683, wR_2 = 0.1273$
<b>Final R indexes [all data]</b>	$R_1 = 0.0720, wR_2 = 0.1287$
<b>Largest diff. peak/hole / e Å<sup>-3</sup></b>	2.02/-2.85

**Table 11** Crystal data and structural refinement parameters for complex  $[\kappa^2(\text{Tp}'^{(\text{NH})})\text{Pt}(\eta^2\text{CH}_2=\text{CHCH}_3)(\text{Me})][\text{B}(\text{Ar}^{\text{F}})_4]$  (**10**).

<b>Empirical formula</b>	C <sub>51</sub> H <sub>44</sub> B <sub>2</sub> F <sub>24</sub> N <sub>6</sub> Pt
<b>Formula weight</b>	1413.63
<b>Temperature/K</b>	100
<b>Crystal system</b>	triclinic
<b>Space group</b>	P-1
<b>a/Å</b>	12.9597(5)
<b>b/Å</b>	14.7320(5)
<b>c/Å</b>	18.0702(6)
<b><math>\alpha/^\circ</math></b>	100.802(2)
<b><math>\beta/^\circ</math></b>	90.788(2)
<b><math>\gamma/^\circ</math></b>	123.8524(17)
<b>Volume/Å<sup>3</sup></b>	2784.70(18)
<b>Z</b>	2
<b><math>\rho_{\text{calc}}/\text{g/cm}^3</math></b>	1.686
<b><math>\mu/\text{mm}^{-1}</math></b>	5.824
<b>F(000)</b>	1392.0
<b>Crystal size/mm<sup>3</sup></b>	0.25 × 0.2 × 0.1
<b>Radiation</b>	CuKα ( $\lambda = 1.54178$ )
<b>2Θ range for data collection/°</b>	5.032 to 133.212
<b>Index ranges</b>	-15 ≤ h ≤ 15, -17 ≤ k ≤ 17, -21 ≤ l ≤ 19
<b>Reflections collected</b>	14926
<b>Independent reflections</b>	9568 [R <sub>int</sub> = 0.0291, R <sub>sigma</sub> = 0.0472]

<b>Data/restraints/parameters</b>	9568/208/840
<b>Goodness-of-fit on <math>F^2</math></b>	1.065
<b>Final R indexes [<math>I \geq 2\sigma(I)</math>]</b>	$R_1 = 0.0638, wR_2 = 0.1659$
<b>Final R indexes [all data]</b>	$R_1 = 0.0711, wR_2 = 0.1721$
<b>Largest diff. peak/hole / e Å<sup>-3</sup></b>	2.70/-2.22

**Table 12** Crystal data and structural refinement parameters for complex  $[\kappa^2(\text{Tp}'^{(\text{NH})})\text{Pt}(\eta^2\text{O}=\text{C}(\text{H})(\text{CH}_3))(\text{Me})][\text{B}(\text{Ar}^{\text{F}})_4]$  (**12**).

<b>Empirical formula</b>	C <sub>50</sub> H <sub>43</sub> B <sub>2</sub> F <sub>24</sub> N <sub>6</sub> OPt
<b>Formula weight</b>	1416.16
<b>Temperature/K</b>	100
<b>Crystal system</b>	triclinic
<b>Space group</b>	P-1
<b>a/Å</b>	12.9607(4)
<b>b/Å</b>	13.1166(4)
<b>c/Å</b>	18.0761(6)
<b><math>\alpha/^\circ</math></b>	77.2110(18)
<b><math>\beta/^\circ</math></b>	89.2287(19)
<b><math>\gamma/^\circ</math></b>	68.7195(19)
<b>Volume/Å<sup>3</sup></b>	2784.81(16)
<b>Z</b>	2
<b><math>\rho_{\text{calc}}/\text{g/cm}^3</math></b>	1.689
<b><math>\mu/\text{mm}^{-1}</math></b>	5.839
<b>F(000)</b>	1394.0
<b>Crystal size/mm<sup>3</sup></b>	0.25 × 0.25 × 0.15
<b>Radiation</b>	CuKα ( $\lambda = 1.54178$ )
<b>2Θ range for data collection/°</b>	5.026 to 136.654
<b>Index ranges</b>	-14 ≤ h ≤ 15, -15 ≤ k ≤ 15, -21 ≤ l ≤ 21
<b>Reflections collected</b>	33177

<b>Independent reflections</b>	9857 [R <sub>int</sub> = 0.0512, R <sub>sigma</sub> = 0.0421]
<b>Data/restraints/parameters</b>	9857/884/875
<b>Goodness-of-fit on F<sup>2</sup></b>	1.056
<b>Final R indexes [I&gt;=2σ (I)]</b>	R <sub>1</sub> = 0.0498, wR <sub>2</sub> = 0.1180
<b>Final R indexes [all data]</b>	R <sub>1</sub> = 0.0592, wR <sub>2</sub> = 0.1239
<b>Largest diff. peak/hole / e Å<sup>-3</sup></b>	1.75/-1.80

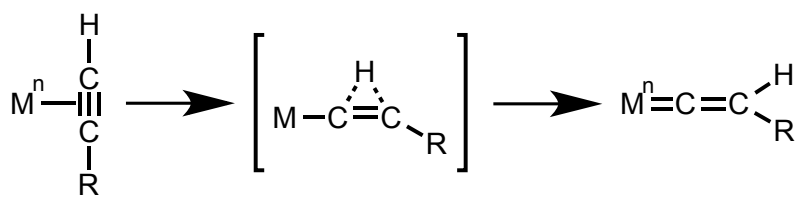
## CHAPTER FOUR

### Investigations into Tp'Pt Vinylidene Complexes

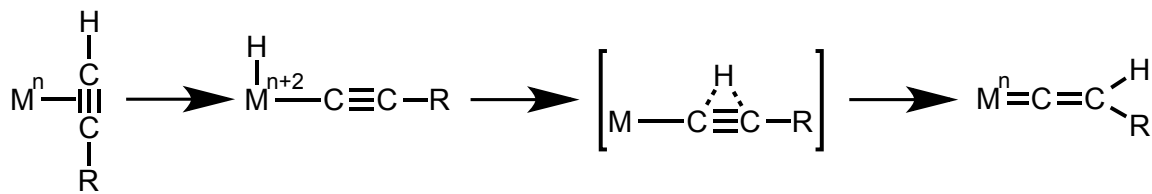
#### 4.1 Introduction

Vinylidene units, :CCR<sub>2</sub>, are unsaturated carbene fragments. Vinylidenes are proposed intermediates for many synthetic transformations and they are the higher energy tautomer of acetylene.<sup>1,2</sup> However, when a transition metal is present, the barrier for interconversion is lowered dramatically, especially if the acetylene is bound to an electron rich metal fragment. Multiple catalysts exploit the different reactivity seen with a M-acetylene ligand versus a M-vinylidene ligand.<sup>3</sup> As a result, intense efforts have been undertaken to reveal the mechanism by which acetylenes tautomerize to a vinylidenes in the presence of a transition metal.

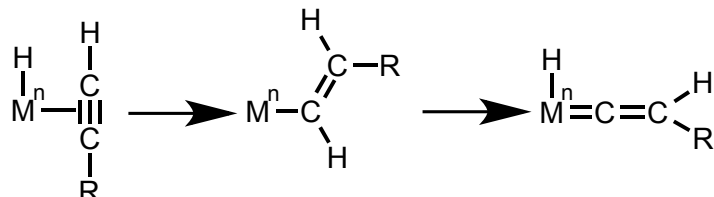
The transformation of acetylene to vinylidene at a metal center occurs in one of four ways. Starting with a M-acetylene, a 1,2-hydrogen atom migration can occur in a concerted mechanism (Scheme 1a).<sup>2,4</sup> Alternatively, if an open coordination site is present, the metal can insert into the terminal C-H bond and undergo a formal oxidation to form a HM(CCR) (alkynyl hydrido complex). A 1,3-hydride migration then generates the M-vinylidene complex, Scheme 1b. A third mechanism requires a M-H ligand in addition to the acetylene. The alkyne inserts into the hydride ligand to from a M-alkenyl intermediate that rearranges to form a M-vinylidene ligand and reestablishes the hydride ligand (Scheme 1c). Add Scheme 1d. Finally, the addition of a base can mediate the acetylene isomerization (Scheme 1d).



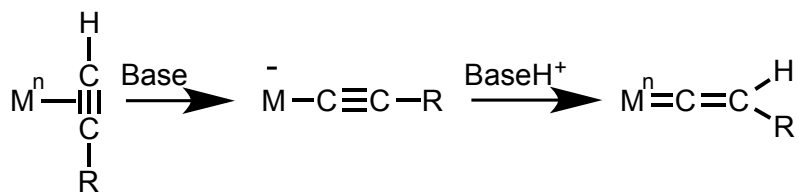
a. 1,2-hydrogen migration



b. 1,3-hydride migration



c. acetylene insertion



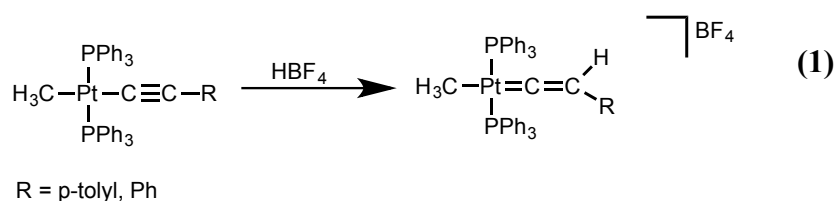
d. base mediated

**Scheme 1** Mechanisms for the isomerization of M-acetylene to M-vinylidene complexes.

There are various examples of late transition metal complexes that, in low oxidation states, have enough electron density to stabilize vinylidene ligands. The complex  $\text{TpOs}(\text{P}^{\text{i}}\text{Pr}_3)\{\kappa^1-\text{C}[\text{NC}_5\text{H}_3\text{Me}]\}\text{(=C=C(H)Ph)}$  ( $\text{Tp}$  = tris(pyrazolyl)borate) is formed from phenyl acetylene displacing acetone and then rearranging to the more

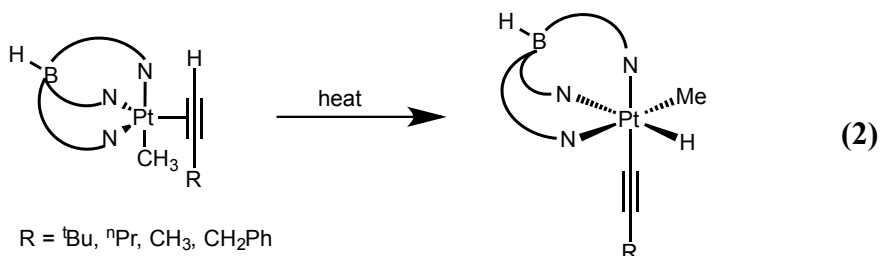
energetically stable vinylidene ligand.<sup>5,6</sup> Under basic conditions the vinylidene ligand is able to insert into the Os-C bond of the pyridyl group to form a new C-C bond. The complex TpRu(PN)(Cl) (PN =  $\kappa^2$ P,N<sup>i</sup>Pr<sub>2</sub>PXPy, X = NH, CH<sub>2</sub>, S) in the presence of an internal alkyne will form a Ru-vinylidene. However, replacing the Tp ligand with cyclopentadienyl results in  $\eta^2$ -binding of the alkyne.<sup>7,8</sup>

It was recently reported that group 7-9 metals are more adept at stabilizing a vinylidene ligand whereas group 10 metals favor the alkyne tautomer.<sup>9</sup> This observation is supported by the lack of published research on platinum vinylidene complexes. While numerous papers propose going through a Pt-vinylidene intermediate, there is only one report of observation of a Pt-vinylidene.<sup>10</sup> Michelin et al. published on the formation and reactivity of trans-[Pt(Me)(C≡CR)(PPh<sub>3</sub>)<sub>2</sub>] (R = *p*-tolyl, Ph), which, when protonated, forms a Pt(II)-vinylidene in situ, eq 1.<sup>11</sup> They followed the reaction by low temperature <sup>1</sup>H NMR, with the proton bound to the carbon beta to the platinum center observed at 3.95 ppm with <sup>3</sup>J<sub>Pt-H</sub> = 42 Hz. Unfortunately they weren't able to observe the vinylidene using C-13 NMR.



Pt alkyne complexes have been reported to facilitate a wide range of transformations. Jones et al. found that the C-C bond of internal alkynes bound to Pt, Pt( $\eta^2$ -R'C≡CR), could be photochemically activated to generate Pt(R')(C≡CR).<sup>12</sup> In a study designed to probe barriers for oxidative addition from d<sup>8</sup> to d<sup>6</sup> platinum, our lab

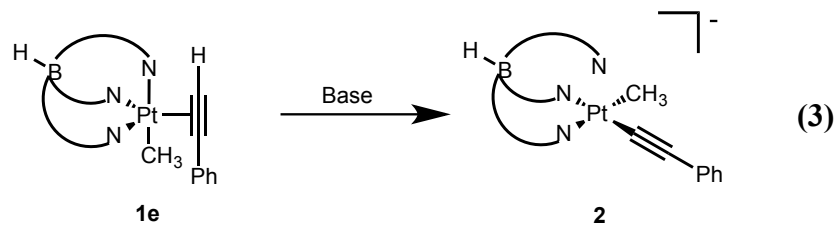
reported a series of  $\text{Tp}'\text{PtMe}(\eta^2\text{-HC}\equiv\text{CR})$  ( $\text{R} = {}^t\text{Bu}$  **1a**,  ${}^n\text{Pr}$  **1b**,  $\text{CH}_3$  **1c**,  $\text{CH}_2\text{Ph}$  **1d**,  $\text{Ph}$  **1e**) ( $\text{Tp}'$  = hydridotris(3,5-dimethylpyrazolyl)borate) complexes.<sup>13</sup> Gentle heating led to oxidative addition to generate  $d^6$ ,  $\text{Tp}'\text{Pt}(\text{Me})(\text{H})(\text{C}\equiv\text{CR})$ , for four of the five complexes, eq 2. Complex **1e** demonstrated no inclination to undergo oxidative addition, presumably due to the less electron rich phenyl substituent of the acetylene fragments investigated.



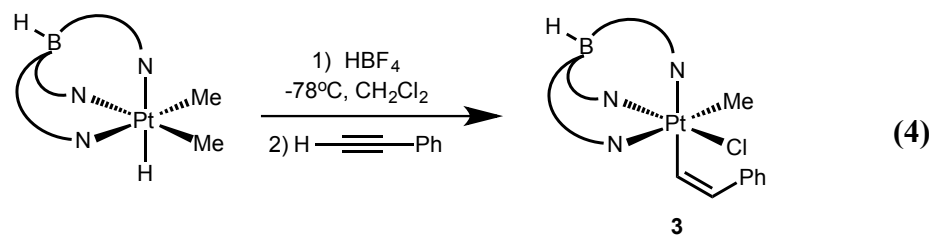
Pt-acetylide complexes seemed promising for the formation of Pt vinylidene complexes. Interested in the formation and isolation of Pt-C<sub>carbene</sub> double bonds, we sought to find another way to synthesize platinum(IV) acetylidyde complexes. We envisioned that similar chemistry could occur with a Pt acetylidyde complex as was seen in chapter 3. Addition of an electrophile to the Pt acetylidyde complex would add at the atom beta to the metal. The Pt center would help stabilize the atom alpha to the metal, resulting in a Pt-vinylidene. We envisioned making the Pt(II) acetylene as previously reported and deprotonating the acetylene unit to yield the Pt(II) acetylidyde anionic complex. Then, addition of acid would form a cationic Pt(II) vinylidene complex. Herein we report our findings.

## 4.2 Results and Discussion

Paralleling our previous work, we sought to mimic chemistry allowing access to Pt carbenes through the addition of an electrophile to a unit of unsaturation. We envisioned deprotonation of **1e** would result in the formation of  $[Tp'Pt(Me)(C\equiv CPh)]^-$  **2**, equation 3.



While attempting to synthesize **1e**, we instead observed the formation of a second product. A solution of  $\text{Tp}'\text{PtMe}_2\text{H}$  was brought to  $-78^\circ\text{C}$ , then phenyl acetylene and  $\text{HBF}_4$  were added sequentially. The reaction was allowed to react at low temperatures for 5 minutes before warming to room temperature. This reaction sequence resulted in the isolation of  $\text{Tp}'\text{PtMeCl}(\text{CH}=\text{C(H)Ph})$  **3**, (eq 4).



The phenylvinyl ligand olefinic protons appear as doublets at 6.95 and 6.49 ppm with 10.5 Hz coupling. They both demonstrate platinum coupling, with  ${}^2J_{\text{Pt-H}} = 51$  Hz and  ${}^3J_{\text{Pt-H}} = 67$  Hz respectively. The chloride ligand pushes the Pt-methyl signal downfield to 2.08 ppm. This is a notable shift compared to most  $\text{Tp}'\text{Pt(IV)}\text{Me}_2$  fragments which commonly appear between 1.20 and 1.50 ppm.<sup>14-16</sup> The C-13 signal for the Pt-methyl signal appears at -3.78 ppm with  ${}^1J_{\text{Pt-C}} = 517$  Hz—around 100 Hz smaller coupling than is seen for analogous complexes with the  $\text{Tp}'\text{Pt(IV)}\text{Me}_2$  fragment.

Intrigued by the new Pt(IV) species, we investigated how this complex was formed. We hypothesized that the Pt(II) acetylene formed *in situ* and then underwent oxidative addition to form  $[\kappa^2(\text{Tp}'^{(\text{NH})})\text{PtCH}_3(\text{H})(\text{C}\equiv\text{CPh})][\text{BF}_4]$ . The protonated pyrazole arm transfers the proton to form the Pt-vinylidene before the hydride adds at the carbon alpha to the metal forming the cis-vinyl ligand, consistent with literature precedent. The resulting Pt center would be electrophilic and able to abstract a  $\text{Cl}^-$  from the solvent (Figure 1).

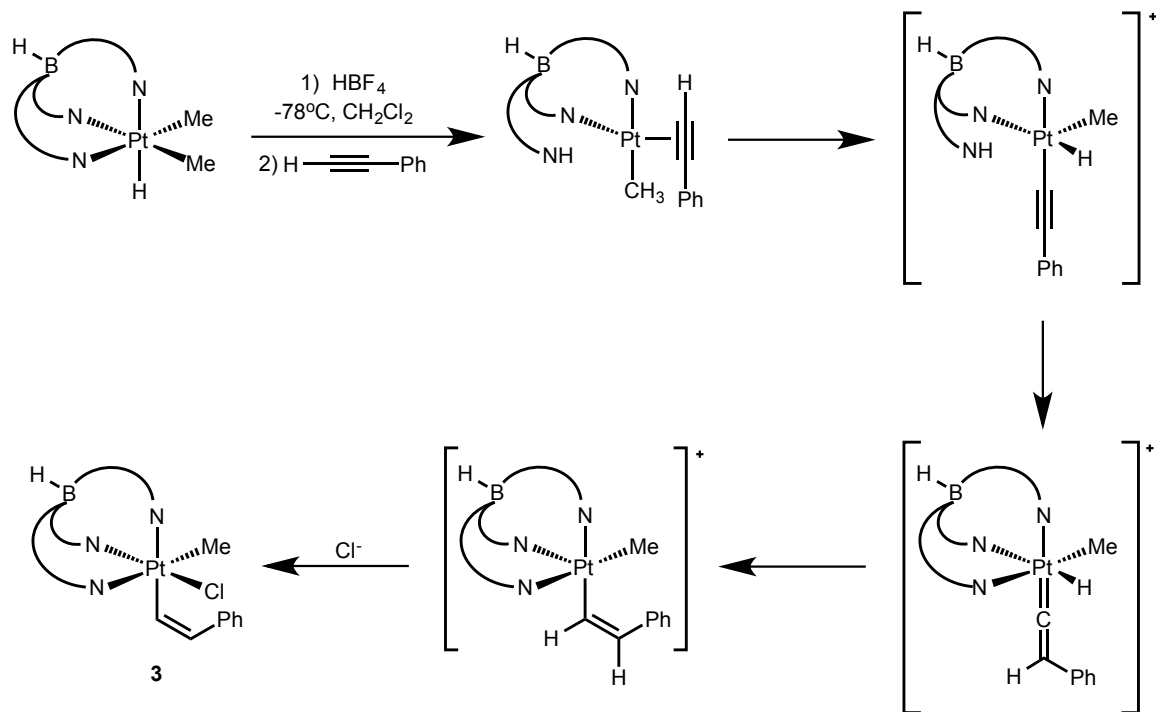


**Figure 1** Proposed mechanism for formation of complex **3**

Finding conditions that allowed isolation of complex **1e** was crucial. Switching to a different solvent, chlorobenzene, allowed isolation of **1e**. Motivated to form an

acetylide ligand, n-butyl lithium was added to **1e** to deprotonate the acetylene ligand.

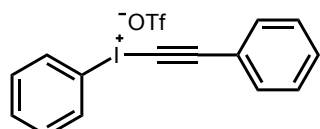
However, the reaction resulted in Pt black, not the desired Pt(II) acetylide complex.

Since the Pt acetylene deprotonation proved problematic

$[Tp'Pt(Me)(phenylacetylide)]^-$  was targeted directly. A solution of phenylene acetylene in dichloromethane was brought to -78 °C and n-Butyl lithium was added slowly to allow for the isolation of lithium phenyl acetylide,  $\text{LiC}\equiv\text{CPh}$ . The addition of tetrafluoroboric acid to  $Tp'PtMe_2\text{H}$  releases methane and forms the  $[(\kappa^2(\text{NH})Tp')\text{PtMe}(\text{solvent})][\text{BF}_4]$ .

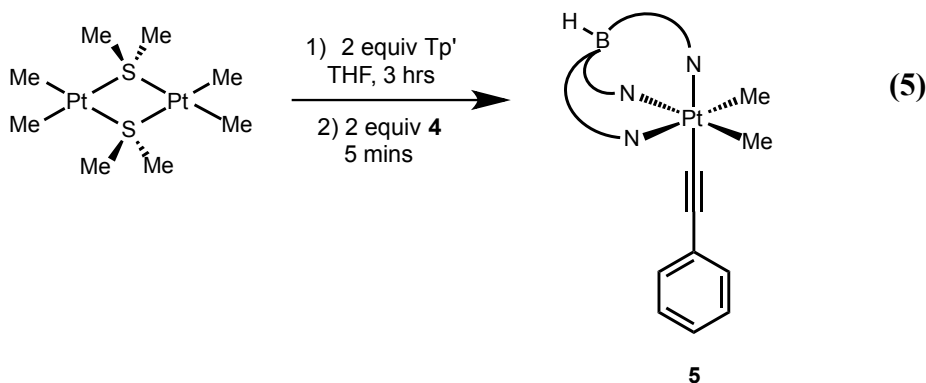
When the reaction was done in acetonitrile, the  $\text{LiCCPh}$  wasn't reactive enough to displace the bound solvent molecule. Repeating the experiment in dichloromethane resulted in platinum black.

Since we were unable to access the desired Pt(II) acetylide, we targeted a Pt(IV) acetylide complex,  $Tp'PtMe_2(\text{C}\equiv\text{CPh})$ . Synthesis of (phenylethynyl)(phenyl)iodonium triflate, **4**, provided a promising cationic acetylide source.<sup>17</sup>



**4**

Metalation of the  $Tp'$  ligand to platinum was achieved by treating one equiv of  $[\text{PtMe}_2(\text{SMe}_2)]_2$  with two equivalents of  $\text{KTp}'$  to generate the  $[\text{K}][\kappa^2-\text{Tp}'\text{PtMe}_2]$ . The addition of the electrophilic reagent **4** oxidatively added the acetylide fragment, allowing for isolation of the desired  $Tp'PtMe_2(\text{C}\equiv\text{CPh})$  complex, **5**; iodobenzene formed as a side product, eq 5. The C-13 NMR spectrum confirmed the formation of the phenyl acetylide ligand, with the carbon alpha to the platinum observed at 69.4 ppm with  ${}^1J_{\text{Pt-C}} = 1370$  Hz. The β-carbon to the metal center is further downfield at 95.4 ppm with  ${}^2J_{\text{Pt-C}} = 296$  Hz.

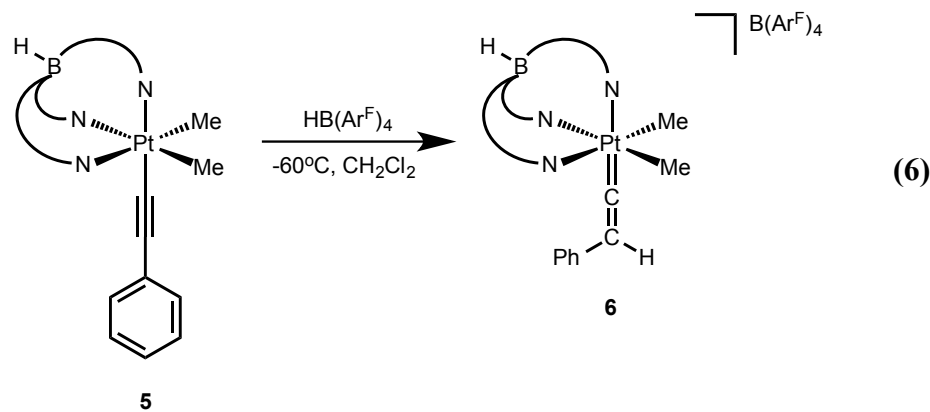


To explore the reactivity of this Pt(IV) acetylidy moiety, a solution of **5** and sodium cyanoborohydride ( $\text{NaBH}_3\text{CN}$ ) was monitored by  $^1\text{H}$  NMR. Letting the mixture stir for 24 hours showed no reactivity. Switching to a stronger hydride reagent, lithium triethylborohydride, also led to no reaction.

Confident that a platinum acetylidy ligand would be electron rich, we sought to investigate the formation of a Pt-vinylidene complex. The addition of a proton to the triple bond of the acetylidy ligand in complex **5** seemed likely to attack at the  $\beta$ -carbon to the metal and formed a  $\text{Pt}=\text{C}=\text{C}(\text{H})(\text{Ph})$  moiety. Addition of  $\text{H}[\text{B}(\text{Ar}^{\text{F}})_4] \bullet (\text{Et}_2\text{O})_2$  to a solution of **5** at low temperatures results in a clean intermediate, but upon warming to room temperature ultimately results in elimination of methane and formation of platinum black and an unidentifiable product in low yield.

To probe the possible formation of a cationic Pt(IV) vinylidene complex, investigations into the low temperature reactivity of **5** with  $\text{H}[\text{B}(\text{Ar}^{\text{F}})_4] \bullet (\text{Et}_2\text{O})_2$  proved informative. As shown in equation 6, the  $\beta$ -carbon of the acetylidy ligand is initially protonated by  $\text{HB}(\text{Ar}^{\text{F}})_4$ , resulting in the desired cationic Pt(IV) vinylidene complex,  $[\text{Tp}'\text{Pt}(=\text{C}=\text{C}(\text{H})(\text{Ph}))(\text{Me})_2][\text{B}(\text{Ar}^{\text{F}})_4]$ , **6**. This intermediate is observable by NMR at 213 K for prolonged periods of time. The proton on the  $\beta$ -carbene of the vinylidene ligand

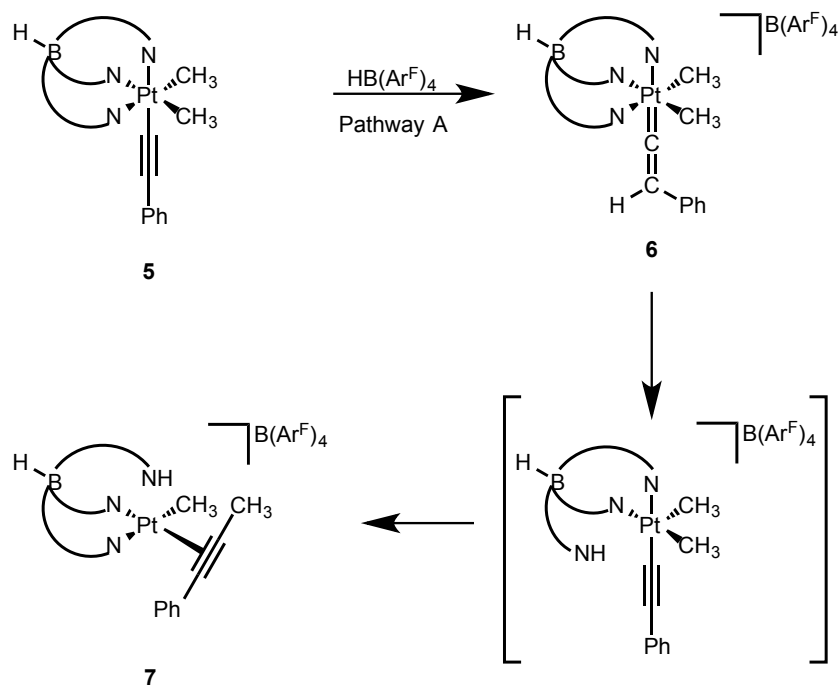
appears as a singlet at 3.03 ppm with  $^3J_{\text{Pt-H}} = 84$  Hz. The C-13 NMR reveals the alpha carbon of the vinylidene moiety at 526 ppm. This is exceedingly low field signal for the carbon alpha to the metal center and is slightly downfield of the cationic Pt(IV) carbene carbon signal which was observed at 500 ppm.<sup>18</sup> This drastic downfield carbon peak indicates the Pt(IV) vinylidene has significant cationic character on the alpha carbon, consistent with the platinum center only weakly donating electrons to stabilize the alpha carbon.



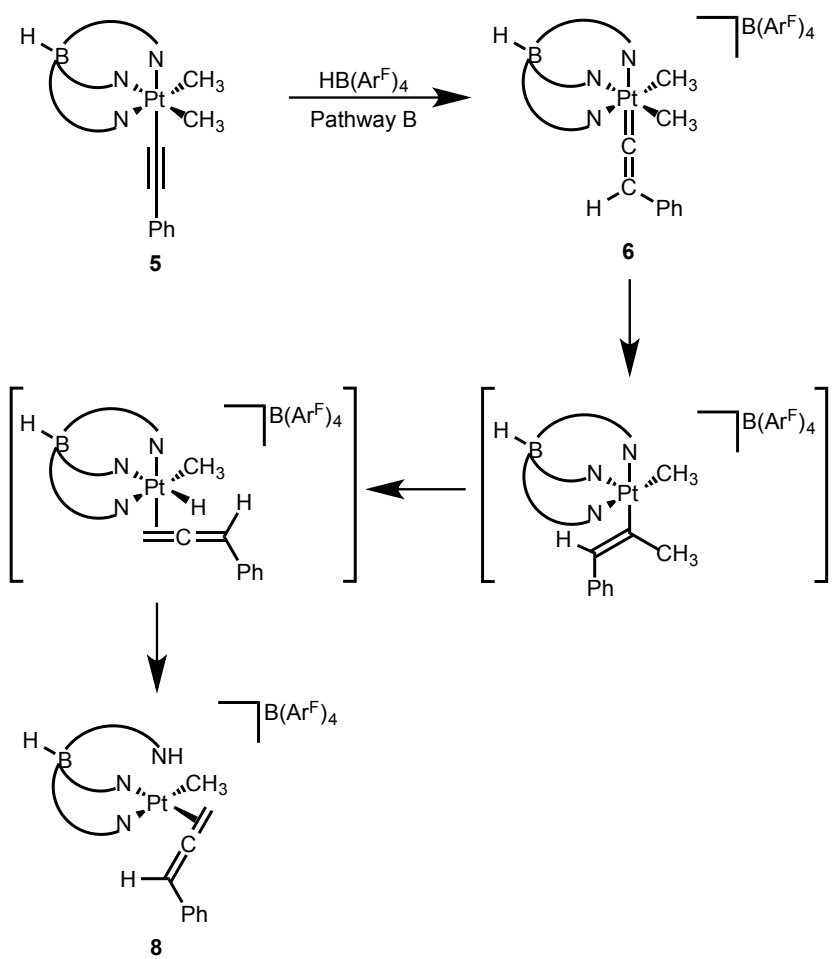
There are several plausible pathways for the cationic Pt(IV) vinylidene complex to react upon warming above 213 K. Once the vinylidene ligand is formed, the proton on the beta carbon is presumably acidic. This proton could protonate the proximal pyrazole arm directly (scheme 2, a). This would generate a 5-coordinate Pt(IV) acetylide cation poised for reductively elimination. Direct C-C bond reductively coupling from the acetylide to an adjacent methyl ligand would generate a d<sup>8</sup> [k<sup>2</sup>(Tp'<sup>(NH)</sup>)PtMe(η<sup>2</sup>-H<sub>3</sub>CC≡CPh)][B(Ar<sup>F</sup>)<sub>4</sub>] 7. Alternatively, the vinylidene ligand could insert into a Pt-methyl bond to form a vinyl ligand. The vinyl ligand is capable of beta hydride elimination to form a Pt-hydride, which would reductively eliminate with a pyrazolyl arm

to generate the final product,  $[\kappa^2(\text{Tp}'^{(\text{NH})})\text{PtMe}(\eta^2\text{-H}_2\text{C}=\text{CPh})] [\text{B}(\text{Ar}^{\text{F}})_4]$  **8**. A third option would involve the isomerization of the vinylidene unit to phenyl acetylene (scheme 2, c). Once formed, the Pt(IV) wouldn't be able to donate enough electron density for the phenyl acetylene to stay in the coordination sphere. Instead it would result in unstable 5-coordinate  $d^6$  cationic complex.

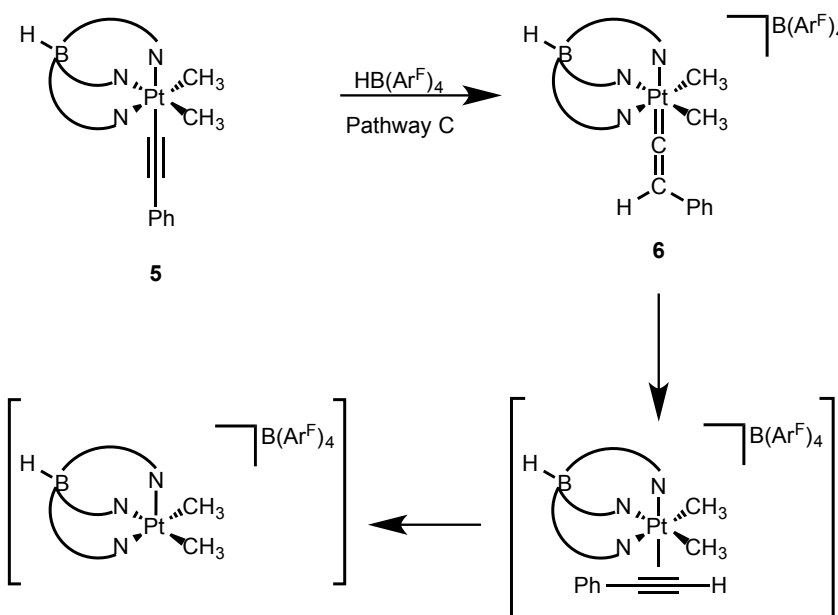
#### a. Vinylidene Protonation of Pyrazole Arm



**b. Vinylidene Migratory Insertion**



c. Vinylidene Isomerization



**Scheme 2** Proposed mechanistic pathways after formation of **6**.

#### 4.3 Conclusion

In summary, we have prepared a  $d^6$  Pt-acetylide complex. Through electrophilic addition, the Pt-acetylide is protonated at the  $\beta$ -carbon to the metal center to form a cationic Pt(IV) vinylidene complex. We observed the Pt(IV) vinylidene with  $^1\text{H}$  and  $^{13}\text{C}$  NMR spectrometry, and the  $\alpha$ -carbon of the vinylidene ligand was difficult to observe at 526 ppm. This is the first reported observation of a Pt(IV) vinylidene.

#### 4.4 Experimental Section

All reactions were performed under an atmosphere of dry argon using standard Schlenk and drybox techniques. Argon was purified by passage through columns of

BASF R3-11 catalyst and 4 Å molecule sieves. Methylene chloride, hexanes, and pentane were purified under an argon atmosphere and passed through a column packed with activated alumina. All other chemicals were used as received without further purification.

<sup>1</sup>H and <sup>13</sup>C NMR spectra were recorded on Bruker Cryoprobe B600 or AV3500 spectrometers. <sup>1</sup>H NMR and <sup>13</sup>C NMR chemical shifts were referenced to residual <sup>1</sup>H and <sup>13</sup>C signals of the deuterated solvents. Elemental analyses were performed by Robertson Microlit Laboratories of Madison, NJ. Tp'PtMe<sub>2</sub>H<sup>19</sup> and complex **4**<sup>17</sup> were prepared following literature procedures

**Tp'Pt(CH=CHPh)(Me)(Cl) (3).** An NMR tube was charged with 0.020g (0.038 mmol) of Tp'PtMe<sub>2</sub>H. Dry CH<sub>2</sub>Cl<sub>2</sub> (0.5 mL) and 4.61 µl (0.040 mmol) of phenylacetylene were added and the tube was sealed. The NMR tube was cooled to -80 °C and 5.2 µl (0.040 mmol) HBF<sub>4</sub> was added. The mixture was left to sit at -80 °C for 3 hours before slowly warming to room temperature; the mixture was chromatographed on alumina with methylene chloride as the elutant. Collection of the elutant followed by removal of solvent resulted in a off white powder. Yield: 10 mg, 40%. <sup>1</sup>H NMR (CD<sub>2</sub>Cl<sub>2</sub>, 298 K δ) 6.95 (d, 1H, Pt-CH=C, <sup>3</sup>J<sub>H-H cis</sub> = 10.5Hz, <sup>2</sup>J<sub>Pt-H</sub> = 51 Hz), 6.79 (t, 1H, *para*-Ph), 6.67 (t, 2H, *meta*-Ph), 6.40 (d, 1H, Pt-CH=CH, <sup>3</sup>J<sub>H-H cis</sub> = 10.5Hz, <sup>3</sup>J<sub>Pt-H</sub> = 66.5 Hz), 6.01 (d, 2H, *ortho*-Ph), 5.85 (s, 1H, Tp'CH), 5.70 (s, 1H, Tp'CH), 5.35 (s, 1H, Tp'CH), 2.53, 2.46, 2.38, 2.37, 2.27, 2.25 (s, 3H each, Tp'CH<sub>3</sub>), 2.08 (s, 3H, Pt-CH<sub>3</sub>, <sup>2</sup>J<sub>Pt-H</sub> = 67 Hz). <sup>13</sup>C NMR (δ, CD<sub>2</sub>Cl<sub>2</sub>, 298 K): 151.63, 151.38, 151.14, 144.83, 144.03, 143.93 (Tp'CCH<sub>3</sub>), 137.88 (*ipso*-Ph), 133.49 (Pt-C=C, <sup>2</sup>J<sub>Pt-C</sub> = 11 Hz), 126.89 (*ortho*-Ph), 126.62 (*meta*-Ph), 125.17 (*para*-Ph), 113.04 (Pt-C=C, <sup>1</sup>J<sub>Pt-C</sub> = 758 Hz) 108.47, 107.97, 107.51 (Tp'CH), 14.17, 13.62, 13.07, 12.80, 12.24, 12.06 (Tp'CH<sub>3</sub>), -3.78 (Pt-CH<sub>3</sub>, <sup>1</sup>J<sub>Pt-C</sub> = 517 Hz). Anal

Calcd for C<sub>24</sub>H<sub>32</sub>B<sub>1</sub>N<sub>6</sub>ClPt: C, 44.63; H, 4.99; N, 13.01. Found: C, 44.12; H, 4.98; N, 12.96.

**Tp'PtMe<sub>2</sub>(C≡CPh) (5).** A vial was charged with 0.020g (0.035 mmol) of [PtMe<sub>2</sub>(SMe<sub>2</sub>)<sub>2</sub>] and 0.024m (0.070 mmol) of KTp' in the box. THF was added (1.5ml) to the vial and the vial was capped and left to stir. After four hours, 0.032g (0.070 mmol) of (phenylethynyl)(phenyl)iodonium triflate<sup>20</sup> was added to the vial. The solution turned yellow and a solid precipitated. The mixture was chromatographed on alumina with methylene chloride as the elutant. The elutant was collected and the solvent was removed via rotary evaporation and the resulting oil was triturated with pentane to afford a yellow solid. The yellow sold was heated to 50 °C under vacuum to pull off the iodobenzene and isolate a mixture of **5** and an unknown Tp'Pt product as a yellow solid. <sup>1</sup>H NMR (CD<sub>2</sub>Cl<sub>2</sub>, 298 K, δ) 7.31 (d, *ortho*-Ph) 7.22 (t, 2H, *meta*-Ph), 7.14 (m, 1H, *para*-Ph), 5.87 (s, 1H, Tp'CH), 5.84 (s, 2H, Tp'CH), 2.57, 2.37 (s, 6H each, Tp'CH<sub>3</sub>), 2.56, 2.39 (s, 3H each, Tp'CH<sub>3</sub>), 1.70 (s, 6H, Pt-CH<sub>3</sub>, <sup>2</sup>J<sub>Pt-H</sub> = 67 Hz). <sup>13</sup>C NMR (CD<sub>2</sub>Cl<sub>2</sub>, 298 K, δ): 152.00, 150.91, 144.69, 144.28 (Tp'CCH<sub>3</sub>), 137 (*ipso*-Ph), 131.79 (*ortho*-Ph), 128.23 (*meta*-Ph), 126.14 (*para*-Ph), 108.44, 107.74 (Tp'CH), 95.35 (Pt-C≡C, <sup>2</sup>J<sub>Pt-C</sub> = 296 Hz), 69.38 (Pt-C≡C, <sup>1</sup>J<sub>Pt-C</sub> = 1370 Hz) 15.30, 13.52, 13.12, 12.77, (Tp'CH<sub>3</sub>), -9.85 (Pt-CH<sub>3</sub>, <sup>1</sup>J<sub>Pt-C</sub> = 565 Hz).

**[Tp'Pt(=C=C(H)(Ph))(Me)<sub>2</sub>][B(Ar<sup>F</sup>)<sub>4</sub>] (6).** An NMR tube was charged with 0.018g (0.018 mmol) of H[B(Ar<sup>F</sup>)<sub>4</sub>]•(Et<sub>2</sub>O)<sub>2</sub> in a glove box. Dry CD<sub>2</sub>Cl<sub>2</sub> (0.3 mL) was added and the tube was sealed. The NMR tube was cooled to -80 °C and a solution of 0.011 g (0.018 mmol) of **5** in 0.3mL of CD<sub>2</sub>Cl<sub>2</sub> was slowly added. The mixture was mixed for 1 min using a thin copper wire. The sample was transported cold (-78 °C) to an NMR probe

cooled to -80 °C and slowly warmed to -60 °C. Complex **6** was only formed in situ, roughly 50% yield, with the rest of the metal present as reagent, complex **9**. <sup>1</sup>H NMR (CD<sub>2</sub>Cl<sub>2</sub>, 213 K, δ), 3.03 (s, 1H, Pt=C=C(H)(Ph), <sup>3</sup>J<sub>Pt-H</sub> = 84 Hz). <sup>13</sup>C NMR (CD<sub>2</sub>Cl<sub>2</sub>, 213 K, δ), 525.8 (1C, Pt=C=C).

## REFERENCES

- (1) Bruce, M. I. *Chem. Rev.* **1991**, *91*, 197.
- (2) Collman, J. P.; Hegedus, L. S.; Norton, J. R.; Finke, R. A. *Principles and Applications of Organotransition Metal Chemistry*, 2nd ed.; Mill Valley, CA.
- (3) Bruneau, C.; Dixneuf, P. H. *Acc. Chem. Res.* **1999**, *32*, 311.
- (4) Crabtree, R. H. *The Organometallic Chemistry of the Transition Metals*, 2nd ed.; Wiley: New York, 1994.
- (5) Bajo, S.; Esteruelas, M. A.; López, A. M.; Oñate, E. *Organometallics* **2014**, *33*, 4057.
- (6) Castro-Rodrigo, R.; Esteruelas, M. A.; López, A. M.; López, F.; Mascareñas, J. L.; Oliván, M.; Oñate, E.; Saya, L.; Villarino, L. *J. Am. Chem. Soc.* **2010**, *132*, 454.
- (7) Singh, V. K.; Bustelo, E.; de los Ríos, I.; Macías-Arce, I.; Puerta, M. C.; Valerga, P.; Ortúño, M. A.; Ujaque, G.; Lledós, A. *Organometallics* **2011**, *30*, 4014.
- (8) Hsu, L.-S.; Lo, Y.-H. *J. Organomet. Chem.* **2016**, *812*, 177.
- (9) Pickup, O. J. S.; Khazal, I.; Smith, E. J.; Whitwood, A. C.; Lynam, J. M.; Bolaky, K.; King, T. C.; Rawe, B. W.; Fey, N. *Organometallics* **2014**, *33*, 1751.
- (10) Belluco, U.; Bertani, R.; Michelin, R. A.; Mozzon, M.; Benetollo, F.; Bombiere, G.; Angelici, R. *Inorganica Chimica Acta* **1995**, *240*, 567.
- (11) Belluco, U.; Bertani, R.; Meneghetti, F.; Michelin, R. A.; Mozzon, M. *J. Organomet. Chem.* **1999**, *583*, 131.
- (12) Gunay, A.; Jones, W. D. *J. Am. Chem. Soc.* **2007**, *129*, 8729.
- (13) Engelman, K. L.; White, P. S.; Templeton, J. L. *Inorganica Chimica Acta* **2009**, *362*, 4461.
- (14) Reinartz, S.; White, P. S.; Brookhart, M.; Templeton, J. L. *J. Am. Chem. Soc.* **2001**, *123*, 12724.
- (15) MacDonald, M. G.; Kostelansky, C. N.; White, P. S.; Templeton, J. L. *Organometallics* **2006**, *25*, 4560.
- (16) Reinartz, S.; White, P. S.; Brookhart, M.; Templeton, J. L. *Organometallics* **2000**, *19*, 3854.

- (17) Höfer, M.; Liska, R. *J. Polym. Sci. A Polym. Chem.* **2009**, *47*, 3419.
- (18) Lavoie, K. D.; Frauhiger, B. E.; White, P. S.; Templeton, J. L. *J. Organomet. Chem.* **2015**, *793*, 182.
- (19) O'Reilly, S. A.; White, P. S.; Templeton, J. L. *J. Am. Chem. Soc.* **1996**, *118*, 5684.
- (20) Bachi, M. D.; Barner, N.; Crittell, C. M.; Stang, P. J.; Willioamson, B. L. *J. Org. Chem.* **1991**, *56*, 3912.

## CHAPTER FIVE

### Syntheses of Cationic Platinum(IV) Complexes Including an Unusual Pt-CH<sub>2</sub>CH<sub>2</sub>-Pt Bridge<sup>1</sup>

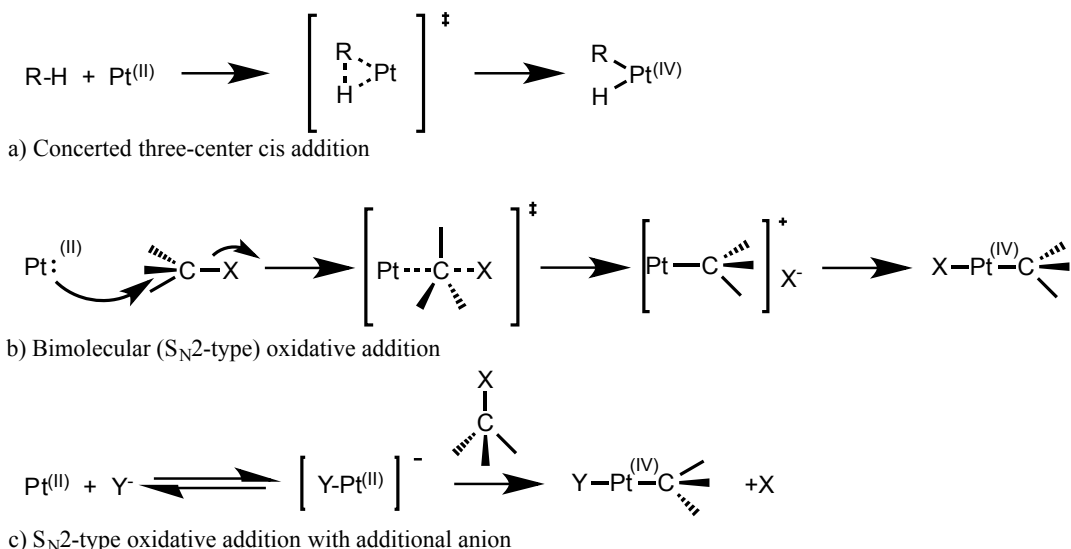
#### 5.1 Introduction

The synthesis of K[Pt(C<sub>2</sub>H<sub>4</sub>)Cl<sub>3</sub>]•H<sub>2</sub>O in 1827 was a seminal event in organometallic chemistry.<sup>1</sup> Existing in d<sup>6</sup>, d<sup>8</sup>, or d<sup>10</sup> configurations, platinum complexes are stable enough for extensive investigations into their reactivity. Perhaps most often probed are oxidative addition and reductive elimination reactions. Oxidative addition reactions are a fundamental process in transition metal chemistry.<sup>2</sup> Substrate activation often is the first step in functionalization of organic compounds needed for synthetic and catalytic processes in organic, inorganic, and organometallic chemistry.<sup>3</sup>

Pt(II) centers oxidatively add electrophiles, a formal 2e<sup>-</sup> process. Oxidative addition can occur as a concerted three-center cis addition, a bimolecular S<sub>N</sub>2 type mechanism, or by following a radical mechanism. The three-center cis addition requires a coordinatively unsaturated metal center and the bond adds across the metal in a concerted fashion (scheme 1a). Alternatively, for a S<sub>N</sub>2 bimolecular addition, platinum acts as a nucleophile, forming a cationic intermediate (scheme 1b). There are a few examples of an anion binding to the platinum center, generating a highly nucleophilic center, which drives the S<sub>N</sub>2 reactivity (scheme 1c). Free radical reactivity can include chain or nonchain inner-sphere electron transfer.

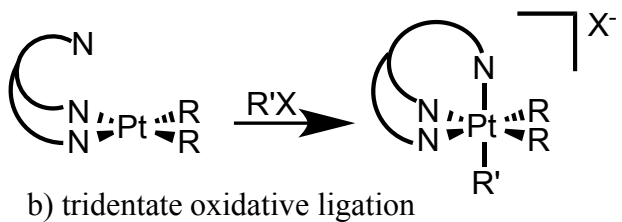
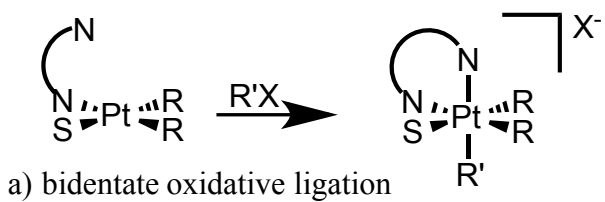
---

<sup>1</sup> Reproduced with permission from Lavoie, K. D., Frauhiger, B. E., White, P.S., Templeton, J. L., DOI: 10.1016/j.molcata.2016.07.002



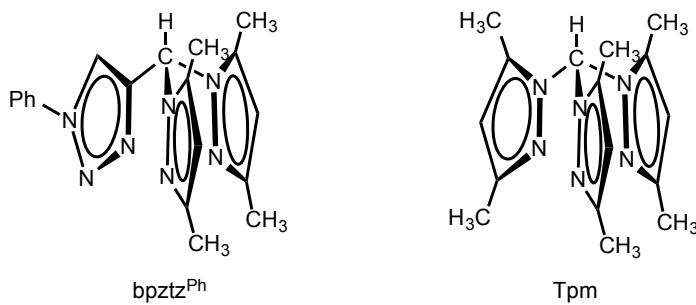
**Scheme 1** Mechanisms for electrophiles adding to  $d^8$  platinum centers.

In 1963, Doyle et al published a report of oxidative addition of methyl iodide to  $cis[Pt(\text{tolyl})_2(\text{py})_2]$ .<sup>4</sup> Since then, Pt(IV) stabilized with nitrogen donors has been an area of expanding impact. Due to the strong  $\sigma$ -donor and weak  $\pi$ -acceptor electronics of amines, they have proven more effective ligands for oxidation state interconversions than the tertiary phosphines or arsine ligands.<sup>5,6</sup> The nucleophilicity of the Pt(II) center is enhanced by the “hard” nature of nitrogen, an important effect for facilitating  $S_N2$ -type reactivity. Investigations into hemilabile ligands with N-donors allows for opening a coordination site while still helping stabilize the platinum center resulted in the common use of heterocycles with  $sp^2$  hybridized nitrogen atoms.<sup>7</sup> These bidentate and tridentate ligands allow for new mechanisms of oxidative addition called oxidative ligation. In oxidative ligation, the platinum center is oxidized by the addition of a new ligand, but instead of a concerted addition, the chelated arm binds to form octahedral Pt(IV) products (scheme 2).<sup>8-10</sup>



**Scheme 2** Oxidative ligation with a bidentate and tridentate nitrogen donor ligands.

In chapter 2 we compared the structures of various scorpionate ligands bound to Pt(IV)trimethyl fragments. Investigations into oxidative addition of Pt centers ligated by either 4-(bis(3,5-dimethyl-1*H*-pyrazol-1-yl)methyl)-1-phenyl-1*H*-1,2,3-triazole ( $\text{bpztz}^{\text{Ph}}$ ) or tris(3,5-dimethylpyrazolyl)methane (Tpm) are reported herein. Comparison of the two ligands explores the difference resulting from the third arm, either a triazole ring or a pyrazole ring, respectively. Electrophilic oxidation of Pt(II) isomers to form Pt(IV) products with electrophilic reagents, including simple acids and acid chlorides leads to isomers in some cases, and the binding properties of the various donor arms dictate the stereochemistry of the products. Investigations into the reactivity of heteroscorpionate tridentate ligands bound to platinum(II) led to C-Cl activation reactions with methylene chloride and 1,2-dichloroethane.



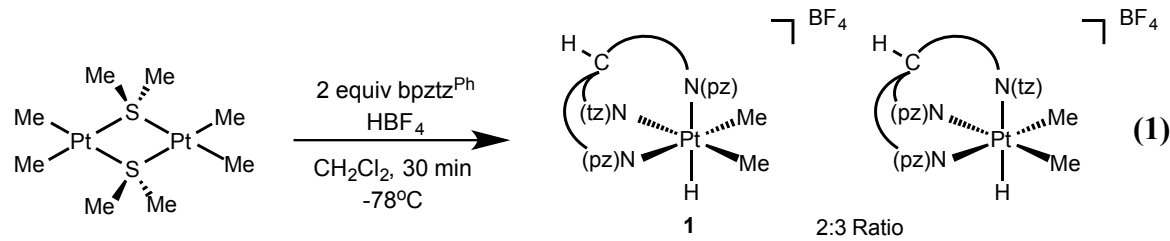
## 5.2 Results and Discussion

### 2.1 Electrophilic Addition: Isomer Preferences for d<sup>8</sup> Pt(II) and d<sup>6</sup> Pt(IV)

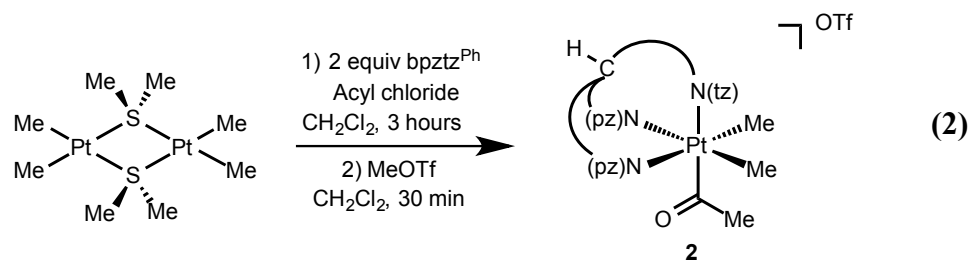
Bidentate binding of the  $\text{bpztz}^{\text{Ph}}$  ligand to form a square planar dimethylPt(II) complex could form two isomers. The ligand could bind either with one free pyrazole arm or with both pyrazole rings bound and with the triazole ring free. If these two isomers were energetically equivalent and isomerization were easily accessible, a statistical 1:2 ratio favoring the asymmetrical isomer should result. The addition of two equivalents of  $\text{bpztz}^{\text{Ph}}$  to one equivalent of  $[\text{PtMe}_2(\text{SMe}_2)]_2$  in tetrahydrofuran initially displayed a 1:1 ratio of the symmetric to asymmetric isomers in the  $^1\text{H}$  NMR spectrum. After 30 minutes a preference (3:1) for the symmetric ( $\kappa^2\text{-bpztz}^{\text{Ph}}$ ) $\text{Pt}(\text{CH}_3)_2$  isomer with the triazolyl arm free was evident. This ratio increased to 5:1 after 90 minutes. This result implies that in the square planar Pt(II) case, the triazole arm binds less tightly than the pyrazole arms, a different conclusion than was drawn above for Pt(IV) based on solid state Pt-N bond distances. The difference in Pt(II) d<sup>8</sup> versus Pt(IV) d<sup>6</sup> binding preferences seemed poised to promote oxidative addition to the metal center: the triazole arm would be non-coordinated in the Pt(II) state then stabilize the high valent Pt(IV) by donating electron density to the metal center and completing a six-coordinate geometry.

Mimicking previous results with  $\text{Tp}'\text{PtMe}_2\text{H}$  [ $\text{Tp}'$  = hydridotris(3,5-dimethylpyrazolyl)borate],<sup>8</sup> we synthesized a Pt(IV) hydride complex by protonation of the Pt(II) intermediate. Metalation of the  $\text{bpztz}^{\text{Ph}}$  ligand followed by low temperature addition of tetrafluoroboric acid resulted in the desired complex,  $[\text{bpztz}^{\text{Ph}}\text{PtMe}_2\text{H}][\text{BF}_4]$ , **1** (eq 1). The  $^1\text{H}$  NMR spectrum of the hydride product displayed two isomers in a 2:3 ratio with the symmetric complex as the major isomer. The major isomer has the hydride trans to the triazole arm and displays  $^1J_{\text{Pt-H}} = 1424$  Hz, while the minor asymmetric isomer has  $^1J_{\text{Pt-H}} = 1480$  Hz. Both  $^1J_{\text{Pt-H}}$  values are typical coupling constants for Pt(IV) hydride complexes.<sup>8,11,12</sup>

The more stable symmetrical isomer of the square planar Pt(II) intermediates with both pyrazole arms bound is presumably trapped by the oxidation of the Pt center as the acid adds to platinum. This places the hydride trans to the triazolyl ligand. However, the hydride is a stronger donating ligand than the methyl groups so it would prefer to bind trans to a pyrazole arm. Isolation of the symmetric Pt(IV) hydride complex demonstrates that once the Pt(IV) complex is formed, the barrier to isomerization increases significantly relative to the Pt(II) barrier. Under the conditions we utilized, isomerization of the mixed ligand only occurs at the Pt(II)  $d^8$  configuration before the complex is oxidized to Pt(IV).



Similar oxidation of Pt(II) to Pt(IV) addition reactions can be observed with other electrophiles. As shown in equation 2, the addition of acyl chloride to a solution of bpztz<sup>Ph</sup> and [PtMe<sub>2</sub>(SMe<sub>2</sub>)<sub>2</sub>] results in a cationic Pt(IV) acyl complex. Anion exchange of chloride to triflate to generate [bpztz<sup>Ph</sup>PtMe<sub>2</sub>(C(O)CH<sub>3</sub>)][OTf], **2**, was accomplished by addition of MeOTf. Only the symmetric isomer with the triazole donor arm trans to the acyl ligand was observed in the <sup>1</sup>H NMR spectrum. We attribute this to the acyl chloride reacting relatively slowly with the Pt(II) complex. Slow electrophilic addition of the acylchloride would allow isomerization at the Pt(II) stage and thus the symmetric isomer could be selectively trapped.



An x-ray structure of **2** was obtained to confirm the geometry of the complex. However, due to disorder between the acyl oxygen and methyl group of the acyl ligand the geometrical parameters are less accurate than other bond distances and angles reported in this thesis. Figure 1 shows the x-ray structure of **2** and selected bond distances and angles are presented in Table 1.

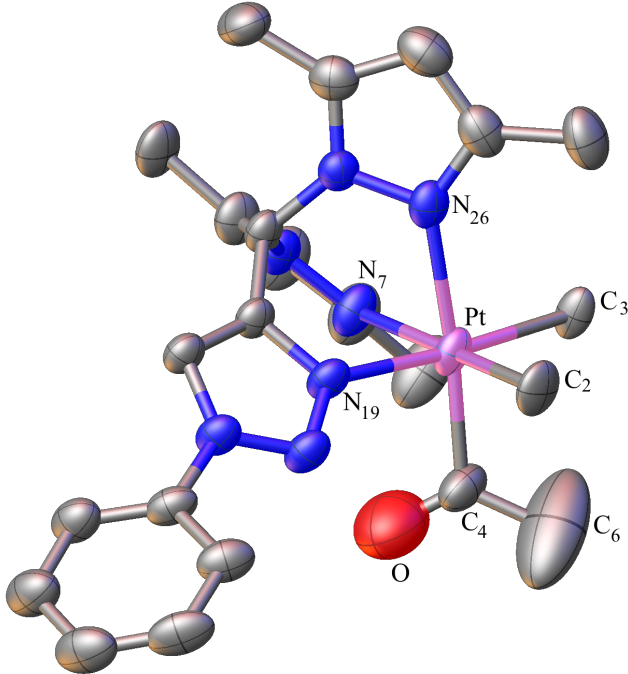


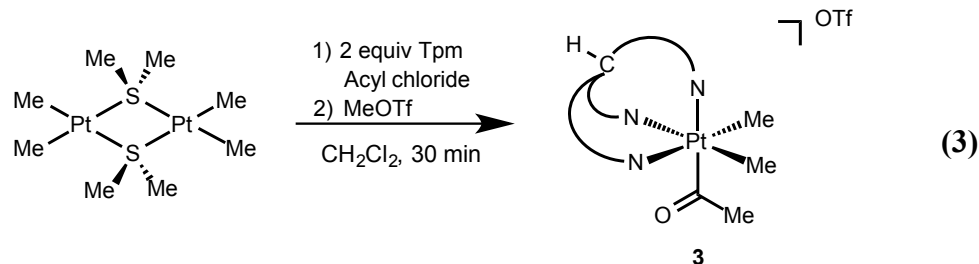
**Figure 1** X-ray structure of  $[bpptz^{Ph}PtMe_2C(O)CH_3][OTf]$  **2**. Ellipsoids are drawn at the 50% probability level. Hydrogen atoms and trifluoromethansulfonate counterion are omitted for clarity.

**Table 1** Selected bond lengths ( $\text{\AA}$ ) and angles (deg) for one monomer of complex **2**.

<u>Bond Lengths</u>			
Pt-N7	2.111(5)	Pt-C2	2.057(5)
Pt-N19	2.188(5)	Pt-C3	2.133(5)
Pt-N26	2.234(5)	Pt-C4	2.030(7)
C4-O	1.173(11)		
<u>Bond Angles</u>			
N7-Pt-N19	84.07(18)	C4-Pt-C3	92.0(3)
C4-Pt-N7	92.0(3)	O-C4-Pt	116.0(6)

Comparable acyl chemistry was observed with Tpm as the tridentate ligand. The addition of acyl chloride to a solution of Tpm and  $[PtMe_2(SMe_2)]_2$  followed by exchange of the anion results in the anticipated  $[TpmPtMe_2(C(O)CH_3)][OTf]$ , **3**, product

(eq 3). The acetyl carbon in the  $^{13}\text{C}$  NMR spectrum is seen at 191.5 ppm with  $^1\text{J}_{\text{Pt-H}} = 894$  Hz, slightly smaller than the coupling seen for complex **2** (ca 912 Hz).



Slow diffusion of pentane into a solution of **3** in dichloromethane produced colorless crystals suitable for X-ray crystallography. Figure 2 shows the x-ray structure of a monomeric unit of **3** and selected bond distances and angles are presented in Table 2.

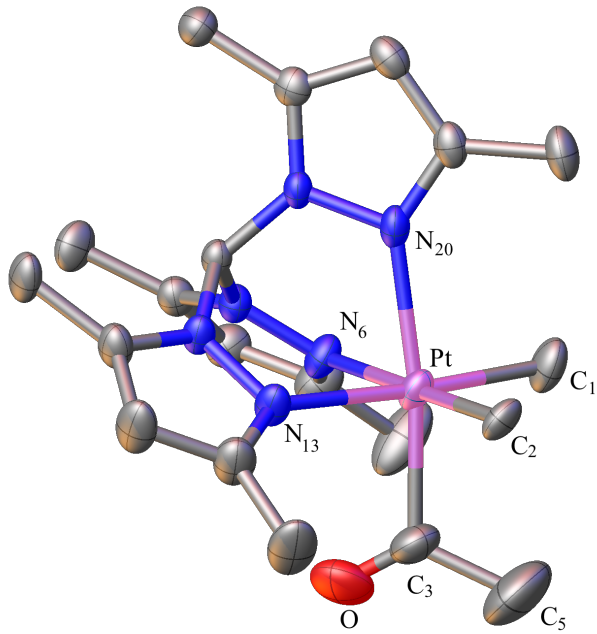


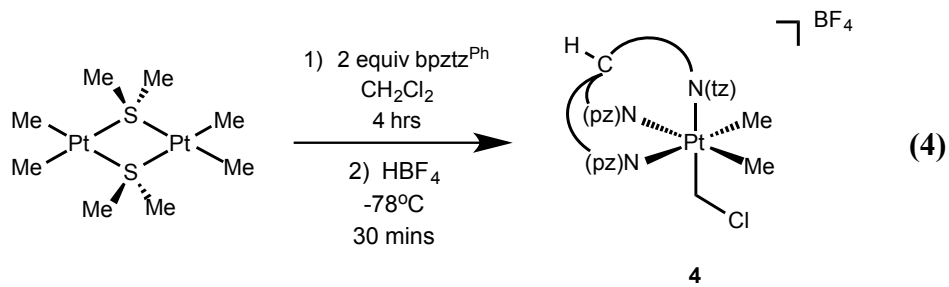
**Figure 2** X-ray structure of  $[\text{TpmPtMe}_2\text{C}(\text{O})\text{CH}_3]\text{[OTf]}$  **3**. Ellipsoids are drawn at the 50% probability level. Hydrogen atoms and trifluoromethanesulfonate counterion are omitted for clarity.

**Table 2** Selected bond lengths (Å) and angles (deg) for one monomer of complex **3**.

<u>Bond Lengths</u>			
Pt-N6	2.188(5)	Pt-C1	2.047(5)
Pt-N13	2.184(4)	Pt-C2	2.024(8)
Pt-N20	2.170(4)	Pt-C3	2.075(12)
C3-O	1.197(10)		
<u>Bond Angles</u>			
N6-Pt-N20	82.52(15)	C3-Pt-N20	166.6(5)
C1-Pt-N6	92.4(2)	O-C3-Pt	130.3(12)

## 2.2 Pt(II) Reactions with Alkyl Chloride Solvents

In the absence of electrophilic reagents, a solution of bpztz<sup>Ph</sup> and [PtMe<sub>2</sub>(SMe<sub>2</sub>)<sub>2</sub>] in dichloromethane results in cleavage of a C-Cl bond of the solvent to form cationic complex [bpztz<sup>Ph</sup>PtMe<sub>2</sub>(CH<sub>2</sub>Cl)]<sup>+</sup>, **4**, with Cl<sup>-</sup> as the leaving group. The addition of tetrafluoroboric acid at low temperature effected anion exchange to produce [bpztz<sup>Ph</sup>PtMe<sub>2</sub>(CH<sub>2</sub>Cl)][BF<sub>4</sub>]<sup>-</sup>, equation 4. In the <sup>1</sup>H NMR spectrum of **4**, a single resonance for both the Pt-CH<sub>2</sub>Cl protons at 4.36 ppm (<sup>2</sup>J<sub>Pt-H</sub> = 50 Hz) along with one resonance for the two aromatic pyrazolyl-protons at 6.06 ppm, indicate C<sub>s</sub> symmetry. A 2D NMR HSQC spectrum displays crosspeaks between the protons at 4.36 ppm and a carbon at 20.3 ppm in the <sup>13</sup>C NMR. The peak at 20.3 ppm in the <sup>13</sup>C NMR displays 841 Hz coupling to Pt, indicative of a one-bond platinum carbon bond, confirming a direct Pt-C bond as opposed to the solvent binding through a chlorine atom of dichloromethane.



Slow evaporation of a solution of **4** in dichloromethane produced pale yellow crystals suitable for X-ray crystallography. Figure 3 shows the x-ray structure of a single unit of **4**, and selected bond distances and angles are presented in Table 3. The metal center adopts a slightly distorted octahedral geometry. The Pt-C<sub>1</sub>-Cl angle through the chloromethyl ligand is 114.8°, surely distorted from the ideal tetrahedral bond angle (109.5°) due to steric effects. The carbon metal bond to the methyl chloride ligand (Pt-C<sub>1</sub>) is the shortest of the Pt-C bonds, at 2.026 Å, consistent with expectations for an electron withdrawing group on the methyl ligand.

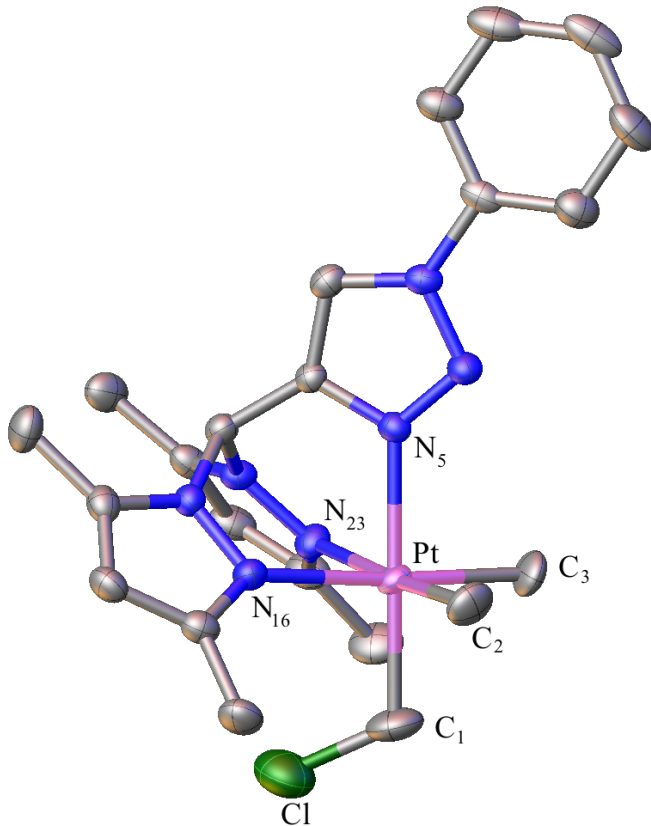
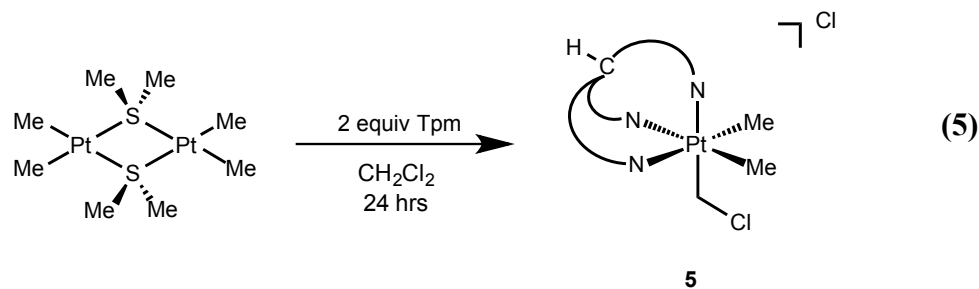


**Figure 3** X-ray structure of  $[bpztt^{Ph}PtMe_2(CH_2Cl)][BF_4]$  **4**. Ellipsoids are drawn at the 50% probability level. Hydrogen atoms and counterion are omitted for clarity.

**Table 3** Selected bond lengths ( $\text{\AA}$ ) and angles (deg) for complex **4**.

<u>Bond Lengths</u>			
Pt-N5	2.110(4)	Pt-C1	2.026(5)
Pt-N16	2.196(4)	Pt-C2	2.056(5)
Pt-N23	2.187(4)	Pt-C3	2.048(5)
C1-Cl	1.775(6)		
<u>Bond Angles</u>			
N5-Pt-N16	83.67(14)	C1-Pt-C2	87.9(2)
C1-Pt-N16	95.64(19)	Cl-C1-Pt	114.8(3)

Intrigued by the proclivity of Pt(II) to break C-Cl bonds, we investigated the possibility of the other tridentate ligands facilitating similar reactivity.<sup>16-19</sup> No reactivity was observed with the POP<sub>3</sub> ligand after a week of stirring in dichloromethane. Due to the low solubility of KTp' in dichloromethane, we first formed the  $\kappa^2$ Pt(II) complex [K][ $\kappa^2$ Tp'PtMe<sub>2</sub>] in tetrahydrofuran, then added dichloromethane to the reaction mixture. Again, no oxidative addition of methylene chloride was observed. In contrast, the reaction of Tpm and [PtMe<sub>2</sub>(SMe<sub>2</sub>)<sub>2</sub>] in dichloromethane resulted in an analogous complex, [TpmPtMe<sub>2</sub>(CH<sub>2</sub>Cl)][Cl] **5**, after 24 hours, equation 5. Complex **5** shows a peak in the <sup>1</sup>H NMR spectrum at 4.34 with 49 Hz platinum coupling for the chloromethyl ligand.



Slow diffusion of pentane into a solution of **13** in dichloromethane produced pale yellow crystals suitable for X-ray crystallography. Figure 4 shows the x-ray structure of a monomeric unit of **5** and selected bond distances and angles are presented in Table 4. The Pt-CH<sub>2</sub>Cl carbon bond length is again shorter than the Pt-C distances to the two methyl ligands, but it is elongated by 0.013 Å compared to the distance in the bpztz<sup>Ph</sup> complex, **5**.

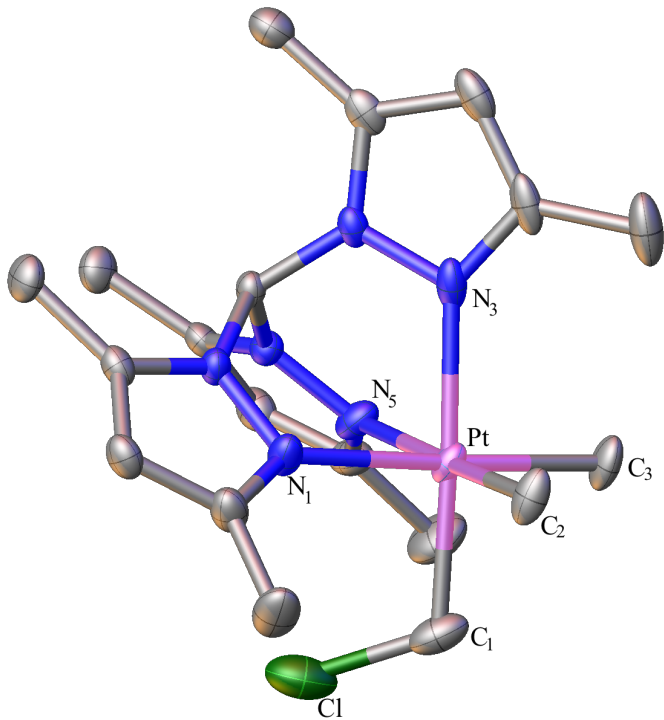


**Figure 4** X-ray structure of  $[\text{TpmpPtMe}_2(\text{CH}_2\text{Cl})][\text{Cl}]$  **5**. Ellipsoids are drawn at the 50% probability level. Hydrogen atoms and counterion are omitted for clarity.

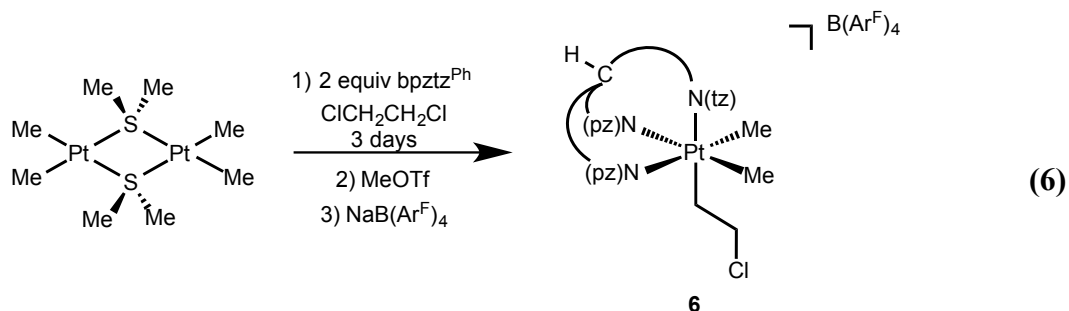
**Table 4** Selected bond lengths ( $\text{\AA}$ ) and angles (deg) for complex **5**.

<u>Bond Lengths</u>			
Pt-N1	2.147(3)	Pt-C1	2.039(7)
Pt-N3	2.109(4)	Pt-C2	2.046(6)
Pt-N5	2.208(4)	Pt-C3	2.060(7)
C1-Cl	1.775(6)		
<u>Bond Angles</u>			
N1-Pt-N5	86.23(14)	C1-Pt-C2	88.9(3)
C1-Pt-N1	93.7(2)	Cl-C1-Pt	114.8(3)

We next attempted the reaction of 1,2-dichloroethane with a Pt(II) precursor.

Stirring a solution of bpztz<sup>Ph</sup> and  $[\text{PtMe}_2(\text{SMe}_2)]_2$  in 1,2-dichloroethane for three days results in the formation of a  $\text{PtCH}_2\text{CH}_2\text{Cl}$  entity. Addition of MeOTf to the complex

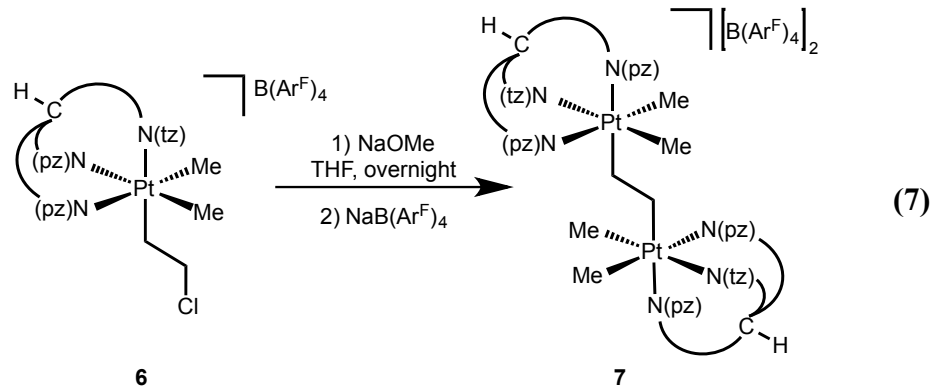
exchanged the anion to the noncoordinating triflate. A secondary anion exchange was accomplished through the addition of sodium tetrakis[(3,5-trifluoromethyl)phenyl]borate ( $\text{NaB}(\text{Ar}^{\text{F}})_4$ ) and led to the isolation of  $[\text{bpztz}^{\text{Ph}}\text{PtMe}_2\text{CH}_2\text{CH}_2\text{Cl}][\text{B}(\text{Ar}^{\text{F}})_4]$ , **6**, (eq 6). In the  $^1\text{H}$  NMR spectrum of **6**, the major isomer is the symmetric product, with the triazole donor trans to the chloroethyl ligand. The two protons bound to the carbon alpha to the metal center appear as a distinctive 8-line pattern at 2.81 ppm. Further downfield at 3.38 ppm is a similar splitting pattern corresponding to the protons bound to the beta carbon of the  $\text{PtCH}_2\text{CH}_2\text{Cl}$  fragment, reflecting the second order AA'XX' pattern typical of  $\text{XCH}_2\text{CH}_2\text{Y}$  entities.



We attempted analogous chemistry with 1,2-dichloroethane and other homoscorpionate ligands to no avail. The ability to activate the C-Cl bond at one end of 1,2-dichloroethane demonstrates the unusual reactivity of this asymmetrical bpztz tridentate ligand.

In an effort to promote elimination from the  $\text{Pt}-\text{CH}_2\text{CH}_2\text{Cl}$  fragment of complex **6** we added a base, sodium methoxide. We anticipated the methoxide would deprotonate the carbon alpha to Pt and perhaps lead to elimination to form a Pt-vinyl ligand. Alternatively methoxide could simply displace the chloride to form a  $\text{Pt}-\text{CH}_2\text{CH}_2\text{OCH}_3$

ligand. The addition of sodium methoxide to cationic complex **6** in THF resulted in the precipitation of a white solid containing platinum. The solid, sparingly soluble in dichloromethane, reacted with  $\text{NaB}(\text{Ar}^{\text{F}})_4$  and led to the isolation of a dicationic, dinuclear product,  $[(\text{bpztz}^{\text{Ph}})\text{Me}_2\text{PtCH}_2\text{CH}_2\text{PtMe}_2(\text{bpztz}^{\text{Ph}})][\text{B}(\text{Ar}^{\text{F}})_4]_2$ , **7**, eq 7.



The  $^1\text{H}$  NMR spectrum was complex due to second order effects so we begin by describing the definitive C-13 NMR spectrum which led to unambiguous identification of the  $\text{PtCH}_2\text{CH}_2\text{Pt}$  unit. The  $^{13}\text{C}$  NMR spectrum indicates the presence of a dinuclear complex containing a  $-\text{CH}_2\text{CH}_2-$  bridge: a single peak centered at 20 ppm exhibits two sets of Pt satellites, one having  $^1J_{\text{Pt-C}} = 622$  Hz and one having  $^2J_{\text{Pt-C}} = 31$  Hz (appendix 5.1). Note that complex **7** proved challenging to identify by  $^1\text{H}$  NMR since “apparent” quartets at 2.92 and 2.06 ppm were misleading (figure 5a). During the formation of **7**, one of the tridentate ligands isomerized, resulting in a pyrazole arm trans to the alkyl bridge, making each of the two Pt centers chiral. The bridging ethylene ligand then becomes an AXA'X' system, but instead of the AA' hydrogens residing on the same carbon as in the XCH<sub>2</sub>CH<sub>2</sub>Y case, the A and A' hydrogens are on C <sub>$\alpha$</sub>  and C <sub>$\beta$</sub> , respectively, as are X and X'. These pairwise diastereotopic protons resemble overlapping doublets ( $^3J_{\text{H-H}} = 9.5$  Hz) that are roofed, appearing roughly as quartets. The Pt satellites are an additional complication

and there are observable satellite peaks due to the proton seeing a spin active platinum center both 2 and 3 bonds away (although not in the same molecule, figure 5a). Simulations supported our analysis, with a geminal proton coupling of -9.5 Hz and vicinal couplings of 5.0 and 9.0 Hz. We were also able to replicate the platinum satellites through simulations of an AXA'X'M system, calculating  $^2J_{\text{Pt-H}}$  and  $^3J_{\text{Pt-H}}$  couplings of 70 and 52 Hz respectively. Overlaying the simulated spectrum allows for easy comparison to the NMR spectra (figure 5b).

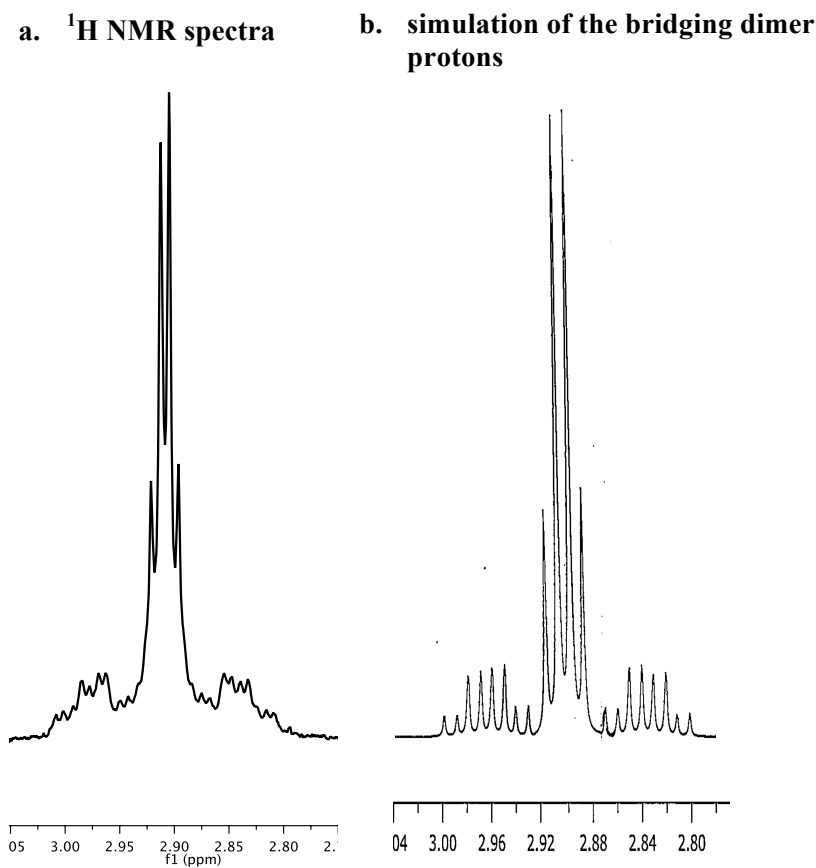
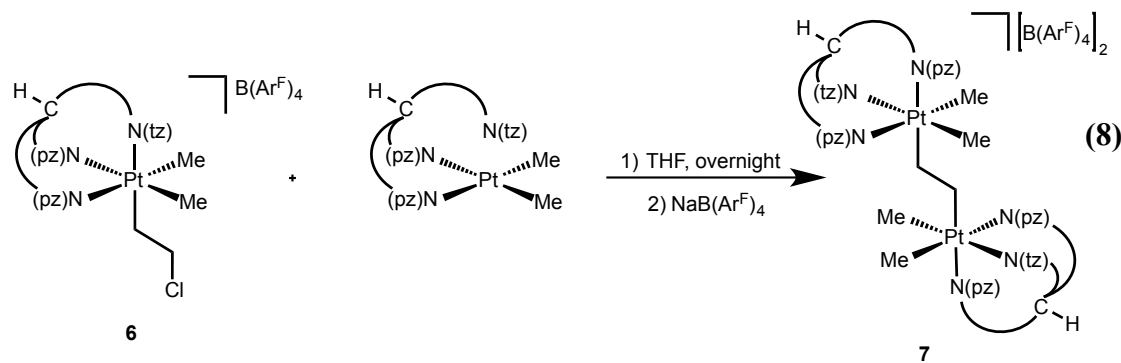


**Figure 5** Observed and simulated spectra of the bridging ligand for complex 7. Calculated with a geminal coupling constant of -9.5 Hz, vicinal coupling constants of 5.0

and 9.0 Hz, two bond platinum proton coupling constant of 70 Hz and three bond coupling constant of 52 Hz.

Preparing a complex with two bridging methylene units between platinum centers is rare, and we probed the importance of the base by adding sodium amide to complex **6**. The result was the same product, indicating that the identity of the base is unimportant in forming the dinuclear product. We propose that the base reacts with the Pt(IV) starting material to reductively eliminate the ethylchloride ligand, perhaps by simply attacking the alpha carbon to form  $\text{MeOCH}_2\text{CH}_2\text{Cl}$  and the reduced Pt complex. This  $\kappa^2\text{-bpztz}^{\text{Ph}}\text{PtMe}_2$  reagent could then react with the C-Cl bond of a second molecule of **7**. Indeed the addition of complex **6** to a solution of  $\kappa^2\text{-bpztz}^{\text{Ph}}\text{Pt}(\text{II})\text{Me}_2$  in THF resulted in precipitation of **7**, eq 8.



### 5.3 Conclusion

Metalation of asymmetrical scorpionate ligands bearing two pyrazolyl rings and one triazolyl ring to generate neutral Pt(II) complexes favors binding only the pyrazole arms rather than the triazole arm. Addition of electrophilic reagents to the dimethylPt(II)

fragment results in stable Pt(IV) complexes with two isomers possible. The  $(\text{bpztz}^{\text{Ph}})\text{PtMe}_2$  d<sup>8</sup> Pt(II) complex displaces chloride from methylene chloride rather than promoting C-H activation as was reported for various Tp' complexes of platinum.<sup>20</sup> The ability to displace chloride from chlorinated solvents led to the synthesis of an unusual dicationic Pt(IV) dimer bridged by an ethylene ligand.<sup>21-23</sup>

#### 5.4 Experimental Section

**Materials and Methods.** All reactions were performed under an atmosphere of dry nitrogen using standard Schlenk and drybox techniques. Nitrogen was purified by passage through columns of BASF R3-11 catalyst and 4 Å molecule sieves. Dichloromethane, dimethyl ether, tetrahydrofuran (THF), and pentane were purified under an argon atmosphere and passed through a column packed with activated alumina. All other chemicals were used as received without further purification. Silica column chromatography was conducted with 230-400 mesh silica gel and alumina column chromatography was conducted with 80-200 mesh alumina.

<sup>1</sup>H and <sup>13</sup>C NMR spectra were recorded on AVANCE500 or ULTRA SHIELD CRYOQNP600 spectrometers. <sup>1</sup>H NMR and <sup>13</sup>C NMR chemical shifts were referenced to residual <sup>1</sup>H and <sup>13</sup>C signals of the deuterated solvents. Elemental analyses were performed by Robertson Microlit Laboratories of Madison, NJ.

Materials: Toluene ( $\text{PhCH}_3$ ), diethyl ether ( $\text{Et}_2\text{O}$ ), dichloromethane ( $\text{CH}_2\text{Cl}_2$ ), and tetrahydrofuran (THF) were dried by passage through a column of neutral alumina under

nitrogen prior to use. All other reagents were purchased from commercial sources and were used as received unless otherwise noted.

**[bpztz<sup>Ph</sup>PtMe<sub>2</sub>H][BF<sub>4</sub>] 1.** A 50-mL Schlenk was charged with 0.030 g (0.05 mmol) of [PtMe<sub>2</sub>(SMe<sub>2</sub>)<sub>2</sub>] and 0.036 g (0.10 mmol) of bpztz<sup>Ph</sup>. The flask was purged with argon and CH<sub>2</sub>Cl<sub>2</sub> (10 mL) was added through the septum. The solution was cooled to -78°C and 7.8 μl (0.06 mmol) of an 8M solution of tetrafluoroboric acid was added. The solution was warmed to room temperature while stirring for 30 minutes. The solvent was removed under reduced pressure and the resulting oil was triturated with pentane to afford **1** as a pale yellow solid in quantitative yield. Major isomer: <sup>1</sup>H NMR ( $\delta$ , CD<sub>2</sub>Cl<sub>2</sub>, 298 K): 9.39 (s, 1H, tz H), 8.26 (s, 1H, HC(pz)<sub>2</sub>(tz)), 7.88 (d, 2H, *o*-Ph), 7.59 (m, 3H, *m*-Ph and *p*-Ph), 6.05 (s, 2H, pz H), 2.63, 2.27 (s, 6H each, pz, CH<sub>3</sub>), 1.36 (s, 3H, <sup>2</sup>J<sub>Pt-H</sub> = 71 Hz, Pt-CH<sub>3</sub>), -19.67 (s, 1H, <sup>1</sup>J<sub>Pt-H</sub> = 1424 Hz). <sup>13</sup>C NMR ( $\delta$ , CD<sub>2</sub>Cl<sub>2</sub>, 298 K): 152.3, 152.0, 142.9, 142.7 (pz C-CH<sub>3</sub>), 139.8 (tz 4-position), 136.0 (ipso-Ph), 130.4 (tz 5-position), 130.2 (*m* -Ph), 124.3, (*p*-Ph), 120.5 (*o*-Ph), 108.8 (pz CH), 60.6 (HC(pz)<sub>2</sub>(tz)), 13.9, 13.6, 12.8, 11.1 (pz CH<sub>3</sub>), -6.0 (<sup>1</sup>J<sub>Pt-C</sub> = 638 Hz, Pt-CH<sub>3</sub>). Minor isomer: <sup>1</sup>H NMR ( $\delta$ , CD<sub>2</sub>Cl<sub>2</sub>, 298 K): 9.34 (s, 1H, tz H), 8.20 (s, 1H, HC(pz)<sub>2</sub>(tz)), 7.83 (d, 2H, *o*-Ph), 7.59 (m, 3H, *m*-Ph and *p*-Ph), 6.07, 6.05 (s, 1H each, pz H), 2.65, 2.64, 2.35, 2.29 (s, 3H each, pz CH<sub>3</sub>), 1.54 (s, 3H, <sup>2</sup>J<sub>Pt-H</sub> = 71 Hz, Pt-CH<sub>3</sub>), 1.33 (s, 3H, <sup>2</sup>J<sub>Pt-H</sub> = 70 Hz, Pt-CH<sub>3</sub>), -21.01 (s, 1H, <sup>1</sup>J<sub>Pt-H</sub> = 1450 Hz). <sup>13</sup>C NMR ( $\delta$ , CD<sub>2</sub>Cl<sub>2</sub>, 298 K): 152.3, 152.0, 142.9, 142.7 (pz C-CH<sub>3</sub>), 139.8 (tz 4-position), 136.0 (ipso-Ph), 130.4 (tz 5-position), 130.2 (*m* -Ph), 124.3, (*p*-Ph), 120.5 (*o*-Ph), 108.8 (pz CH), 60.6 (HC(pz)<sub>2</sub>(tz)), 13.9, 13.6, 12.8, 11.1 (pz CH<sub>3</sub>), -6.5 (<sup>1</sup>J<sub>Pt-C</sub> = 709 Hz, Pt-CH<sub>3</sub>), -8.3 (<sup>1</sup>J<sub>Pt-C</sub> = 603 Hz, Pt-CH<sub>3</sub>).

**[bpztz<sup>Ph</sup>PtMe<sub>2</sub>C(O)CH<sub>3</sub>][OTf] 2.** A 50-mL Schlenk was charged with 0.030 g (0.05 mmol) of [PtMe<sub>2</sub>(SMe<sub>2</sub>)<sub>2</sub>] and 0.036 g (0.10 mmol) of bpztz<sup>Ph</sup>. The flask was purged with argon and CH<sub>2</sub>Cl<sub>2</sub> (10 mL) was added through the septum. The solution was treated with 63 μL (0.06 mmol) of a 1M solution of acetyl chloride and stirred overnight at room temperature. The solvent was removed under reduced pressure to remove any excess acetyl chloride. The resulting oil was dissolved in dichloromethane and 6.2 μL (0.055 mmol) of methyl trifluoromethanesulfonate was added. The solvent was removed under reduced pressure and the resulting oil was triturated with pentane to afford **2** as a pale yellow solid in quantitative yield. <sup>1</sup>H NMR ( $\delta$ , CD<sub>2</sub>Cl<sub>2</sub>, 298 K): 10.50 (s, 1H, tz H), 9.35 (s, 1H, HC(pz)<sub>2</sub>(tz)), 7.95 (d, 2H, *o*-Ph), 7.54 (m, 3H, *m*-Ph and *p*-Ph), 6.10, 6.01 (s, 1H each, pz H), 2.52 (br s, 6H, pz, CH<sub>3</sub>), 2.34, 2.18 (s, 3H each, pz CH<sub>3</sub>), 2.31 (s, 3H, PtC(O)CH<sub>3</sub>), 1.58 (s, 3H, <sup>2</sup>J<sub>Pt-H</sub> = 76 Hz, Pt-CH<sub>3</sub>), 1.52 (s, 3H, <sup>2</sup>J<sub>Pt-H</sub> = 72 Hz, Pt-CH<sub>3</sub>). <sup>13</sup>C NMR ( $\delta$ , CD<sub>2</sub>Cl<sub>2</sub>, 298 K): 189.6 (<sup>1</sup>J<sub>Pt-C</sub> = 912 Hz, PtCO), 153.1, 152.0, 143.5, 143.3 (pz C-CH<sub>3</sub>), 140.6 (tz 4-position), 136.0 (ipso-Ph), 130.3 (*m*-Ph), 130.0, (*p*-Ph), 121.1 (tz 5-position), 121.0 (*o*-Ph), 108.5, 180.4 (pz CH), 61.3 (HC(pz)<sub>2</sub>(tz)), 35.8 (<sup>2</sup>J<sub>Pt-C</sub> = 190 Hz, C(O)CH<sub>3</sub>), 13.6, 12.8, 12.1, 11.9 (pz CH<sub>3</sub>), -5.9 (<sup>1</sup>J<sub>Pt-C</sub> = 691 Hz, Pt-CH<sub>3</sub>), -16.3 (<sup>1</sup>J<sub>Pt-C</sub> = 685 Hz, Pt-CH<sub>3</sub>).

**[TpmpPtMe<sub>2</sub>C(O)CH<sub>3</sub>][OTf] 3.** A 50-mL Schlenk was charged with 0.030 g (0.05 mmol) of [PtMe<sub>2</sub>(SMe<sub>2</sub>)<sub>2</sub>] and 0.031 g (0.10 mmol) of tris(3,5-dimethylpyrazolyl)methane. The flask was purged with argon and CH<sub>2</sub>Cl<sub>2</sub> (10 mL) was added through the septum. The solution was treated with 63 μL (0.06 mmol) of a 1M solution of acetyl chloride and stirred for 30 minutes at room temperature. The solvent was removed under reduced pressure to remove any excess acyl chloride. The oil was

dissolved in dichloromethane and 6.0  $\mu$ L (0.055 mmol) of methyl trifluoromethanesulfonate was added. The solvent was removed under reduced pressure and the resulting oil was triturated with pentane to afford **3** as a pale yellow solid in quantitative yield.  $^1\text{H}$  NMR ( $\delta$ , CD<sub>2</sub>Cl<sub>2</sub>, 298 K): 7.96 (s, 1H, HC(pz)<sub>3</sub>), 6.20 (s, 2H, pz H), 6.16 (s, 1H, pz H), 2.63, 2.16 (s, 6H each, pz CH<sub>3</sub>) 2.99, 2.63 (s, 3H each, pz CH<sub>3</sub>), 2.37 (s, 3H, PtC(O)CH<sub>3</sub>), 1.64 (s, 3H,  $^2J_{\text{Pt-H}} = 72$  Hz, Pt-CH<sub>3</sub>).  $^{13}\text{C}$  NMR ( $\delta$ , CD<sub>2</sub>Cl<sub>2</sub>, 298 K): 191.5 ( $^1J_{\text{Pt-C}} = 894$  Hz, PtCO), 154.3, 152.9, 142.0, 141.9 (pz C-CH<sub>3</sub>), 121.9 (triflate), 110.4, 109.7 (pz CH), 69.6 (HC(pz)<sub>3</sub>), 34.5 ( $^2J_{\text{Pt-C}} = 202.5$  Hz, C(O)CH<sub>3</sub>), 13.9, 13.7, 12.8, 12.6 (pz CH<sub>3</sub>), -7.4 ( $^1J_{\text{Pt-C}} = 717$  Hz, Pt-CH<sub>3</sub>).

**[bpztz<sup>Ph</sup>PtMe<sub>2</sub>(CH<sub>2</sub>Cl)][BF<sub>4</sub>] 4.** A 50-mL Schlenk was charged with 0.030 g (0.05 mmol) of [PtMe<sub>2</sub>(SMe<sub>2</sub>)]<sub>2</sub> and 0.037 g (0.10 mmol) of bpztz<sup>Ph</sup>. The flask was purged with argon and CH<sub>2</sub>Cl<sub>2</sub> (10 mL) was added through the septum. The yellow solution was stirred overnight at room temperature. The reaction was cooled to -78°C and 7.5  $\mu$ L (0.06 mmol) of tetrafluoroboric acid was added. The solution was warmed to room temperature while stirring for 30 minutes. The solvent was removed under reduced pressure and the resulting oil was triturated with pentane to afford **4** as a pale yellow solid in quantitative yield.  $^1\text{H}$  NMR ( $\delta$ , CD<sub>2</sub>Cl<sub>2</sub>, 298 K): 9.41 (s, 1H, tz H), 8.23 (s, 1H, HC(pz)<sub>2</sub>(tz)), 7.84 (d, 2H, *o*-Ph), 7.55 (m, 3H, *m*-Ph and *p*-Ph), 6.06 (s, 2H, pz H), 4.36 (2H,  $^2J_{\text{Pt-H}} = 50$  Hz, CH<sub>2</sub>Cl), 2.634, 2.43 (s, 6H each, pz CH<sub>3</sub>), 1.48 (s, 6H,  $^2J_{\text{Pt-H}} = 71$  Hz, Pt-CH<sub>3</sub>).  $^{13}\text{C}$  NMR ( $\delta$ , CD<sub>2</sub>Cl<sub>2</sub>, 298 K): 152.7, 142.2 (pz C-CH<sub>3</sub>), 139.4 (tz 4-position), 136.0 (ipso-Ph), 130.5, (*p*-Ph), 130.3 (*m*-Ph), 124.2 (tz 5-position), 120.6 (*o*-Ph), 108.6 (pz CH), 60.6 (HC(pz)<sub>2</sub>(tz)), 20.3 ( $^1J_{\text{Pt-C}} = 841$  Hz, CH<sub>2</sub>Cl), 13.1, 10.8 (pz CH<sub>3</sub>), -5.6 ( $^1J_{\text{Pt-C}} = 717$  Hz, Pt-CH<sub>3</sub>).

$\text{C} = 662$  Hz, Pt-CH<sub>3</sub>). Anal Calcd for C<sub>22</sub>H<sub>30</sub>N<sub>7</sub>F<sub>5</sub>IPt: C, 37.28; H, 4.12; N, 13.83. Found: C, 37.58; H, 3.60; N, 13.51.

**[TpmPtMe<sub>2</sub>(CH<sub>2</sub>Cl)][Cl] 5.** A 50-mL Schlenk was charged with 0.030 g (0.05 mmol) of [PtMe<sub>2</sub>(SMe<sub>2</sub>)<sub>2</sub>] and 0.031 g (0.10 mmol) of tris(3,5-dimethylpyrazolyl)methane. The flask was purged with argon and CH<sub>2</sub>Cl<sub>2</sub> (10 mL) was added through the septum. The yellow solution was stirred 24 hours at room temperature. The solvent was removed under reduced pressure and the resulting oil was triturated with pentane to afford **5** as white solid in quantitative yield. <sup>1</sup>H NMR ( $\delta$ , CD<sub>2</sub>Cl<sub>2</sub>, 298 K): 7.96 (s, 1H, HC(pz)<sub>3</sub>), 6.19 (s, 1H, Pz H), 6.17 (s, 2H, pz H), 4.34 (s, 2H, <sup>2</sup>J<sub>Pt-H</sub> = 49 Hz, CH<sub>2</sub>Cl), 2.75, 2.34 (s, 3H each, pz CH<sub>3</sub>), 2.72, 2.45 (s, 6H each, pz CH<sub>3</sub>), 1.50 (s, 6H, <sup>2</sup>J<sub>Pt-H</sub> = 70 Hz, Pt-CH<sub>3</sub>). <sup>13</sup>C NMR ( $\delta$ , CD<sub>2</sub>Cl<sub>2</sub>, 298 K): 153.7, 153.5, 142.4, 141.7 (pz C-CH<sub>3</sub>), 110.1, 109.6 (pz CH), 69.7 (HC(pz)<sub>3</sub>), 20.9 (<sup>1</sup>J<sub>Pt-C</sub> = 840 Hz, CH<sub>2</sub>Cl), 13.2, 13.1, 12.1, 12.0, 11.9 (pz CH<sub>3</sub>), -6.6 (<sup>1</sup>J<sub>Pt-C</sub> = 670 Hz, Pt-CH<sub>3</sub>). Anal Calcd for C<sub>19</sub>H<sub>30</sub>N<sub>6</sub>Cl<sub>2</sub>Pt: C, 37.50; H, 4.97; N, 13.81. Found: C, 37.21; H, 3.60; N, 12.51.

**[bpztz<sup>Ph</sup>PtMe<sub>2</sub>(CH<sub>2</sub>CH<sub>2</sub>Cl)][BAr<sup>F</sup>] 6.** In the glove box, a vial was charged with 0.030 g (0.05 mmol) of [PtMe<sub>2</sub>(SMe<sub>2</sub>)<sub>2</sub>] and 0.037 g (0.10 mmol) of bpztz<sup>Ph</sup>. The solids were dissolved in 1,2-dichloroethane (0.4 ml) and the vial was capped. The yellow solution was stirred 3 days at room temperature. The solvent was removed under reduced pressure and dissolved in dichloromethane. The addition of 6.6  $\mu$ L (0.06 mmol) methyl trifluoromethanesulfonate followed by solvent removal under reduced pressure gave the triflate anion for the complex. Dissolving the complex in dichloromethane followed by addition of 0.05 g (0.06 mmol) NaB(Ar<sup>F</sup>)<sub>4</sub> followed by filtration gave the B(Ar<sup>F</sup>)<sub>4</sub> anion for the complex. The solvent was removed under reduced pressure resulting in a clear oil.

The resulting oil was triturated with pentane to afford **6** as a white solid in 67% yield (100 mg).  $^1\text{H}$  NMR ( $\delta$ , CD<sub>2</sub>Cl<sub>2</sub>, 298 K): 8.92 (s, 1H, tz H), 7.83 (s, 1H, HC(pz)<sub>2</sub>(tz)), 7.75, 7.57 (s, 8H, 4H, B(Ar<sup>F</sup>)<sub>4</sub>), 7.74 (d, 2H, *o*-Ph), 7.54 (m, 3H, *m*-Ph and *p*-Ph), 6.01 (s, 2H, pz H), 3.38 (m, 2H, PtCH<sub>2</sub>CH<sub>2</sub>Cl), 2.66, 2.40 (s, 6H each, pz CH<sub>3</sub>), 2.81 (m, 2H, PtCH<sub>2</sub>CH<sub>2</sub>Cl), 1.47 (s, 6H,  $^2J_{\text{Pt-H}} = 71$  Hz, Pt-CH<sub>3</sub>).  $^{13}\text{C}$  NMR ( $\delta$ , CD<sub>2</sub>Cl<sub>2</sub>, 298 K): 162.0 (B(Ar<sup>F</sup>)<sub>4</sub>), 153.3, 143.0 (pz C-CH<sub>3</sub>), 139.5 (tz 4-position), 136.3 (ipso-Ph), 131.0, (*p*-Ph), 130.7 (*m*-Ph), 129.3, 121, 117 (B(Ar<sup>F</sup>)<sub>4</sub>), 124.2 (tz 5-position), 121.0 (*o*-Ph), 109.4 (pz CH), 60.9 (HC(pz)<sub>2</sub>(tz)), 45 (PtCH<sub>2</sub>CH<sub>2</sub>Cl), 30.1 (PtCH<sub>2</sub>CH<sub>2</sub>Cl), 13.5, 10.1 (pz CH<sub>3</sub>), -6.1 ( $^1J_{\text{Pt-C}} = 675$  Hz, Pt-CH<sub>3</sub>).

**[bpztz<sup>Ph</sup>Me<sub>2</sub>PtCH<sub>2</sub>CH<sub>2</sub>PtMe<sub>2</sub>bpztz<sup>Ph</sup>][BAr<sup>F</sup>]<sub>2</sub> 7.** In the glove box, a vial was charged with 0.030 g (0.02 mmol) of **6** and 0.1mg (0.02 mmol) of NaOMe. The solids were dissolved in THF and the vial was capped overnight. The next morning the solvent was filtered away from the solid. The remaining solid was then washed with dichloromethane and the solution was collected. 0.022 g (0.025 mmol) of NaB(Ar<sup>F</sup>)<sub>4</sub> was added to the solution, and the solution was filtered. Removal of the solvent under reduced pressure resulted in a white powder to afford **7** in 41% yield (0.012 g).  $^1\text{H}$  NMR ( $\delta$ , CD<sub>2</sub>Cl<sub>2</sub>, 298 K): 8.41 (s, 2H, tz H), 7.71 (s, 16H, B(Ar<sup>F</sup>)<sub>4</sub>), 7.54 (s, 8H, B(Ar<sup>F</sup>)<sub>4</sub>), 7.70 (d, 4H, *o*-Ph), 7.62 (m, 6H, *m*-Ph and *p*-Ph), 7.36 (s, 2H, HC(pz)<sub>2</sub>(tz)), 6.10 (s, 2H, pz H), 6.00 (s, 2H, pz H), 2.92 (sloping doublets, 2H,  $^2J_{\text{Pt-H}} = 71$  Hz,  $^3J_{\text{Pt-H}} = 48$  Hz, PtCH<sub>2</sub>CH<sub>2</sub>HPt), 2.51 (s, 12 H, pz CH<sub>3</sub>), 2.47, 2.19 (s, 6H each, pz CH<sub>3</sub>), 2.06 (sloping doublets, 2H,  $^2J_{\text{Pt-H}} = 44$  Hz,  $^3J_{\text{Pt-H}} = 23$  Hz, PtCH<sub>2</sub>CH<sub>2</sub>HPt), 1.36 (s, 6H,  $^2J_{\text{Pt-H}} = 74$  Hz, Pt-CH<sub>3</sub>), 1.21 (s, 6H,  $^2J_{\text{Pt-H}} = 74$  Hz, Pt-CH<sub>3</sub>).  $^{13}\text{C}$  NMR ( $\delta$ , CD<sub>2</sub>Cl<sub>2</sub>, 298 K): 152.7, 142.8 (pz C-CH<sub>3</sub>), 142.2 (tz 4-position), 140.0 (ipso-Ph), 136.4, (*p*-Ph), 130.7 (*m*-Ph),

122.1 (tz 5-position), 120.1 (*o*-Ph), 109.3, 108.8 (pz CH), 60.9 (HC(pz)<sub>2</sub>(tz)), 16.2 (<sup>1</sup>J<sub>Pt-C</sub> = 622 Hz, <sup>2</sup>J<sub>Pt-C</sub> = 31 Hz, PtCH<sub>2</sub>CH<sub>2</sub>Pt), 14.1, 13.8, 11.5, 11.2 (pz CH<sub>3</sub>), -6.7 (<sup>1</sup>J<sub>Pt-C</sub> = 718 Hz, Pt-CH<sub>3</sub>), -9.2 (<sup>1</sup>J<sub>Pt-C</sub> = 730 Hz, Pt-CH<sub>3</sub>). Anal Calcd for C<sub>76</sub>H<sub>70</sub>N<sub>14</sub>ClF<sub>24</sub>BPt<sub>2</sub>: C, 44.06; H, 3.41; N, 9.47. Found: C, 43.62; H, 3.16; N, 9.51.

## REFERENCES

- (1) Zeise, W. C. *Ann. Phys.* **1827**, 9, 932.
- (2) Collman, J. P.; Hegedus, L. S.; Norton, J. R.; Finke, R. A. *Principles and Applications of Organotransition Metal Chemistry*, 2nd ed.; Mill Valley, CA.
- (3) Crabtree, R. H. *The Organometallic Chemistry of the Transition Metals*, 2nd ed.; Wiley: New York, 1994.
- (4) Kistner, C. R.; Hutchinson, J. H.; Doyle, J. R. *Inorg. Chem.* **1963**, 2, 1255.
- (5) Puddephatt, R. J. *Pure and Applied Chemistry* **1990**, 62, 1161.
- (6) Canty, A. J.; van Koten, G. *Acc. Chem. Res.* **1995**, 28, 406.
- (7) Togni, A.; Venanzi, L. M. *Angew. Chemie. Int. Ed.* **1994**, 33, 497.
- (8) Jensen, M. P.; Wick, D. D.; Reinartz, S.; White, P. S.; Templeton, J. L.; Goldberg, K. I. *J. Am. Chem. Soc.* **2003**, 125, 8614.
- (9) Frauhiger, B. E.; White, P. S.; Templeton, J. L. *Organometallics* **2011**, 31, 225.
- (10) Goldberg, K. I.; Yan, J. Y.; Winter, E. L. *J. Am. Chem. Soc.* **1994**, 116, 1573.
- (11) O'Reilly, S. A.; White, P. S.; Templeton, J. L. *J. Am. Chem. Soc.* **1996**, 118, 5684.
- (12) Reinartz, S.; White, P. S.; Brookhart, M.; Templeton, J. L. *Organometallics* **2000**, 19, 3748.
- (13) Tellers, D. M.; Yung, C. M.; Arndtsen, B. A.; Adamson, D. R.; Bergman, R. G. *J. Am. Chem. Soc.* **2002**, 124, 1400.
- (14) Butts, M. D.; Scott, B. L.; Kubas, G. J. *J. Am. Chem. Soc.* **1996**, 118, 11831.
- (15) Kulawiec, R. J.; Crabtree, R. H. *Coord. Chem. Rev.* **1990**, 99, 89.
- (16) Burkhill, H. A.; Vilar, R.; White, A. *Inorganica. Chimica. Acta.* **2006**, 359, 3709.
- (17) Ho, J.; Black, D.; Messerle, B. A.; Clegg, J. K. *Organometallics* **2006**, 25, 5800.
- (18) Ito, J.; Miyakawa, T.; Nishiyama, H. *Organometallics* **2006**, 25, 5216.
- (19) Tejel, C.; Ciriano, M. A.; López, J. A.; Jiménez, S.; Bordonaba, M.; Oro, L. A. *Chem. Eur. J.* **2007**, 13, 2044.

- (20) Jiao, Y.; Brennessel, W. W.; Jones, W. D. *Organometallics* **2015**, *34*, 1552.
- (21) Wei, M. L.; Wayland, B. B. *Organometallics* **1996**, *15*, 4681.
- (22) Campazzi, E.; Solari, E.; Scopelliti, R.; Floriani, C. *Chem. Commun.* **1999**, 1617.
- (23) de Bruin, B.; Hetterscheid, D. G. H. *Eur. J. Inorg. Chem.* **2007**, *2007*, 211.

**Table 5** Crystal data and structural refinement parameters complex [bpztz<sup>Ph</sup>PtMe<sub>2</sub>C(O)CH<sub>3</sub>][OTf] (**2**).

---

<b>Empirical formula</b>	C <sub>24</sub> H <sub>30</sub> F <sub>3</sub> N <sub>7</sub> O <sub>4</sub> PtS
<b>Formula weight</b>	764.70
<b>Temperature/K</b>	100.15
<b>Crystal system</b>	triclinic
<b>Space group</b>	P-1
<b>a/Å</b>	9.5435(7)
<b>b/Å</b>	10.9989(7)
<b>c/Å</b>	13.7606(9)
<b>α/°</b>	78.506(3)
<b>β/°</b>	77.315(4)
<b>γ/°</b>	85.146(3)
<b>Volume/Å<sup>3</sup></b>	1379.64(16)
<b>Z</b>	2
<b>ρ<sub>calc</sub>g/cm<sup>3</sup></b>	1.841
<b>μ/mm<sup>-1</sup></b>	10.795
<b>F(000)</b>	752.0
<b>Crystal size/mm<sup>3</sup></b>	0.304 × 0.166 × 0.074
<b>Radiation</b>	CuKα ( $\lambda = 1.54178$ )
<b>2Θ range for data collection/°</b>	6.7 to 140.2
<b>Index ranges</b>	-11 ≤ h ≤ 11, -13 ≤ k ≤ 13, -16 ≤ l ≤ 16

<b>Reflections collected</b>	82587
<b>Independent reflections</b>	5106 [ $R_{\text{int}} = 0.0394$ , $R_{\text{sigma}} = 0.0166$ ]
<b>Data/restraints/parameters</b>	5106/0/368
<b>Goodness-of-fit on <math>F^2</math></b>	1.140
<b>Final R indexes [<math>I \geq 2\sigma(I)</math>]</b>	$R_1 = 0.0385$ , $wR_2 = 0.0923$
<b>Final R indexes [all data]</b>	$R_1 = 0.0406$ , $wR_2 = 0.0936$
<b>Largest diff. peak/hole / e Å<sup>-3</sup></b>	2.36/-1.39

**Table 6** Crystal data and structural refinement parameters complex [TpmpMe<sub>2</sub>C(O)CH<sub>3</sub>][OTf] (**3**).

---

<b>Empirical formula</b>	C <sub>21</sub> H <sub>31</sub> F <sub>3</sub> N <sub>6</sub> O <sub>4</sub> PtS
<b>Formula weight</b>	715.67
<b>Temperature/K</b>	100
<b>Crystal system</b>	orthorhombic
<b>Space group</b>	Pbca
<b>a/Å</b>	15.5752(2)
<b>b/Å</b>	13.7902(2)
<b>c/Å</b>	23.7500(3)
<b>α/°</b>	90
<b>β/°</b>	90
<b>γ/°</b>	90
<b>Volume/Å<sup>3</sup></b>	5101.15(12)
<b>Z</b>	8
<b>ρ<sub>calc</sub>g/cm<sup>3</sup></b>	1.864
<b>μ/mm<sup>-1</sup></b>	11.609
<b>F(000)</b>	2816.0
<b>Crystal size/mm<sup>3</sup></b>	0.218 × 0.214 × 0.09
<b>Radiation</b>	CuKα ( $\lambda = 1.54178$ )
<b>2Θ range for data collection/°</b>	7.444 to 144.254
<b>Index ranges</b>	-19 ≤ h ≤ 19, -14 ≤ k ≤ 17, -28 ≤ l ≤ 29

<b>Reflections collected</b>	42651
<b>Independent reflections</b>	4988 [ $R_{\text{int}} = 0.0315$ , $R_{\text{sigma}} = 0.0171$ ]
<b>Data/restraints/parameters</b>	4988/90/361
<b>Goodness-of-fit on <math>F^2</math></b>	1.167
<b>Final R indexes [<math>I \geq 2\sigma(I)</math>]</b>	$R_1 = 0.0381$ , $wR_2 = 0.0811$
<b>Final R indexes [all data]</b>	$R_1 = 0.0389$ , $wR_2 = 0.0816$
<b>Largest diff. peak/hole / e Å<sup>-3</sup></b>	2.20/-1.54

**Table 7** Crystal data and structural refinement parameters complex [bpztz<sup>Ph</sup>PtMe<sub>2</sub>CH<sub>2</sub>Cl][BF<sub>4</sub>] (**4**).

---

<b>Empirical formula</b>	C <sub>22</sub> H <sub>29</sub> BClF <sub>4</sub> N <sub>7</sub> Pt
<b>Formula weight</b>	708.87
<b>Temperature/K</b>	100
<b>Crystal system</b>	monoclinic
<b>Space group</b>	P2 <sub>1</sub> /c
<b>a/Å</b>	21.6316(5)
<b>b/Å</b>	10.1043(2)
<b>c/Å</b>	23.7979(6)
<b>α/°</b>	90
<b>β/°</b>	95.9347(11)
<b>γ/°</b>	90
<b>Volume/Å<sup>3</sup></b>	5173.7(2)
<b>Z</b>	8
<b>ρ<sub>calc</sub>g/cm<sup>3</sup></b>	1.820
<b>μ/mm<sup>-1</sup></b>	11.579
<b>F(000)</b>	2768.0
<b>Crystal size/mm<sup>3</sup></b>	0.222 × 0.181 × 0.075
<b>Radiation</b>	CuKα ( $\lambda = 1.54178$ )
<b>2Θ range for data collection/°</b>	4.106 to 133.198
<b>Index ranges</b>	-24 ≤ h ≤ 25, -12 ≤ k ≤ 12, -28 ≤ l ≤ 28

<b>Reflections collected</b>	63378
<b>Independent reflections</b>	9023 [ $R_{\text{int}} = 0.0443$ , $R_{\text{sigma}} = 0.0268$ ]
<b>Data/restraints/parameters</b>	9023/0/661
<b>Goodness-of-fit on <math>F^2</math></b>	1.070
<b>Final R indexes [<math>I \geq 2\sigma(I)</math>]</b>	$R_1 = 0.0330$ , $wR_2 = 0.0852$
<b>Final R indexes [all data]</b>	$R_1 = 0.0368$ , $wR_2 = 0.0875$
<b>Largest diff. peak/hole / e Å<sup>-3</sup></b>	1.36/-1.56

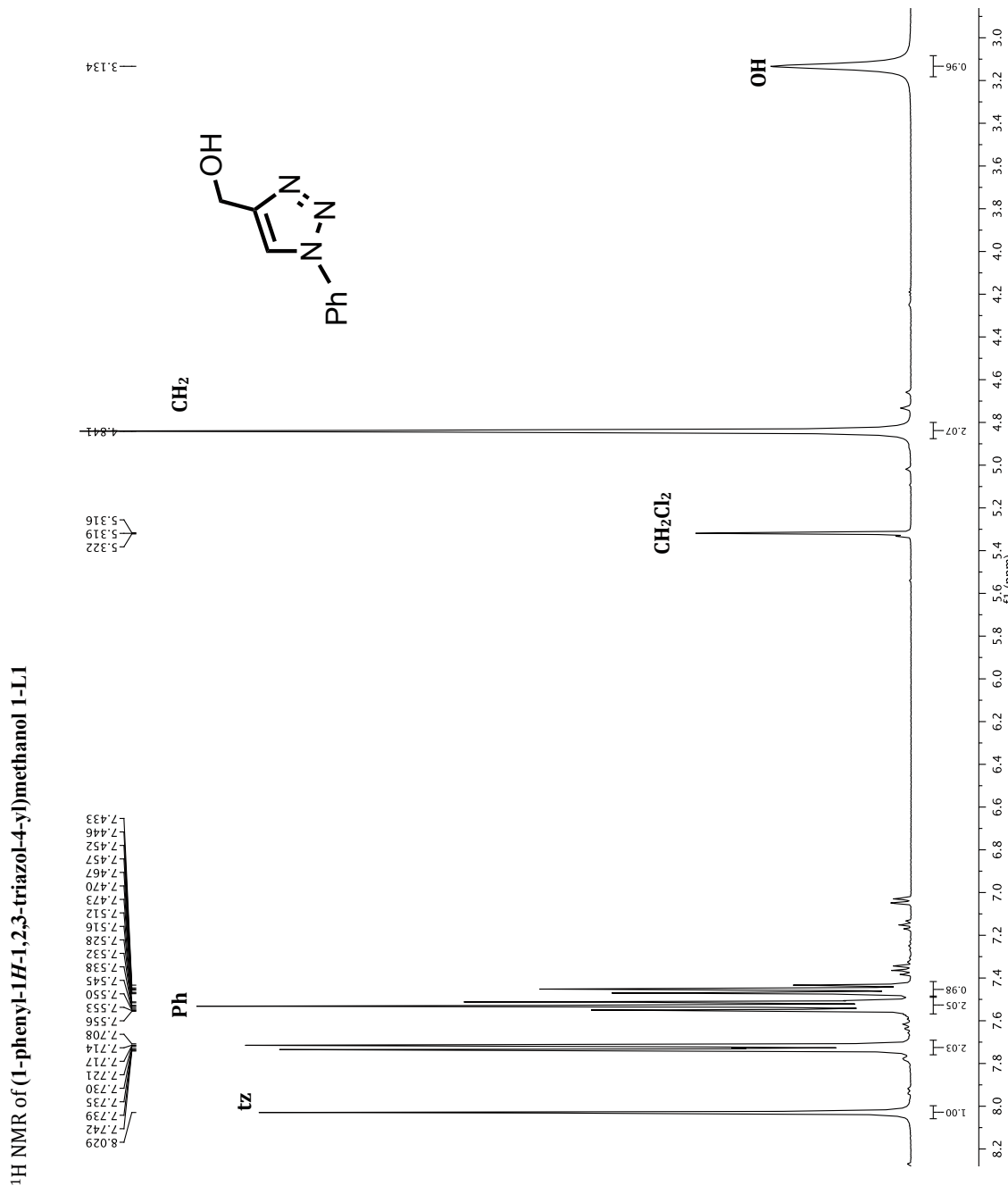
**Table 8** Crystal data and structural refinement parameters complex [TpmpPtMe<sub>2</sub>CH<sub>2</sub>Cl][Cl] (**5**).

<b>Empirical formula</b>	C <sub>19</sub> H <sub>30</sub> Cl <sub>2</sub> N <sub>6</sub> Pt
<b>Formula weight</b>	608.48
<b>Temperature/K</b>	100
<b>Crystal system</b>	monoclinic
<b>Space group</b>	P2 <sub>1</sub> /c
<b>a/Å</b>	13.4026(12)
<b>b/Å</b>	15.9431(14)
<b>c/Å</b>	11.1625(10)
<b>α/°</b>	90
<b>β/°</b>	113.265(2)
<b>γ/°</b>	90
<b>Volume/Å<sup>3</sup></b>	2191.2(3)
<b>Z</b>	4
<b>ρ<sub>calc</sub>g/cm<sup>3</sup></b>	1.844
<b>μ/mm<sup>-1</sup></b>	14.356
<b>F(000)</b>	1192.0
<b>Crystal size/mm<sup>3</sup></b>	0.251 × 0.169 × 0.146
<b>Radiation</b>	CuKα ( $\lambda = 1.54178$ )
<b>2Θ range for data collection/°</b>	7.18 to 144.774
<b>Index ranges</b>	-16 ≤ h ≤ 16, -18 ≤ k ≤ 19, -13 ≤ l ≤ 13

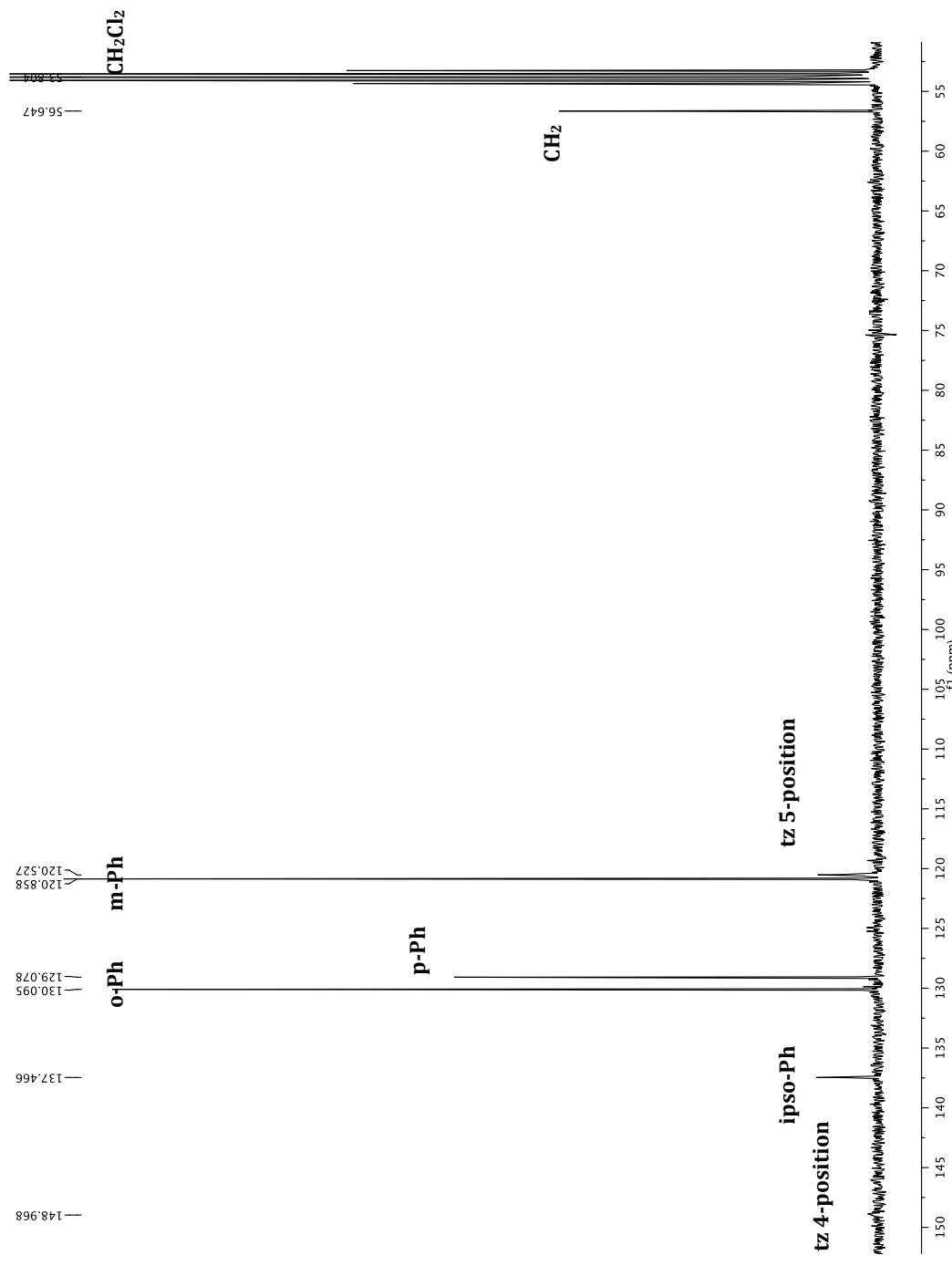
<b>Reflections collected</b>	26590
<b>Independent reflections</b>	4315 [ $R_{\text{int}} = 0.0288$ , $R_{\text{sigma}} = 0.0200$ ]
<b>Data/restraints/parameters</b>	4315/1/285
<b>Goodness-of-fit on <math>F^2</math></b>	1.304
<b>Final R indexes [<math>I \geq 2\sigma(I)</math>]</b>	$R_1 = 0.0311$ , $wR_2 = 0.0660$
<b>Final R indexes [all data]</b>	$R_1 = 0.0314$ , $wR_2 = 0.0662$
<b>Largest diff. peak/hole / e Å<sup>-3</sup></b>	0.91/-1.18

## APPENDIX 2.1

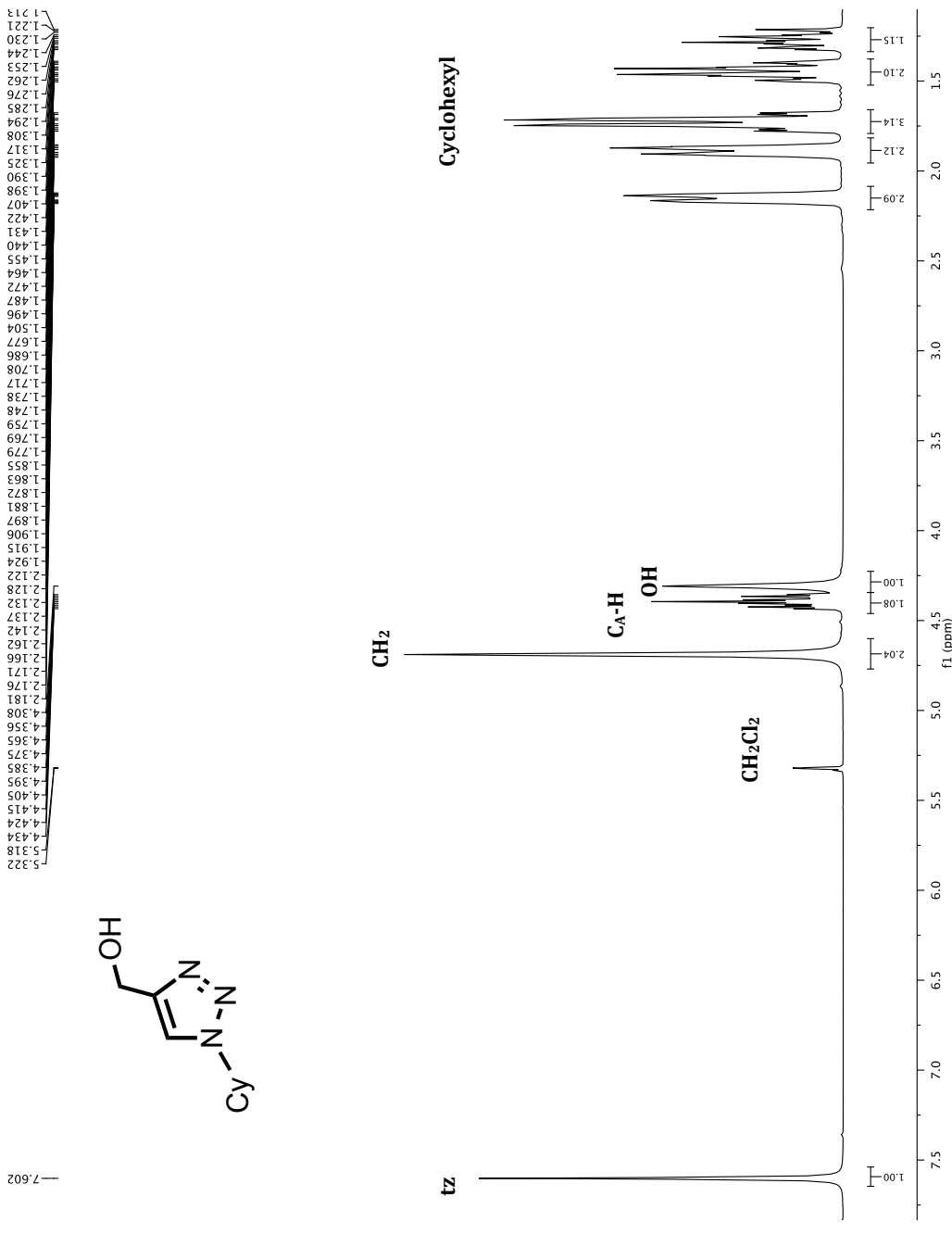
### Representative NMR Data for Chapter 2



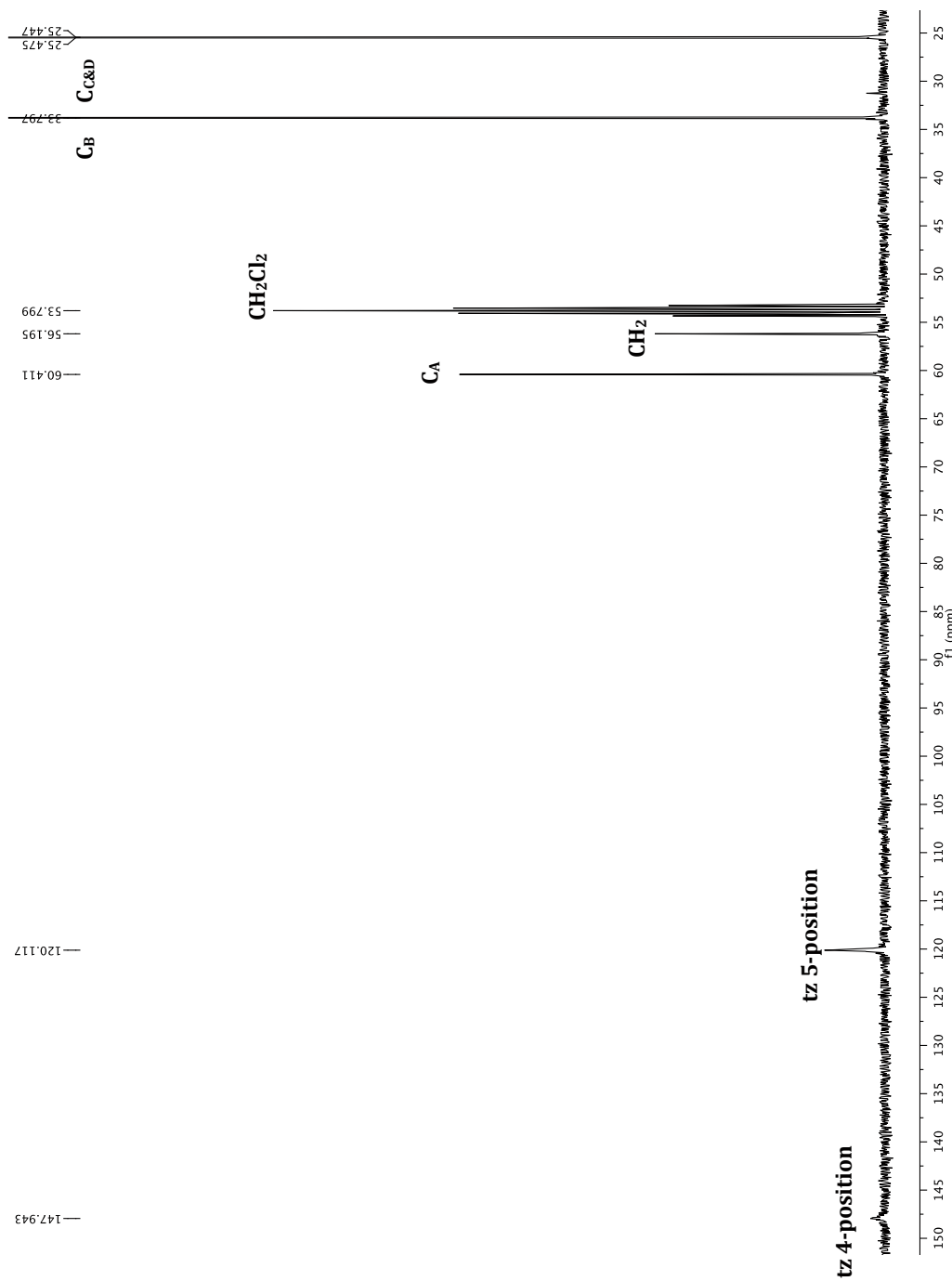
<sup>13</sup>C NMR of (1-phenyl-1*H*-1,2,3-triazol-4-yl)methanol 1-L1



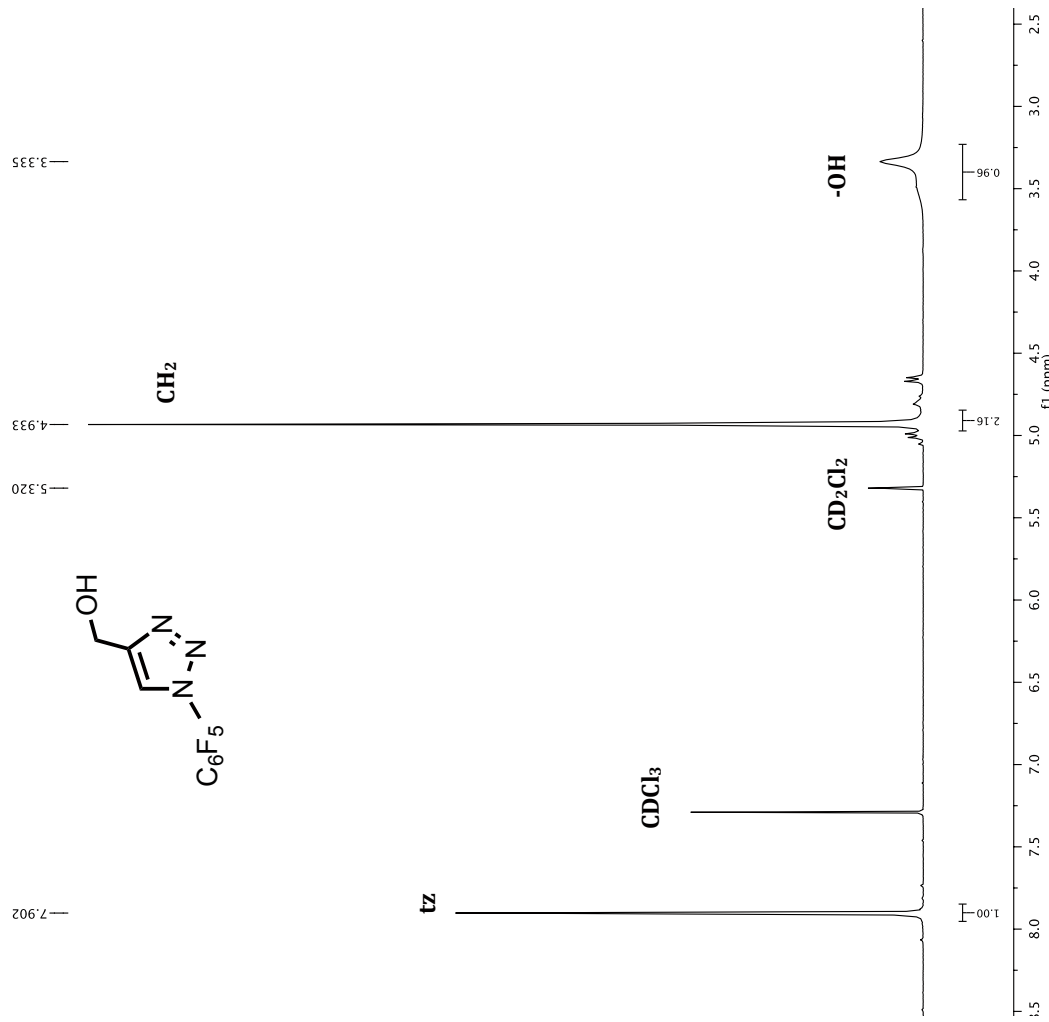
<sup>1</sup>H NMR of (1-cyclohexyl-1*H*-1,2,3-triazol-4-yl)methanol 1-L2

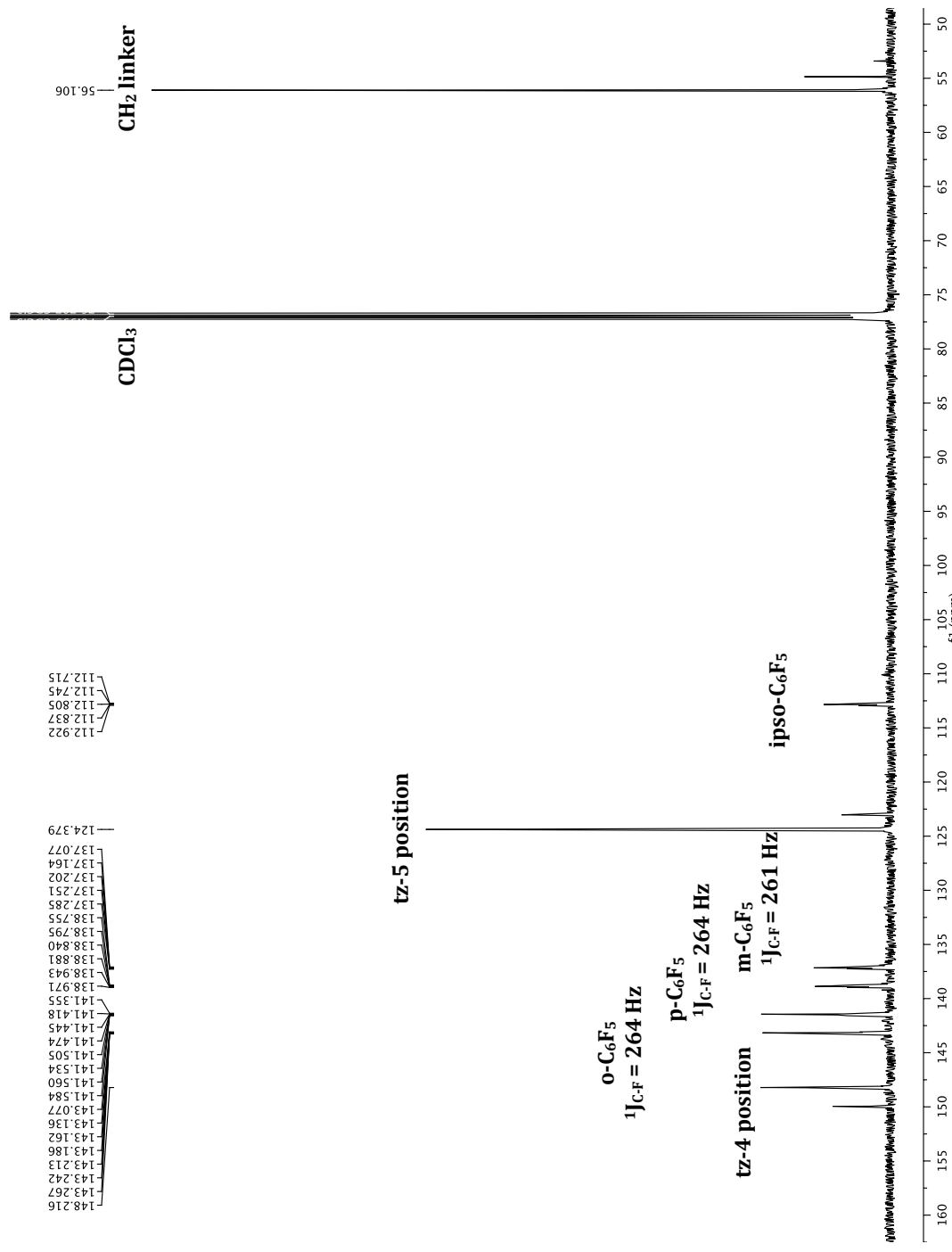


<sup>13</sup>C NMR of (1-cyclohexyl-1*H*-1,2,3-triazol-4-*y*)methanol 1-L2

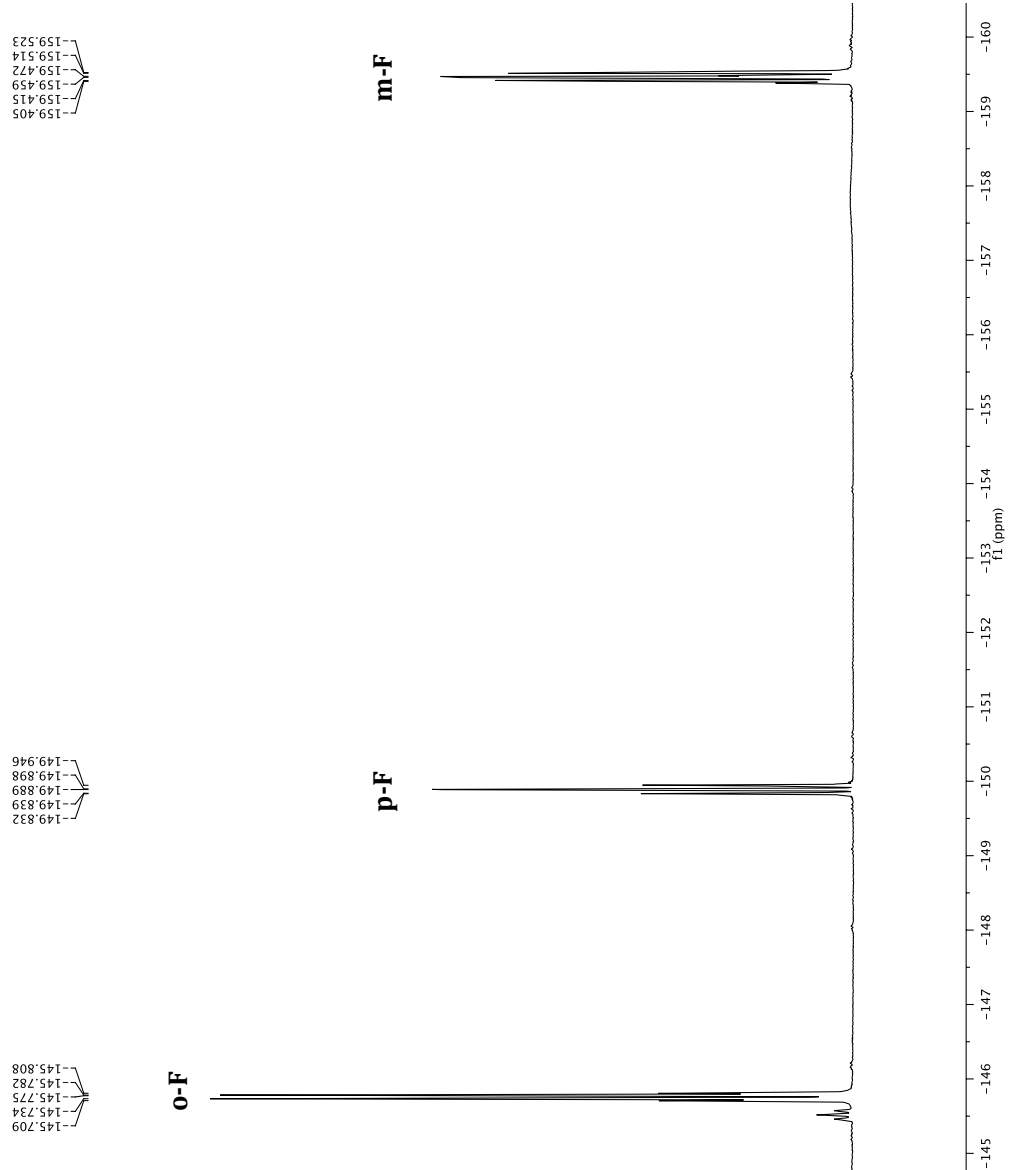


<sup>1</sup>H NMR of (1-pentafluorophenyl-1*H*-1,2,3-triazol-4-yl)methanol 1-L3

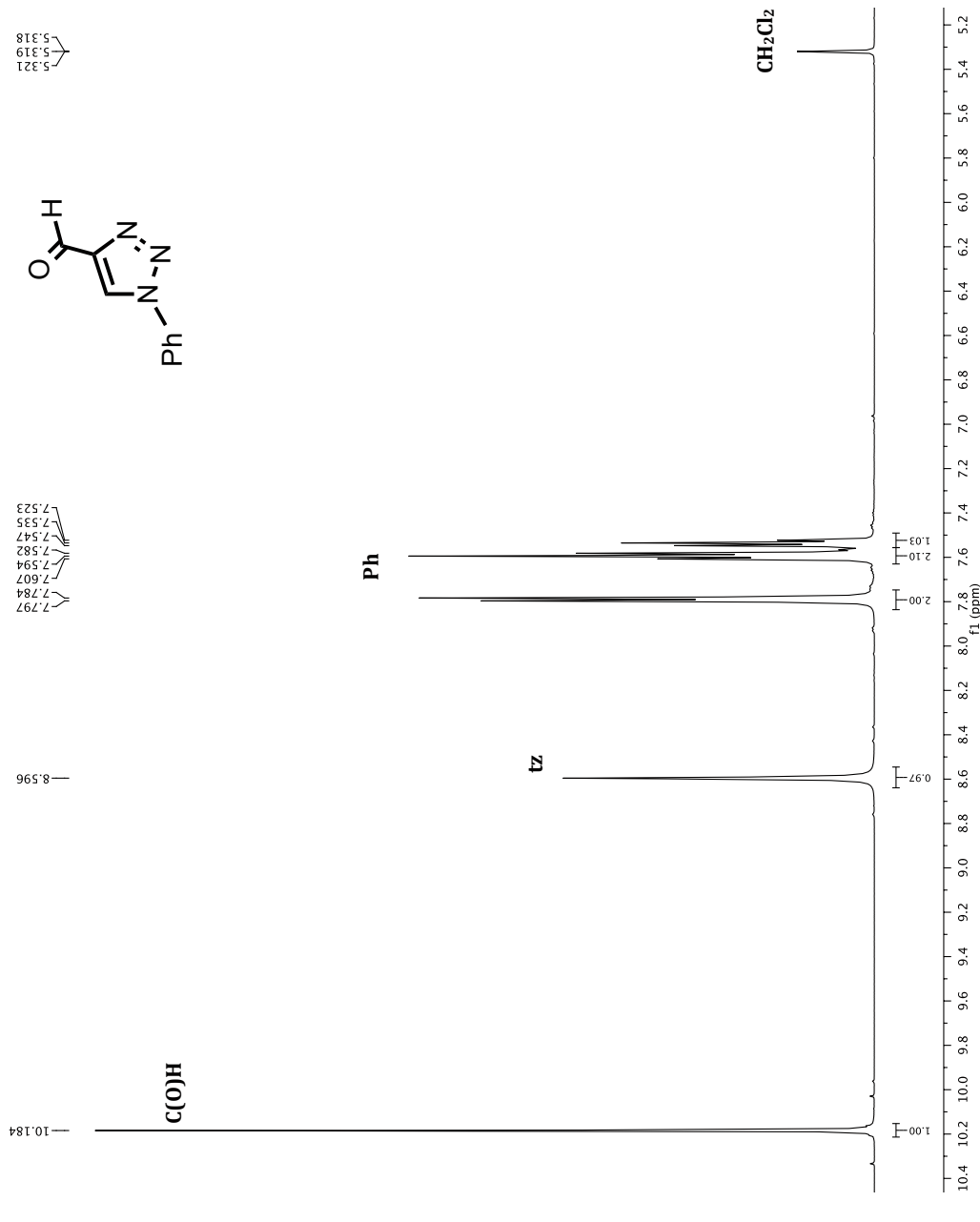


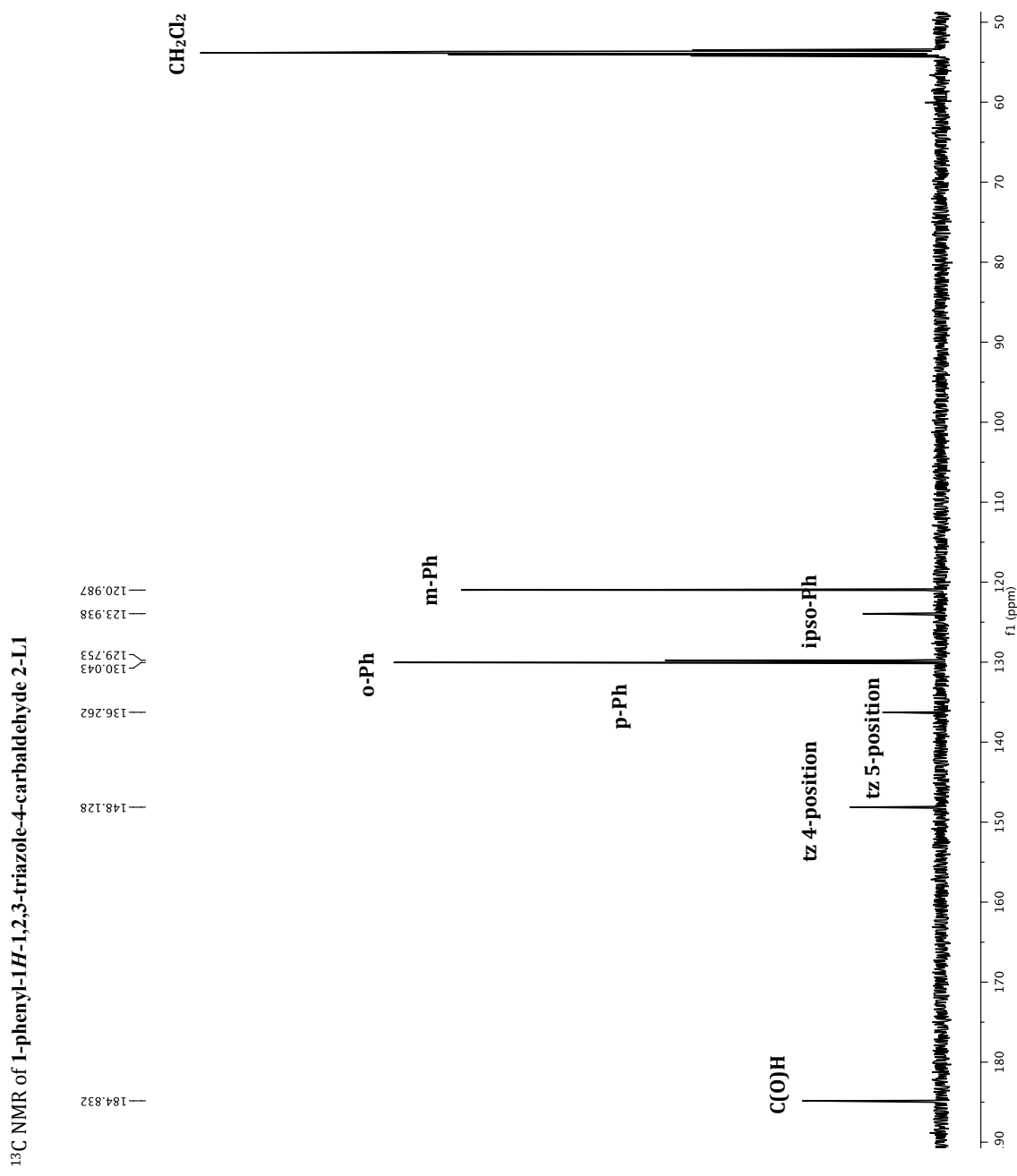


<sup>19</sup>F NMR of (1-pentafluorophenyl-1*H*-1,2,3-triazol-4-yl)methanol 1-L3

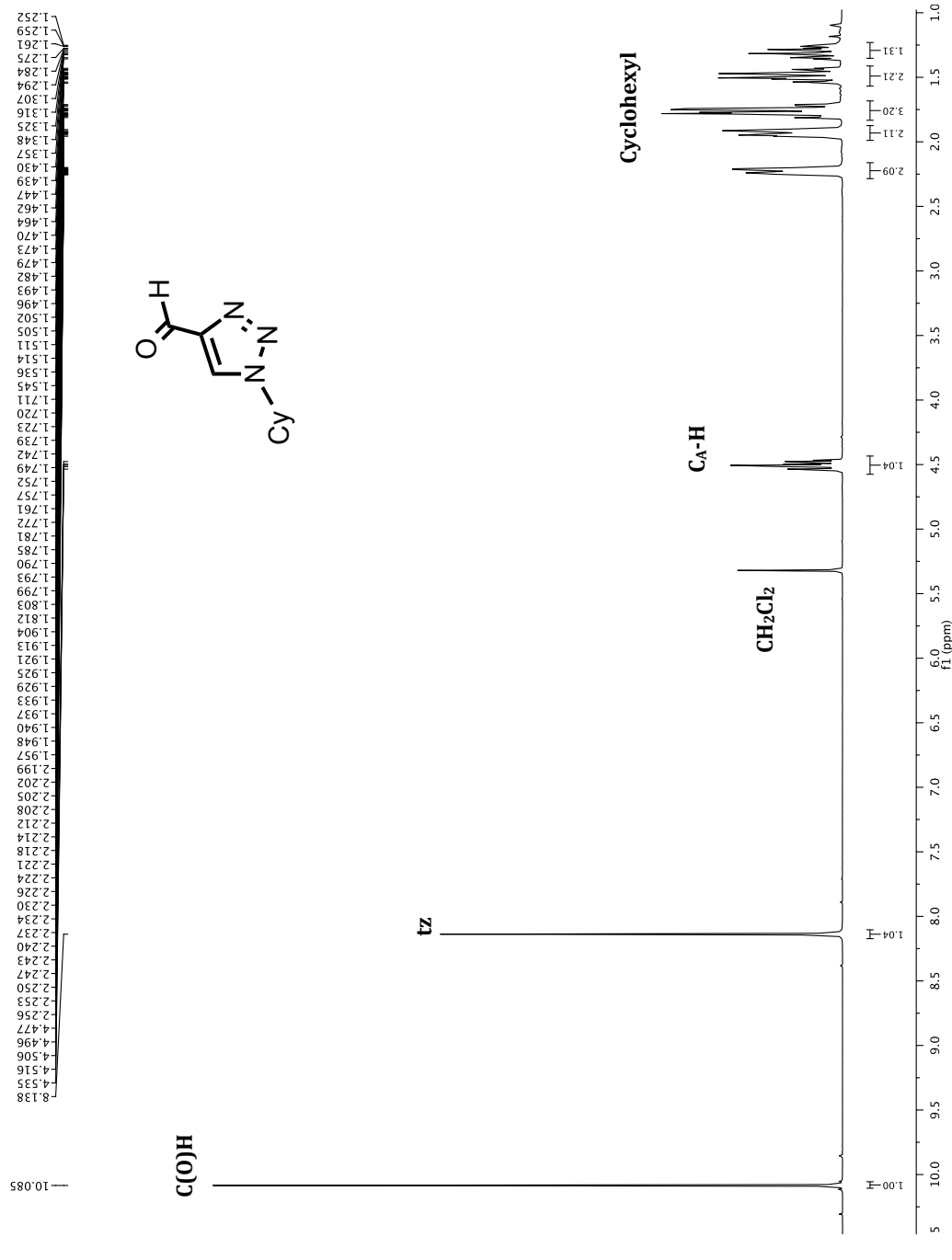


<sup>1</sup>H NMR of 1-phenyl-1*H*-1,2,3-triazole-4-carbaldehyde 2-L1

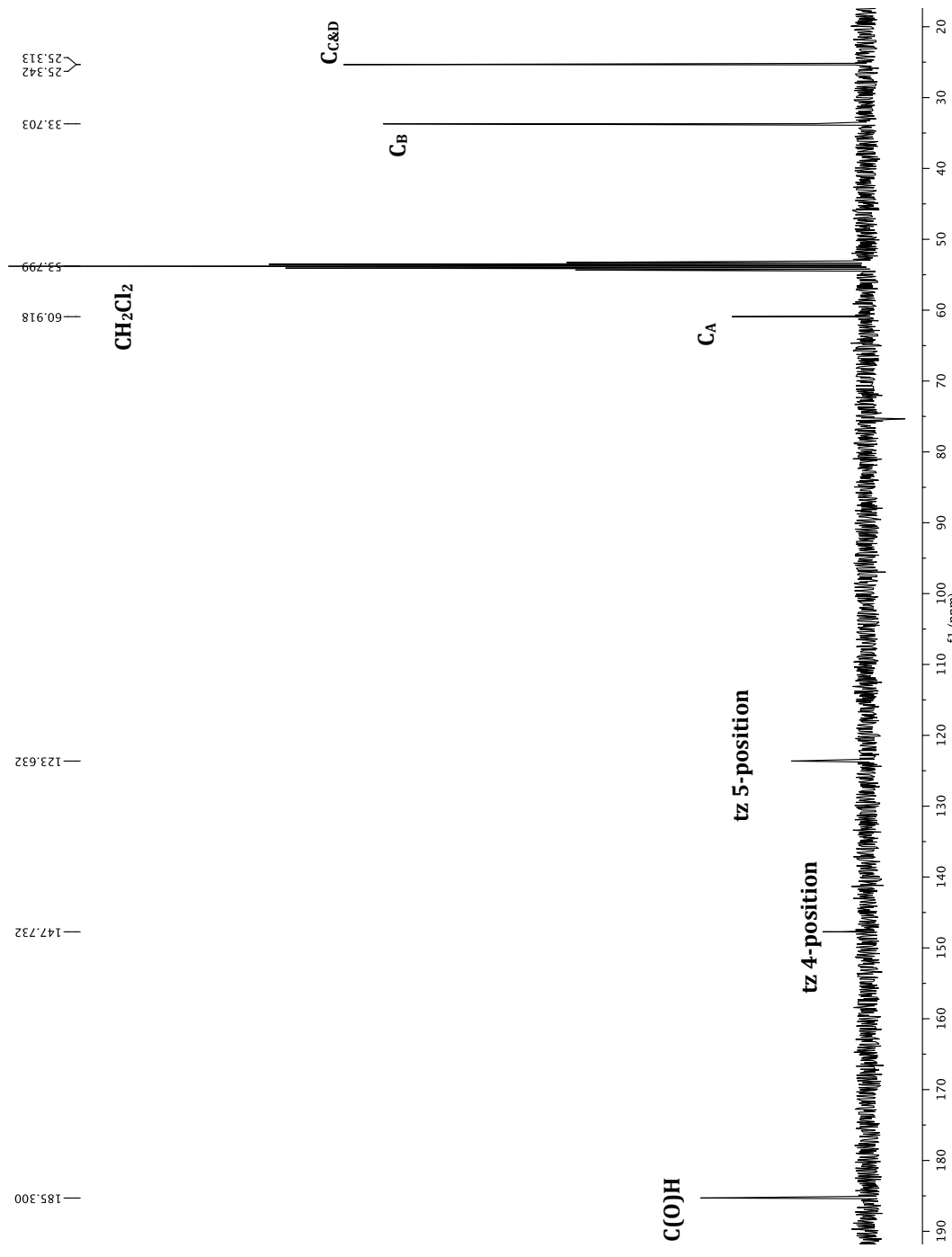




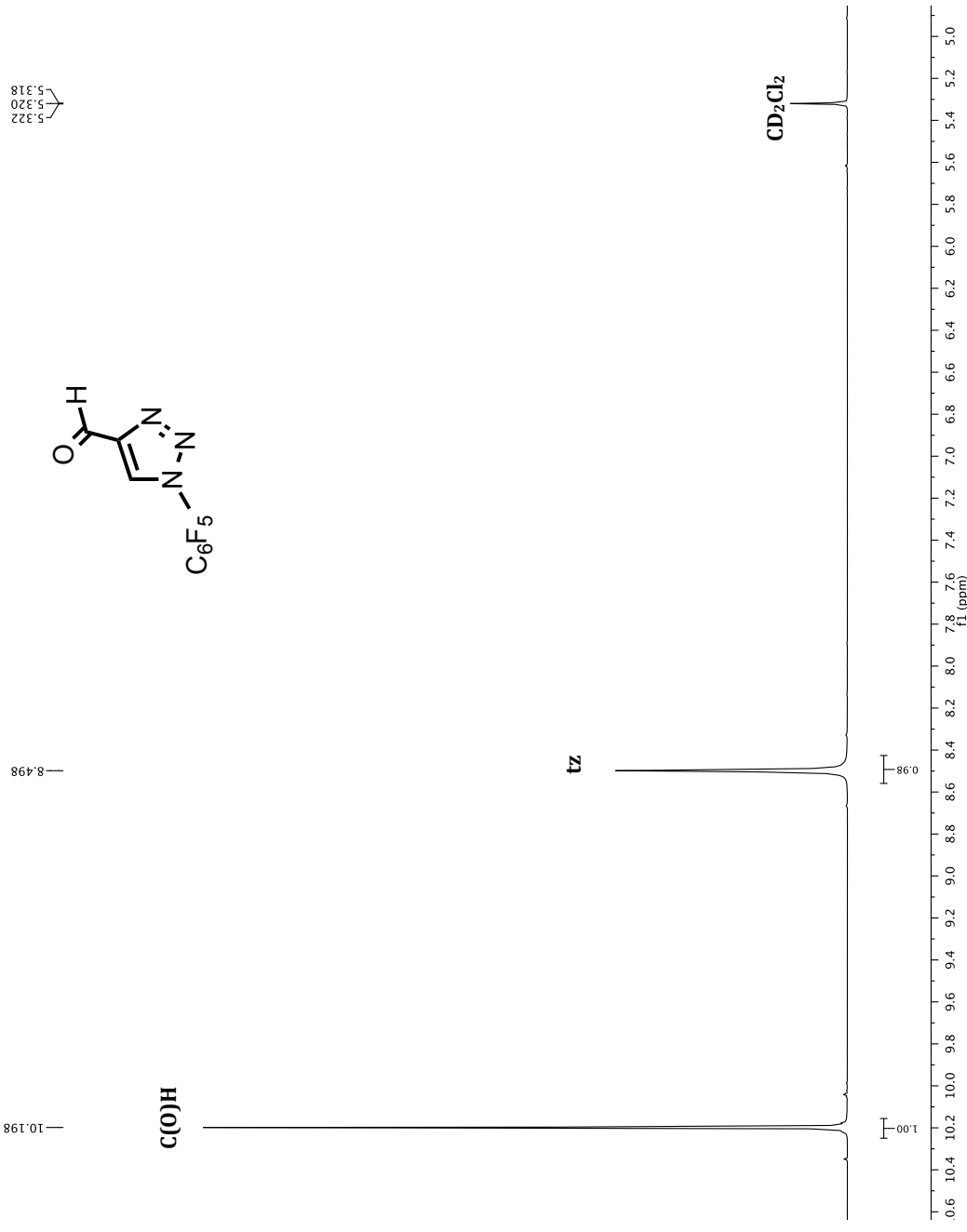
<sup>1</sup>H NMR of 1-cyclohexyl-1*H*-1,2,3-triazole-4-carbaldehyde 2-L2



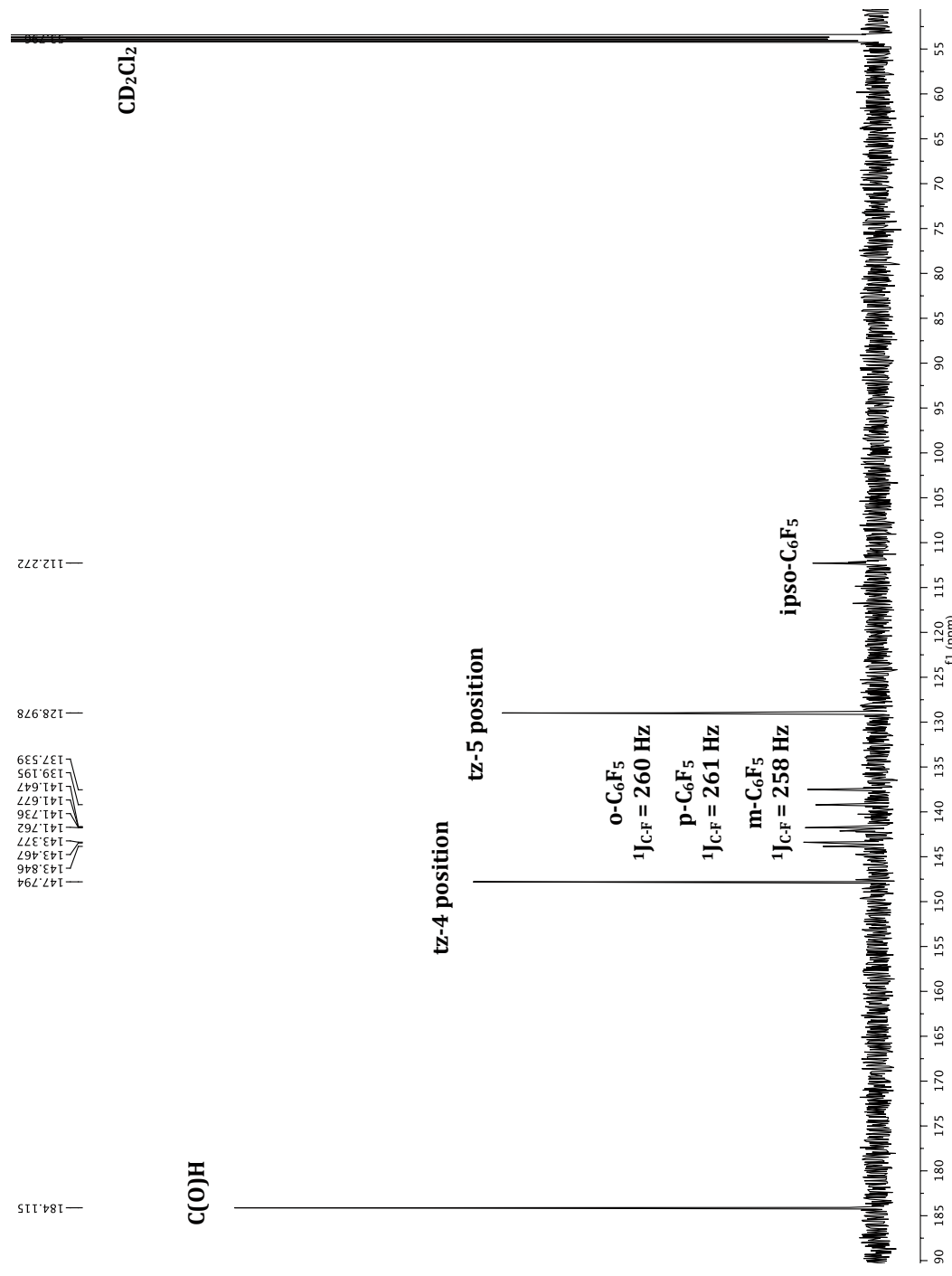
<sup>13</sup>C NMR of 1-cyclohexyl-1*H*-1,2,3-triazole-4-carbaldehyde 2-1.2



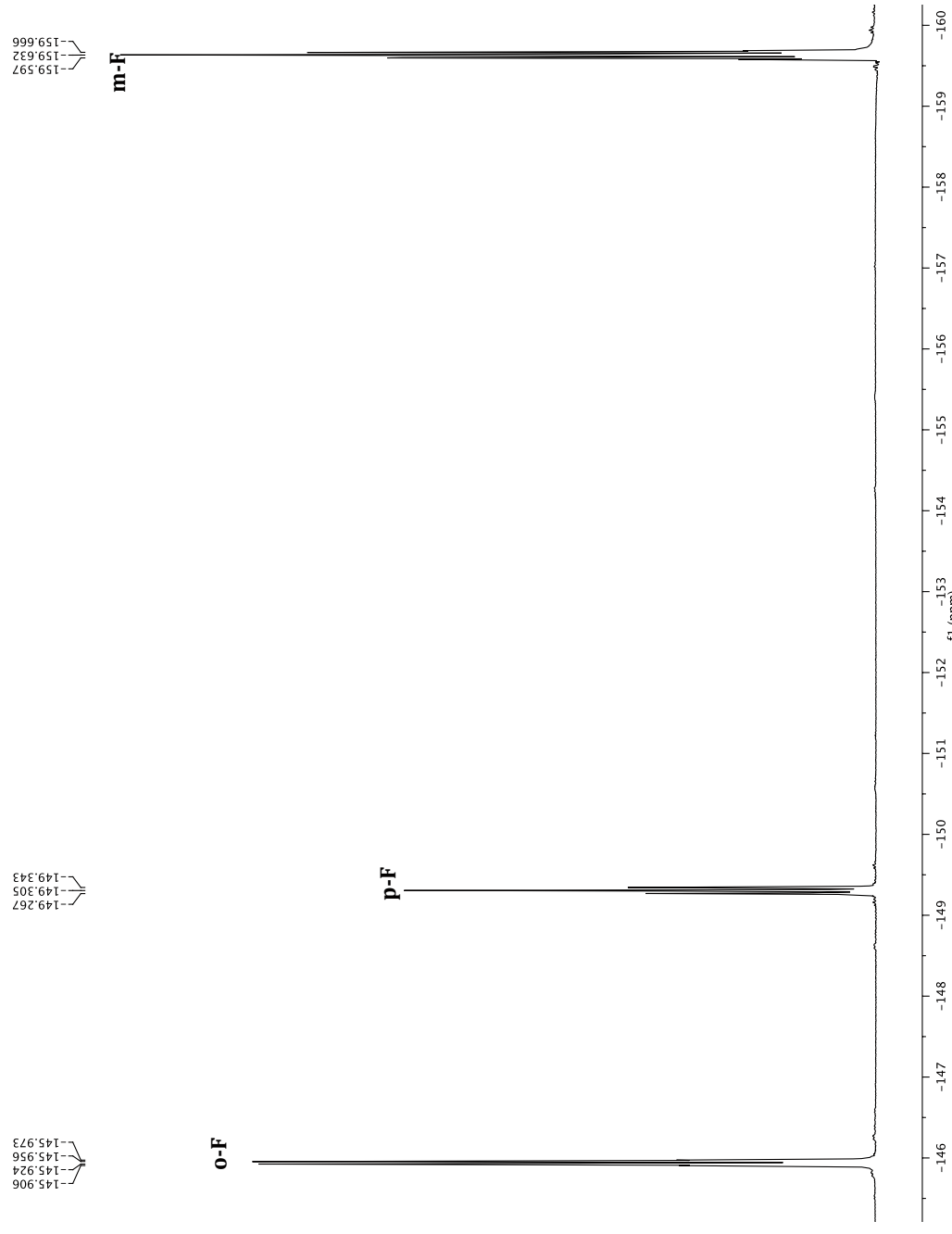
<sup>1</sup>H NMR of 1-pentafluorophenyl-1*H*-1,2,3-triazole-4-carbaldehyde 2-L3



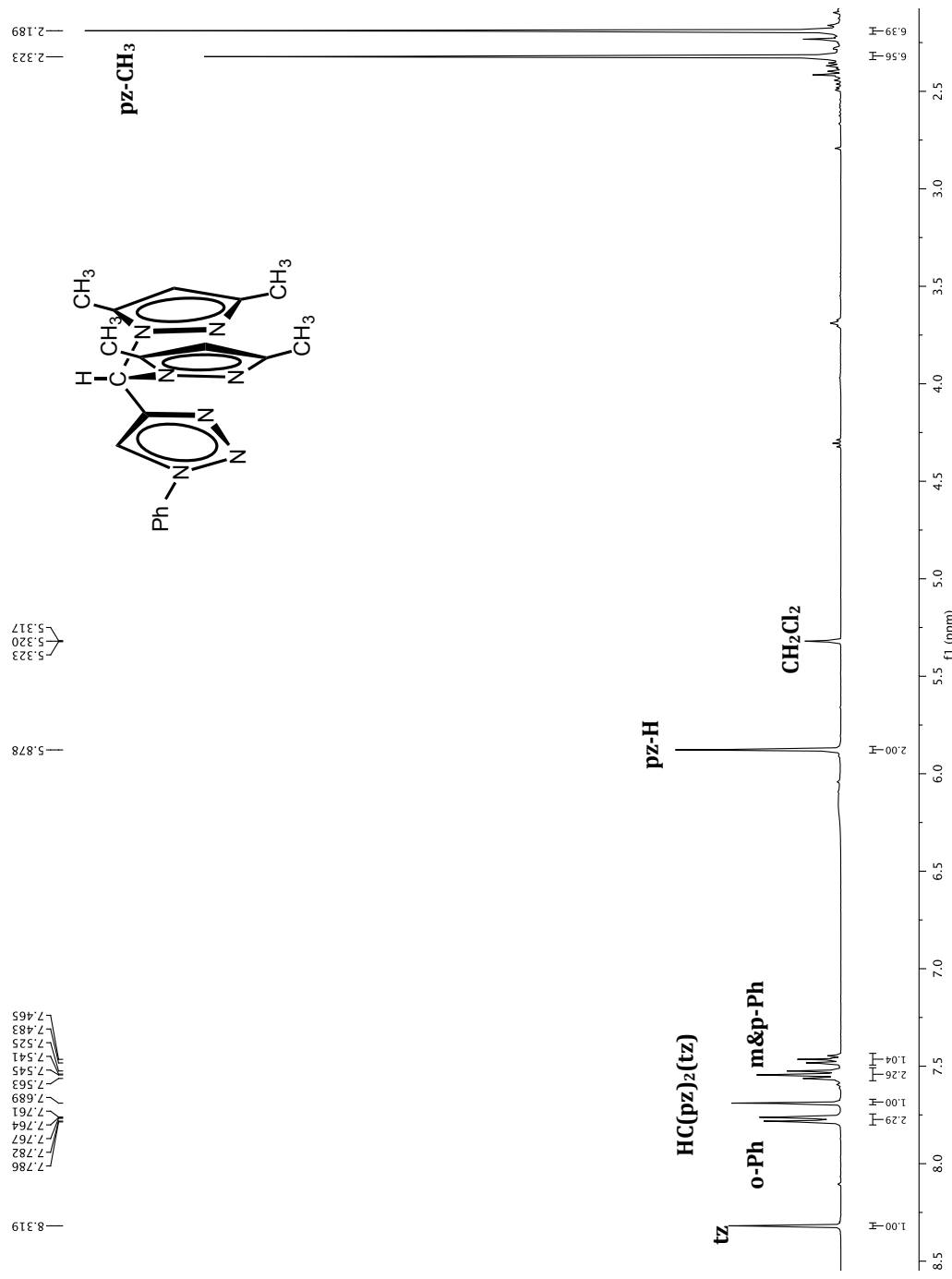
<sup>13</sup>C NMR of 1-pentafluorophenyl-1*H*-1,2,3-triazole-4-carbaldehyde 2-L3



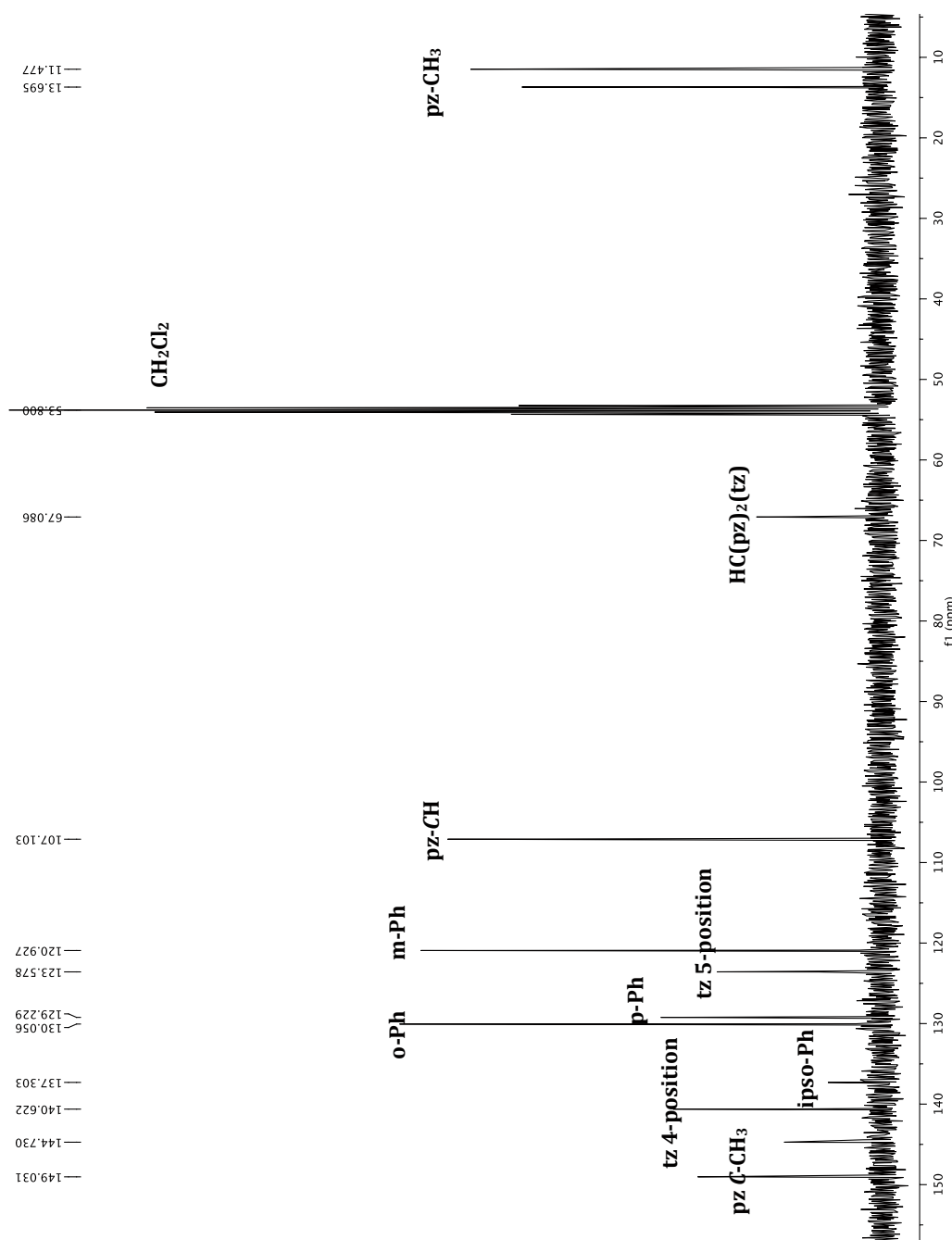
<sup>19</sup>F NMR of 1-pentafluorophenyl-1*H*-1,2,3-triazole-4-carbaldehyde 2-L3



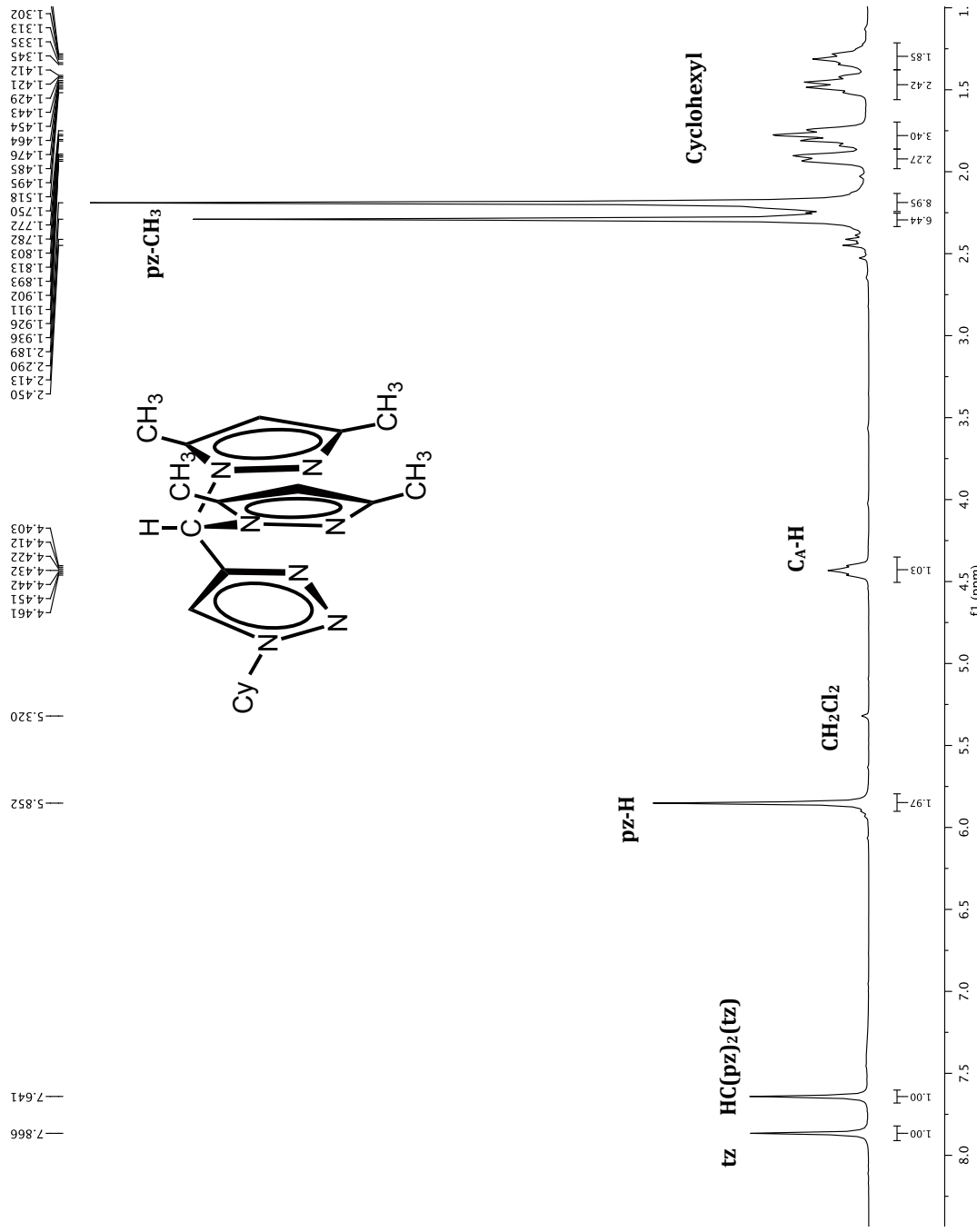
<sup>1</sup>H NMR of 4-(bis(3,5-dimethyl-1*H*-pyrazol-1-yl)methyl)-1-phenyl-1*H*-1,2,3-triazole (bp<sub>tz</sub><sup>Ph</sup>) 4-L1



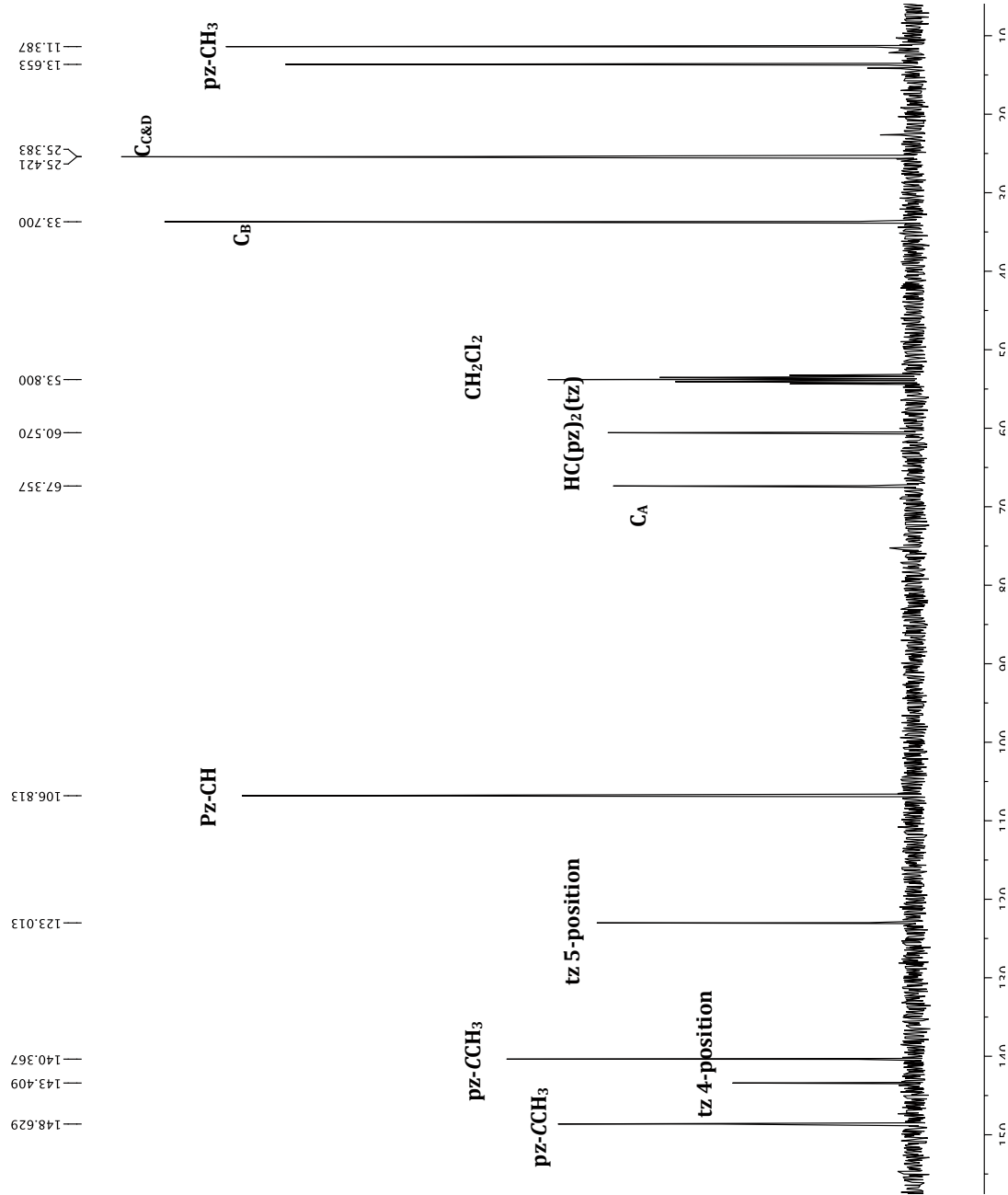
<sup>13</sup>C NMR of 4-(bis(3,5-dimethyl-1*H*-pyrazol-1-yl)methyl)-1-phenyl-1*H*-1,2,3-triazole (bpztz<sup>Pb</sup>) 4-L1

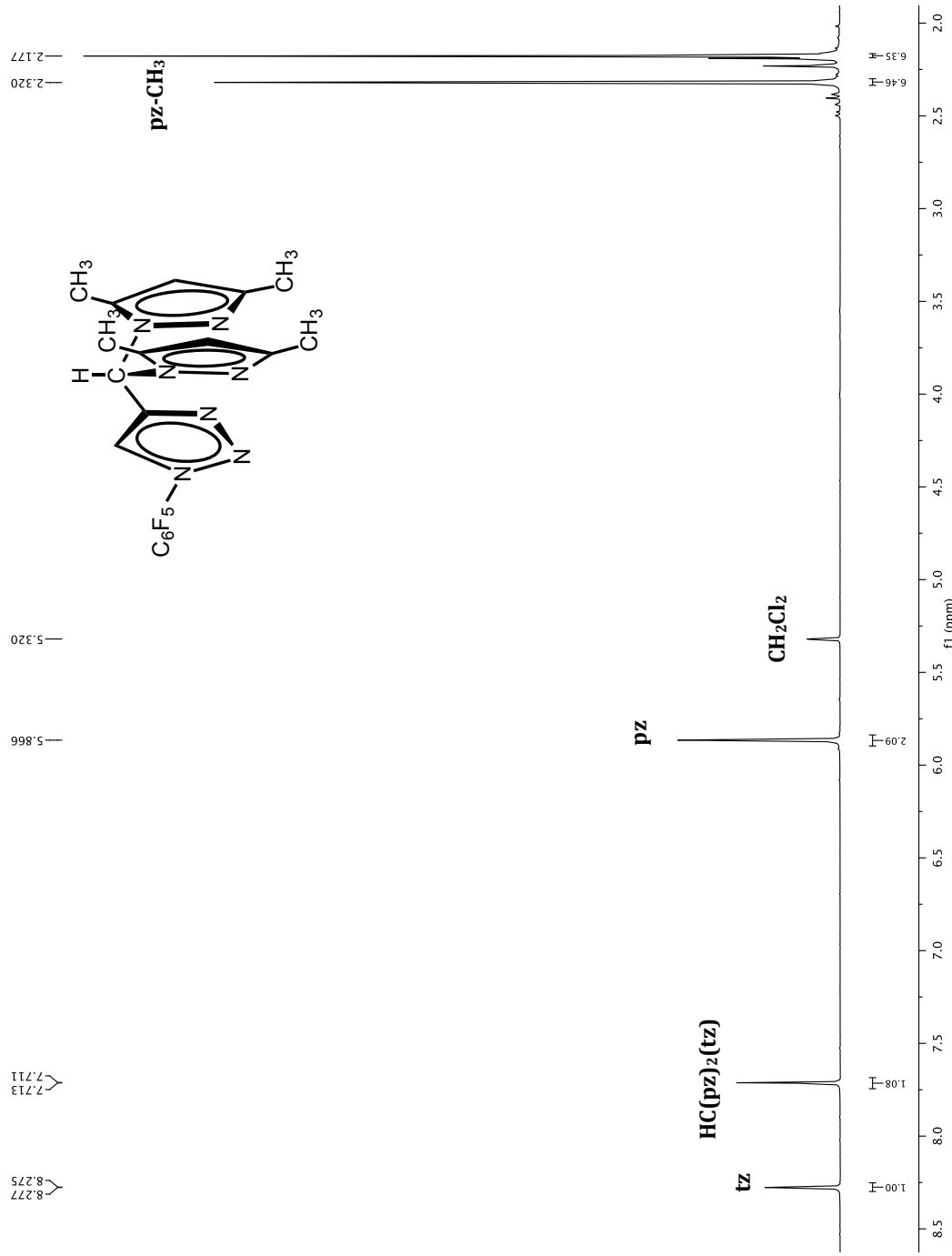
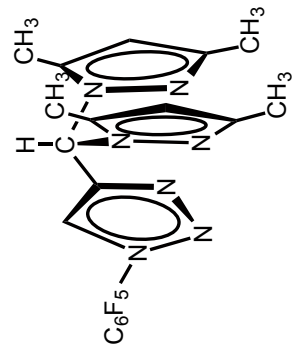
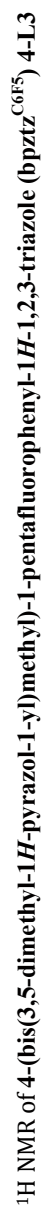


<sup>1</sup>H NMR of 4-(bis(3,5-dimethyl-1*H*-pyrazol-1-*y*)dimethyl)-1-cyclohexyl-1*H*-1,2,3-triazole (*bpztcy*) 4-L2

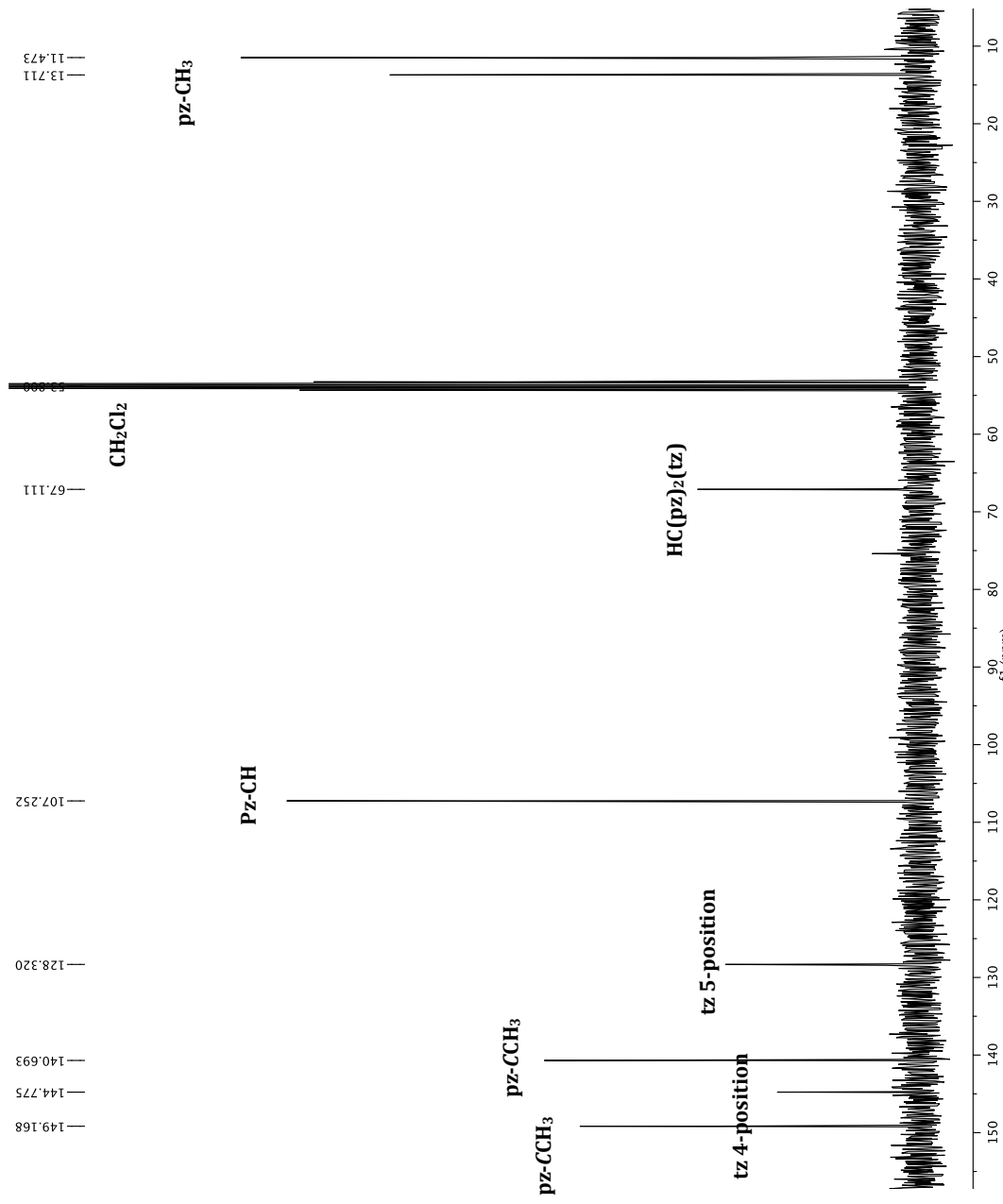


<sup>13</sup>C NMR of 4-(bis(3,5-dimethyl-1*H*-pyrazol-1-yl)methyl)-1-cyclohexyl-1*H*-1,2,3-triazole (bpztz<sup>CY</sup>) 4-L2

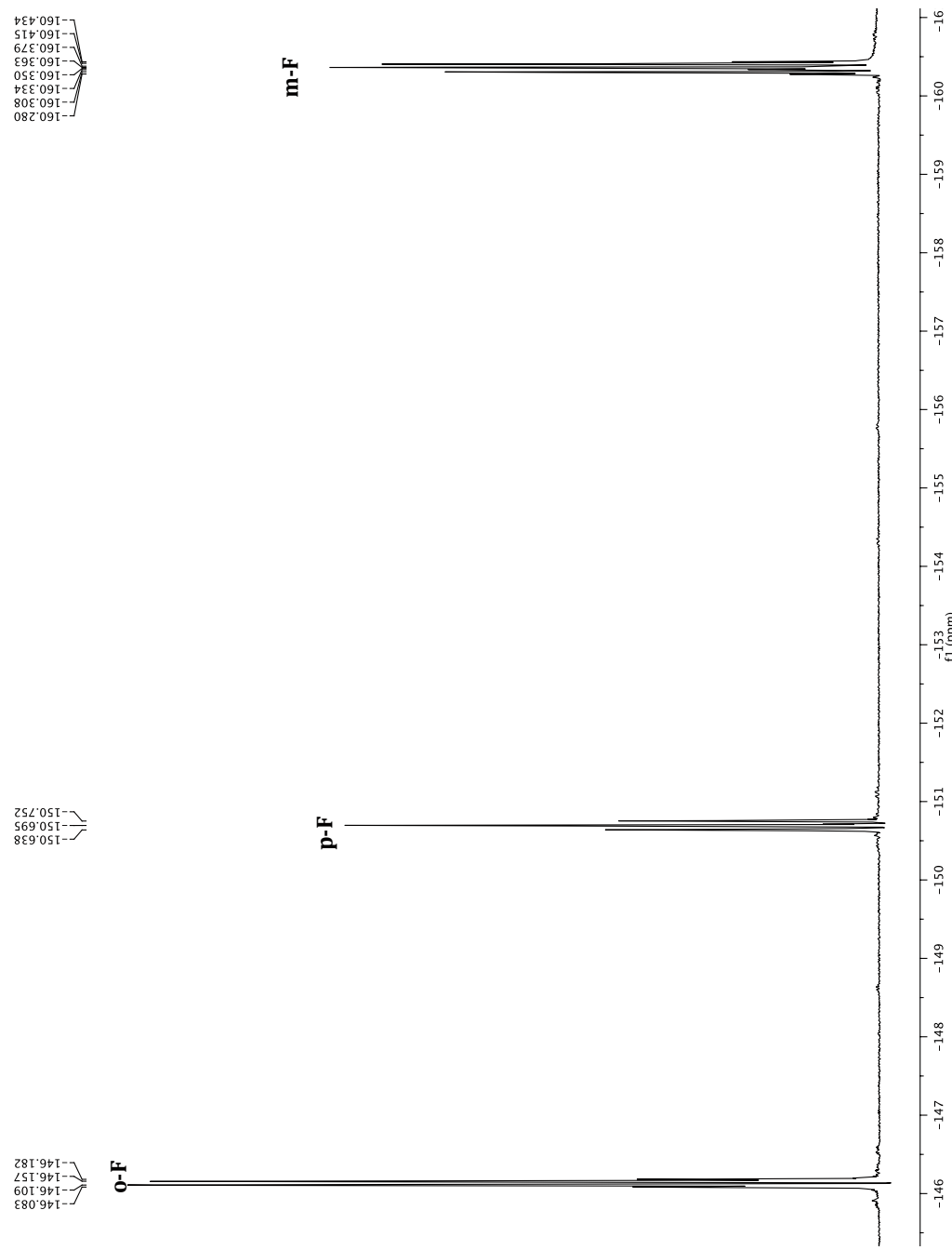


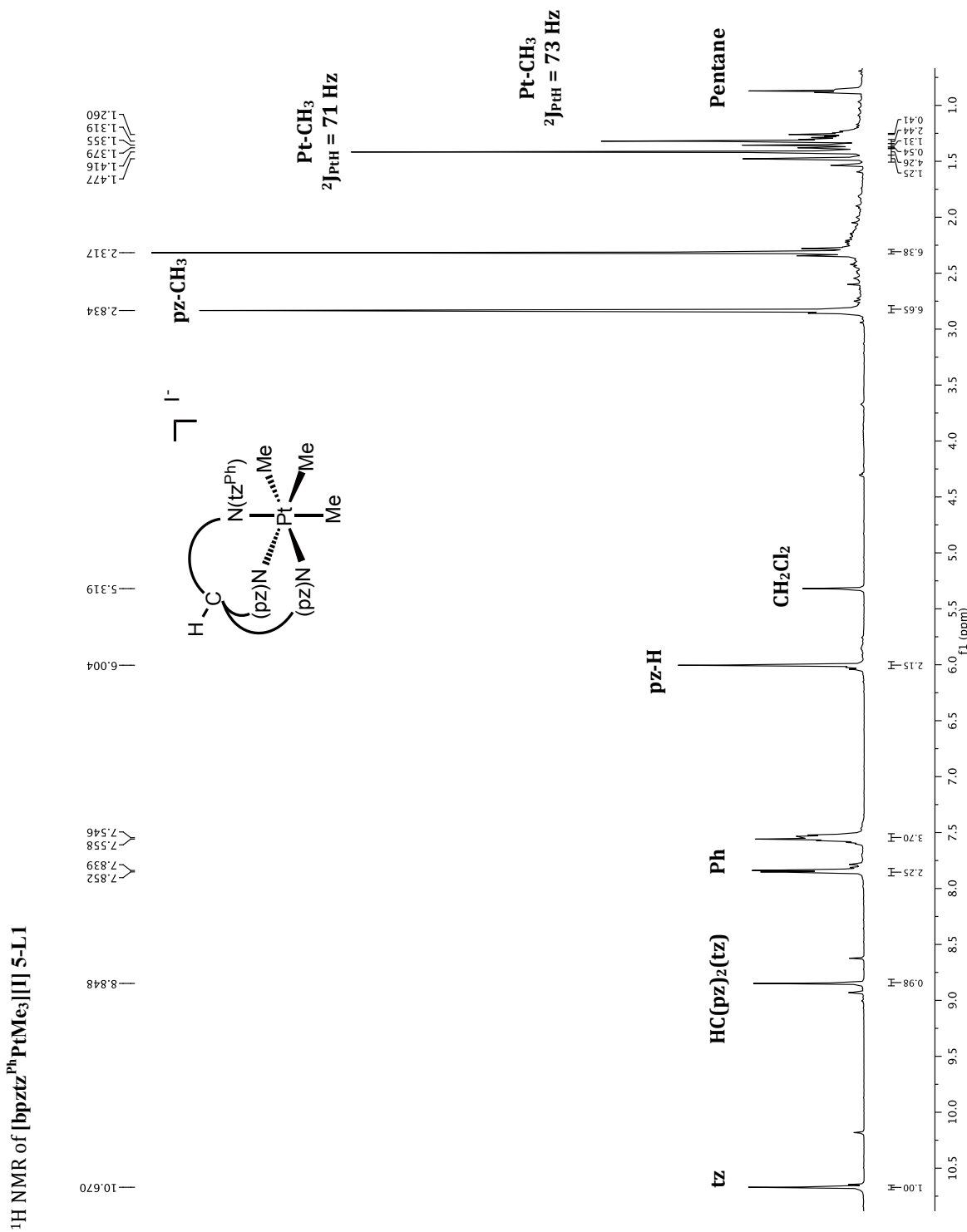


<sup>13</sup>C NMR of 4-(bis(3,5-dimethyl-1*H*-pyrazol-1-yl)methyl)-1-pentafluorophenyl-1*H*-1,2,3-triazole (*b*pztz <sup>CF<sub>3</sub></sup>) 4-L3

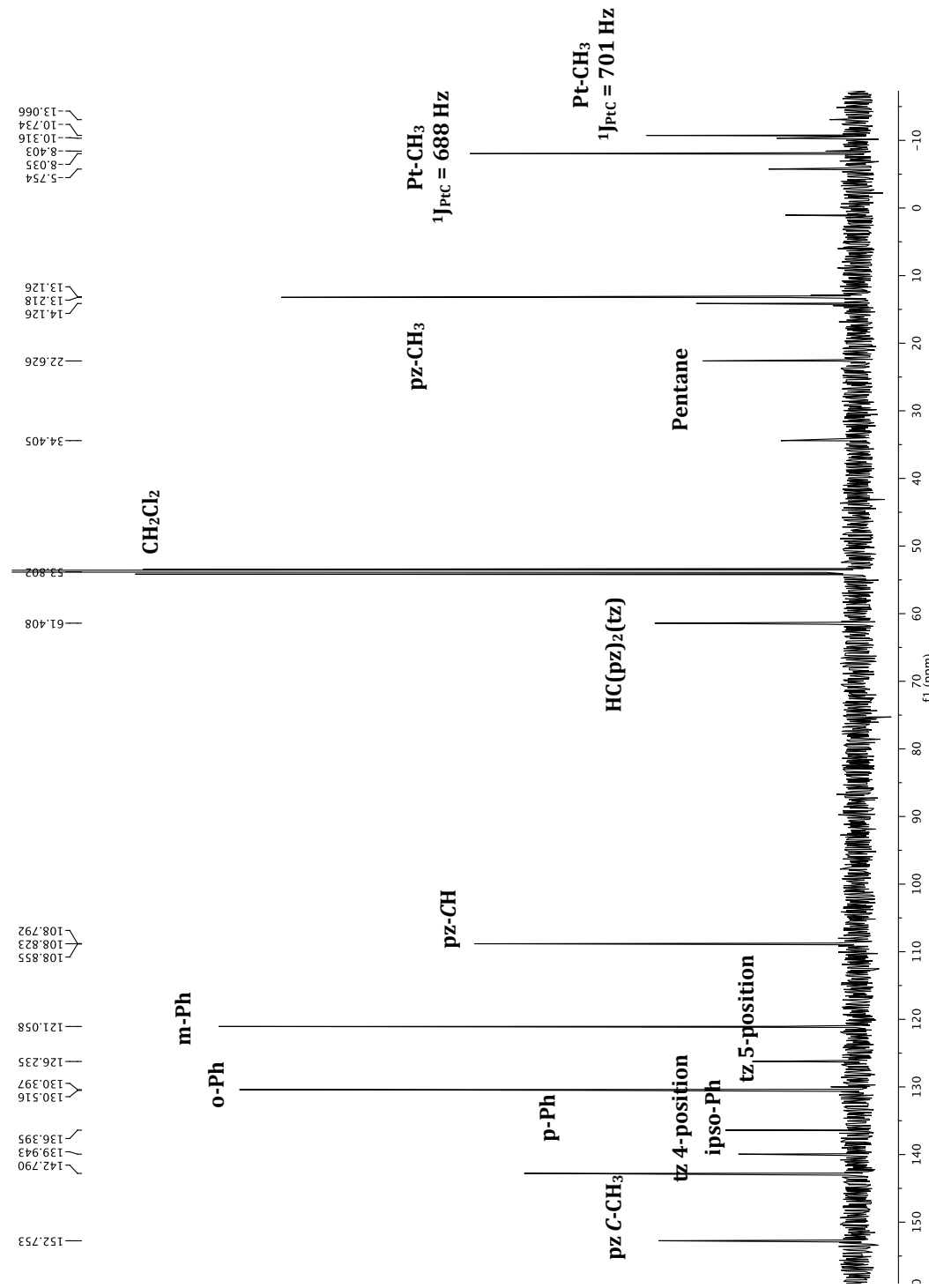


<sup>19</sup>F NMR of 4-(bis(3,5-dimethyl-1*H*-pyrazol-1-yl)methyl)-1-pentafluorophenyl-1*H*-1,2,3-triazole (bpptz<sup>C6F<sub>5</sub></sup>) 4-L3

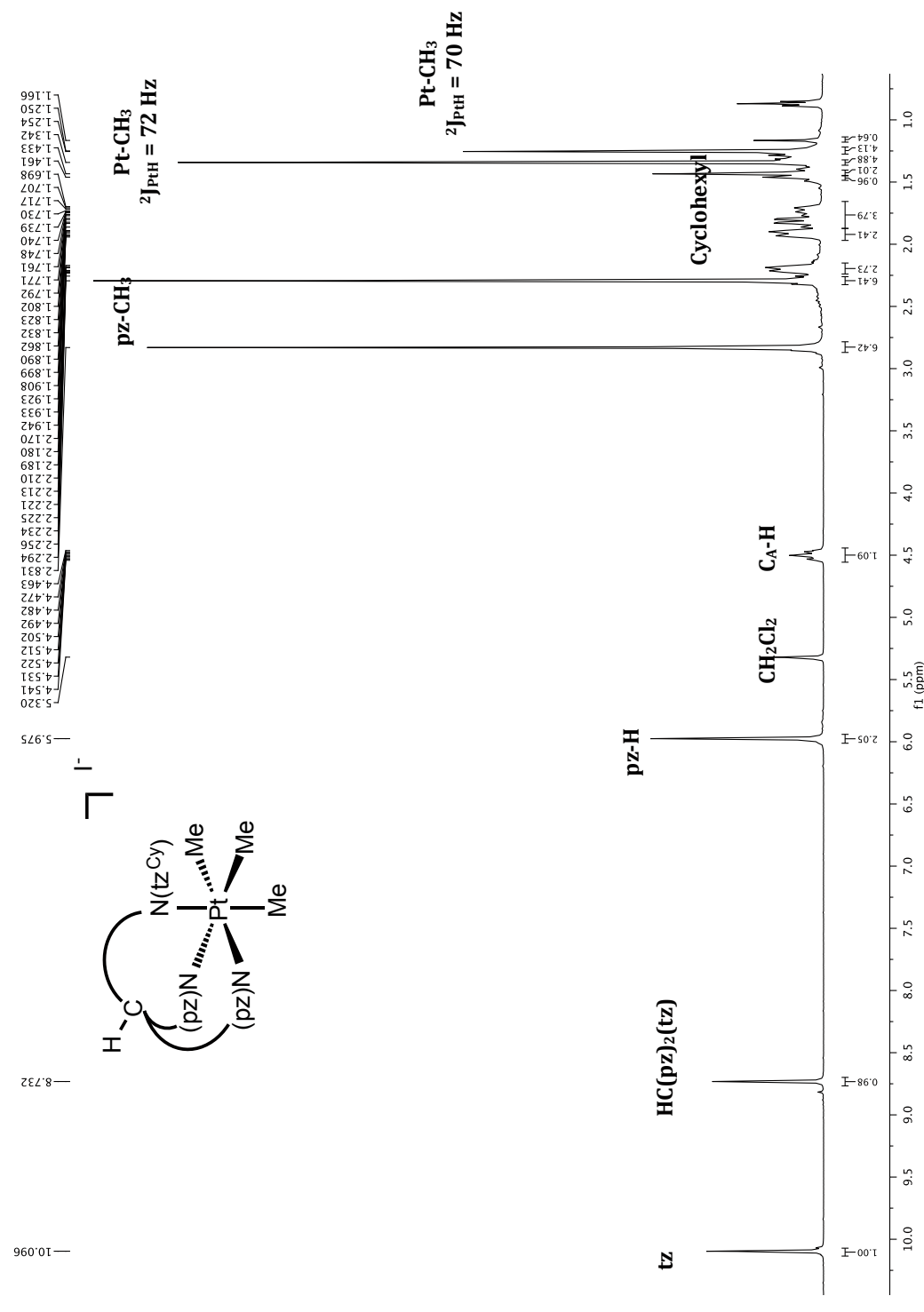




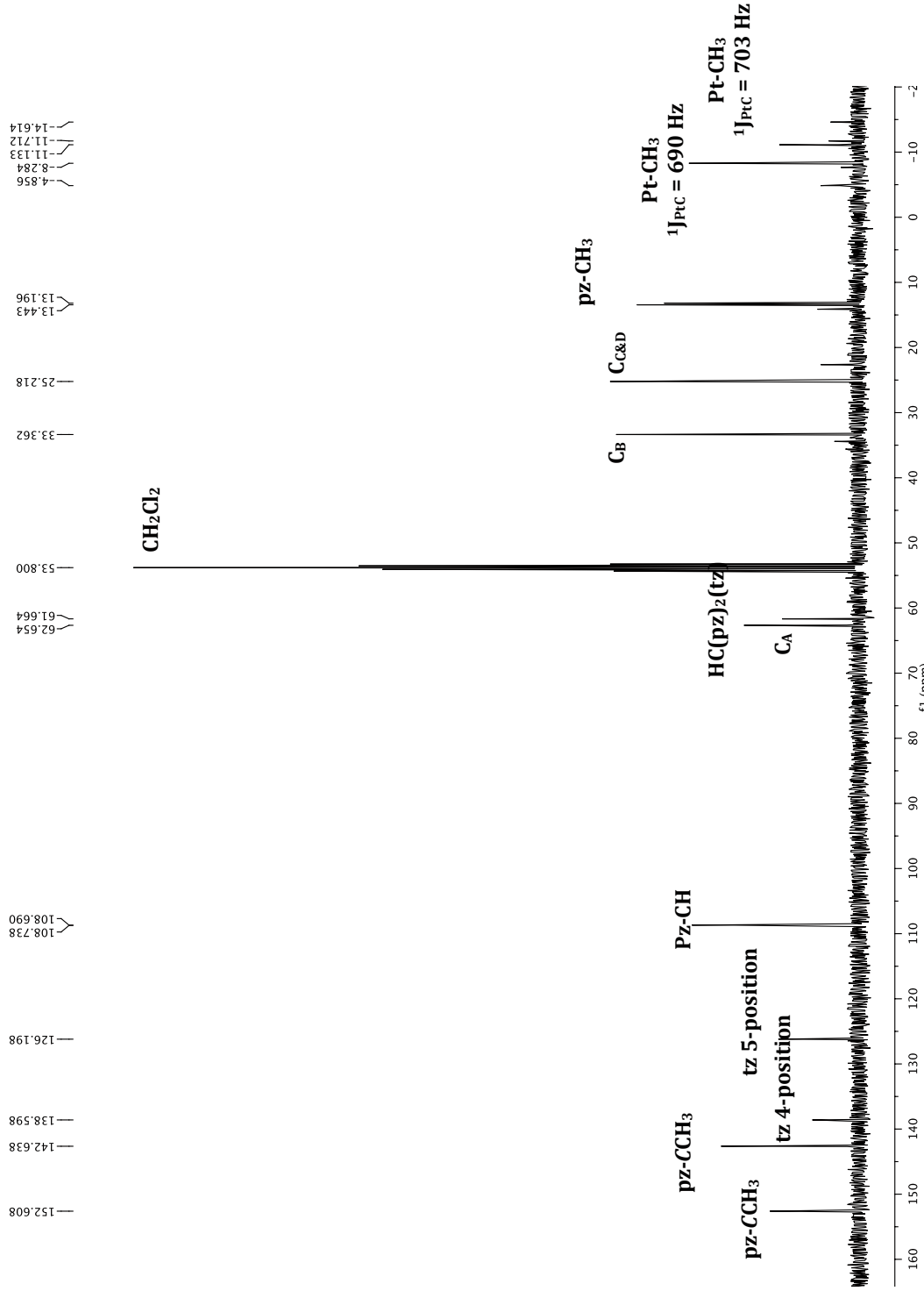
<sup>13</sup>C NMR of [bp<sup>tz</sup><sup>Ph</sup>PtMe<sub>3</sub>]<sup>II</sup>] 5-L1



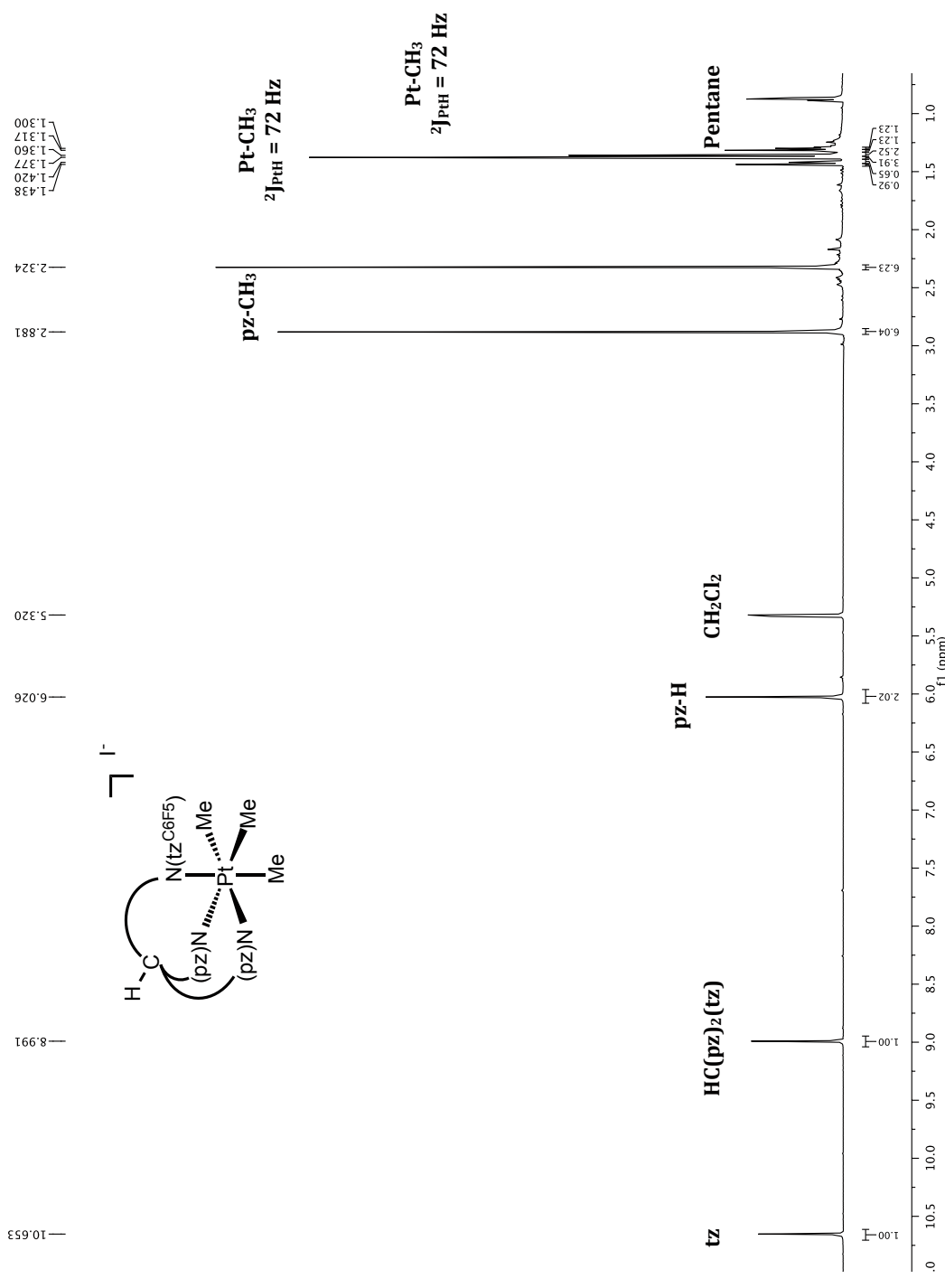
<sup>1</sup>H NMR of [bpz]tz<sup>Cy</sup>Pt(Me<sub>3</sub>)**I**] 5-12



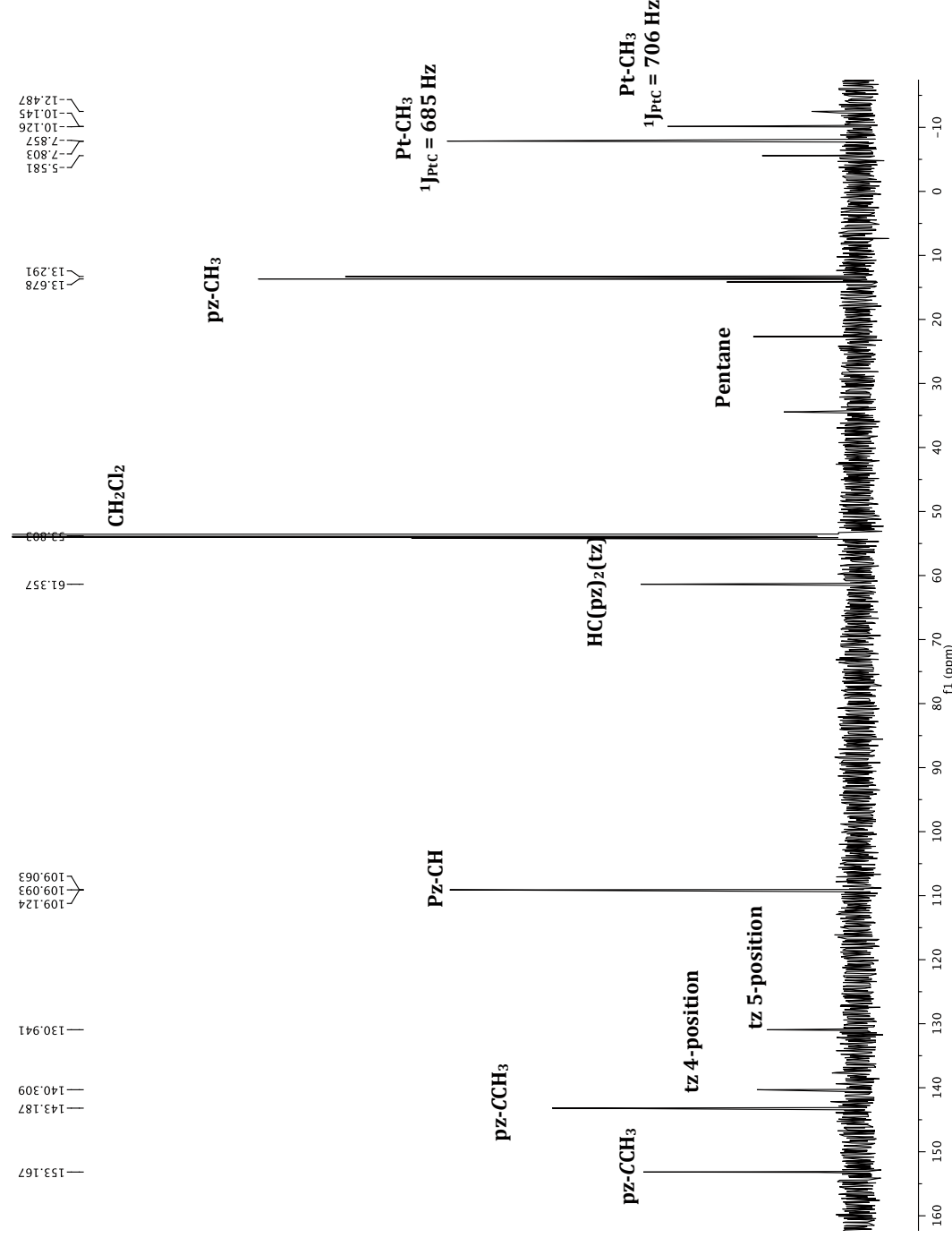
<sup>13</sup>C NMR of [bp<sup>y</sup>tz PtMe<sub>3</sub>]<sup>+</sup>[I] 5-L2



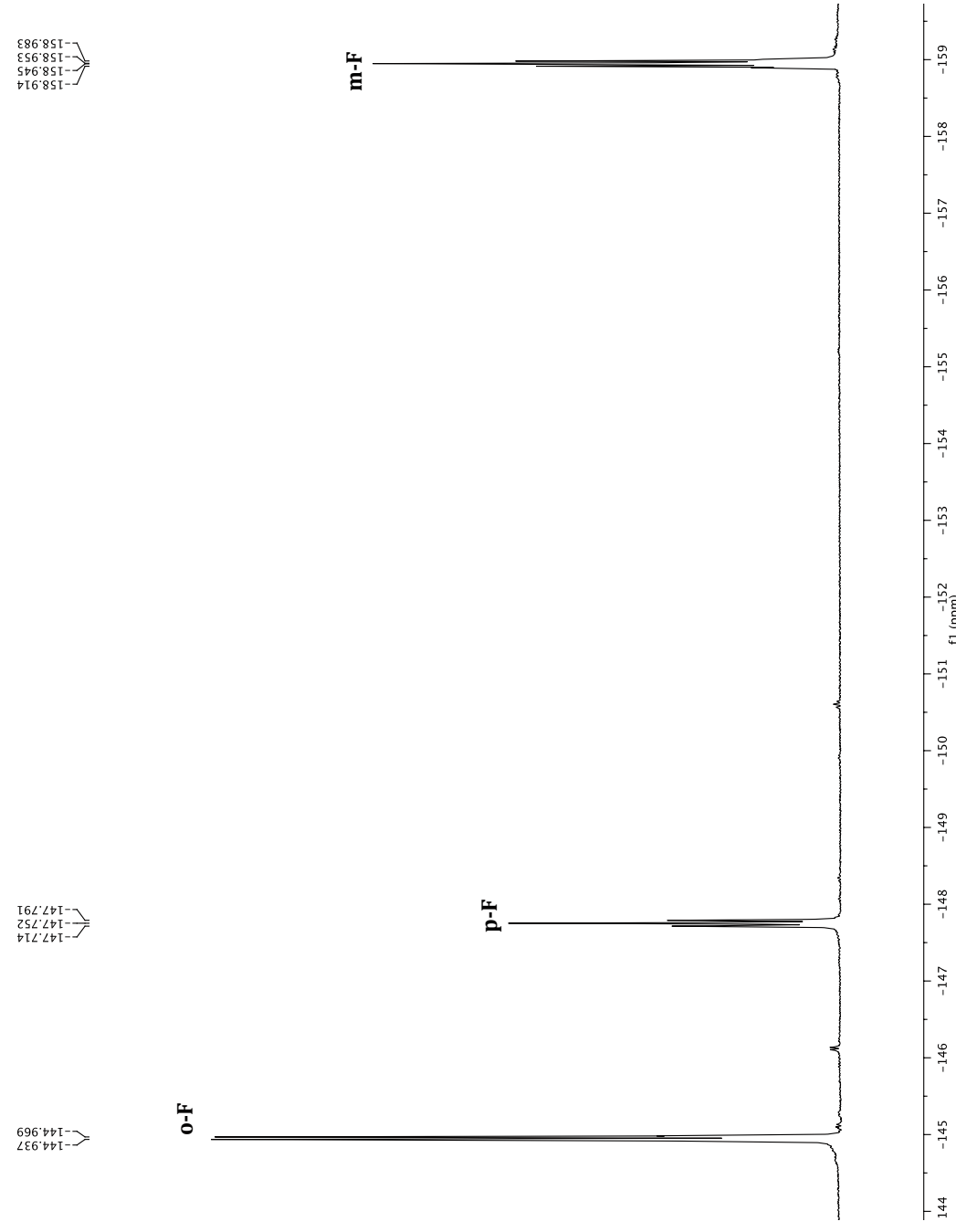
<sup>1</sup>H NMR of [bpz<sub>2</sub>CoF<sub>5</sub>Pt(Me<sub>3</sub>)<sub>2</sub>]I 5-L<sub>3</sub>



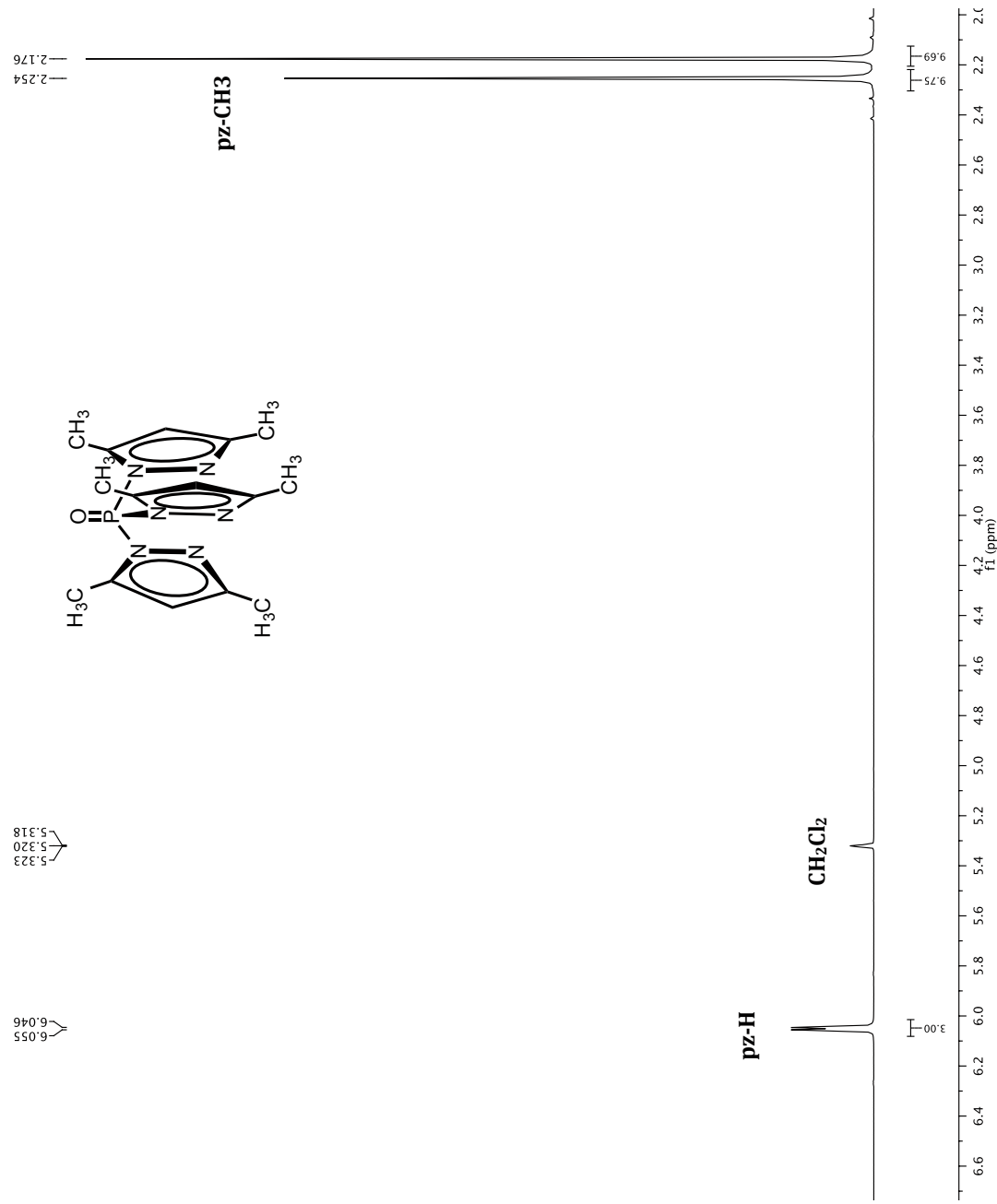
<sup>13</sup>C NMR of [bp<sub>2</sub>tz-C<sub>6</sub>F<sub>5</sub>PtMe<sub>3</sub>][I] 5-L3



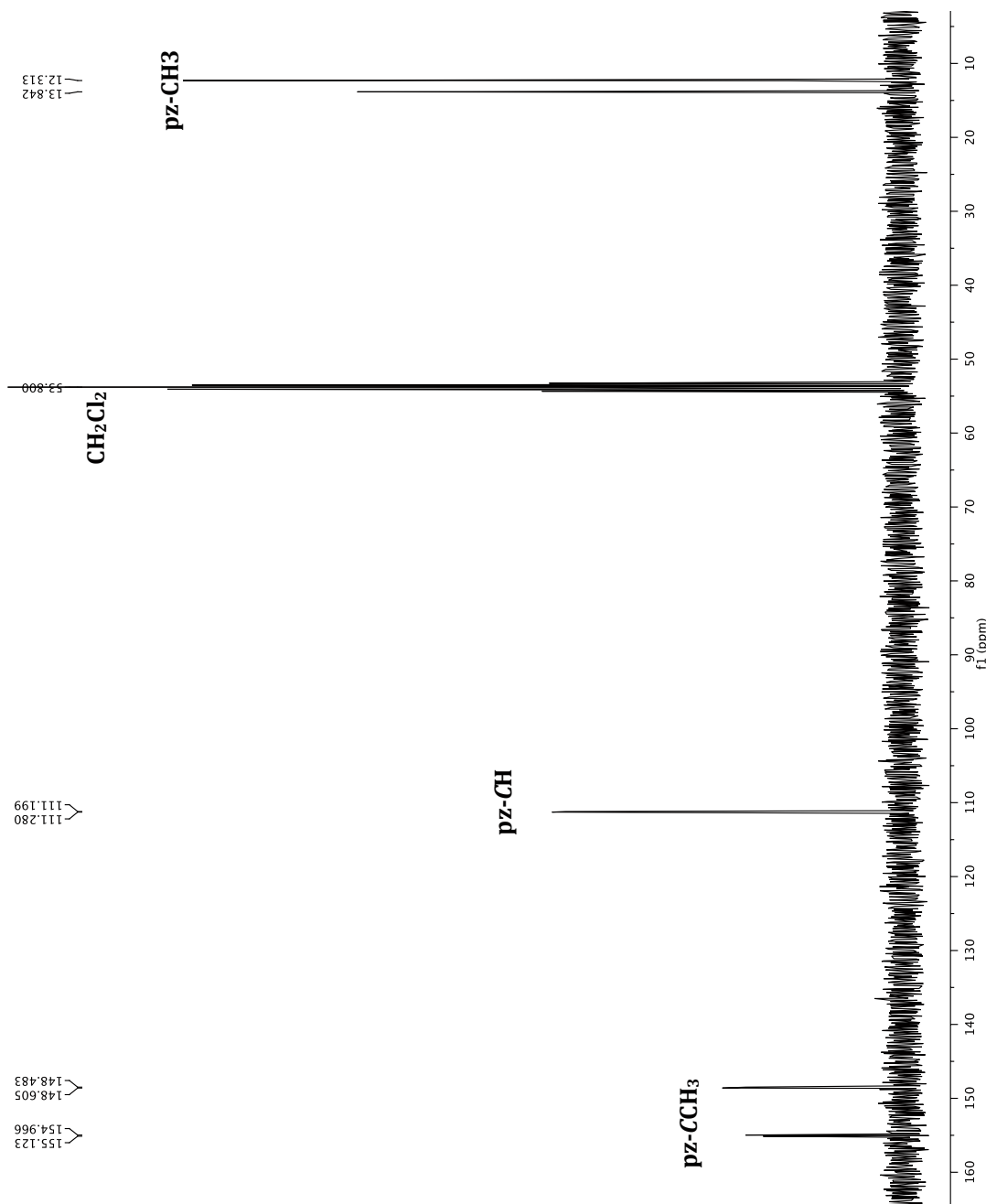
<sup>19</sup>F NMR of [bpzTzC<sup>6</sup>F<sub>5</sub>PtMe<sub>3</sub>][I] 5-L3



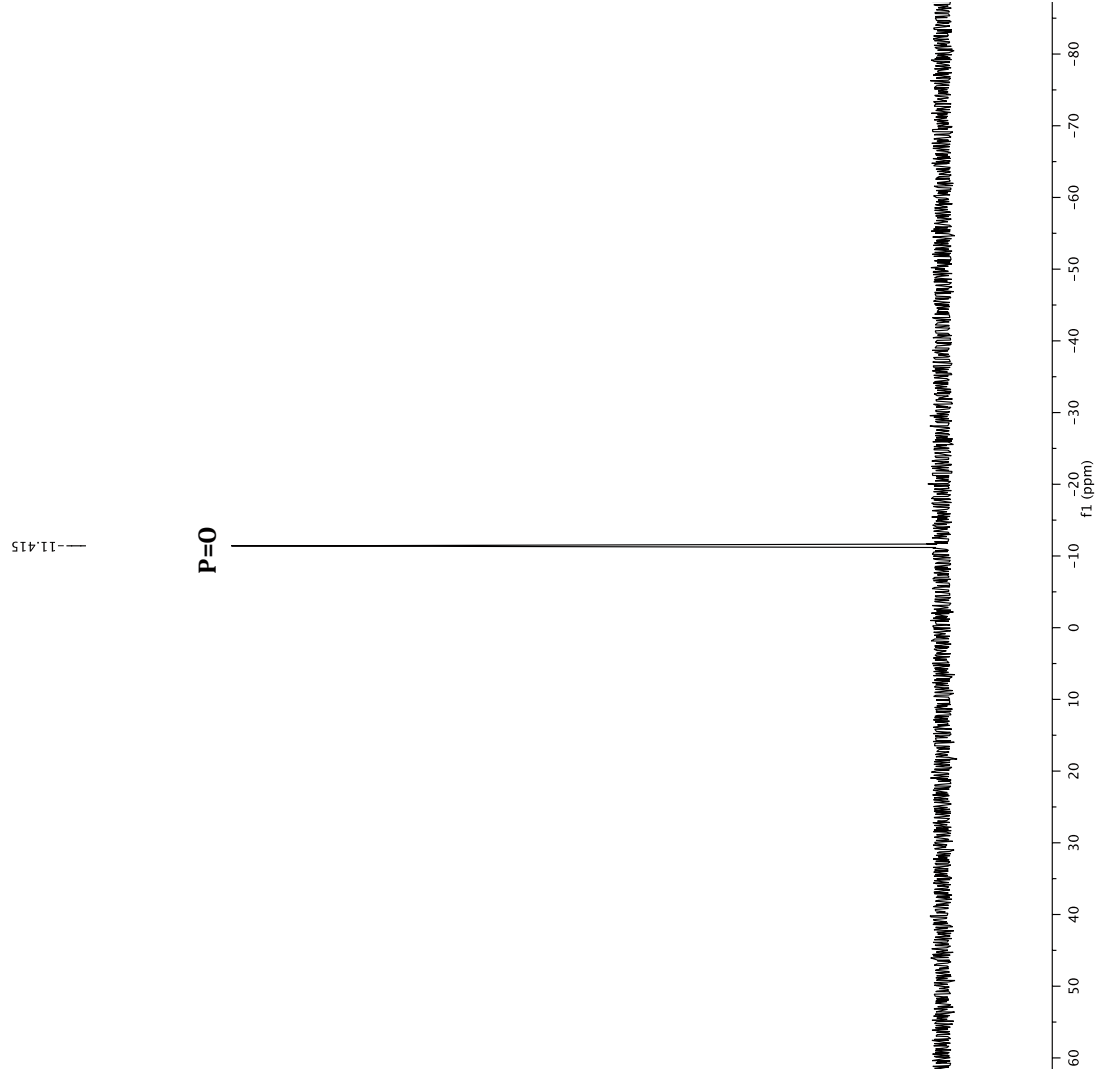
<sup>1</sup>H NMR of tris(3,5-dimethylpyrazoly)phosphine oxide (POPz<sub>3</sub>) 6



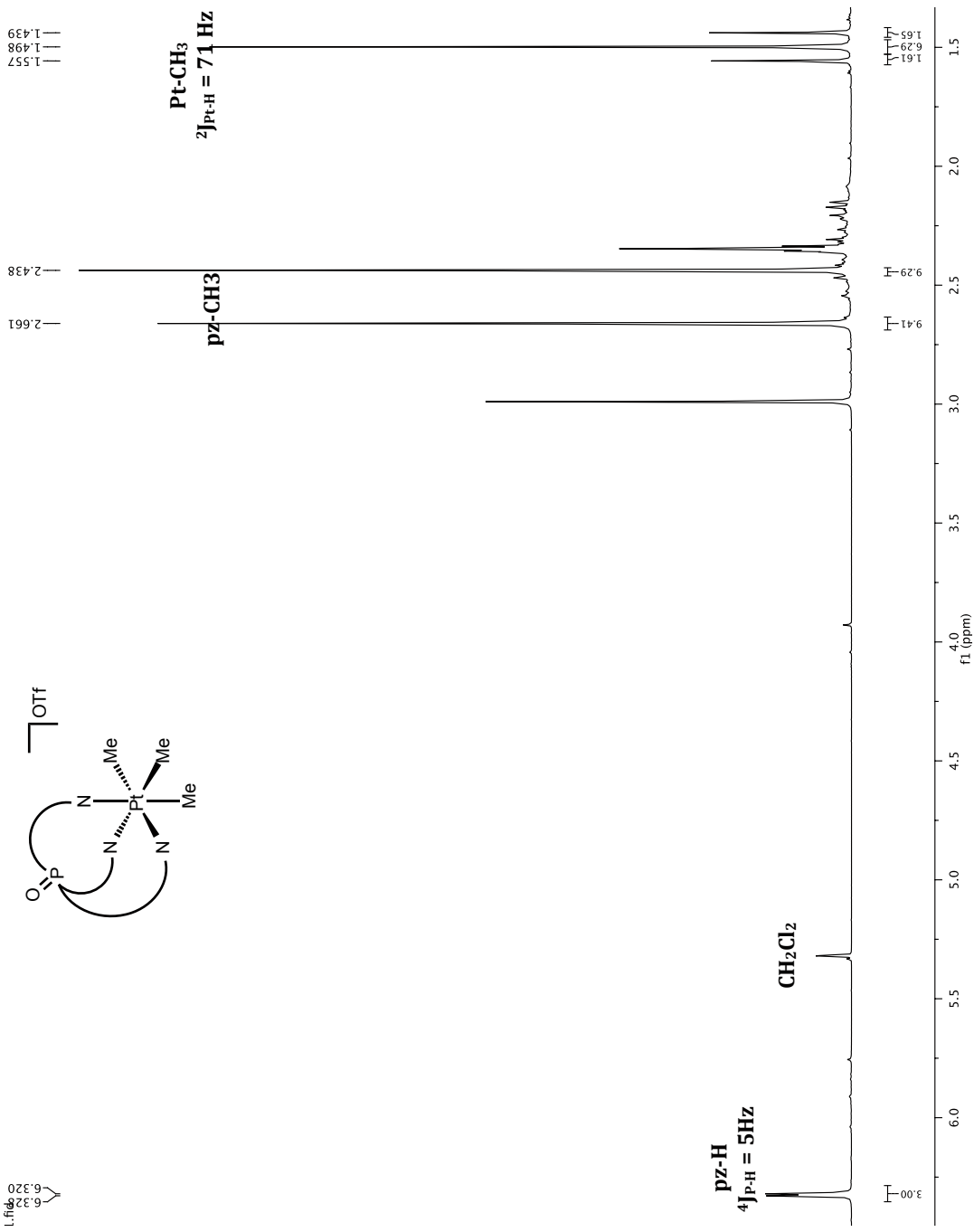
$^{13}\text{C}$  NMR of tris(3,5-dimethylpyrazolyl)phosphine oxide (POP $\text{P}_3$ ) 6



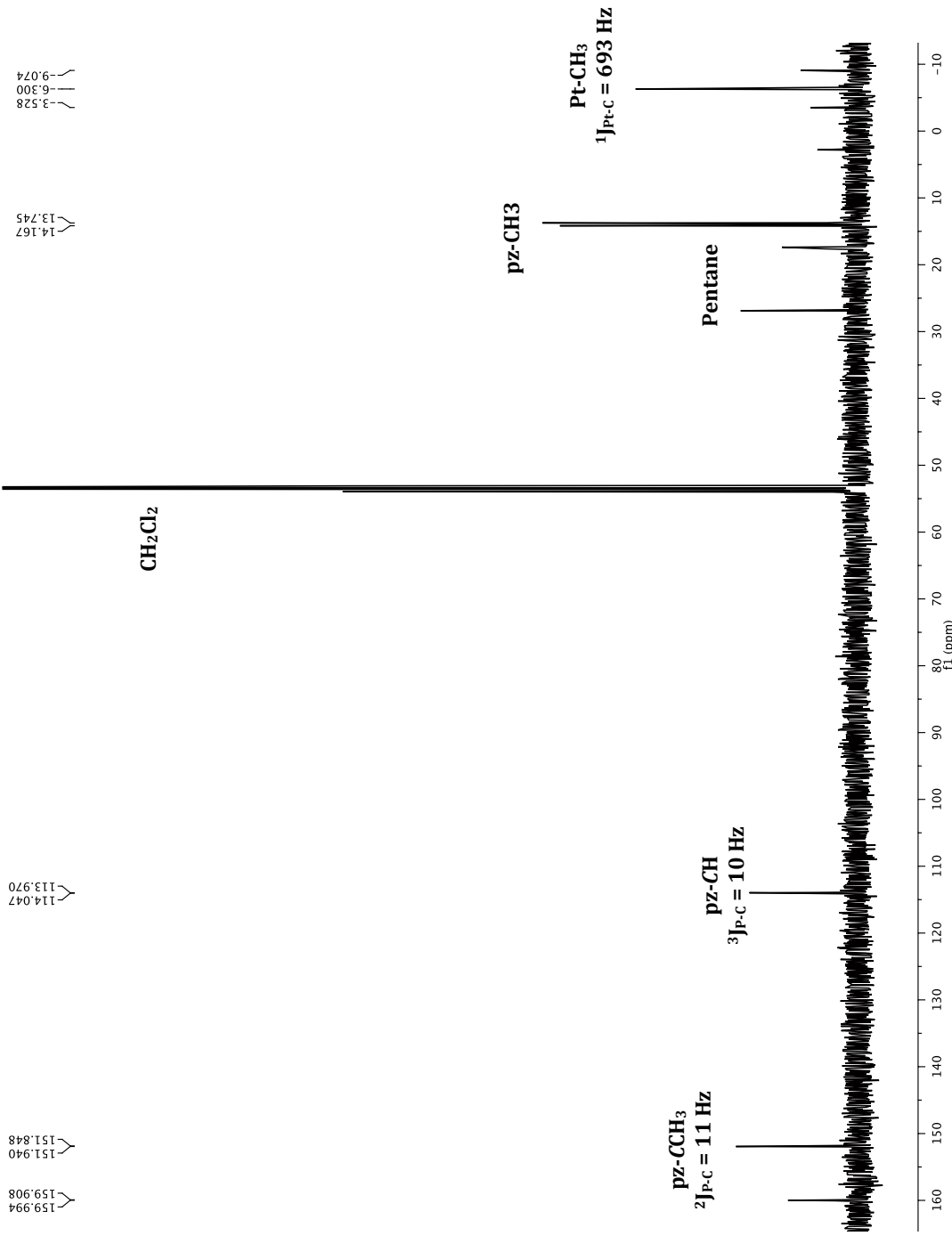
$^{31}\text{P}$  NMR of tris(3,5-dimethylpyrazoly)phosphine oxide) (POPz<sub>3</sub>) 6



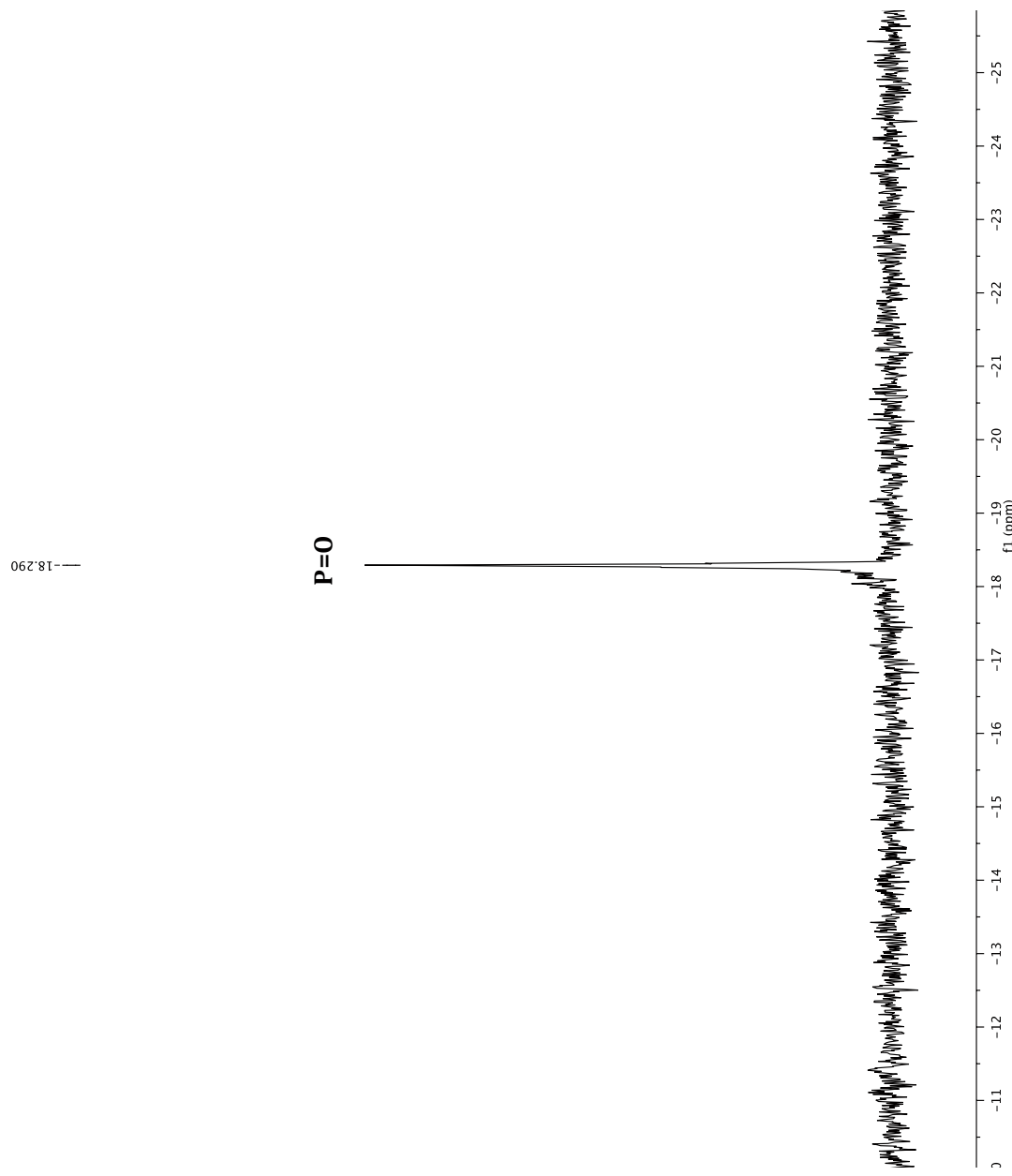
<sup>1</sup>H NMR of [POP<sub>2</sub>PtMe<sub>3</sub>][OTf] 7



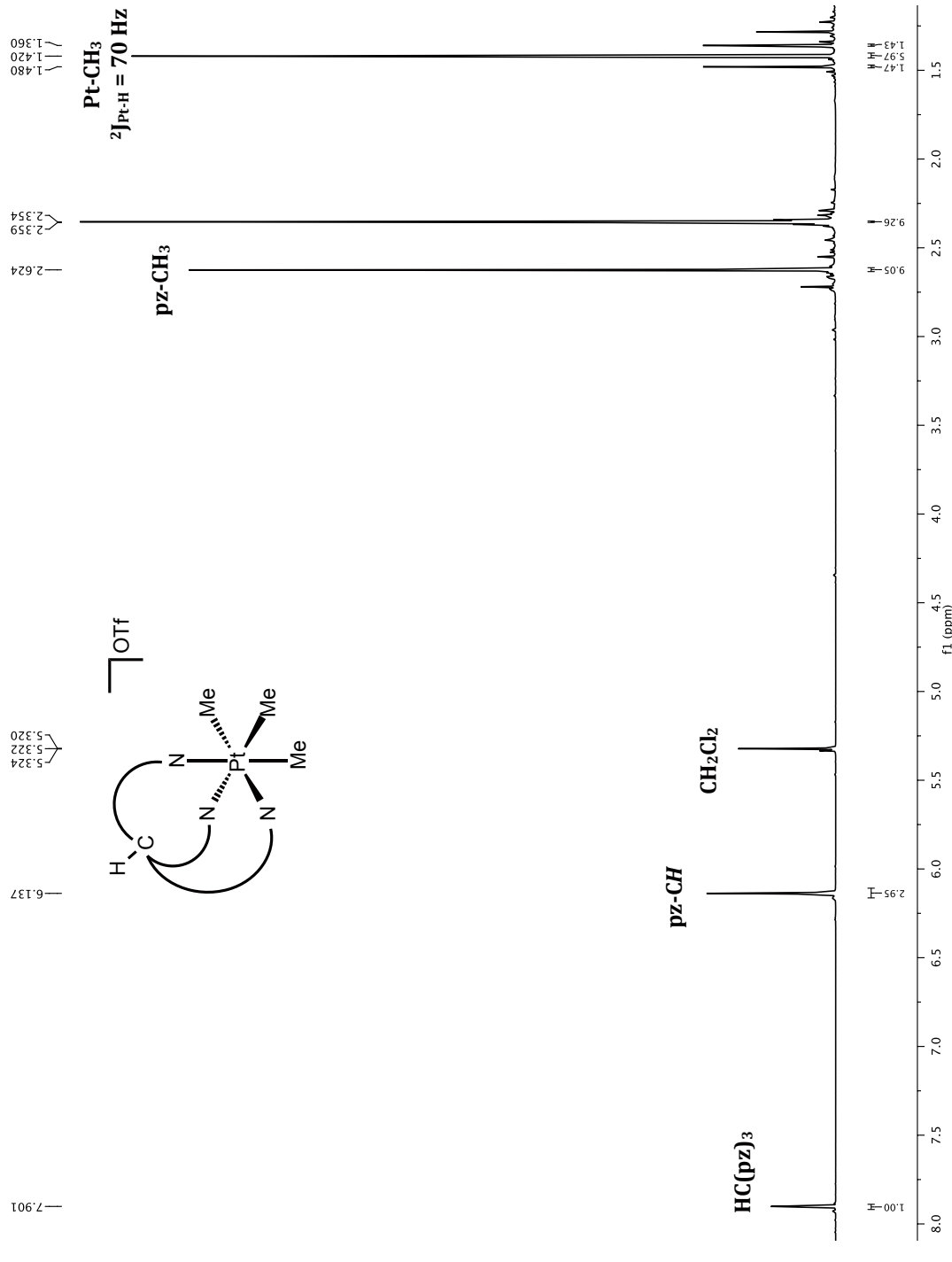
$^{13}\text{C}$  NMR of  $[\text{POPz}_3\text{PtMe}_3]\text{[OTf}]$  7



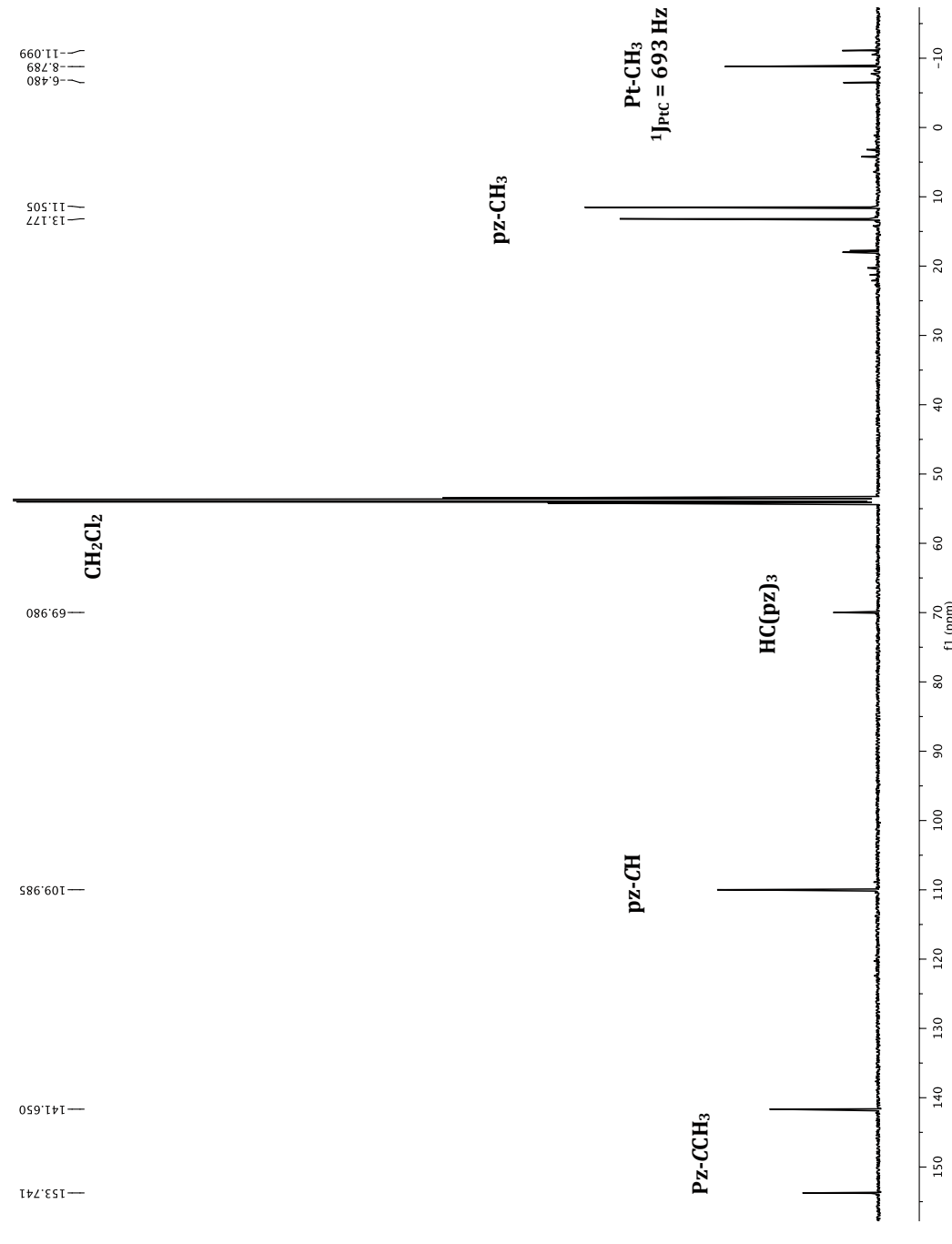
$^{31}\text{P}$  NMR of  $[\text{POP}_{\text{z}_3}\text{PtMe}_3]\text{[OTf]}_7$



$^1\text{H}$  NMR of  $[\text{Tp}^{\text{m}}\text{PtMe}_3]\text{OTf}$  8



$^{13}\text{C}$  NMR of  $[\text{Tp}^{\text{m}}\text{PtMe}_3]\text{OTf}$  8



## APPENDIX 2.2

### Atomic coordinates and isotropic displacement parameters for [bpztz<sup>Cy</sup>PtMe<sub>3</sub>][I] (5-L2)

U(eq) is defines as one third of the trace of the orthogonalized U<sub>ij</sub> tensor.

<b>Atom</b>	<b>x/a</b>	<b>y/b</b>	<b>z/c</b>	<b>U(eq)</b>
Pt1	2059.7(2)	6676.85(17)	3679.62(14)	21.18(8)
N1	986(4)	4587(4)	2892(3)	21.9(8)
N2	-115(4)	3612(4)	2980(3)	25.3(8)
N3	-283(4)	2488(4)	2336(3)	23.9(8)
N4	2047(4)	7083(4)	2139(3)	23.6(8)
N5	2344(4)	6176(4)	1533(3)	22.4(8)
N6	4124(4)	6245(4)	3821(3)	22.7(8)
N7	4162(4)	5620(4)	2915(3)	22.1(8)
C1	2001(6)	6239(5)	5112(4)	32.2(11)
C2	50(5)	6960(5)	3447(4)	30.1(10)
C3	3202(6)	8686(4)	4422(4)	29(1)
C4	2766(5)	5064(4)	1965(3)	20.2(9)
C5	1518(5)	4112(4)	2211(3)	19.9(9)
C6	697(5)	2742(5)	1847(4)	22.6(9)
C7	-1464(5)	1179(4)	2237(4)	24.7(10)
C8	-1062(6)	648(5)	3275(4)	30.1(11)
C9	-2280(6)	-722(5)	3156(5)	35.1(12)
C10	-3864(6)	-609(5)	2794(4)	32.9(11)
C11	-4215(6)	-24(5)	1790(4)	31.2(11)
C12	-3007(5)	1341(5)	1908(4)	29.3(10)
C13	1842(5)	8053(5)	1586(4)	24.0(9)
C14	1993(5)	7769(5)	633(4)	28.2(10)
C15	2322(5)	6582(5)	602(4)	26.3(10)
C16	1495(6)	9257(5)	1971(4)	33.5(11)
C17	2641(7)	5803(5)	-206(4)	37.8(12)
C18	5562(5)	6642(4)	4526(4)	25.7(10)
C19	6475(5)	6279(5)	4053(4)	29.5(10)
C20	5569(5)	5643(5)	3027(4)	27.4(10)
C21	6052(6)	7352(5)	5639(4)	34.4(11)
C22	5938(6)	5090(6)	2158(5)	36.5(12)
I1	2708.1(4)	1966.1(3)	117.7(3)	32.34(10)

### Bond Lengths (Å)

<b>Atom</b>	<b>Atom</b>	<b>Length/Å</b>	<b>Atom</b>	<b>Atom</b>	<b>Length/Å</b>
Pt1	N1	2.135(4)	N7	C20	1.359(6)
Pt1	N4	2.178(4)	C4	C5	1.506(6)
Pt1	N6	2.193(4)	C5	C6	1.375(6)
Pt1	C1	2.061(5)	C7	C8	1.530(7)
Pt1	C2	2.042(5)	C7	C12	1.520(7)
Pt1	C3	2.054(4)	C8	C9	1.537(6)
N1	N2	1.310(5)	C9	C10	1.536(7)
N1	C5	1.351(6)	C10	C11	1.517(8)
N2	N3	1.345(5)	C11	C12	1.529(6)
N3	C6	1.343(6)	C13	C14	1.385(7)
N3	C7	1.482(5)	C13	C16	1.502(7)
N4	N5	1.374(5)	C14	C15	1.371(7)
N4	C13	1.327(6)	C15	C17	1.498(7)
N5	C4	1.445(6)	C18	C19	1.404(7)
N5	C15	1.366(6)	C18	C21	1.491(7)
N6	N7	1.375(5)	C19	C20	1.372(8)
N6	C18	1.352(6)	C20	C22	1.485(7)
N7	C4	1.471(6)			

### Bond Angles (°)

<b>Atom</b>	<b>Atom</b>	<b>Atom</b>	<b>Angle/°</b>	<b>Atom</b>	<b>Atom</b>	<b>Atom</b>	<b>Angle/°</b>
N1	Pt1	N4	84.85(14)	C20	N7	N6	112.6(4)
N1	Pt1	N6	83.31(14)	C20	N7	C4	128.1(4)
N4	Pt1	N6	83.68(14)	N5	C4	N7	109.5(3)
C1	Pt1	N1	93.54(17)	N5	C4	C5	111.3(4)
C1	Pt1	N4	178.01(17)	N7	C4	C5	111.1(4)
C1	Pt1	N6	97.30(18)	N1	C5	C4	120.4(4)
C2	Pt1	N1	92.68(17)	N1	C5	C6	107.2(4)
C2	Pt1	N4	94.06(18)	C6	C5	C4	132.4(4)
C2	Pt1	N6	175.55(16)	N3	C6	C5	104.4(4)
C2	Pt1	C1	84.8(2)	N3	C7	C8	110.1(4)
C2	Pt1	C3	90.4(2)	N3	C7	C12	111.0(4)
C3	Pt1	N1	176.67(17)	C12	C7	C8	111.6(4)
C3	Pt1	N4	93.79(17)	C7	C8	C9	109.6(4)
C3	Pt1	N6	93.52(17)	C10	C9	C8	112.1(4)
C3	Pt1	C1	87.9(2)	C11	C10	C9	111.1(4)

N2	N1	Pt1	130.7(3)	C10	C11	C12	112.0(4)
N2	N1	C5	111.1(4)	C7	C12	C11	110.3(4)
C5	N1	Pt1	118.2(3)	N4	C13	C14	109.8(4)
N1	N2	N3	105.1(4)	N4	C13	C16	123.4(4)
N2	N3	C7	119.4(4)	C14	C13	C16	126.9(4)
C6	N3	N2	112.2(4)	C15	C14	C13	107.9(5)
C6	N3	C7	128.4(4)	N5	C15	C14	105.3(4)
N5	N4	Pt1	117.8(3)	N5	C15	C17	122.6(4)
C13	N4	Pt1	136.1(3)	C14	C15	C17	132.0(5)
C13	N4	N5	106.1(4)	N6	C18	C19	109.9(4)
N4	N5	C4	119.5(4)	N6	C18	C21	123.4(4)
C15	N5	N4	110.9(4)	C19	C18	C21	126.6(5)
C15	N5	C4	129.3(4)	C20	C19	C18	107.4(4)
N7	N6	Pt1	117.0(3)	N7	C20	C19	105.6(4)
C18	N6	Pt1	137.1(3)	N7	C20	C22	123.7(5)
C18	N6	N7	104.5(4)	C19	C20	C22	130.7(5)
N6	N7	C4	119.3(4)				

## APPENDIX 2.3

### Atomic coordinates and isotropic displacement parameters for [bpztz<sup>C6F5</sup>PtMe<sub>3</sub>][I] (5-L3)

U(eq) is defines as one third of the trace of the orthogonalized U<sub>ij</sub> tensor.

<b>Atom</b>	<b>x/a</b>	<b>y/b</b>	<b>z/c</b>	<b>U(eq)</b>
Pt1	6064.91(10)	2112.89(12)	3680.06(12)	14.37(7)
F1	6752.7(18)	6245.9(19)	5234(2)	26.0(5)
F2	6854(2)	8348(2)	5293(2)	30.8(6)
F3	7545(2)	9399(2)	3983(2)	34.6(6)
F4	8053.8(19)	8338(2)	2559(2)	31.2(6)
F5	7998.2(19)	6223.2(19)	2529(2)	28.2(6)
N1	6840(2)	3534(2)	3773(2)	15.3(6)
N2	6585(2)	4516(3)	3747(3)	16.3(6)
N3	7370(2)	5075(3)	3871(3)	17.1(7)
N4	6900(2)	1538(2)	2761(3)	15.5(6)
N5	7835(2)	1773(3)	3083(3)	16.5(6)
N6	7271(2)	1633(3)	4948(3)	16.1(6)
N7	8137(2)	1834(3)	4873(3)	16.2(6)
C1	8222(3)	2393(3)	3995(3)	15.1(7)
C2	7766(3)	3455(3)	3914(3)	16.3(8)
C3	8133(3)	4454(3)	3979(3)	17.4(8)
C4	7353(3)	6189(3)	3866(3)	17.8(8)
C5	7067(3)	6747(3)	4567(3)	20.6(8)
C6	7124(3)	7831(3)	4609(4)	23.6(9)
C7	7467(3)	8360(3)	3938(3)	23.5(9)
C8	7744(3)	7819(3)	3218(3)	21.9(9)
C9	7694(3)	6735(3)	3194(3)	20.0(8)
C10	5867(3)	367(3)	1447(3)	24.7(9)
C11	6778(3)	880(3)	1977(3)	19.6(8)
C12	7628(3)	714(3)	1798(3)	22.0(8)
C13	8294(3)	1265(3)	2520(3)	20.7(8)
C14	9321(3)	1328(4)	2714(4)	27.8(10)
C15	6645(3)	816(4)	6214(3)	25.4(9)
C16	7421(3)	1157(3)	5839(3)	19.9(8)
C17	8381(3)	1050(3)	6338(3)	24.7(9)
C18	8820(3)	1491(3)	5706(3)	21.4(8)
C19	9834(3)	1604(4)	5842(4)	30.9(10)

C20	5350(3)	2720(3)	4575(3)	23.2(9)
C21	5370(3)	720(3)	3611(3)	21.1(8)
C22	4978(3)	2645(3)	2475(3)	18.8(8)
I1	517.11(17)	3806.7(2)	4047.56(19)	20.83(8)

### Bond Lengths (Å)

Atom	Atom	Length/Å	Atom	Atom	Length/Å
Pt1	N1	2.138(3)	N6	N7	1.372(5)
Pt1	N4	2.188(3)	N6	C16	1.334(5)
Pt1	N6	2.188(3)	N7	C1	1.455(5)
Pt1	C20	2.042(4)	N7	C18	1.359(5)
Pt1	C21	2.050(4)	C1	C2	1.507(5)
Pt1	C22	2.058(4)	C2	C3	1.380(6)
F1	C5	1.333(5)	C4	C5	1.383(6)
F2	C6	1.323(5)	C4	C9	1.389(6)
F3	C7	1.328(5)	C5	C6	1.383(6)
F4	C8	1.330(5)	C6	C7	1.379(7)
F5	C9	1.326(5)	C7	C8	1.386(6)
N1	N2	1.307(5)	C8	C9	1.384(6)
N1	C2	1.357(5)	C10	C11	1.495(6)
N2	N3	1.348(5)	C11	C12	1.401(6)
N3	C3	1.368(5)	C12	C13	1.371(6)
N3	C4	1.420(5)	C13	C14	1.494(6)
N4	N5	1.376(5)	C15	C16	1.492(6)
N4	C11	1.342(5)	C16	C17	1.406(6)
N5	C1	1.452(5)	C17	C18	1.378(6)
N5	C13	1.363(5)	C18	C19	1.493(6)

### Bond Angles (°)

Atom	Atom	Atom	Angle/°	Atom	Atom	Atom	Angle/°
N1	Pt1	N4	84.95(12)	N1	C2	C1	120.3(3)
N1	Pt1	N6	83.43(12)	N1	C2	C3	108.5(3)
N6	Pt1	N4	83.63(12)	C3	C2	C1	131.2(4)
C20	Pt1	N1	91.61(15)	N3	C3	C2	102.6(3)
C20	Pt1	N4	176.33(15)	C5	C4	N3	121.4(4)
C20	Pt1	N6	94.72(16)	C5	C4	C9	118.9(4)
C20	Pt1	C21	89.67(18)	C9	C4	N3	119.6(4)

C20	Pt1	C22	86.03(18)	F1	C5	C4	120.3(4)
C21	Pt1	N1	177.77(15)	F1	C5	C6	118.7(4)
C21	Pt1	N4	93.73(15)	C4	C5	C6	120.9(4)
C21	Pt1	N6	94.64(15)	F2	C6	C5	119.9(4)
C21	Pt1	C22	88.89(17)	F2	C6	C7	120.7(4)
C22	Pt1	N1	93.02(14)	C7	C6	C5	119.5(4)
C22	Pt1	N4	95.42(15)	F3	C7	C6	120.2(4)
C22	Pt1	N6	176.39(14)	F3	C7	C8	119.2(4)
N2	N1	Pt1	131.2(3)	C6	C7	C8	120.7(4)
N2	N1	C2	110.9(3)	F4	C8	C7	120.3(4)
C2	N1	Pt1	117.9(2)	F4	C8	C9	120.5(4)
N1	N2	N3	105.2(3)	C9	C8	C7	119.2(4)
N2	N3	C3	112.8(3)	F5	C9	C4	120.5(4)
N2	N3	C4	120.9(3)	F5	C9	C8	118.7(4)
C3	N3	C4	126.3(3)	C8	C9	C4	120.8(4)
N5	N4	Pt1	117.5(2)	N4	C11	C10	122.9(4)
C11	N4	Pt1	136.7(3)	N4	C11	C12	110.0(4)
C11	N4	N5	105.3(3)	C12	C11	C10	127.0(4)
N4	N5	C1	119.5(3)	C13	C12	C11	107.2(4)
C13	N5	N4	111.6(3)	N5	C13	C12	105.9(4)
C13	N5	C1	128.5(3)	N5	C13	C14	124.1(4)
N7	N6	Pt1	117.4(2)	C12	C13	C14	129.9(4)
C16	N6	Pt1	136.9(3)	N6	C16	C15	122.4(4)
C16	N6	N7	105.6(3)	N6	C16	C17	110.4(4)
N6	N7	C1	119.6(3)	C17	C16	C15	127.2(4)
C18	N7	N6	111.3(3)	C18	C17	C16	106.1(4)
C18	N7	C1	129.0(3)	N7	C18	C17	106.6(4)
N5	C1	N7	110.5(3)	N7	C18	C19	123.5(4)
N5	C1	C2	112.0(3)	C17	C18	C19	129.9(4)
N7	C1	C2	110.1(3)				

## APPENDIX 2.4

### Atomic coordinates and isotropic displacement parameters for [POPz<sub>3</sub>PtMe<sub>3</sub>][OTf] (7)

U(eq) is defines as one third of the trace of the orthogonalized U<sub>ij</sub> tensor.

<b>Atom</b>	<b>x/a</b>	<b>y/b</b>	<b>z/c</b>	<b>U(eq)</b>
Pt1	727.4(2)	3682.0(2)	5052.8(2)	14.02(6)
P1	3594.0(13)	4715.8(7)	5132.7(6)	14.7(3)
O1	4828(4)	5159(2)	5174.3(18)	19.3(8)
N1	2353(5)	3713(4)	4305(2)	15.8(9)
N2	3467(5)	4192(3)	4428(2)	14.3(9)
N3	917(4)	4958(2)	5144(2)	16.0(9)
N4	2210(4)	5277(2)	5154(2)	15.8(9)
N5	2282(5)	3596(4)	5823(2)	14.9(10)
N6	3422(5)	4071(3)	5763(2)	15.7(10)
C1	-760(7)	3654(5)	5757(2)	23.8(11)
C2	-713(7)	3781(4)	4325(3)	21.4(13)
C3	559(5)	2491(3)	4977(3)	22.4(10)
C4	2597(6)	3386(3)	3711(3)	16.6(11)
C5	3832(5)	3638(4)	3448(2)	18.3(11)
C6	4385(7)	4146(3)	3903(2)	17.3(11)
C7	1690(6)	2824(4)	3369(3)	22.2(13)
C8	5681(7)	4572(3)	3887(3)	23.8(12)
C9	86(6)	5560(3)	5186(3)	20.5(12)
C10	811(6)	6265(3)	5219(2)	21.9(10)
C11	2156(6)	6084(3)	5198(2)	19.4(11)
C12	-1410(6)	5486(3)	5202(3)	23.5(13)
C13	3336(6)	6616(3)	5206(3)	25.6(13)
C14	2486(6)	3185(3)	6382(3)	15.7(11)
C15	3717(6)	3381(3)	6669(3)	18.1(12)
C16	4308(7)	3935(3)	6284(2)	16.4(10)
C17	1514(6)	2599(4)	6657(3)	21.2(13)
C18	5646(6)	4323(3)	6355(3)	21.2(11)
S1	6821.4(15)	7048.6(10)	3326.0(7)	23.0(3)
F1	9046(4)	6646(2)	3948.1(17)	33.7(9)
F2	9167(4)	6591(2)	2872.6(16)	31.9(8)
F3	8096(4)	5702(2)	3418(2)	39.9(10)
O2	6088(4)	6841(3)	3924(2)	36.4(11)

O3	7336(5)	7835(3)	3311(2)	31.2(10)
O4	6250(5)	6775(3)	2704(2)	37.2(12)
C19	8353(6)	6466(3)	3398(3)	21.3(12)
C20	2108(7)	5497(4)	3232(3)	32.0(15)
C21	1428(7)	4950(4)	2865(3)	31.8(16)
C22	1972(7)	4653(4)	2282(3)	30.3(14)
C23	3222(7)	4930(4)	2068(3)	27.9(15)
C24	3907(6)	5478(4)	2430(3)	26.8(14)
C25	3340(7)	5768(4)	3016(3)	29.1(14)
C26	6896(8)	7233(4)	6509(4)	34.5(17)
C27	8271(6)	7138(4)	6452(3)	28.3(13)
C28	8901(6)	6509(4)	6746(3)	27.0(15)
C29	8151(7)	5967(4)	7099(3)	32.7(15)
C30	6784(7)	6069(4)	7164(3)	36.6(17)
C31	6144(7)	6698(4)	6871(3)	36.2(17)

### Bond Lengths (Å)

Atom	Atom	Length/Å	Atom	Atom	Length/Å
Pt1	N1	2.201(4)	C10	C11	1.374(8)
Pt1	N3	2.199(4)	C11	C13	1.486(7)
Pt1	N5	2.185(5)	C14	C15	1.392(8)
Pt1	C1	2.041(6)	C14	C17	1.497(7)
Pt1	C2	2.047(5)	C15	C16	1.354(8)
Pt1	C3	2.052(4)	C16	C18	1.494(8)
P1	O1	1.446(4)	S1	O2	1.444(4)
P1	N2	1.672(5)	S1	O3	1.440(5)
P1	N4	1.679(4)	S1	O4	1.442(5)
P1	N6	1.681(5)	S1	C19	1.827(6)
N1	N2	1.401(7)	F1	C19	1.332(7)
N1	C4	1.333(7)	F2	C19	1.341(6)
N2	C6	1.392(7)	F3	C19	1.333(7)
N3	N4	1.398(6)	C20	C21	1.366(10)
N3	C9	1.325(7)	C20	C25	1.380(10)
N4	C11	1.386(6)	C21	C22	1.381(10)
N5	N6	1.401(7)	C22	C23	1.398(10)
N5	C14	1.334(7)	C23	C24	1.366(9)
N6	C16	1.384(7)	C24	C25	1.391(9)
C4	C5	1.403(8)	C26	C27	1.382(10)

C4	C7	1.484(7)	C26	C31	1.386(10)
C5	C6	1.372(8)	C27	C28	1.378(9)
C6	C8	1.482(9)	C28	C29	1.384(9)
C9	C10	1.407(8)	C29	C30	1.377(10)
C9	C12	1.494(8)	C30	C31	1.381(10)

### Bond Angles (°)

Atom	Atom	Atom	Angle/°	Atom	Atom	Atom	Angle/°
N3	Pt1	N1	88.2(2)	C6	C5	C4	107.4(5)
N5	Pt1	N1	87.61(15)	N2	C6	C8	124.0(5)
N5	Pt1	N3	87.0(2)	C5	C6	N2	105.7(5)
C1	Pt1	N1	179.2(2)	C5	C6	C8	130.3(5)
C1	Pt1	N3	91.6(3)	N3	C9	C10	110.5(5)
C1	Pt1	N5	91.58(19)	N3	C9	C12	123.9(6)
C1	Pt1	C2	89.0(2)	C10	C9	C12	125.6(5)
C1	Pt1	C3	88.2(3)	C11	C10	C9	107.8(5)
C2	Pt1	N1	91.8(2)	N4	C11	C13	125.6(5)
C2	Pt1	N3	92.1(2)	C10	C11	N4	105.3(5)
C2	Pt1	N5	178.9(3)	C10	C11	C13	129.1(5)
C2	Pt1	C3	88.4(3)	N5	C14	C15	110.5(5)
C3	Pt1	N1	91.9(2)	N5	C14	C17	124.2(5)
C3	Pt1	N3	179.5(2)	C15	C14	C17	125.3(5)
C3	Pt1	N5	92.5(2)	C16	C15	C14	108.5(5)
O1	P1	N2	113.2(2)	N6	C16	C18	124.3(5)
O1	P1	N4	113.2(2)	C15	C16	N6	105.5(6)
O1	P1	N6	112.8(2)	C15	C16	C18	130.2(5)
N2	P1	N4	105.4(2)	O2	S1	C19	102.8(3)
N2	P1	N6	105.6(2)	O3	S1	O2	115.3(3)
N4	P1	N6	105.9(2)	O3	S1	O4	115.2(3)
N2	N1	Pt1	118.5(3)	O3	S1	C19	102.4(3)
C4	N1	Pt1	136.6(4)	O4	S1	O2	115.6(3)
C4	N1	N2	104.9(4)	O4	S1	C19	102.6(3)
N1	N2	P1	121.4(3)	F1	C19	S1	111.7(4)
C6	N2	P1	127.9(4)	F1	C19	F2	107.1(5)
C6	N2	N1	110.7(4)	F1	C19	F3	107.6(5)
N4	N3	Pt1	117.9(3)	F2	C19	S1	110.8(4)
C9	N3	Pt1	136.5(4)	F3	C19	S1	112.2(4)
C9	N3	N4	105.6(4)	F3	C19	F2	107.2(5)

N3	N4	P1	122.0(3)	C21	C20	C25	120.2(6)
C11	N4	P1	127.1(4)	C20	C21	C22	120.7(7)
C11	N4	N3	110.8(4)	C21	C22	C23	118.8(6)
N6	N5	Pt1	118.3(3)	C24	C23	C22	121.0(6)
C14	N5	Pt1	137.0(4)	C23	C24	C25	119.1(6)
C14	N5	N6	104.7(4)	C20	C25	C24	120.2(6)
N5	N6	P1	121.8(4)	C27	C26	C31	120.0(7)
C16	N6	P1	127.4(4)	C28	C27	C26	120.4(6)
C16	N6	N5	110.7(5)	C27	C28	C29	119.7(6)
N1	C4	C5	111.3(5)	C30	C29	C28	119.7(7)
N1	C4	C7	124.7(6)	C29	C30	C31	120.9(7)
C5	C4	C7	124.1(5)	C30	C31	C26	119.2(7)

## APPENDIX 2.5

### Atomic coordinates and isotropic displacement parameters for [TpmpMe<sub>3</sub>][OTf] (8)

U(eq) is defines as one third of the trace of the orthogonalized U<sub>ij</sub> tensor.

<b>Atom</b>	<b>x/a</b>	<b>y/b</b>	<b>z/c</b>	<b>U(eq)</b>
Pt1	86.8(2)	7018.4(2)	3069.5(2)	18.84(9)
C1	-704(7)	6391(3)	2606(4)	35(2)
C2	975(6)	6431(3)	3532(4)	36(2)
C3	1043(6)	7003(4)	2468(4)	30.9(19)
N4	838(4)	7710(3)	3559(3)	19.8(13)
N5	232(4)	8111(2)	3740(3)	20.9(13)
C6	753(6)	8533(3)	4026(3)	24.5(16)
C7	1733(6)	8393(3)	4038(3)	25.4(17)
C8	1752(5)	7888(3)	3743(3)	22.2(15)
C9	290(7)	9025(4)	4261(4)	40(2)
C10	2640(6)	7573(4)	3634(4)	38(2)
N11	-844(5)	7668(2)	2630(3)	20.5(13)
N12	-1131(4)	8085(3)	2969(3)	20.5(13)
C13	-1627(6)	8502(3)	2644(4)	28.2(18)
C14	-1663(6)	8335(4)	2085(4)	35(2)
C15	-1173(6)	7827(4)	2079(4)	30.3(18)
C16	-1995(8)	9014(4)	2904(5)	45(2)
C17	-983(9)	7491(5)	1567(4)	53(3)
N18	-924(5)	7054(3)	3695(3)	22.3(13)
N19	-1210(4)	7575(3)	3845(3)	20.2(13)
C20	-1833(6)	7550(3)	4250(3)	24.9(16)
C21	-1961(6)	6993(4)	4352(3)	27.4(17)
C22	-1379(6)	6704(3)	4012(3)	24.5(16)
C23	-2250(7)	8053(4)	4495(4)	39(2)
C24	-1286(7)	6084(4)	3985(4)	37(2)
C25	-836(5)	8065(3)	3588(3)	20.0(15)
Pt2	2384.4(2)	4920.2(2)	2412.4(2)	15.16(8)
C26	1724(6)	5504(3)	1843(3)	23.9(16)
C27	3578(6)	4923(3)	1962(4)	30.5(19)
C28	1757(6)	4301(3)	1873(3)	27.3(17)
N29	3084(4)	4340(2)	3073(2)	16.9(12)
N30	2982(4)	4458(2)	3634(2)	13.1(11)

C31	3462(5)	4079(3)	4004(3)	19.1(15)
C32	3890(6)	3708(3)	3677(3)	22.8(16)
C33	3637(5)	3885(3)	3097(3)	18.9(15)
C34	3496(6)	4115(3)	4651(3)	25.2(17)
C35	3931(8)	3615(4)	2573(4)	37(2)
N36	3039(4)	5546(2)	3037(2)	14.7(11)
N37	2941(4)	5455(2)	3602(2)	13.8(11)
C38	3398(5)	5855(3)	3960(3)	15.7(14)
C39	3795(5)	6220(3)	3608(3)	19.3(15)
C40	3564(5)	6018(3)	3042(3)	16.0(14)
C41	3416(6)	5859(3)	4601(3)	22.8(16)
C42	3819(6)	6273(3)	2502(3)	28.1(17)
N43	1174(4)	4922(2)	2910(2)	16.4(12)
N44	1429(4)	4933(2)	3503(2)	14.9(12)
C45	610(5)	4926(3)	3769(3)	18.8(15)
C46	-181(5)	4909(3)	3339(3)	18.8(15)
C47	188(5)	4910(3)	2812(3)	17.2(14)
C48	656(6)	4923(3)	4412(3)	23.8(16)
C49	-402(6)	4880(3)	2218(3)	25.8(16)
C50	2458(5)	4953(3)	3765(3)	14.1(13)
Pt3	5265.5(2)	2242.2(2)	8424.4(2)	28.71(10)
C51	4565(9)	1519(4)	8157(6)	58(3)
C52	6233(7)	1795(4)	9029(5)	48(3)
C53	6220(7)	2107(4)	7833(4)	38(2)
N54	4245(5)	2751(3)	7823(3)	23.3(14)
N55	4007(4)	3255(2)	8037(3)	18.0(12)
C56	3551(5)	3594(3)	7609(3)	21.1(15)
C57	3499(6)	3289(4)	7109(3)	28.8(18)
C58	3928(6)	2772(4)	7256(4)	31.6(19)
C59	3260(6)	4178(3)	7713(4)	30.0(18)
C60	4007(8)	2281(5)	6874(4)	52(3)
N61	4252(5)	2420(3)	9030(3)	31.0(16)
N62	3840(5)	2937(3)	8992(3)	25.6(14)
C63	3139(6)	2995(4)	9346(3)	30.5(19)
C64	3104(7)	2497(4)	9619(4)	39(2)
C65	3795(7)	2147(4)	9418(4)	40(2)
C66	2569(7)	3513(4)	9377(4)	39(2)
C67	4013(9)	1557(5)	9596(5)	59(3)
N68	5928(5)	3042(3)	8729(3)	24.8(14)
N69	5277(4)	3446(3)	8831(3)	21.4(13)

C70	5748(6)	3903(3)	9084(3)	24.0(16)
C71	6729(6)	3786(4)	9144(3)	27.9(18)
C72	6822(6)	3250(4)	8913(3)	28.7(18)
C73	5211(6)	4411(4)	9230(3)	29.9(18)
C74	7755(6)	2947(5)	8856(4)	43(2)
C75	4226(5)	3366(3)	8654(3)	19.2(15)
S1	2689.8(15)	5109.9(8)	9357.3(9)	28.7(4)
O76	2973(6)	5689(3)	9354(4)	62(2)
O77	3185(5)	4808(3)	9847(3)	45.5(17)
O78	2615(6)	4823(3)	8824(3)	54.3(19)
C79	1423(7)	5139(5)	9515(5)	46(3)
F80	858(6)	5448(4)	9128(3)	95(3)
F81	1384(4)	5370(3)	10023(3)	53.8(15)
F82	1030(5)	4639(3)	9491(4)	92(3)
S3	4982.4(15)	7415.2(9)	4862.7(10)	32.1(5)
O90	5875(8)	7249(3)	5185(5)	100(4)
O91	4053(7)	7227(4)	4977(4)	76(3)
O92	5040(6)	7350(4)	4238(3)	61(2)
C93	4936(7)	8168(4)	4900(6)	49(3)
F94	4137(4)	8389(3)	4640(3)	57.0(16)
F95	5718(4)	8425(2)	4871(4)	77(2)
F96	4843(6)	8281(3)	5495(4)	80(2)
S2	2928.7(13)	5273.8(8)	6041.1(8)	22.4(4)
O83	2522(4)	5155(3)	6564(2)	33.9(14)
O84	3195(5)	5845(2)	5964(3)	38.1(15)
O85	2438(4)	5009(2)	5524(2)	26.2(12)
C86	4115(6)	4917(4)	6177(4)	36(2)
F87	4659(4)	5082(3)	6655(2)	58.5(18)
F88	4647(4)	4995(2)	5746(2)	40.8(13)
F89	3977(4)	4367(3)	6220(3)	58.4(17)

### Bond Lengths (Å)

Atom	Atom	Length/Å	Atom	Atom	Length/Å
Pt1	C1	2.062(8)	C45	C46	1.359(11)
Pt1	C2	2.057(8)	C45	C48	1.492(10)
Pt1	C3	2.060(8)	C46	C47	1.397(10)
Pt1	N4	2.183(6)	C47	C49	1.496(10)
Pt1	N11	2.169(6)	Pt3	C51	2.035(10)

Pt1	N18	2.159(6)	Pt3	C52	2.079(9)
N4	N5	1.379(8)	Pt3	C53	2.065(9)
N4	C8	1.328(10)	Pt3	N54	2.194(6)
N5	C6	1.353(10)	Pt3	N61	2.166(7)
N5	C25	1.454(9)	Pt3	N68	2.194(7)
C6	C7	1.378(11)	N54	N55	1.368(8)
C6	C9	1.485(12)	N54	C58	1.329(11)
C7	C8	1.397(11)	N55	C56	1.361(9)
C8	C10	1.485(12)	N55	C75	1.450(9)
N11	N12	1.369(9)	C56	C57	1.370(11)
N11	C15	1.351(10)	C56	C59	1.487(11)
N12	C13	1.372(10)	C57	C58	1.393(12)
N12	C25	1.440(9)	C58	C60	1.492(12)
C13	C14	1.359(13)	N61	N62	1.361(10)
C13	C16	1.491(12)	N61	C65	1.347(11)
C14	C15	1.394(13)	N62	C63	1.365(10)
C15	C17	1.495(13)	N62	C75	1.445(9)
N18	N19	1.374(9)	C63	C64	1.360(12)
N18	C22	1.335(10)	C63	C66	1.476(13)
N19	C20	1.367(10)	C64	C65	1.397(14)
N19	C25	1.449(9)	C65	C67	1.494(13)
C20	C21	1.376(12)	N68	N69	1.363(9)
C20	C23	1.485(12)	N68	C72	1.330(10)
C21	C22	1.392(11)	N69	C70	1.360(10)
C22	C24	1.497(11)	N69	C75	1.446(9)
Pt2	C26	2.044(7)	C70	C71	1.357(11)
Pt2	C27	2.072(8)	C70	C73	1.488(12)
Pt2	C28	2.049(8)	C71	C72	1.409(13)
Pt2	N29	2.187(6)	C72	C74	1.493(12)
Pt2	N36	2.189(6)	S1	O76	1.444(8)
Pt2	N43	2.162(6)	S1	O77	1.434(7)
N29	N30	1.367(8)	S1	O78	1.413(7)
N29	C33	1.324(9)	S1	C79	1.826(10)
N30	C31	1.353(9)	C79	F80	1.322(13)
N30	C50	1.443(8)	C79	F81	1.316(11)
C31	C32	1.362(10)	C79	F82	1.313(13)
C31	C34	1.506(10)	S3	O90	1.390(9)
C32	C33	1.410(10)	S3	O91	1.412(9)
C33	C35	1.493(10)	S3	O92	1.479(8)
N36	N37	1.362(8)	S3	C93	1.812(10)

N36	C40	1.341(9)	C93	F94	1.281(11)
N37	C38	1.362(9)	C93	F95	1.246(11)
N37	C50	1.452(8)	C93	F96	1.437(14)
C38	C39	1.368(10)	S2	O83	1.444(6)
C38	C41	1.491(10)	S2	O84	1.438(6)
C39	C40	1.398(10)	S2	O85	1.437(5)
C40	C42	1.489(10)	S2	C86	1.819(9)
N43	N44	1.375(8)	C86	F87	1.303(11)
N43	C47	1.333(9)	C86	F88	1.342(10)
N44	C45	1.361(9)	C86	F89	1.341(11)
N44	C50	1.447(9)			

### Bond Angles (°)

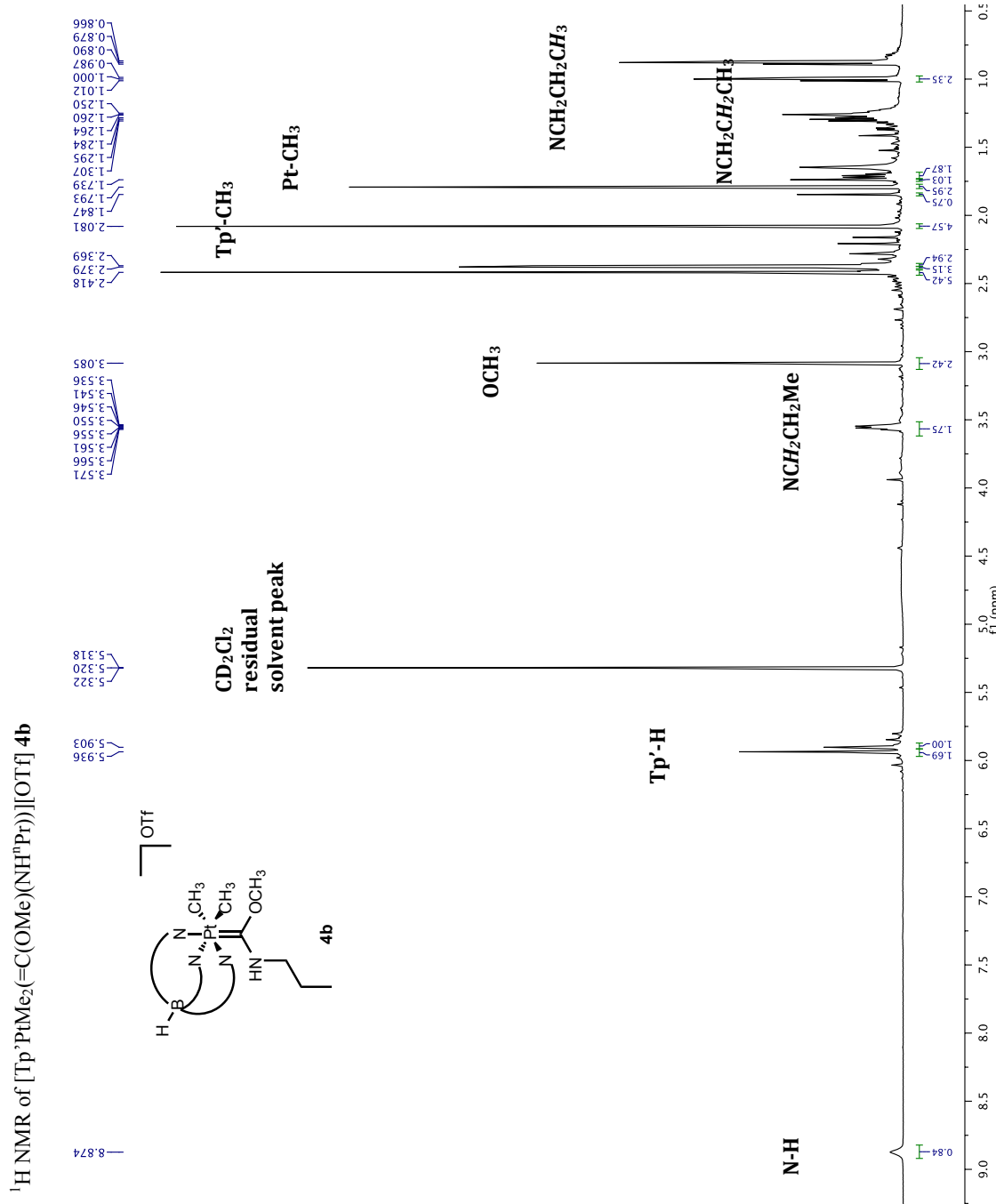
Atom	Atom	Atom	Angle/°	Atom	Atom	Atom	Angle/°
C1	Pt1	N4	176.5(3)	N44	C45	C48	123.2(7)
C1	Pt1	N11	93.1(3)	C46	C45	N44	106.4(6)
C1	Pt1	N18	92.5(3)	C46	C45	C48	130.4(7)
C2	Pt1	C1	89.7(4)	C45	C46	C47	107.2(6)
C2	Pt1	C3	87.7(4)	N43	C47	C46	110.0(6)
C2	Pt1	N4	93.1(3)	N43	C47	C49	123.2(7)
C2	Pt1	N11	176.5(3)	C46	C47	C49	126.8(7)
C2	Pt1	N18	93.5(3)	N30	C50	N37	111.6(5)
C3	Pt1	C1	88.0(3)	N30	C50	N44	111.4(5)
C3	Pt1	N4	94.2(3)	N44	C50	N37	111.6(5)
C3	Pt1	N11	94.6(3)	C51	Pt3	C52	89.3(5)
C3	Pt1	N18	178.7(3)	C51	Pt3	C53	88.7(5)
N11	Pt1	N4	84.0(2)	C51	Pt3	N54	93.2(4)
N18	Pt1	N4	85.1(2)	C51	Pt3	N61	92.8(4)
N18	Pt1	N11	84.3(2)	C51	Pt3	N68	176.2(4)
N5	N4	Pt1	115.8(4)	C52	Pt3	N54	176.8(4)
C8	N4	Pt1	139.3(5)	C52	Pt3	N61	93.7(4)
C8	N4	N5	104.9(6)	C52	Pt3	N68	92.5(4)
N4	N5	C25	120.0(6)	C53	Pt3	C52	88.2(4)
C6	N5	N4	112.2(6)	C53	Pt3	N54	93.8(3)
C6	N5	C25	127.7(6)	C53	Pt3	N61	177.6(3)
N5	C6	C7	105.4(7)	C53	Pt3	N68	94.8(3)
N5	C6	C9	123.7(7)	N61	Pt3	N54	84.2(2)
C7	C6	C9	130.9(8)	N61	Pt3	N68	83.7(3)

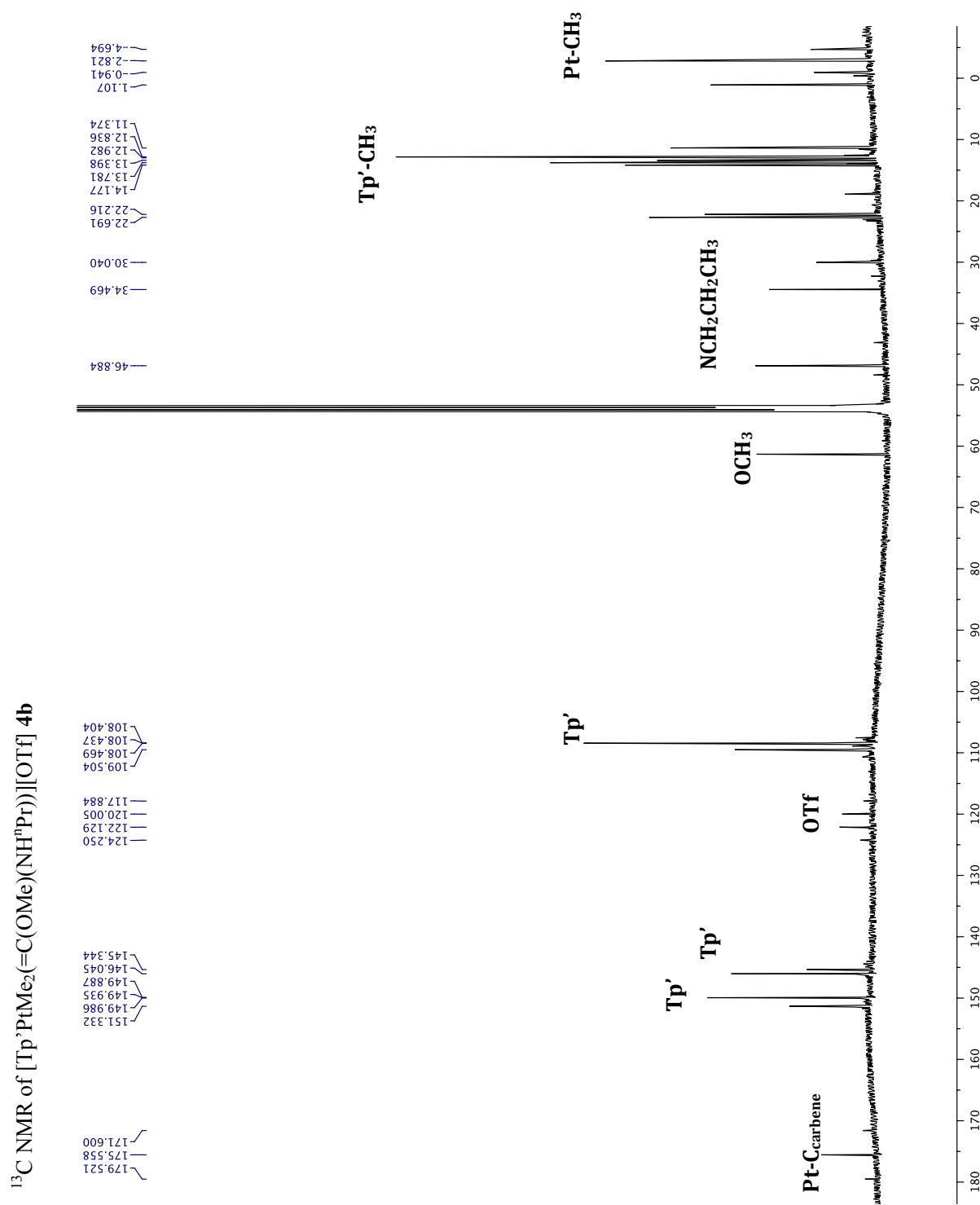
C6	C7	C8	107.0(7)	N68	Pt3	N54	84.9(2)
N4	C8	C7	110.5(7)	N55	N54	Pt3	115.1(4)
N4	C8	C10	122.4(7)	C58	N54	Pt3	137.5(5)
C7	C8	C10	127.1(7)	C58	N54	N55	105.6(6)
N12	N11	Pt1	116.9(4)	N54	N55	C75	119.9(6)
C15	N11	Pt1	137.6(6)	C56	N55	N54	111.7(6)
C15	N11	N12	105.1(6)	C56	N55	C75	128.4(6)
N11	N12	C13	112.2(6)	N55	C56	C57	105.3(7)
N11	N12	C25	119.6(6)	N55	C56	C59	123.2(7)
C13	N12	C25	128.0(7)	C57	C56	C59	131.4(7)
N12	C13	C16	123.2(8)	C56	C57	C58	107.5(7)
C14	C13	N12	104.8(7)	N54	C58	C57	109.9(7)
C14	C13	C16	131.9(8)	N54	C58	C60	121.4(8)
C13	C14	C15	108.7(7)	C57	C58	C60	128.6(8)
N11	C15	C14	109.2(7)	N62	N61	Pt3	115.9(5)
N11	C15	C17	122.4(8)	C65	N61	Pt3	138.8(6)
C14	C15	C17	128.4(8)	C65	N61	N62	104.9(7)
N19	N18	Pt1	116.4(4)	N61	N62	C63	112.1(7)
C22	N18	Pt1	138.7(5)	N61	N62	C75	120.2(6)
C22	N18	N19	104.9(6)	C63	N62	C75	127.4(7)
N18	N19	C25	120.2(6)	N62	C63	C66	122.7(7)
C20	N19	N18	111.6(6)	C64	C63	N62	105.8(8)
C20	N19	C25	128.2(6)	C64	C63	C66	131.5(8)
N19	C20	C21	105.7(7)	C63	C64	C65	107.3(8)
N19	C20	C23	123.1(7)	N61	C65	C64	110.0(8)
C21	C20	C23	131.1(8)	N61	C65	C67	123.7(9)
C20	C21	C22	106.7(7)	C64	C65	C67	126.3(9)
N18	C22	C21	110.9(7)	N69	N68	Pt3	115.6(5)
N18	C22	C24	123.5(7)	C72	N68	Pt3	138.4(6)
C21	C22	C24	125.5(7)	C72	N68	N69	105.6(7)
N12	C25	N5	111.1(6)	N68	N69	C75	120.1(6)
N12	C25	N19	112.3(6)	C70	N69	N68	111.9(6)
N19	C25	N5	111.4(6)	C70	N69	C75	128.0(7)
C26	Pt2	C27	88.4(3)	N69	C70	C73	122.9(7)
C26	Pt2	C28	89.8(3)	C71	C70	N69	105.8(7)
C26	Pt2	N29	175.8(3)	C71	C70	C73	131.3(7)
C26	Pt2	N36	93.3(3)	C70	C71	C72	107.2(7)
C26	Pt2	N43	92.8(3)	N68	C72	C71	109.6(7)
C27	Pt2	N29	93.8(3)	N68	C72	C74	123.0(8)
C27	Pt2	N36	93.6(3)	C71	C72	C74	127.5(8)

C27	Pt2	N43	178.0(3)	N62	C75	N55	112.0(6)
C28	Pt2	C27	88.8(3)	N62	C75	N69	111.7(6)
C28	Pt2	N29	93.9(3)	N69	C75	N55	110.8(6)
C28	Pt2	N36	176.1(3)	O76	S1	C79	103.2(5)
C28	Pt2	N43	92.7(3)	O77	S1	O76	113.4(5)
N29	Pt2	N36	83.0(2)	O77	S1	C79	101.9(5)
N43	Pt2	N29	84.9(2)	O78	S1	O76	116.6(5)
N43	Pt2	N36	84.8(2)	O78	S1	O77	114.7(4)
N30	N29	Pt2	116.4(4)	O78	S1	C79	104.7(5)
C33	N29	Pt2	137.8(5)	F80	C79	S1	111.0(8)
C33	N29	N30	105.7(6)	F81	C79	S1	111.6(6)
N29	N30	C50	120.0(5)	F81	C79	F80	106.2(8)
C31	N30	N29	111.2(5)	F82	C79	S1	110.5(7)
C31	N30	C50	128.8(6)	F82	C79	F80	106.8(9)
N30	C31	C32	106.9(6)	F82	C79	F81	110.6(10)
N30	C31	C34	122.6(6)	O90	S3	O91	123.2(7)
C32	C31	C34	130.4(7)	O90	S3	O92	109.2(7)
C31	C32	C33	106.0(6)	O90	S3	C93	107.1(5)
N29	C33	C32	110.2(6)	O91	S3	O92	109.6(5)
N29	C33	C35	123.1(7)	O91	S3	C93	105.7(5)
C32	C33	C35	126.7(7)	O92	S3	C93	99.2(5)
N37	N36	Pt2	116.3(4)	F94	C93	S3	115.1(7)
C40	N36	Pt2	138.5(5)	F94	C93	F96	100.7(8)
C40	N36	N37	105.1(5)	F95	C93	S3	117.0(7)
N36	N37	C38	112.1(5)	F95	C93	F94	116.5(10)
N36	N37	C50	120.1(5)	F95	C93	F96	99.3(9)
C38	N37	C50	127.6(6)	F96	C93	S3	104.1(7)
N37	C38	C39	105.7(6)	O83	S2	C86	102.0(4)
N37	C38	C41	123.7(6)	O84	S2	O83	115.6(4)
C39	C38	C41	130.6(6)	O84	S2	C86	103.5(4)
C38	C39	C40	107.0(6)	O85	S2	O83	115.5(3)
N36	C40	C39	110.1(6)	O85	S2	O84	114.3(4)
N36	C40	C42	122.4(7)	O85	S2	C86	103.2(4)
C39	C40	C42	127.4(7)	F87	C86	S2	112.6(7)
N44	N43	Pt2	116.2(4)	F87	C86	F88	107.2(7)
C47	N43	Pt2	138.2(5)	F87	C86	F89	107.7(8)
C47	N43	N44	105.5(6)	F88	C86	S2	112.0(6)
N43	N44	C50	120.5(5)	F89	C86	S2	110.1(6)
C45	N44	N43	111.0(6)	F89	C86	F88	107.0(8)
C45	N44	C50	128.6(6)				

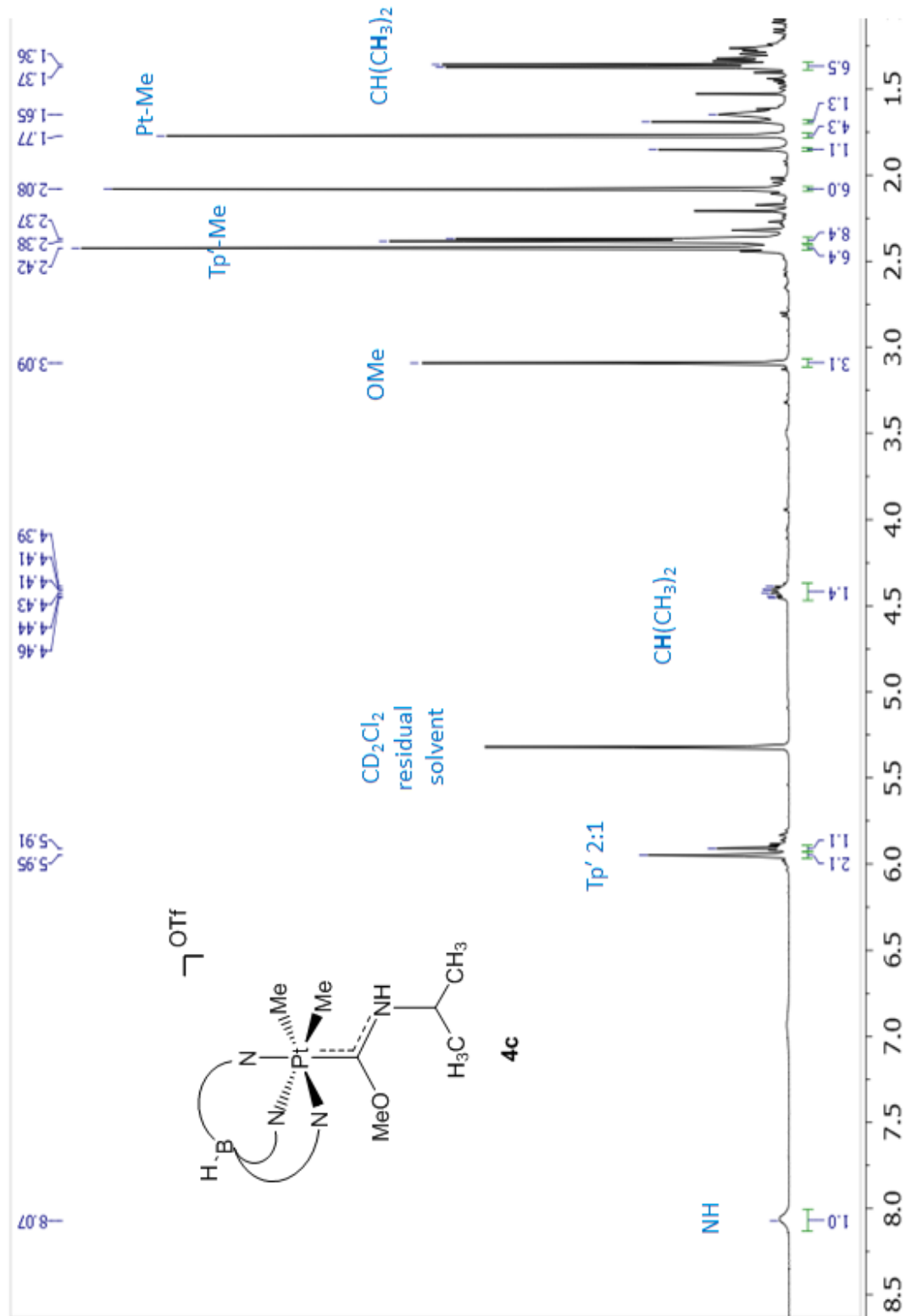
## APPENDIX 3.1

### Representative NMR Data for Chapter 3

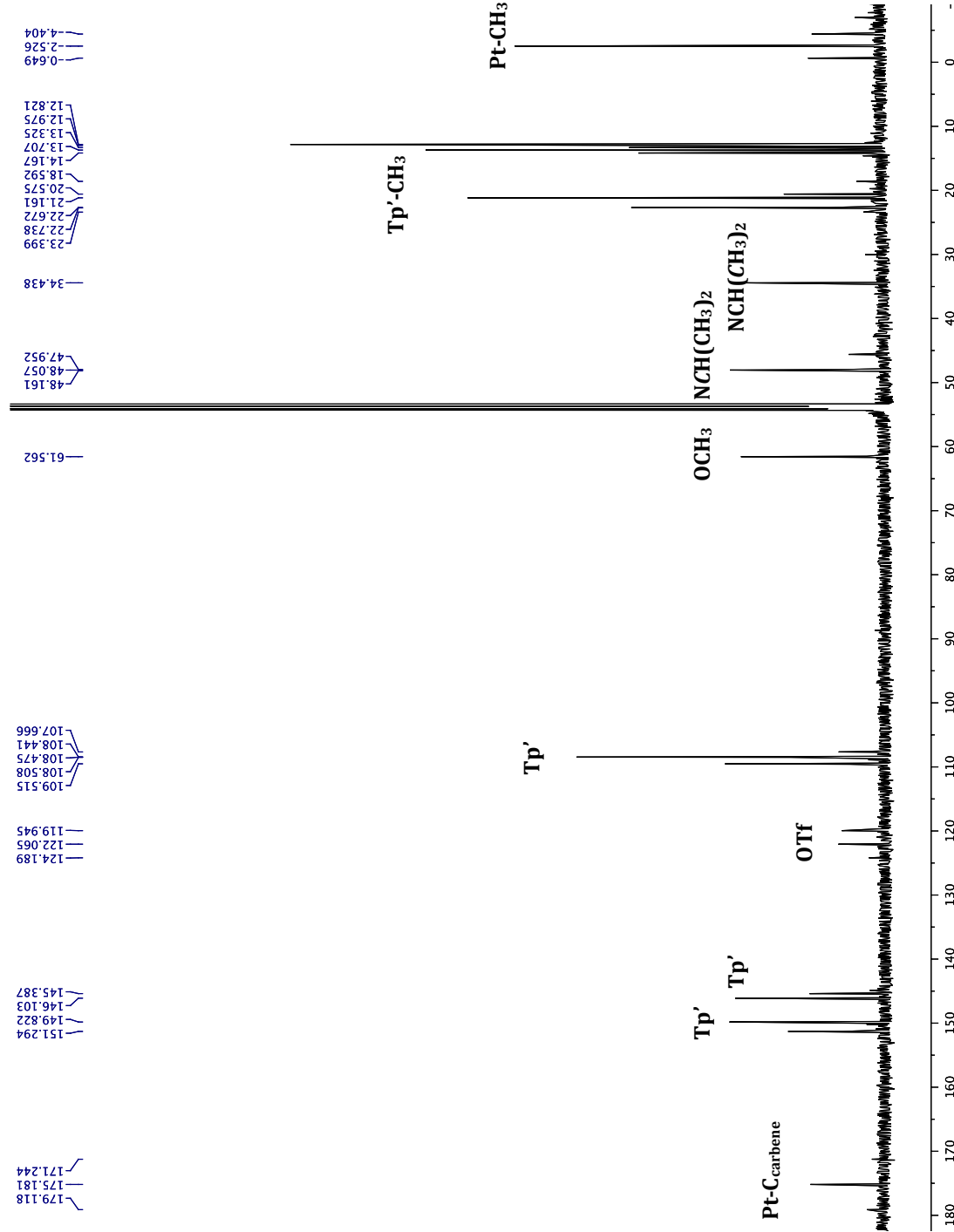




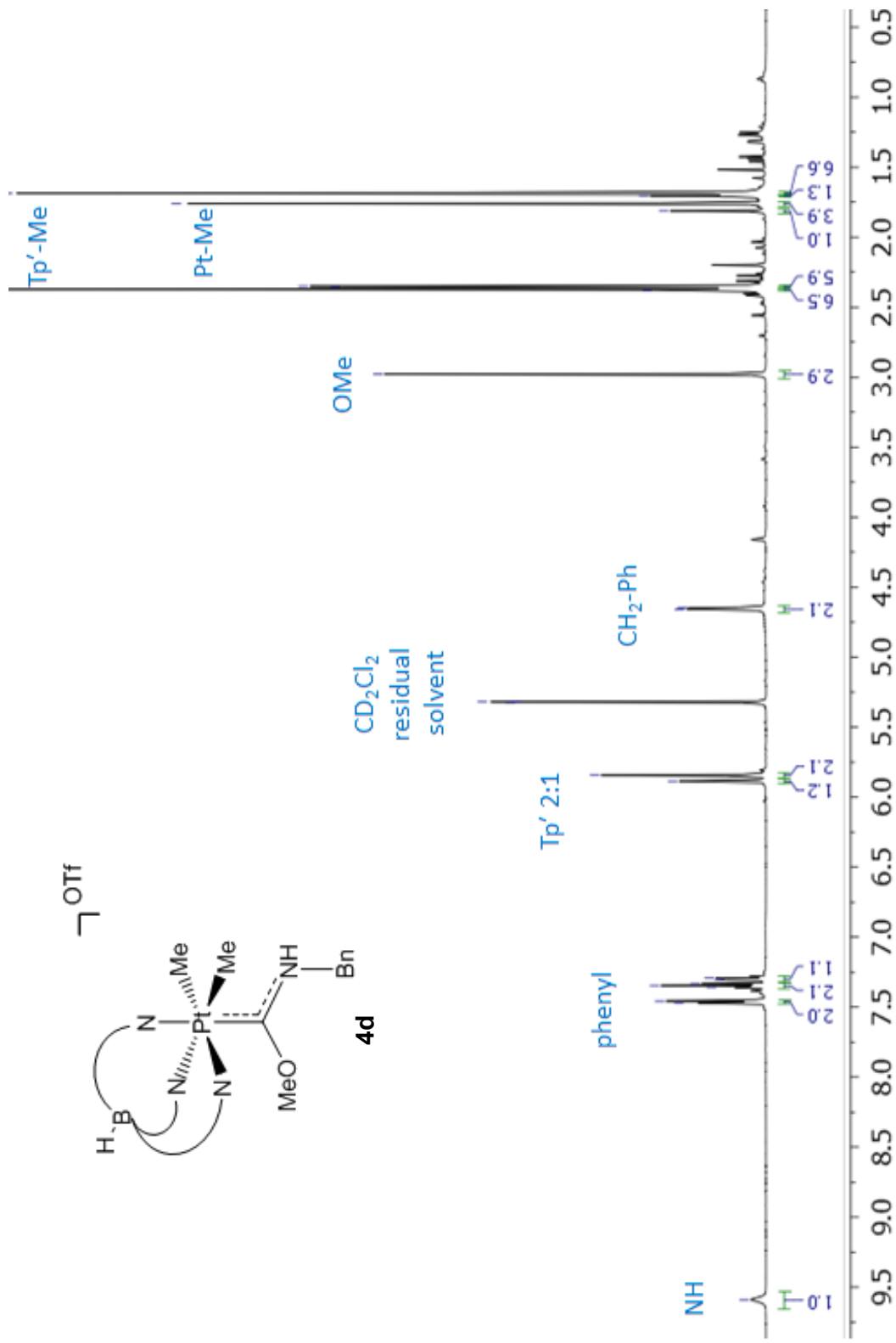
<sup>1</sup>H NMR of [Tp'PtMe<sub>2</sub>(=C(OMe)NH*i*Pr)][OTf] **4c**

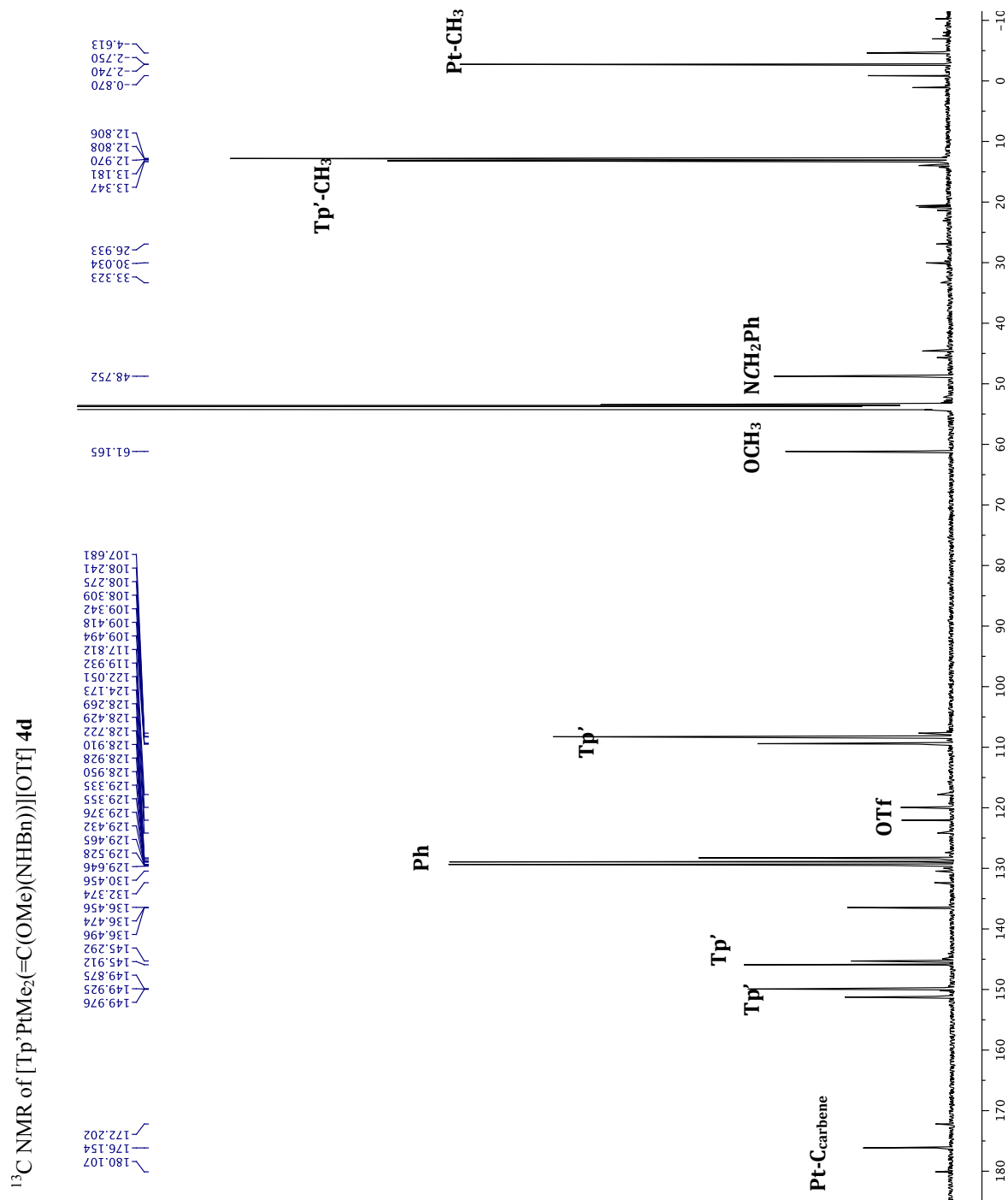


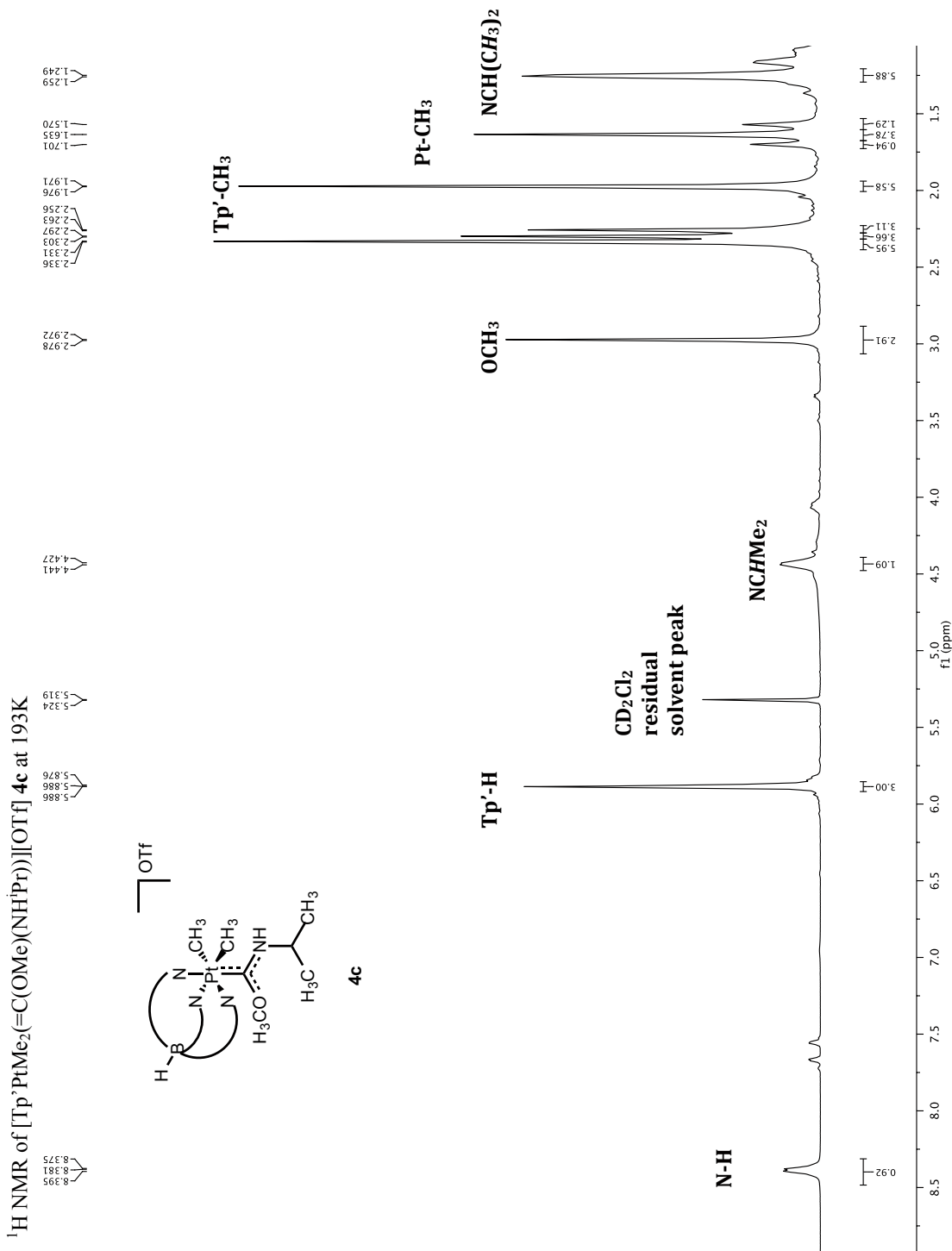
$^{13}\text{C}$  NMR of [Tp'PtMe<sub>2</sub>(=C(OMe)(NH<sup>i</sup>Pr))][OTf] **4c**



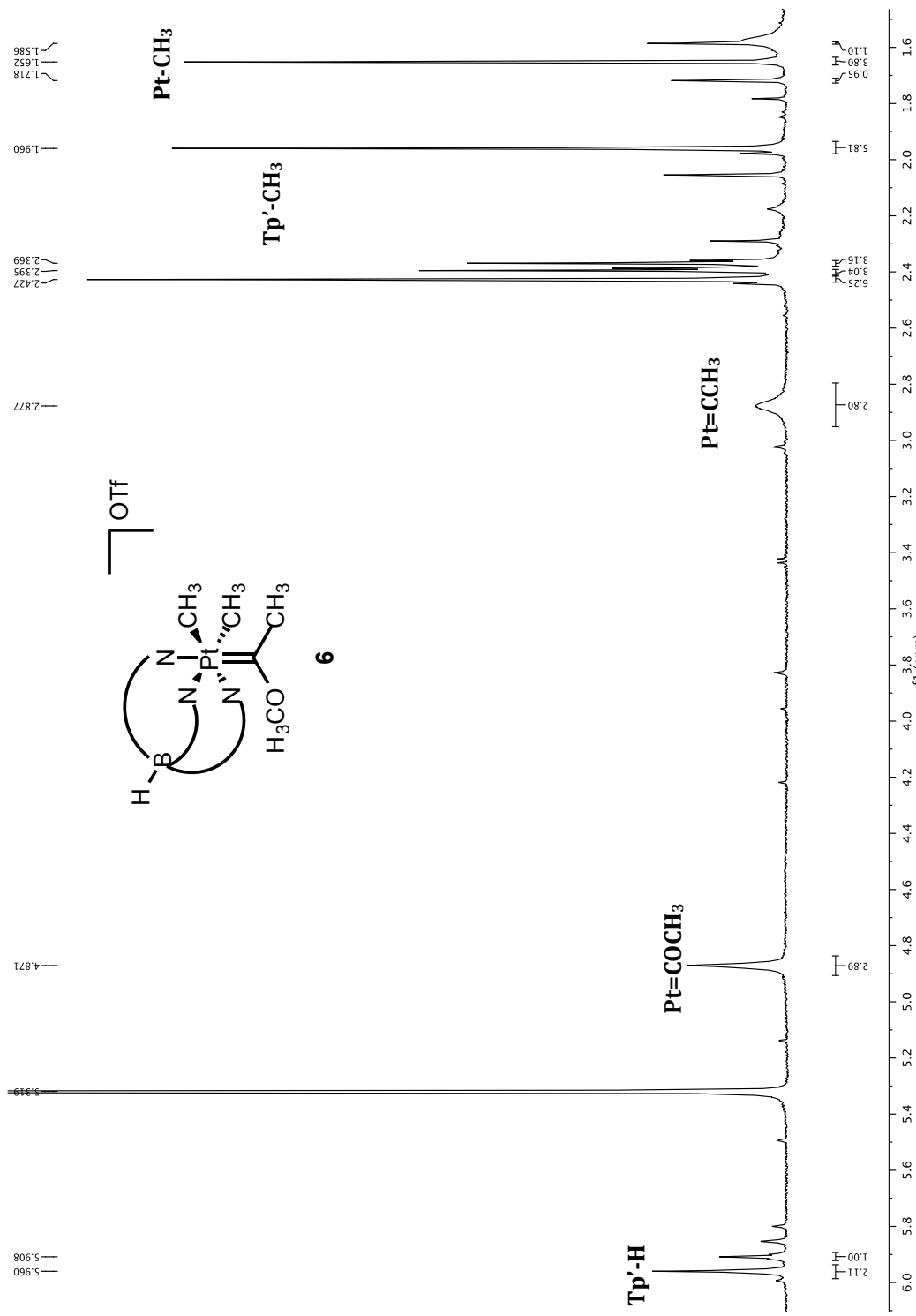
<sup>1</sup>H NMR of [(Tp')Pt(=C(OCH<sub>3</sub>)(NHBn))Me<sub>2</sub>][OTf] 4d

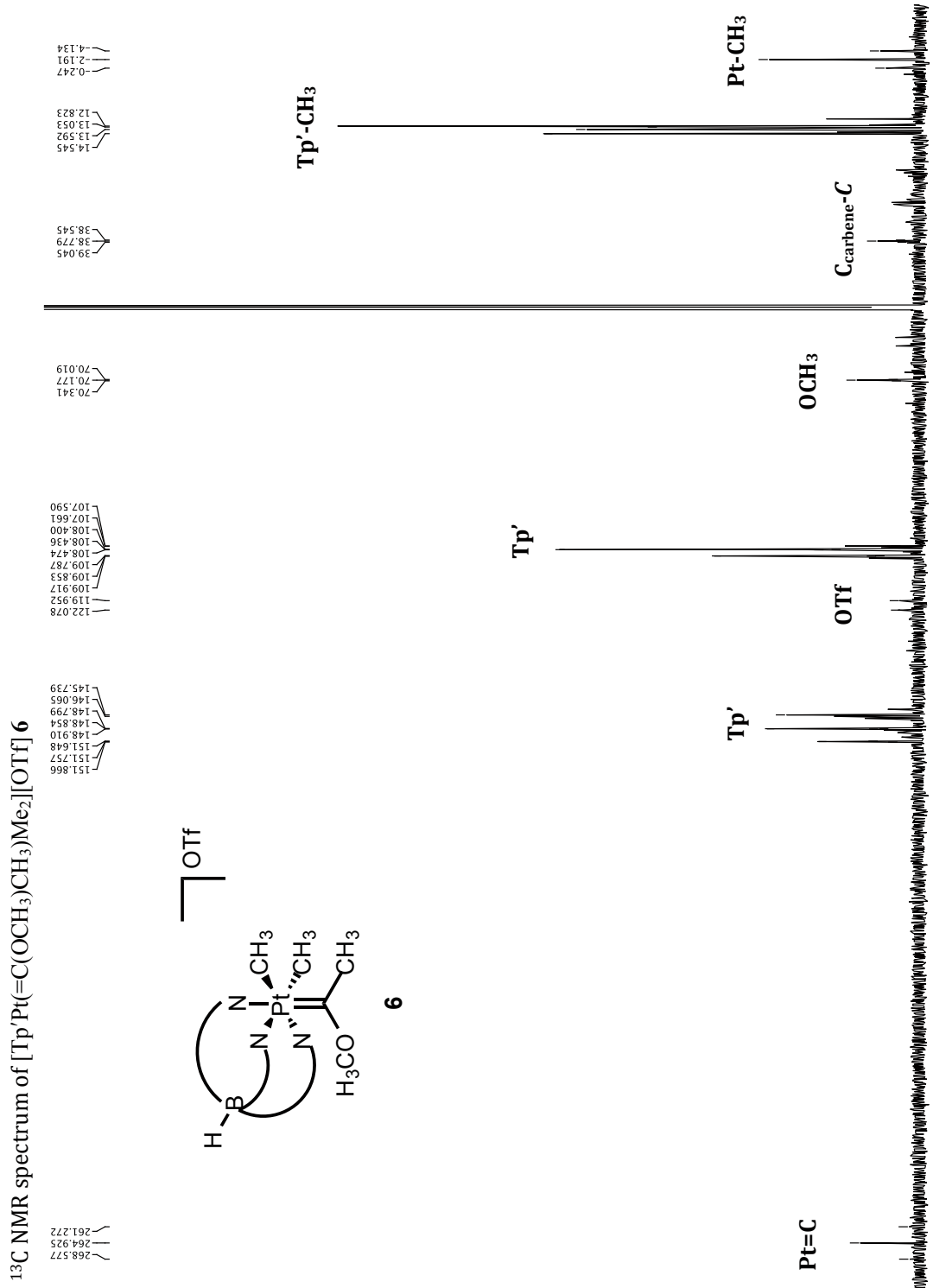




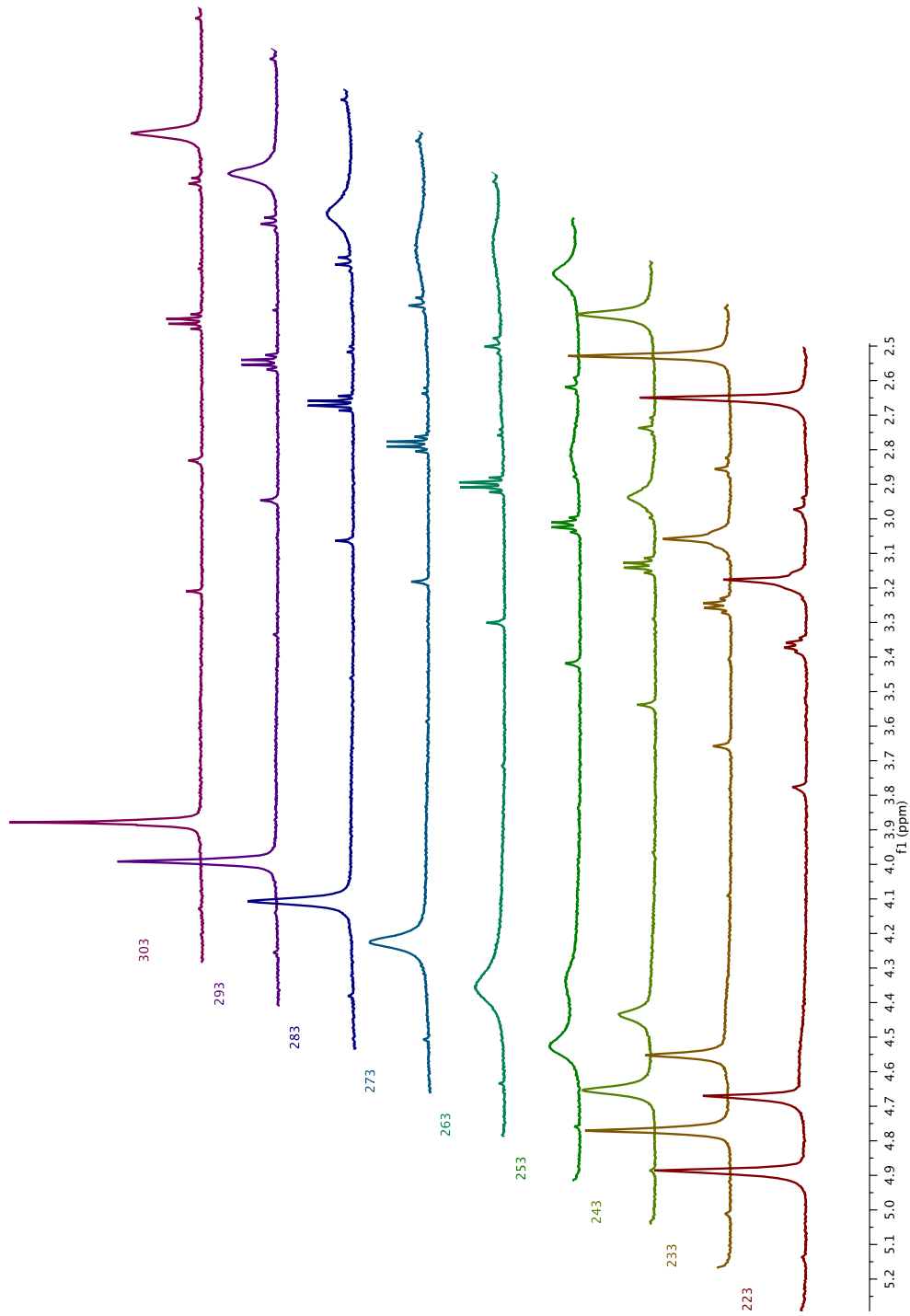


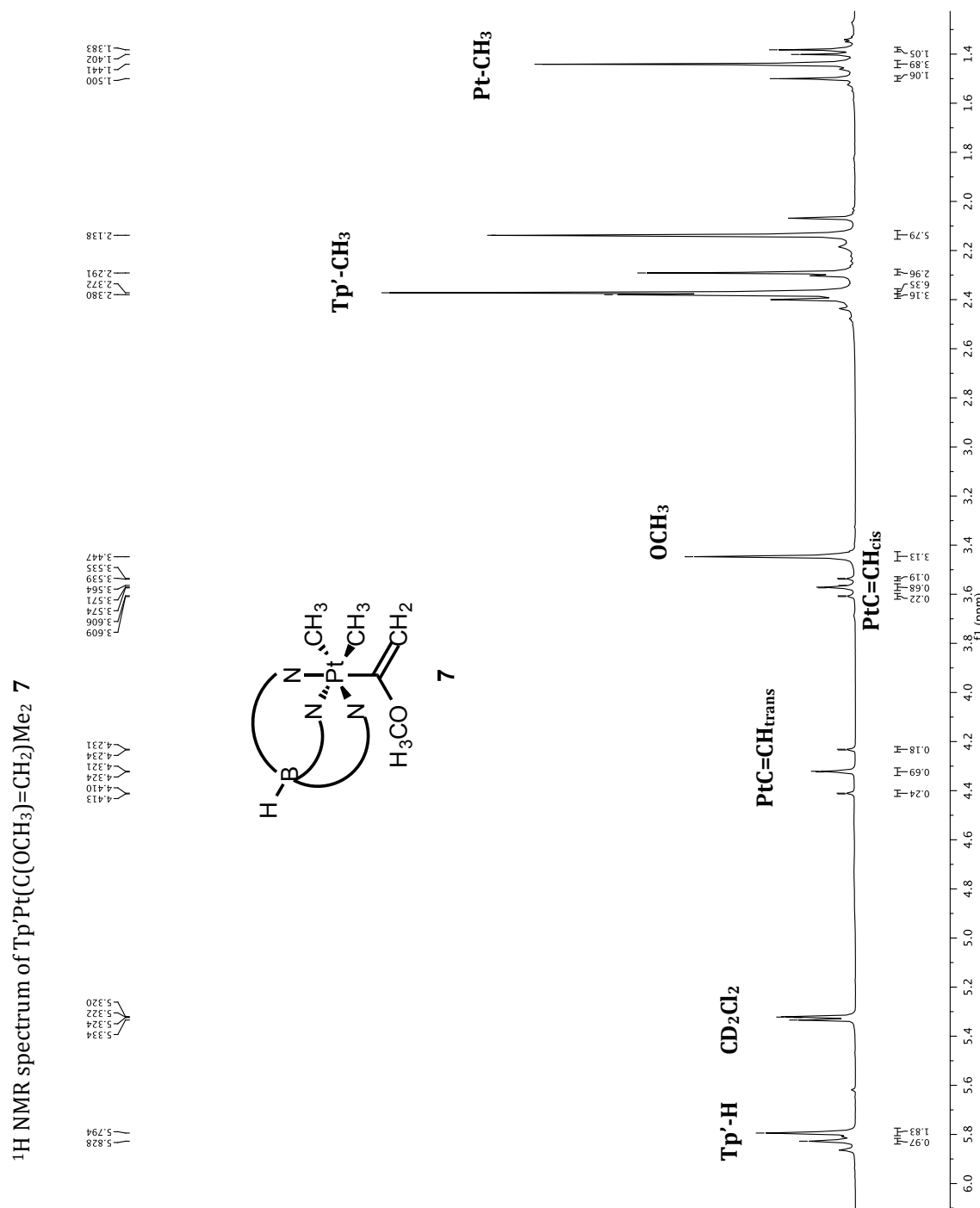
$^1\text{H}$  NMR spectrum of  $[\text{Tp}'\text{Pt}(\text{=C(OCH}_3)\text{CH}_3)\text{Me}_2]\text{[OTf]}$  6



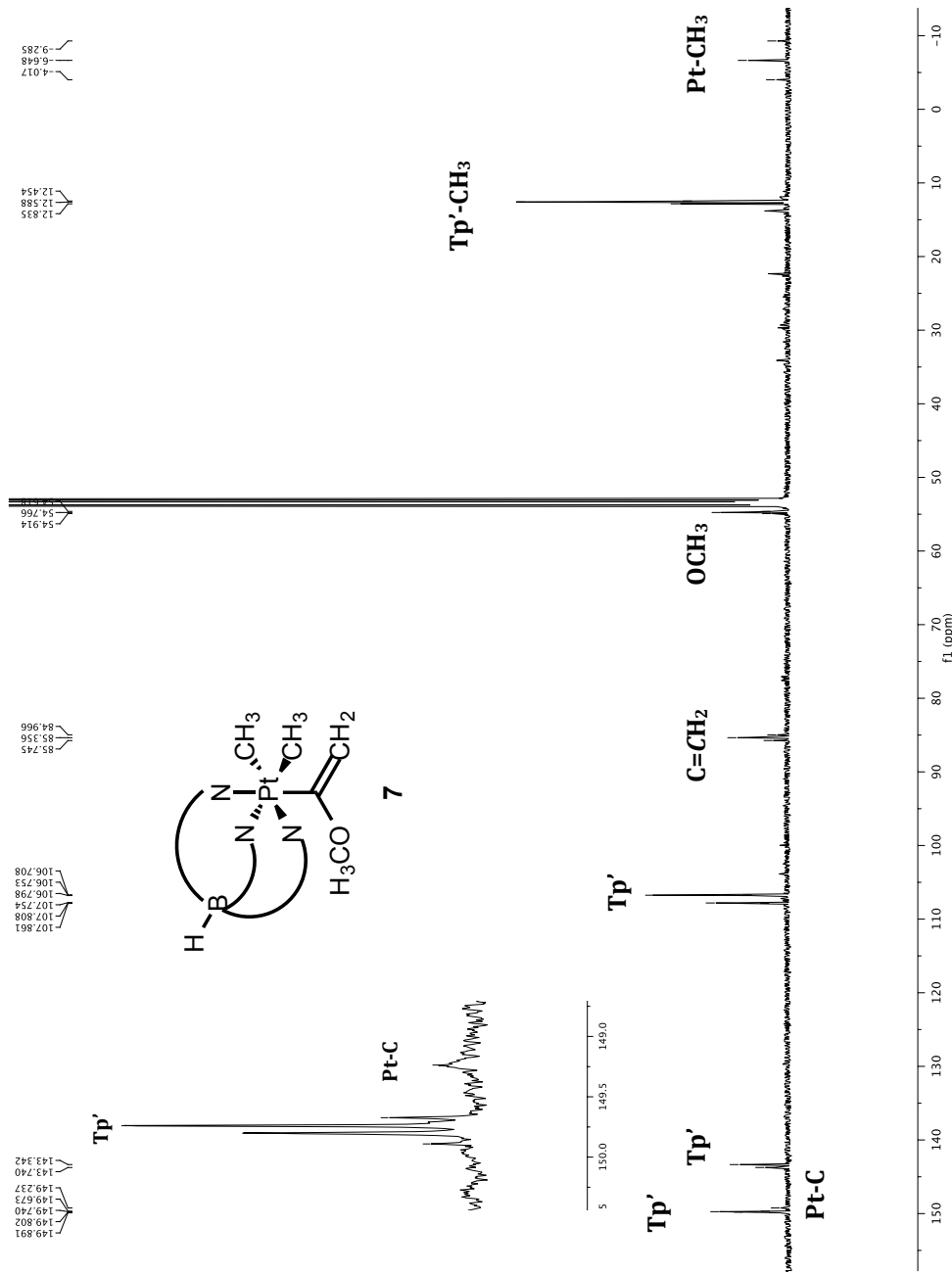


Variable temperature  $^1\text{H}$  NMR spectrum of  $[\text{Tp}'\text{Pt}(\text{=C(OCH}_3)\text{CH}_3)\text{Me}_2]\text{[OTf]}$  **6** of the carbene ligands

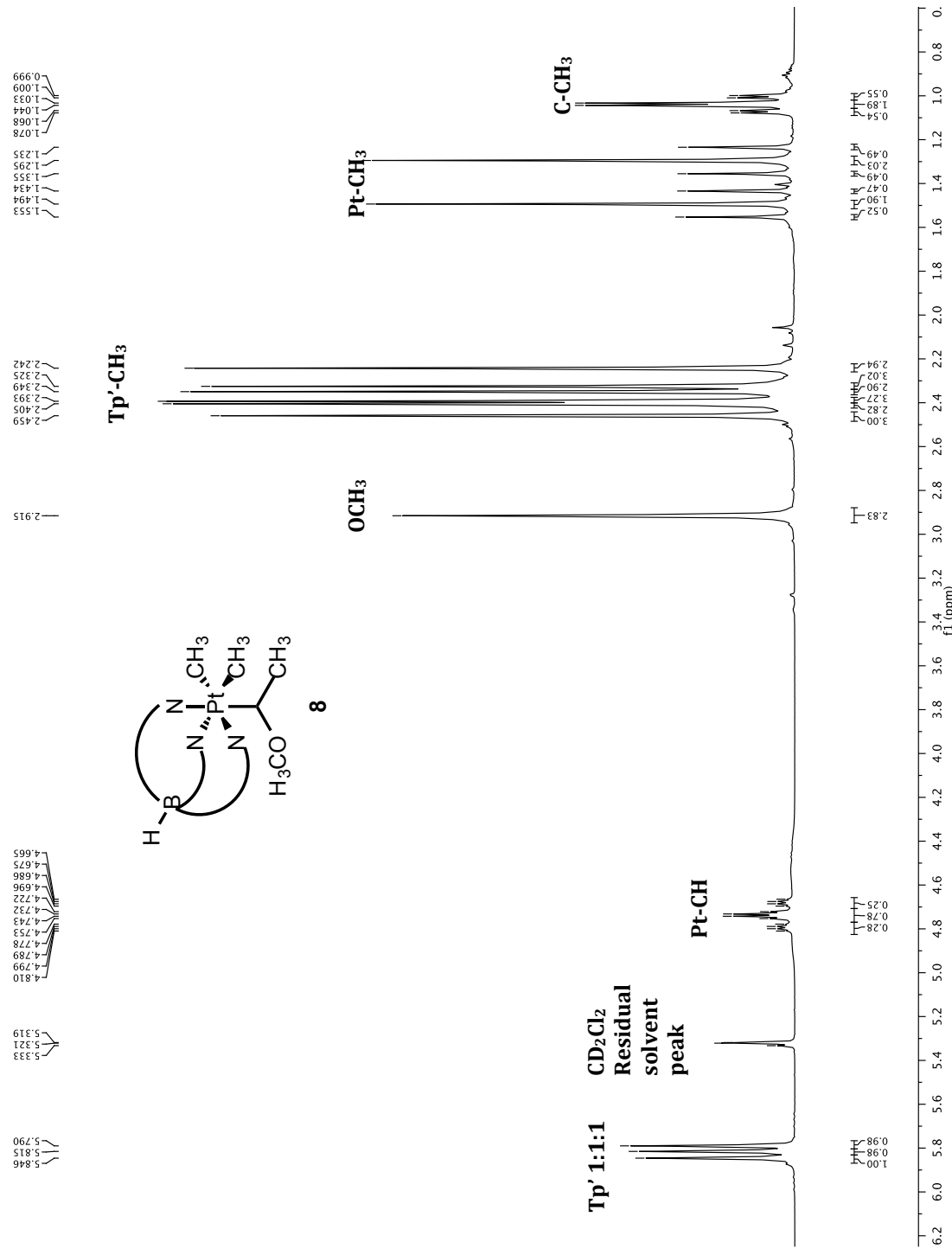


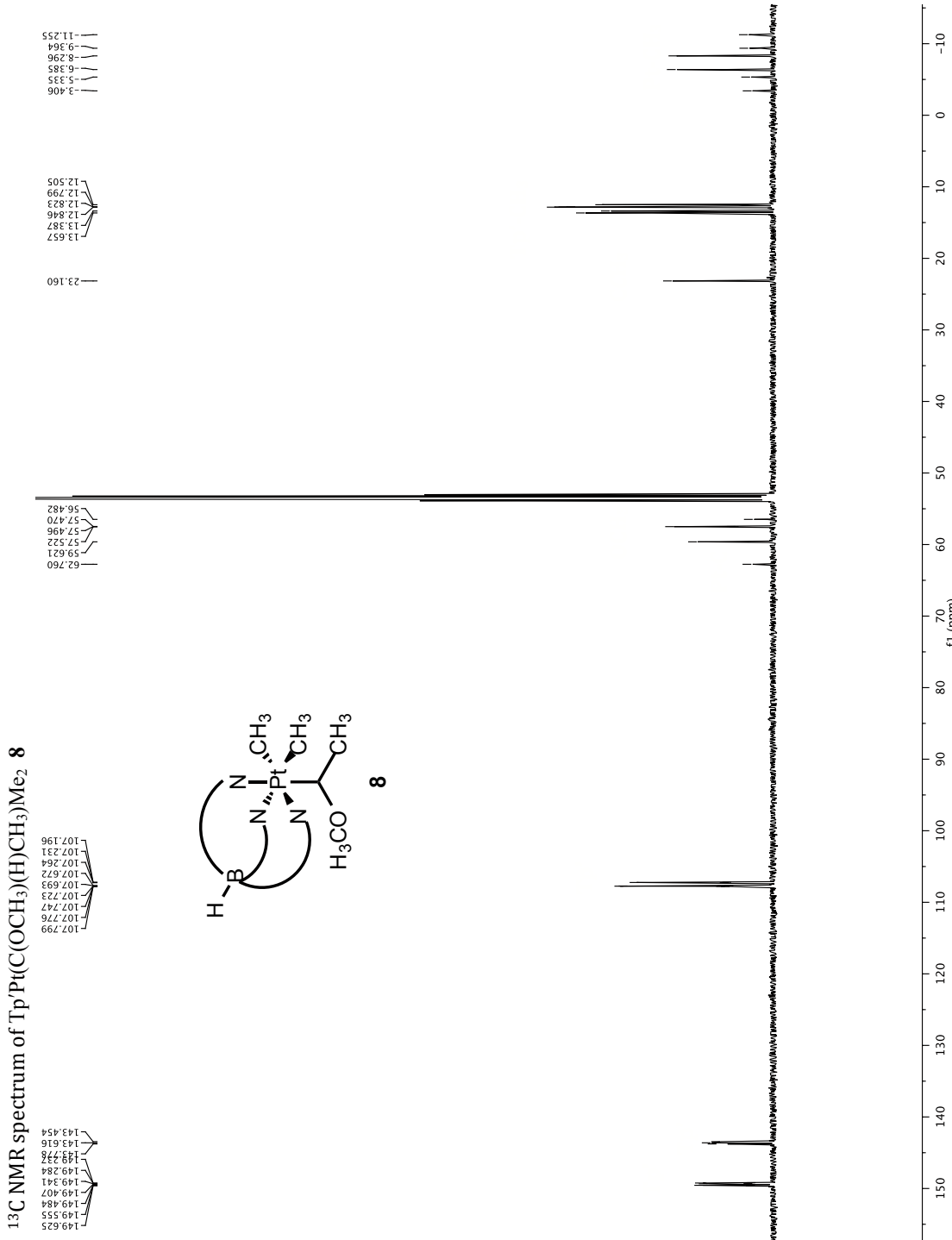


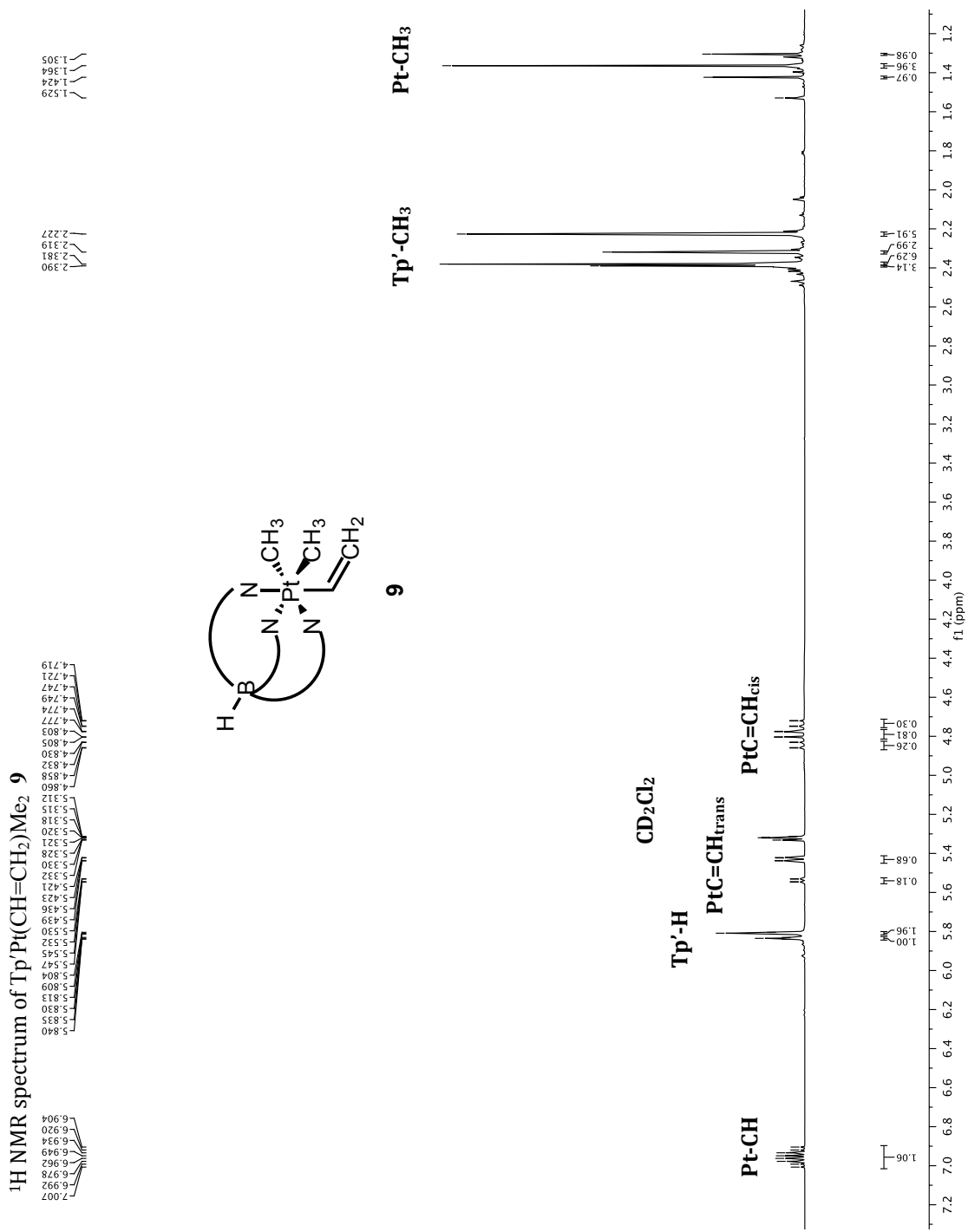
$^{13}\text{C}$  NMR spectrum of  $\text{Tp}'\text{Pt}(\text{C}(\text{OCH}_3)=\text{CH}_2)\text{Me}_2$  7

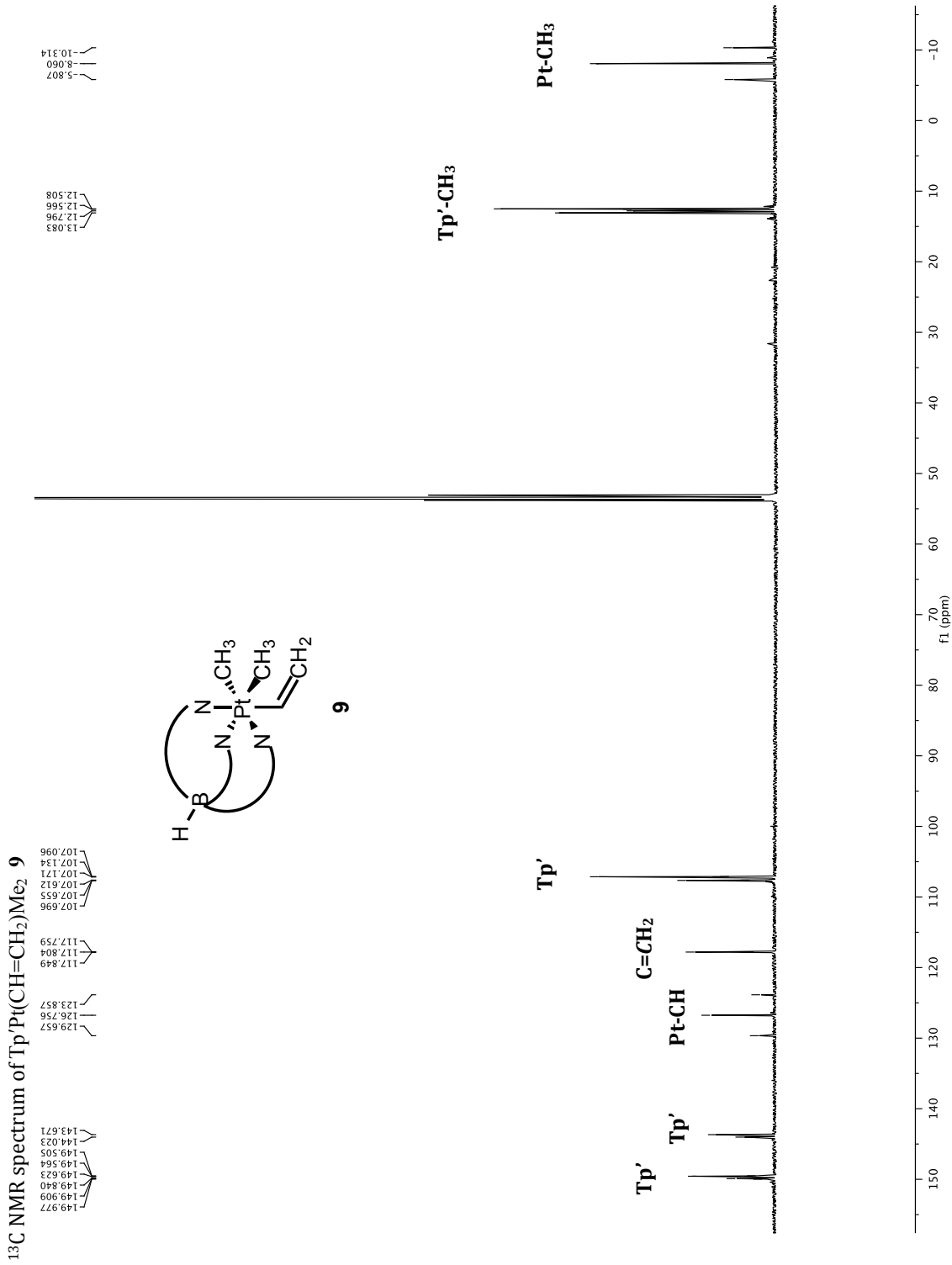


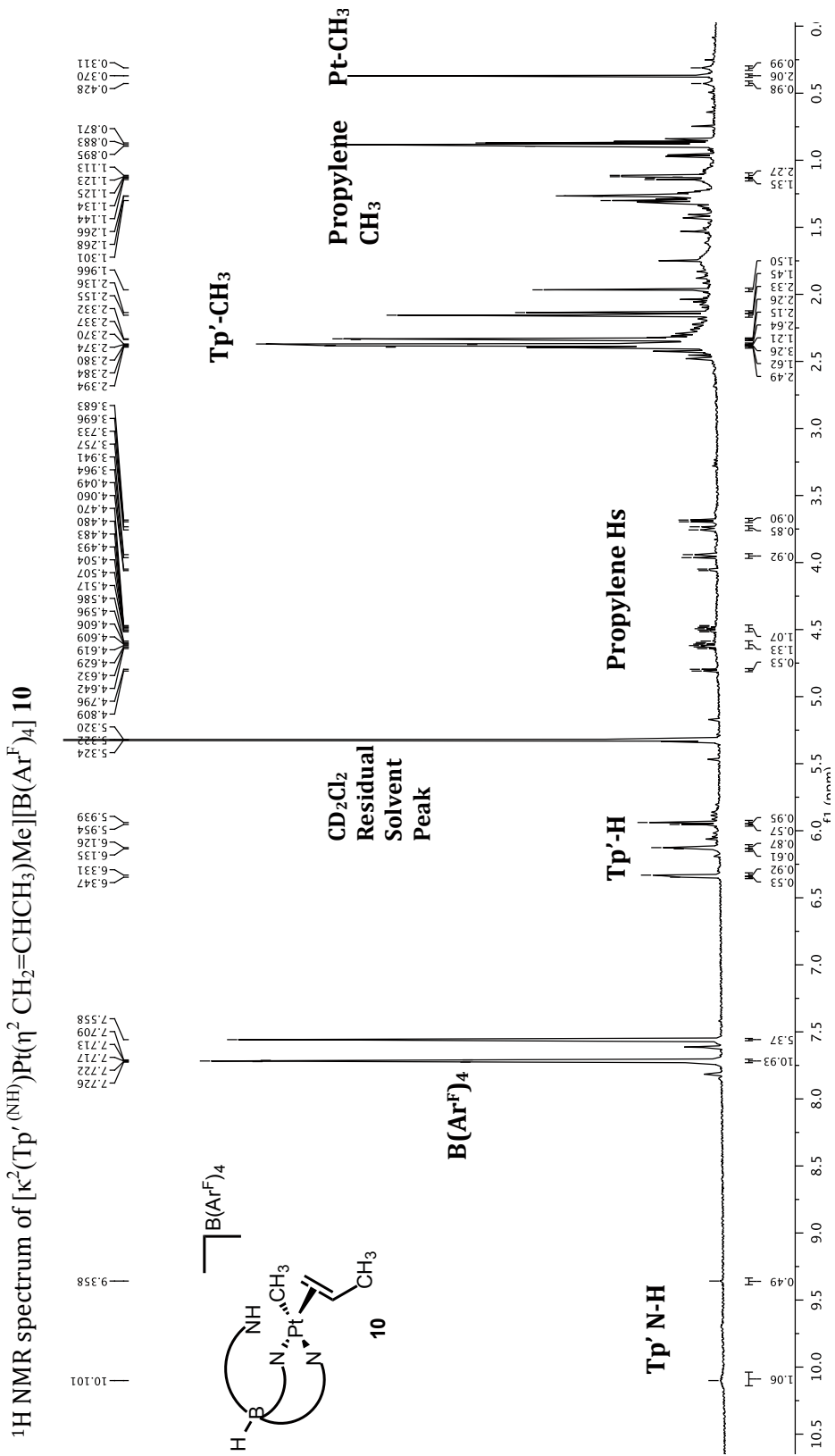
<sup>1</sup>H NMR spectrum of Tp'Pt(C(OCH<sub>3</sub>)(H)CH<sub>3</sub>)Me<sub>2</sub> **8**



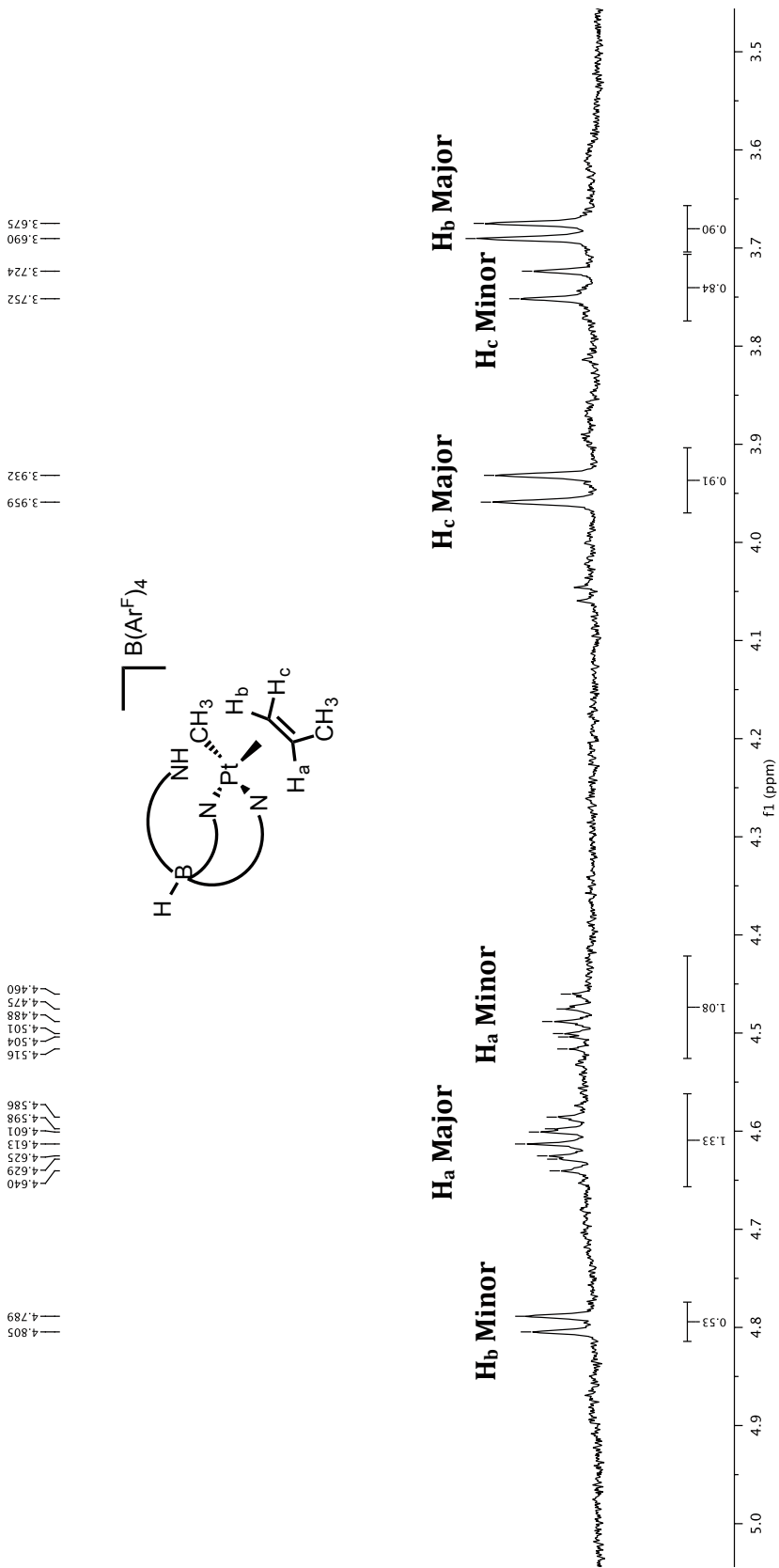




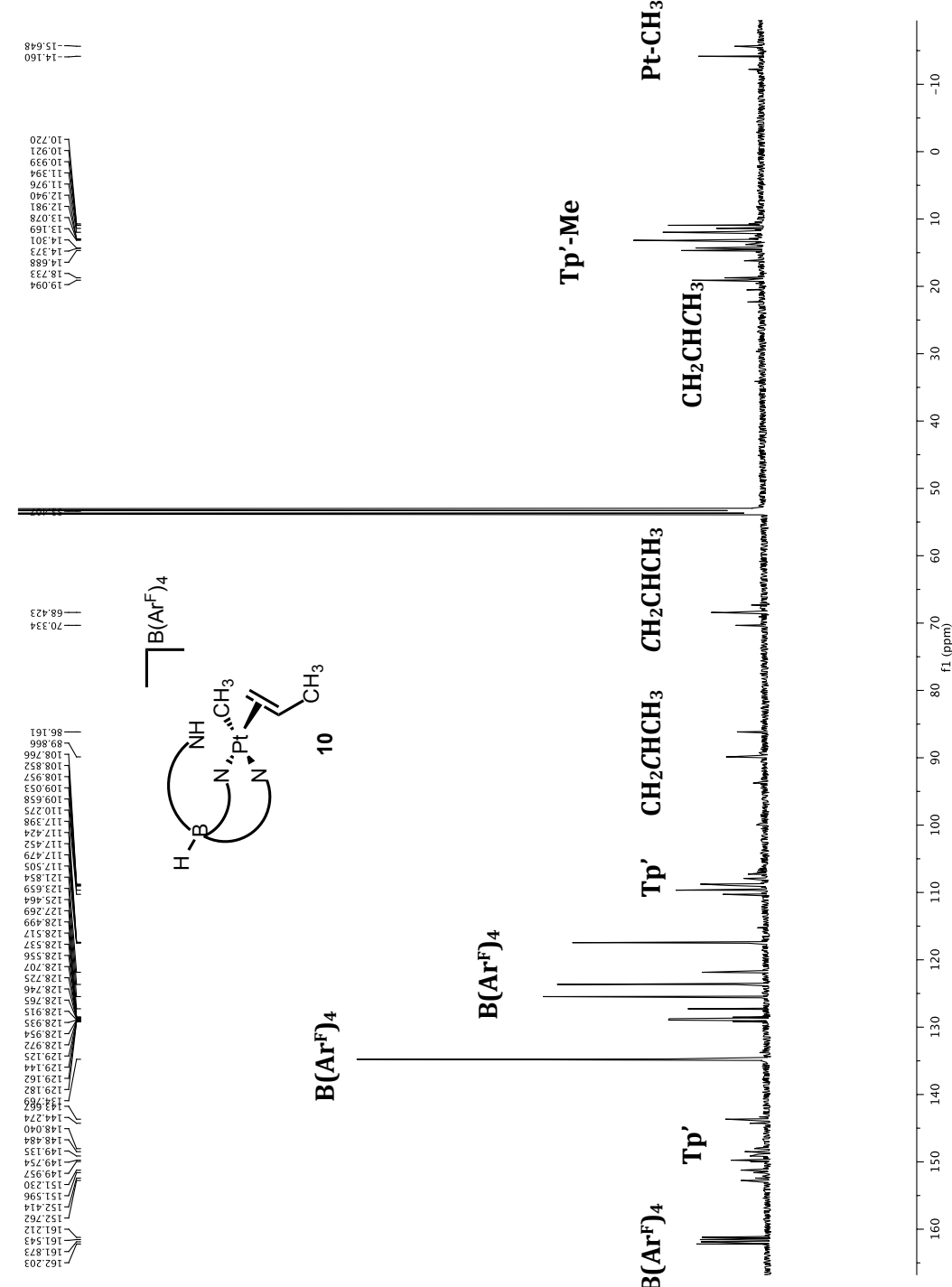




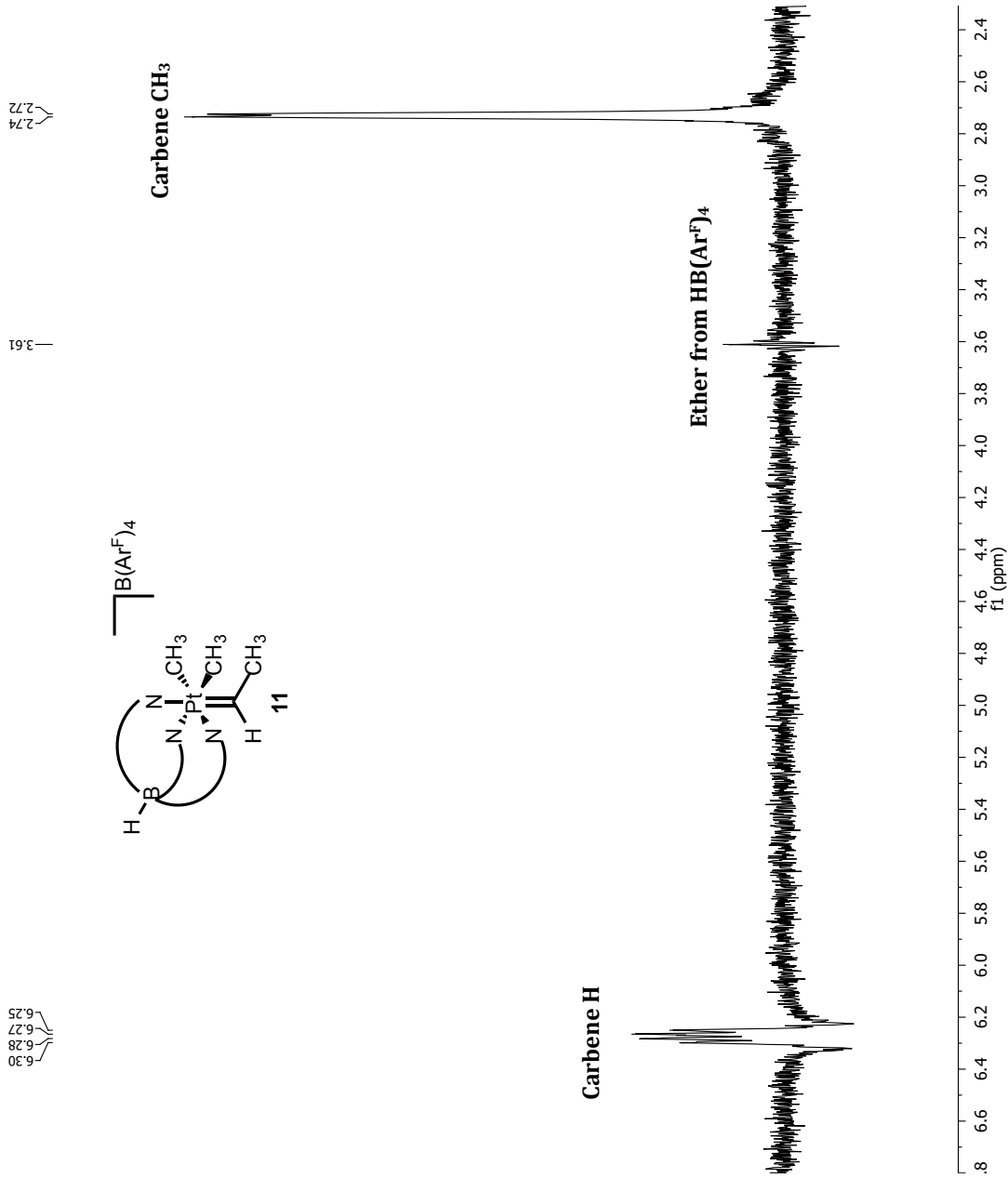
<sup>1</sup>H NMR spectrum zoomed in of [ $\kappa^2(\text{Tp}'^{(\text{NH})})\text{Pt}(\eta^2\text{CH}_2=\text{CHCH}_3)\text{Me}] [\text{B}(\text{Ar}^{\text{F}})_4]$ ] 10



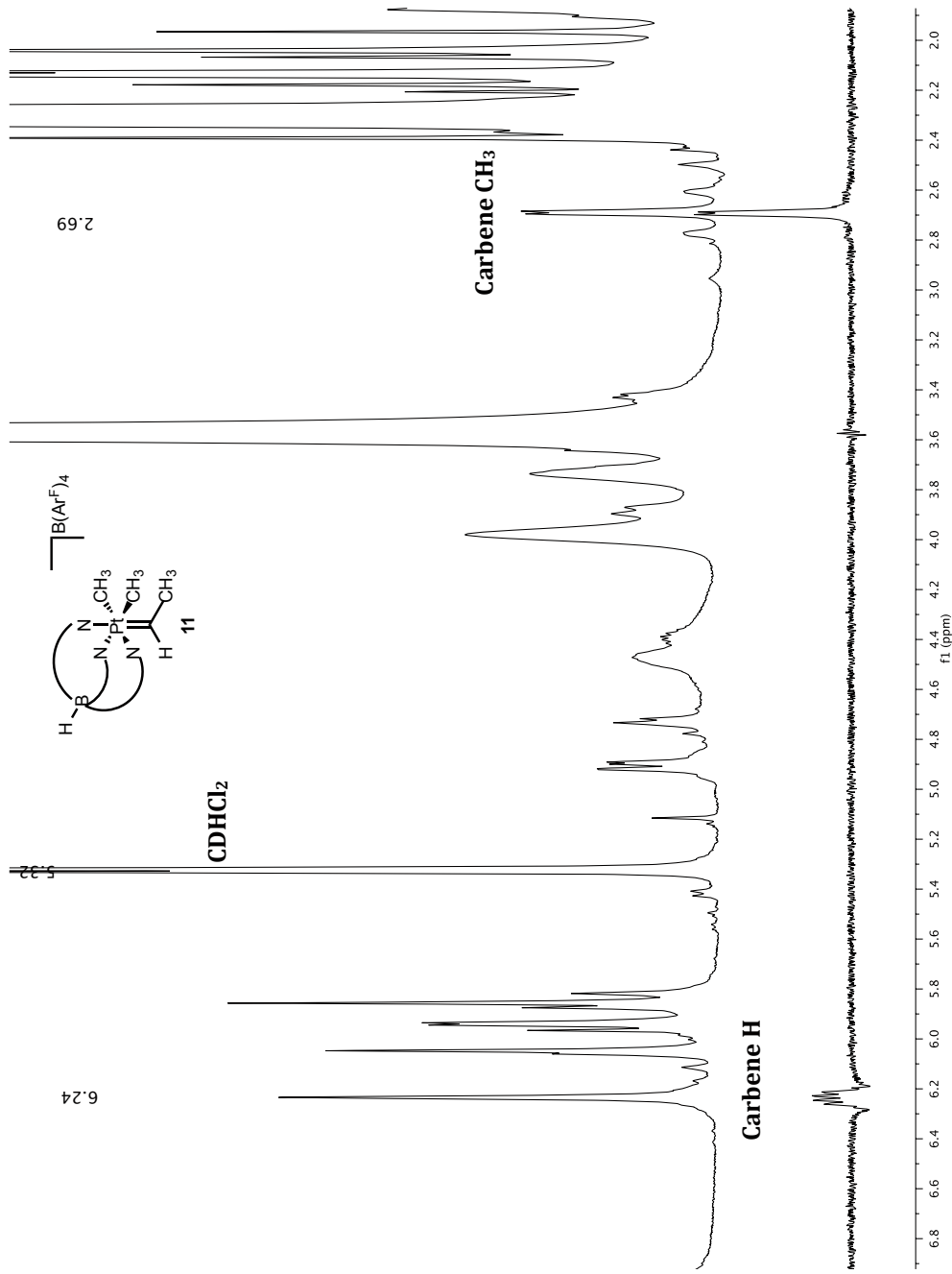
$^{13}\text{C}$  NMR spectrum of  $[\kappa^2(\text{Tp}'(\text{NH}))\text{Pt}(\eta^2\text{CH}_2=\text{CHCH}_3)\text{Me}][\text{B}(\text{Ar}^F)_4]$  10



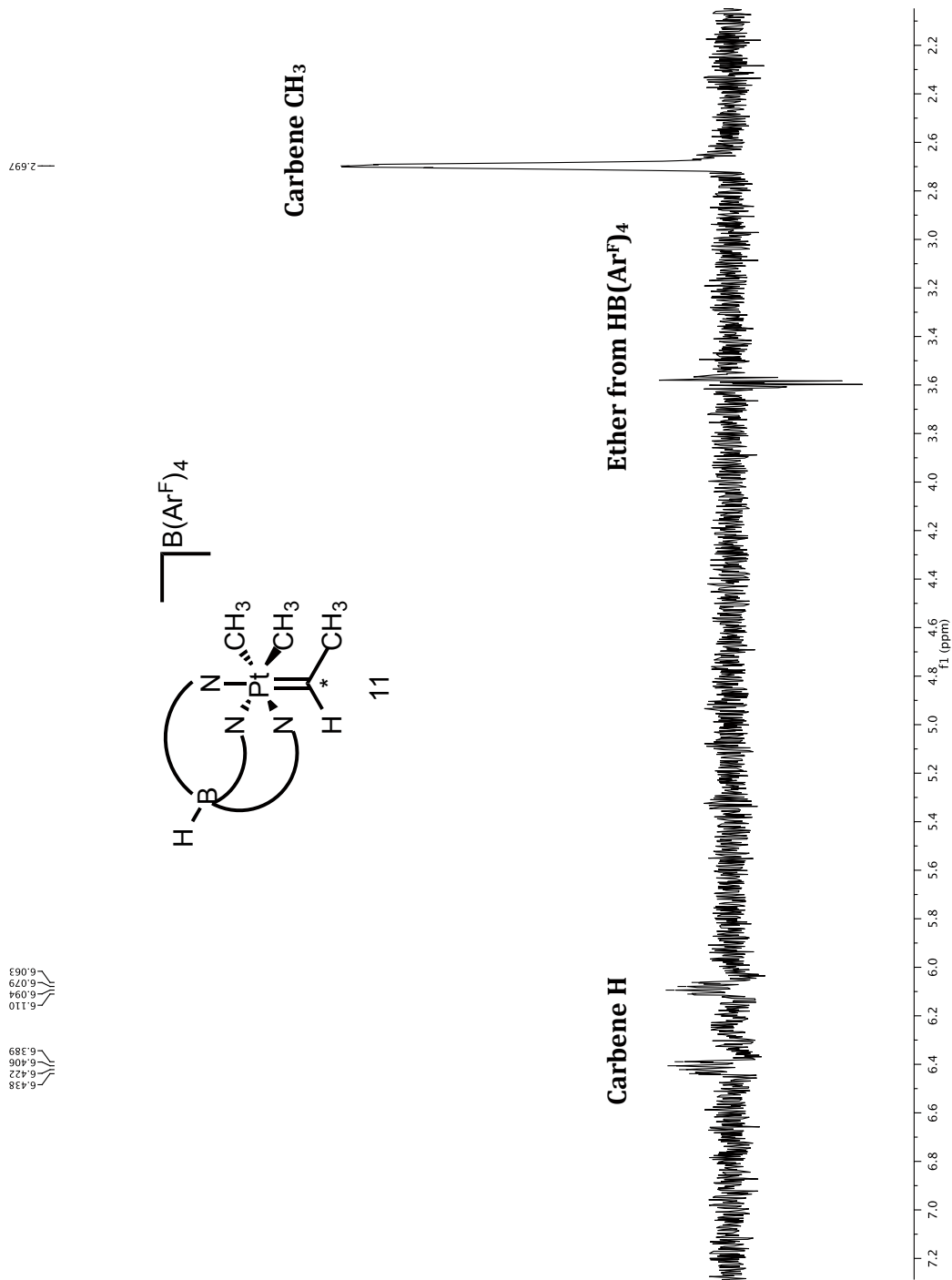
1D COSY spectrum of ethylidene carbene intermediate  $[\text{Tp}'\text{Pt}(\text{=C}(\text{CH}_3)(\text{H}))\text{Me}_2][\text{B}(\text{Ar}^F)_4]$  11



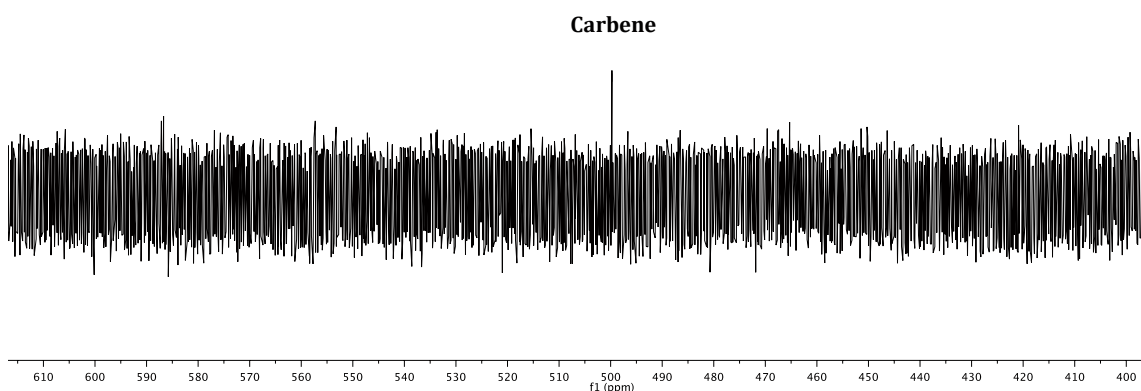
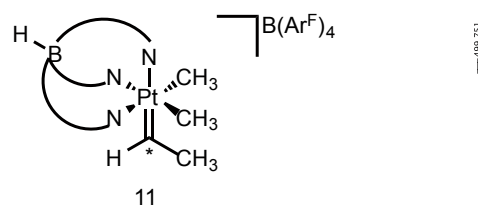
$^1\text{H}$  NMR spectrum of *in situ* ethylidene carbene  $[\text{Tp}'\text{Pt}(\text{=C}(\text{CH}_3)(\text{H}))\text{Me}_2][\text{B}(\text{Ar}^{\text{F}})_4]$  **11**. Stacked plots of  $^1\text{H}$  NMR spectrum (top) and 1D COSY spectrum (bottom).



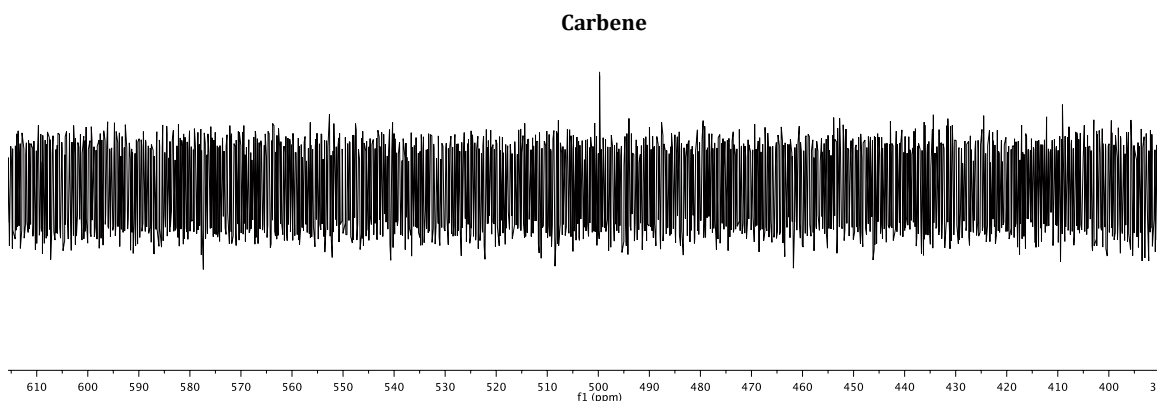
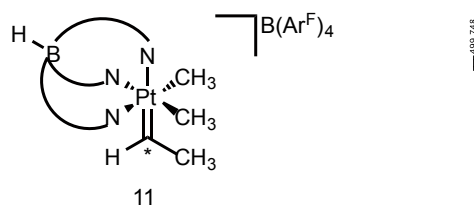
1D COSY spectrum of  $^{13}\text{C}$  labeled ethylidene carbene [ $\text{Tp}'\text{Pt}(\text{=}\text{CH}_3)(\text{H})\text{Me}_2][\text{B}(\text{Ar}^{\text{F}})_4]$  11



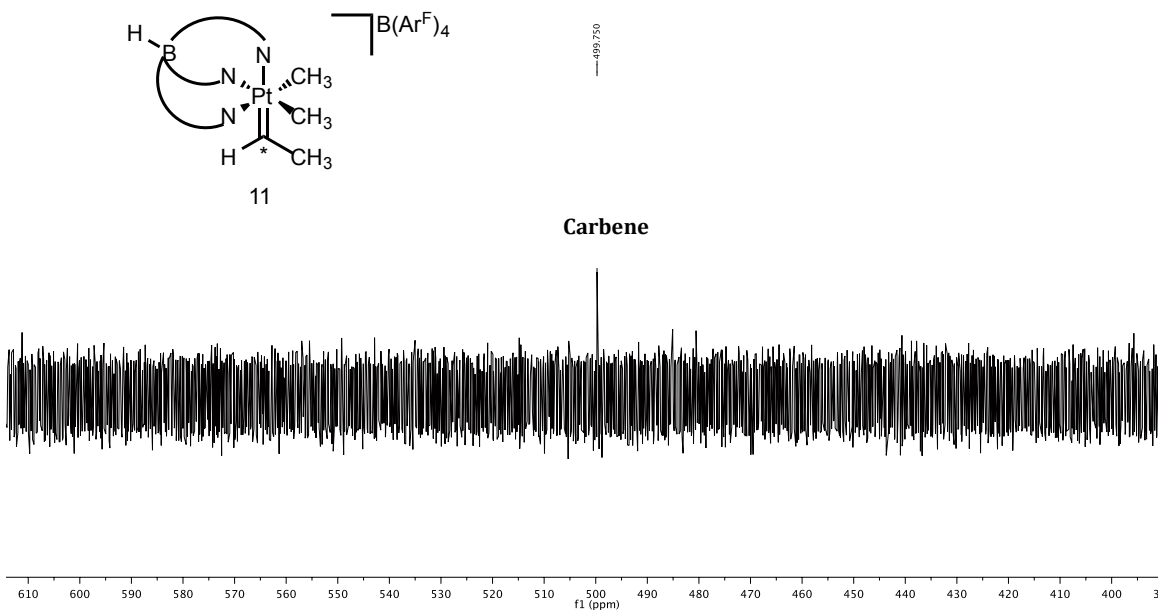
$^{13}\text{C}$  NMR spectrum of  $^{13}\text{C}$  labeled ethylidene carbene [ $\text{Tp}'\text{Pt}(=\text{CH}_3)(\text{H})\text{Me}_2][\text{B}(\text{Ar}^F)_4]$  **11** on 500MHz BBI NMR

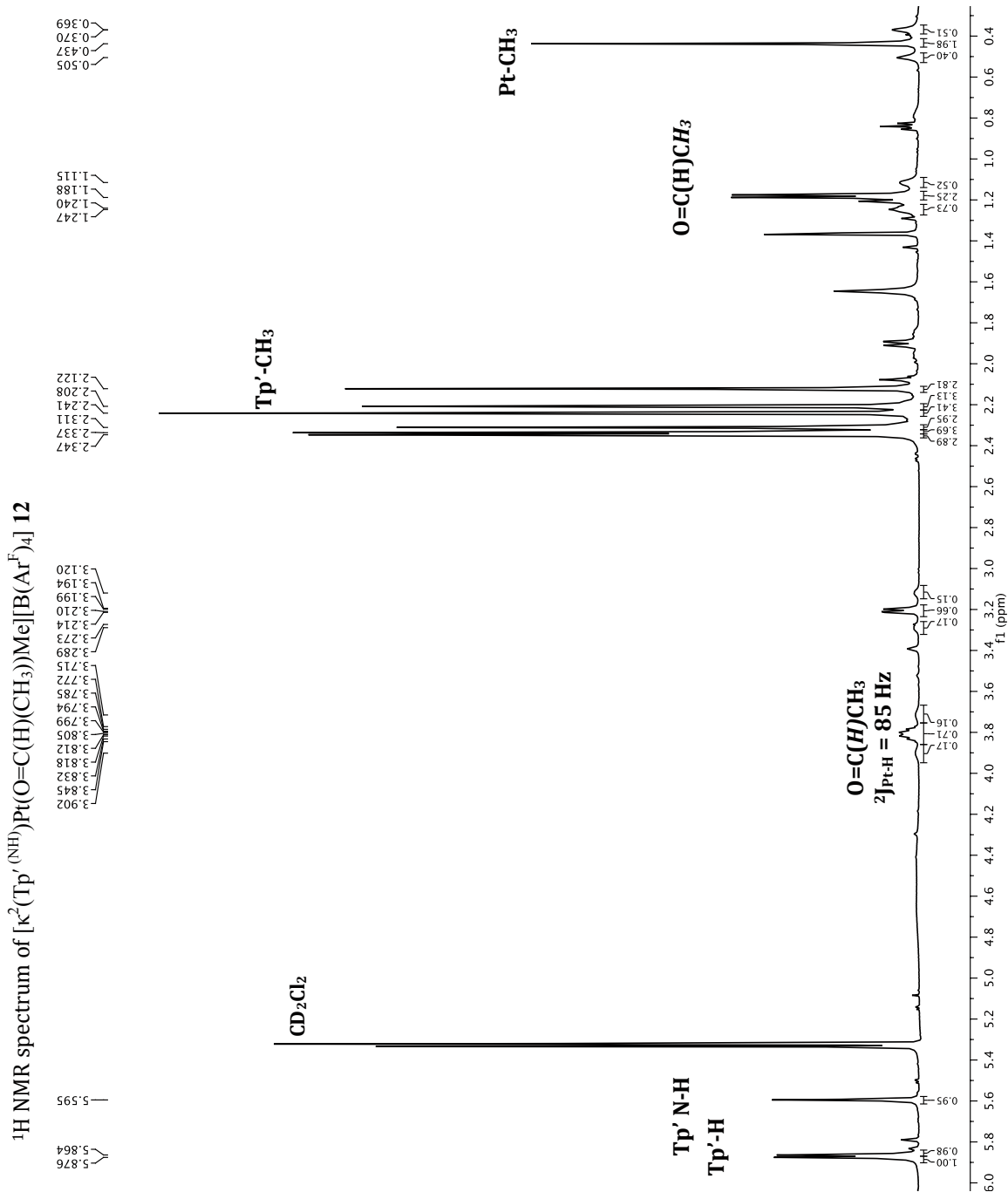


$^{13}\text{C}$  NMR spectrum of  $^{13}\text{C}$  labeled ethylidene carbene [ $\text{Tp}'\text{Pt}(=\text{CH}_3)(\text{H})\text{Me}_2][\text{B}(\text{Ar}^F)_4]$  **11** on 600MHz BBFO NMR



$^{13}\text{C}$  NMR spectrum of  $^{13}\text{C}$  labeled ethylidene carbene [ $\text{Tp}'\text{Pt}(=\text{C}(\text{CH}_3)(\text{H}))\text{Me}_2][\text{B}(\text{Ar}^F)_4]$  **11** on 400MHz BBFO NMR





## APPENDIX 3.2

### Atomic coordinates and isotropic displacement parameters for [Tp'Pt(=C(OMe)NHCH<sub>2</sub>Ph)(CH<sub>3</sub>)<sub>2</sub>][OTf] (4d)

U(eq) is defines as one third of the trace of the orthogonalized U<sub>ij</sub> tensor.

<b>Atom</b>	<b>x/a</b>	<b>y/b</b>	<b>z/c</b>	<b>U(eq)</b>
Pt1	8568.49(13)	3384.68(12)	8486.61(7)	20.05(8)
O1	7035(2)	5219(2)	8586.1(13)	26.8(6)
N1	7149(3)	4100(3)	9342.9(16)	26.8(8)
N2	9685(3)	2352(3)	8157.8(15)	23.8(7)
N3	9952(3)	2579(3)	7584.1(16)	25.9(7)
N4	9657(3)	4594(3)	8216.9(15)	22.0(7)
N5	9857(3)	4514(3)	7616.5(15)	22.3(7)
N6	7472(3)	3401(3)	7529.9(16)	23.3(7)
N7	8070(3)	3510(3)	7058.0(17)	25.8(8)
C1	7503(3)	4332(4)	8831.1(19)	24.8(9)
C2	7210(4)	5690(3)	8002.6(19)	28.6(9)
C3	6219(4)	4639(4)	9586(2)	31(1)
C3A	6219(4)	4639(4)	9586(2)	31(1)
C4	6573(5)	5465(5)	10071(3)	25.2(13)
C4A	5073(6)	4171(7)	9362(4)	27(3)
C5A	4690(7)	3272(7)	9607(4)	30(3)
C6A	3578(8)	2865(7)	9338(6)	30(3)
C7A	2849(7)	3356(10)	8824(6)	35(5)
C8A	3232(7)	4254(9)	8579(5)	39(4)
C9A	4344(8)	4662(6)	8848(4)	35(3)
C5	7018(5)	5163(5)	10697(3)	28.4(13)
C6	7292(6)	5896(7)	11170(3)	31.2(15)
C7	7116(9)	6930(9)	11024(5)	34(2)
C8	6682(7)	7241(6)	10420(4)	36.6(18)
C9	6407(7)	6505(5)	9933(3)	34.2(16)
C10	7578(4)	2153(3)	8693(2)	29.1(9)
C11	9690(4)	3337(3)	9382.9(19)	27.4(9)
C12	10252(5)	973(4)	8993(2)	40.2(11)
C13	10262(4)	1478(3)	8373(2)	26.9(9)
C14	10894(4)	1143(4)	7935(2)	33.3(10)
C15	10699(4)	1851(4)	7450(2)	31.5(10)
C16	11161(5)	1884(5)	6863(3)	54.5(16)
C17	10059(4)	5873(4)	9100(2)	30.0(9)

C18	10115(4)	5504(4)	8458.0(19)	25.3(9)
C19	10637(4)	5994(3)	8019.5(19)	26.2(9)
C20	10459(4)	5366(3)	7499.8(19)	26.4(9)
C21	10814(4)	5516(4)	6879(2)	35.0(11)
C22	5357(4)	3381(4)	7640(2)	31.6(10)
C23	6304(4)	3429(3)	7269(2)	27.2(9)
C24	6154(4)	3541(4)	6628(2)	33.9(10)
C25	7270(4)	3600(4)	6503(2)	28.7(9)
C26	7602(5)	3758(5)	5883(2)	48.8(14)
B1	9439(4)	3550(4)	7205(2)	24.4(10)
S1	7759(1)	1676.5(8)	589.9(5)	28.4(2)
F1	6663(3)	-108(2)	480.7(14)	45.2(7)
F2	6054(3)	916(2)	-304.9(12)	41.7(7)
F3	5554(2)	1189(2)	584.6(12)	39.2(6)
O2	8020(3)	1548(3)	1268.8(16)	41.4(9)
O3	8617(3)	1240(3)	275.2(15)	37.8(8)
O4	7342(3)	2693(3)	366.4(16)	36.6(7)
C27	6436(4)	882(4)	327(2)	32.1(10)

### Bond Lengths (Å)

Atom	Atom	Length/Å	Atom	Atom	Length/Å
Pt1	N2	2.090(3)	C5A	C6A	1.39
Pt1	N4	2.168(3)	C6A	C7A	1.39
Pt1	N6	2.175(4)	C7A	C8A	1.39
Pt1	C1	1.997(4)	C8A	C9A	1.39
Pt1	C10	2.069(4)	C5	C6	1.380(10)
Pt1	C11	2.081(4)	C6	C7	1.378(12)
O1	C1	1.327(5)	C7	C8	1.354(12)
O1	C2	1.459(5)	C8	C9	1.403(10)
N1	C1	1.301(5)	C12	C13	1.497(6)
N1	C3	1.473(5)	C13	C14	1.392(6)
N2	N3	1.379(5)	C14	C15	1.374(7)
N2	C13	1.341(5)	C15	C16	1.488(7)
N3	C15	1.352(6)	C17	C18	1.487(5)
N3	B1	1.544(6)	C18	C19	1.388(6)
N4	N5	1.376(4)	C19	C20	1.366(6)
N4	C18	1.346(6)	C20	C21	1.505(5)
N5	C20	1.357(5)	C22	C23	1.497(6)

N5	B1	1.545(6)	C23	C24	1.371(7)
N6	N7	1.365(5)	C24	C25	1.378(7)
N6	C23	1.341(6)	C25	C26	1.492(6)
N7	C25	1.348(6)	S1	O2	1.444(4)
N7	B1	1.542(6)	S1	O3	1.439(3)
C3	C4	1.491(7)	S1	O4	1.446(3)
C4	C5	1.396(8)	S1	C27	1.824(5)
C4	C9	1.381(9)	F1	C27	1.334(6)
C4A	C5A	1.39	F2	C27	1.342(5)
C4A	C9A	1.39	F3	C27	1.329(5)

### Bond Angles (°)

Atom	Atom	Atom	Angle/°	Atom	Atom	Atom	Angle/°
N2	Pt1	N4	85.94(13)	C6A	C7A	C8A	120
N2	Pt1	N6	87.30(13)	C7A	C8A	C9A	120
N4	Pt1	N6	89.11(13)	C8A	C9A	C4A	120
C1	Pt1	N2	177.61(15)	C6	C5	C4	120.2(6)
C1	Pt1	N4	95.87(16)	C7	C6	C5	119.8(8)
C1	Pt1	N6	94.29(15)	C8	C7	C6	120.9(9)
C1	Pt1	C10	88.49(18)	C7	C8	C9	119.9(8)
C1	Pt1	C11	88.60(17)	C4	C9	C8	120.0(7)
C10	Pt1	N2	89.75(16)	N2	C13	C12	125.2(4)
C10	Pt1	N4	175.36(14)	N2	C13	C14	108.7(4)
C10	Pt1	N6	88.97(16)	C14	C13	C12	126.0(4)
C10	Pt1	C11	91.94(17)	C15	C14	C13	107.1(4)
C11	Pt1	N2	89.84(15)	N3	C15	C14	107.6(4)
C11	Pt1	N4	89.76(15)	N3	C15	C16	122.2(5)
C11	Pt1	N6	177.00(14)	C14	C15	C16	130.2(4)
C1	O1	C2	125.8(3)	N4	C18	C17	123.2(4)
C1	N1	C3	126.2(4)	N4	C18	C19	109.1(4)
N3	N2	Pt1	116.9(3)	C19	C18	C17	127.7(4)
C13	N2	Pt1	135.7(3)	C20	C19	C18	106.6(4)
C13	N2	N3	107.4(3)	N5	C20	C19	108.5(4)
N2	N3	B1	121.1(3)	N5	C20	C21	121.7(4)
C15	N3	N2	109.2(4)	C19	C20	C21	129.8(4)
C15	N3	B1	129.7(4)	N6	C23	C22	124.0(4)
N5	N4	Pt1	115.6(3)	N6	C23	C24	108.4(4)
C18	N4	Pt1	136.6(3)	C24	C23	C22	127.5(4)

C18	N4	N5	107.4(3)	C23	C24	C25	107.2(4)
N4	N5	B1	120.6(3)	N7	C25	C24	107.7(4)
C20	N5	N4	108.5(3)	N7	C25	C26	123.6(4)
C20	N5	B1	130.9(3)	C24	C25	C26	128.7(4)
N7	N6	Pt1	115.6(3)	N3	B1	N5	108.4(3)
C23	N6	Pt1	135.9(3)	N7	B1	N3	109.6(3)
C23	N6	N7	108.2(3)	N7	B1	N5	108.7(3)
N6	N7	B1	121.1(3)	O2	S1	O4	115.1(2)
C25	N7	N6	108.5(4)	O2	S1	C27	102.8(2)
C25	N7	B1	130.4(4)	O3	S1	O2	115.5(2)
O1	C1	Pt1	127.6(3)	O3	S1	O4	114.3(2)
N1	C1	Pt1	121.1(3)	O3	S1	C27	104.4(2)
N1	C1	O1	111.3(4)	O4	S1	C27	102.4(2)
N1	C3	C4	119.0(4)	F1	C27	S1	111.0(3)
C5	C4	C3	118.0(6)	F1	C27	F2	106.8(4)
C9	C4	C3	122.8(6)	F2	C27	S1	111.1(3)
C9	C4	C5	119.1(6)	F3	C27	S1	111.6(3)
C5A	C4A	C9A	120	F3	C27	F1	107.9(4)
C4A	C5A	C6A	120	F3	C27	F2	108.2(4)
C7A	C6A	C5A	120				

### APPENDIX 3.3

**Atomic coordinates and isotropic displacement parameters for  
[Tp'Pt(=C(OMe)CH<sub>3</sub>)(Me)<sub>2</sub>][OTf] (6)**

<b>Atom</b>	<b>x/a</b>	<b>y/b</b>	<b>z/c</b>	<b>U(eq)</b>
Pt1	6917.0(2)	7776.43(18)	8017.37(18)	16.29(10)
O1	6556(4)	5604(3)	9513(3)	23.3(8)
N1	6370(4)	9412(4)	7015(4)	20.1(10)
N2	5056(5)	9579(4)	6899(4)	19.5(9)
N3	5250(4)	8153(4)	9251(4)	19.8(9)
N4	4092(5)	8481(4)	8810(4)	18.4(9)
N5	5546(4)	6841(4)	7231(4)	18.0(9)
N6	4344(4)	7393(4)	7116(4)	18.8(9)
C1	8421(6)	7492(5)	6741(5)	23.4(12)
C2	8169(6)	8721(5)	8782(5)	23.9(12)
C3	7483(6)	6293(5)	8960(5)	21.0(11)
C4	8862(6)	5934(5)	9081(5)	24.6(12)
C5	6845(6)	4477(5)	10286(6)	28.9(13)
C6	7007(6)	10414(5)	6453(5)	24.9(12)
C7	6085(6)	11220(5)	5982(5)	26.5(13)
C8	4872(6)	10676(5)	6268(5)	24.1(12)
C9	8465(7)	10585(6)	6361(6)	35.3(15)
C10	3566(6)	11149(6)	5952(5)	29.4(13)
C11	5004(6)	8100(5)	10381(5)	21.0(11)
C12	3678(6)	8379(5)	10682(5)	22.6(11)
C13	3133(5)	8623(5)	9670(5)	19.8(11)
C14	6024(6)	7800(6)	11184(5)	25.5(12)
C15	1728(5)	8942(5)	9475(5)	24.2(12)
C16	5509(5)	5746(5)	6870(5)	19.6(11)
C17	4280(6)	5619(5)	6534(5)	25.8(12)
C18	3565(6)	6656(5)	6705(5)	22.1(11)
C19	6636(6)	4851(5)	6850(6)	29.4(13)
C20	2155(6)	6966(6)	6550(6)	29.6(13)
B1	4028(6)	8634(6)	7506(5)	19.2(12)
S1	431.9(14)	3095.7(13)	7855.6(12)	24.0(3)
F1	-117(5)	3098(4)	5773(4)	48.7(11)
F2	77(4)	4872(3)	6205(3)	34.8(8)
F3	1800(4)	3765(4)	5841(3)	42.5(10)
O2	916(5)	1864(4)	7872(4)	34.7(10)
O3	-960(4)	3216(4)	8232(4)	36(1)

O4	1265(5)	3909(4)	8268(4)	35.2(10)
C21	561(6)	3724(5)	6333(5)	26.2(13)

### Bond Lengths (Å)

Atom	Atom	Length/Å	Atom	Atom	Length/Å
Pt1	N1	2.111(4)	C3	C4	1.469(8)
Pt1	N3	2.178(5)	C6	C7	1.387(9)
Pt1	N5	2.165(5)	C6	C9	1.495(9)
Pt1	C1	2.073(6)	C7	C8	1.375(9)
Pt1	C2	2.070(6)	C8	C10	1.489(8)
Pt1	C3	1.957(5)	C11	C12	1.392(8)
O1	C3	1.282(7)	C11	C14	1.501(8)
O1	C5	1.477(7)	C12	C13	1.382(8)
N1	N2	1.369(6)	C13	C15	1.506(7)
N1	C6	1.344(8)	C16	C17	1.386(8)
N2	C8	1.349(7)	C16	C19	1.496(8)
N2	B1	1.536(8)	C17	C18	1.373(9)
N3	N4	1.372(6)	C18	C20	1.497(8)
N3	C11	1.334(8)	S1	O2	1.439(4)
N4	C13	1.349(7)	S1	O3	1.442(5)
N4	B1	1.551(7)	S1	O4	1.447(5)
N5	N6	1.367(6)	S1	C21	1.831(6)
N5	C16	1.360(7)	F1	C21	1.311(7)
N6	C18	1.351(7)	F2	C21	1.345(7)
N6	B1	1.538(8)	F3	C21	1.322(8)

### Bond Angles (°)

Atom	Atom	Atom	Angle/°	Atom	Atom	Atom	Angle/°
N1	Pt1	N3	85.70(17)	N1	C6	C7	108.3(5)
N1	Pt1	N5	87.93(17)	N1	C6	C9	124.4(5)
N5	Pt1	N3	87.23(17)	C7	C6	C9	127.4(6)
C1	Pt1	N1	90.3(2)	C8	C7	C6	107.3(5)
C1	Pt1	N3	175.38(19)	N2	C8	C7	107.4(5)
C1	Pt1	N5	90.4(2)	N2	C8	C10	124.0(6)
C2	Pt1	N1	90.6(2)	C7	C8	C10	128.6(5)
C2	Pt1	N3	90.9(2)	N3	C11	C12	109.5(5)
C2	Pt1	N5	177.70(19)	N3	C11	C14	124.3(5)

C2	Pt1	C1	91.4(2)	C12	C11	C14	126.2(5)
C3	Pt1	N1	177.8(2)	C13	C12	C11	105.9(5)
C3	Pt1	N3	94.9(2)	N4	C13	C12	108.0(5)
C3	Pt1	N5	94.2(2)	N4	C13	C15	122.5(5)
C3	Pt1	C1	89.2(2)	C12	C13	C15	129.5(5)
C3	Pt1	C2	87.3(2)	N5	C16	C17	108.8(5)
C3	O1	C5	121.4(5)	N5	C16	C19	124.2(5)
N2	N1	Pt1	116.9(3)	C17	C16	C19	127.0(5)
C6	N1	Pt1	135.3(4)	C18	C17	C16	106.8(5)
C6	N1	N2	107.7(4)	N6	C18	C17	107.9(5)
N1	N2	B1	121.2(4)	N6	C18	C20	122.8(5)
C8	N2	N1	109.4(5)	C17	C18	C20	129.3(6)
C8	N2	B1	129.3(5)	N2	B1	N4	108.4(4)
N4	N3	Pt1	115.6(3)	N2	B1	N6	110.4(5)
C11	N3	Pt1	137.0(4)	N6	B1	N4	108.4(4)
C11	N3	N4	107.3(4)	O2	S1	O3	115.2(3)
N3	N4	B1	120.9(4)	O2	S1	O4	115.8(3)
C13	N4	N3	109.3(4)	O2	S1	C21	103.9(3)
C13	N4	B1	129.8(5)	O3	S1	O4	114.7(3)
N6	N5	Pt1	116.7(3)	O3	S1	C21	102.8(3)
C16	N5	Pt1	136.3(4)	O4	S1	C21	101.7(3)
C16	N5	N6	106.8(4)	F1	C21	S1	112.1(4)
N5	N6	B1	120.2(4)	F1	C21	F2	107.4(5)
C18	N6	N5	109.7(4)	F1	C21	F3	108.2(5)
C18	N6	B1	129.9(5)	F2	C21	S1	109.5(4)
O1	C3	Pt1	115.9(4)	F3	C21	S1	112.0(4)
O1	C3	C4	119.0(5)	F3	C21	F2	107.5(5)
C4	C3	Pt1	125.2(4)				

## APPENDIX 3.4

### Atomic coordinates and isotropic displacement parameters for Tp'Pt(C(OCH<sub>3</sub>)=CH<sub>2</sub>)(Me)<sub>2</sub> (7)

<b>Atom</b>	<b>x</b>	<b>y</b>	<b>z</b>	<b>U(eq)</b>
Pt1	3735.4(2)	3768.4(2)	1941.6(2)	18.03(7)
O1	5501(4)	4552.5(14)	3956(3)	23.5(7)
N1	2516(4)	4535.2(15)	1701(4)	17.9(8)
N2	1316(4)	4488.4(15)	1942(4)	17.7(8)
N3	3466(4)	3630.1(15)	3908(4)	19.0(8)
N4	2125(4)	3722.7(15)	3813(4)	19.1(8)
N5	1714(4)	3350.6(15)	765(4)	17.9(8)
N6	651(4)	3473.4(15)	1178(4)	18.7(8)
C1	3894(6)	3921(2)	37(5)	26.3(10)
C2	4814(5)	3012.7(19)	2209(6)	26.4(10)
C3	5605(5)	4165.0(19)	2999(5)	20.2(9)
C4	6789(6)	4087(2)	2819(6)	29.2(11)
C5	6690(6)	4913(2)	4683(6)	29.8(11)
C6	2679(5)	5082.2(19)	1474(5)	20.9(9)
C7	1561(5)	5390.4(19)	1557(5)	21.9(10)
C8	729(5)	5004.2(19)	1863(5)	19.7(9)
C9	3881(5)	5308(2)	1186(5)	25.6(10)
C10	-547(5)	5106(2)	2145(5)	25.4(10)
C11	4325(5)	3510.7(19)	5294(5)	22.4(10)
C12	3508(6)	3527.2(19)	6088(5)	23.8(10)
C13	2140(5)	3660.3(18)	5134(5)	21.9(9)
C14	5883(5)	3390(2)	5848(6)	29.0(11)
C15	829(5)	3732(2)	5392(5)	27.5(10)
C16	1169(5)	2980.6(18)	-331(5)	21.2(9)
C17	-239(5)	2865.7(19)	-618(5)	24.2(10)
C18	-547(5)	3181.8(19)	348(5)	21.6(10)
C19	1988(6)	2733(2)	-1104(5)	25.5(10)
C20	-1905(5)	3210(2)	518(6)	27.7(11)
B1	900(6)	3917(2)	2370(6)	18(1)

### Bond Lengths (Å)

<b>Atom</b>	<b>Atom</b>	<b>Length/Å</b>	<b>Atom</b>	<b>Atom</b>	<b>Length/Å</b>
Pt1	N1	2.165(4)	N5	C16	1.340(6)

Pt1	N3	2.171(4)	N6	C18	1.352(6)
Pt1	N5	2.153(4)	N6	B1	1.543(6)
Pt1	C1	2.055(4)	C3	C4	1.329(7)
Pt1	C2	2.065(4)	C6	C7	1.402(7)
Pt1	C3	1.998(4)	C6	C9	1.496(7)
O1	C3	1.379(5)	C7	C8	1.383(7)
O1	C5	1.417(6)	C8	C10	1.488(7)
N1	N2	1.371(5)	C11	C12	1.404(7)
N1	C6	1.340(6)	C11	C14	1.489(7)
N2	C8	1.352(6)	C12	C13	1.365(7)
N2	B1	1.541(6)	C13	C15	1.500(7)
N3	N4	1.368(5)	C16	C17	1.384(7)
N3	C11	1.338(6)	C16	C19	1.505(6)
N4	C13	1.352(6)	C17	C18	1.381(7)
N4	B1	1.544(6)	C18	C20	1.492(7)
N5	N6	1.370(5)			

### Bond Angles (°)

Atom	Atom	Atom	Angle/°	Atom	Atom	Atom	Angle/°
N1	Pt1	N3	85.99(14)	N5	N6	B1	120.3(4)
N5	Pt1	N1	86.77(14)	C18	N6	N5	109.8(4)
N5	Pt1	N3	88.04(14)	C18	N6	B1	129.7(4)
C1	Pt1	N1	91.51(17)	O1	C3	Pt1	110.1(3)
C1	Pt1	N3	177.13(18)	C4	C3	Pt1	126.6(4)
C1	Pt1	N5	90.40(18)	C4	C3	O1	123.4(4)
C1	Pt1	C2	91.0(2)	N1	C6	C7	108.9(4)
C2	Pt1	N1	176.53(18)	N1	C6	C9	123.9(4)
C2	Pt1	N3	91.41(18)	C7	C6	C9	127.2(4)
C2	Pt1	N5	90.86(18)	C8	C7	C6	106.3(4)
C3	Pt1	N1	92.77(17)	N2	C8	C7	107.6(4)
C3	Pt1	N3	92.95(16)	N2	C8	C10	123.3(4)
C3	Pt1	N5	178.87(17)	C7	C8	C10	129.0(4)
C3	Pt1	C1	88.6(2)	N3	C11	C12	108.4(4)
C3	Pt1	C2	89.6(2)	N3	C11	C14	124.0(4)
C3	O1	C5	117.2(4)	C12	C11	C14	127.6(4)
N2	N1	Pt1	116.2(3)	C13	C12	C11	107.0(4)
C6	N1	Pt1	136.1(3)	N4	C13	C12	107.4(4)
C6	N1	N2	107.5(4)	N4	C13	C15	122.8(4)

N1	N2	B1	120.5(4)	C12	C13	C15	129.7(4)
C8	N2	N1	109.6(4)	N5	C16	C17	109.3(4)
C8	N2	B1	129.6(4)	N5	C16	C19	124.3(4)
N4	N3	Pt1	116.3(3)	C17	C16	C19	126.3(4)
C11	N3	Pt1	136.1(3)	C18	C17	C16	106.8(4)
C11	N3	N4	107.4(4)	N6	C18	C17	107.1(4)
N3	N4	B1	120.4(4)	N6	C18	C20	124.0(4)
C13	N4	N3	109.8(4)	C17	C18	C20	128.9(4)
C13	N4	B1	129.7(4)	N2	B1	N4	108.5(4)
N6	N5	Pt1	116.5(3)	N2	B1	N6	110.2(4)
C16	N5	Pt1	136.5(3)	N6	B1	N4	109.9(4)
C16	N5	N6	107.0(4)				

## APPENDIX 3.5

### Atomic coordinates and isotropic displacement parameters for Tp'Pt(CH=CH<sub>2</sub>)(Me)<sub>2</sub> (9)

<b>Atom</b>	<b>x</b>	<b>y</b>	<b>Z</b>	<b>U(eq)</b>
Pt1	4324.0(5)	7208.1(4)	3605.0(2)	35.52(15)
N1	5986(10)	8401(7)	4013(5)	35(2)
N2	6366(10)	8455(7)	4729(5)	34(2)
N3	2982(10)	7463(5)	4472(4)	25.8(17)
N4	3959(10)	7611(6)	5123(4)	30.6(19)
N5	6001(10)	6315(6)	4331(4)	27.7(18)
N6	6557(9)	6680(7)	4991(4)	29.1(18)
C1	6625(15)	9151(10)	3733(7)	49(3)
C2	7442(15)	9715(10)	4281(8)	54(3)
C3	7238(14)	9280(9)	4906(7)	45(3)
C4	6550(20)	9314(12)	2963(8)	74(5)
C5	7806(17)	9606(11)	5650(7)	62(4)
C6	1404(12)	7482(7)	4562(6)	35(2)
C7	1330(13)	7624(8)	5265(6)	41(3)
C8	2971(14)	7715(8)	5614(6)	38(2)
C9	-70(13)	7305(12)	3978(7)	60(4)
C10	3641(15)	7902(10)	6377(6)	48(3)
C11	6697(12)	5452(8)	4313(5)	34(2)
C12	7725(13)	5261(9)	4965(6)	36(2)
C13	7598(12)	6041(8)	5375(5)	32(2)
C14	6403(16)	4793(9)	3685(6)	47(3)
C15	8396(14)	6222(9)	6129(5)	41(3)
C16	2737(15)	8098(10)	2953(6)	48(3)
C17	5619(13)	6944(8)	2794(6)	36(2)
C18	2787(14)	6085(10)	3272(6)	45(3)
C19	2737(15)	8098(10)	2953(6)	48(3)
C20	1940(60)	8870(20)	3020(30)	64(14)
C21	5619(13)	6944(8)	2794(6)	36(2)
C22	4840(60)	6590(40)	2200(20)	45(11)
C23	2787(14)	6085(10)	3272(6)	45(3)
C24	2240(30)	5969(15)	2629(12)	34(6)
B1	5895(14)	7645(10)	5205(6)	35(3)

### Bond Lengths (Å)

<b>Atom</b>	<b>Atom</b>	<b>Length/Å</b>	<b>Atom</b>	<b>Atom</b>	<b>Length/Å</b>
Pt1	N1	2.194(9)	N5	C11	1.332(13)
Pt1	N3	2.171(7)	N6	C13	1.352(13)
Pt1	N5	2.161(8)	N6	B1	1.531(16)
Pt1	C16	2.047(11)	C1	C2	1.386(19)
Pt1	C17	2.059(10)	C1	C4	1.490(18)
Pt1	C18	2.031(13)	C2	C3	1.382(18)
N1	N2	1.360(12)	C3	C5	1.495(18)
N1	C1	1.321(14)	C6	C7	1.379(16)
N2	C3	1.360(15)	C6	C9	1.506(16)
N2	B1	1.544(14)	C7	C8	1.381(16)
N3	N4	1.373(11)	C8	C10	1.496(16)
N3	C6	1.316(12)	C11	C12	1.402(14)
N4	C8	1.347(12)	C11	C14	1.503(15)
N4	B1	1.544(13)	C12	C13	1.359(15)
N5	N6	1.368(11)	C13	C15	1.500(14)

### Bond Angles (°)

<b>Atom</b>	<b>Atom</b>	<b>Atom</b>	<b>Angle/°</b>	<b>Atom</b>	<b>Atom</b>	<b>Atom</b>	<b>Angle/°</b>
N3	Pt1	N1	87.6(3)	N5	N6	B1	120.3(8)
N5	Pt1	N1	86.1(3)	C13	N6	N5	109.4(8)
N5	Pt1	N3	86.5(3)	C13	N6	B1	130.2(9)
C16	Pt1	N1	92.1(5)	N1	C1	C2	108.0(11)
C16	Pt1	N3	91.6(4)	N1	C1	C4	125.1(14)
C16	Pt1	N5	177.4(5)	C2	C1	C4	126.8(13)
C17	Pt1	N1	92.6(4)	C3	C2	C1	107.3(11)
C17	Pt1	N3	178.9(4)	N2	C3	C2	106.8(12)
C17	Pt1	N5	92.4(4)	N2	C3	C5	123.7(11)
C18	Pt1	N1	177.5(4)	C2	C3	C5	129.4(12)
C18	Pt1	N3	90.5(4)	N3	C6	C7	110.0(9)
C18	Pt1	N5	92.2(4)	N3	C6	C9	123.7(10)
N2	N1	Pt1	114.8(6)	C7	C6	C9	126.1(10)
C1	N1	Pt1	135.5(9)	C6	C7	C8	106.6(9)
C1	N1	N2	109.4(10)	N4	C8	C7	106.6(10)
N1	N2	C3	108.4(9)	N4	C8	C10	123.4(10)
N1	N2	B1	121.7(9)	C7	C8	C10	130.0(10)
C3	N2	B1	129.9(10)	N5	C11	C12	109.5(10)

N4	N3	Pt1	116.1(6)	N5	C11	C14	124.5(10)
C6	N3	Pt1	136.9(8)	C12	C11	C14	125.9(11)
C6	N3	N4	106.9(8)	C13	C12	C11	105.9(10)
N3	N4	B1	120.5(8)	N6	C13	C12	108.3(9)
C8	N4	N3	109.8(8)	N6	C13	C15	122.5(10)
C8	N4	B1	129.7(9)	C12	C13	C15	129.2(10)
N6	N5	Pt1	116.8(6)	N2	B1	N4	108.1(9)
C11	N5	Pt1	136.3(7)	N6	B1	N2	110.5(8)
C11	N5	N6	106.8(8)	N6	B1	N4	109.9(9)

### APPENDIX 3.6

**Atomic coordinates and isotropic displacement parameters for  $[\kappa^2(\text{Tp}'^{(\text{NH})}\text{Pt}(\eta^2\text{CH}_2=\text{CHCH}_3)\text{Me})][\text{B}(\text{Ar}^F)_4]$  (10)**

<b>Atom</b>	<b>x/a</b>	<b>y/b</b>	<b>z/c</b>	<b>U(eq)</b>
Pt1	3071.6(3)	1172.5(3)	6417.0(2)	47.47(14)
N1	3427(6)	2601(6)	6055(3)	43.3(14)
N2	3963(6)	3594(5)	6600(4)	43.4(14)
N3	4911(5)	2256(5)	6952(3)	35.7(12)
N4	5292(5)	3279(4)	7397(3)	33.5(11)
N5	3413(5)	2412(5)	8317(4)	41.6(13)
N6	3319(5)	2975(4)	7829(3)	32.4(11)
C1	1429(11)	-193(11)	5647(7)	95.9(16)
C2	1082(19)	140(17)	6251(9)	95.3(19)
C3	521(17)	793(15)	6233(13)	93(3)
C4	2853(13)	-103(7)	6874(7)	91(4)
C5	3283(8)	2829(9)	5394(5)	58(2)
C6	3719(8)	3949(9)	5508(6)	61(2)
C7	4139(7)	4410(8)	6260(5)	53(2)
C8	2749(10)	1935(10)	4669(5)	77(3)
C9	4676(9)	5581(8)	6687(7)	73(3)
C10	5915(7)	2200(7)	6964(4)	44.5(17)
C11	6917(7)	3178(7)	7414(4)	46.5(18)
C12	6527(6)	3851(6)	7693(4)	42.3(16)
C13	5864(10)	1215(9)	6533(5)	65(2)
C14	7228(8)	4977(7)	8213(6)	63(2)
C15	2393(7)	1913(6)	8658(4)	42.9(16)
C16	1605(6)	2165(6)	8395(4)	39.0(15)
C17	2202(6)	2831(6)	7882(4)	35.5(14)
C18	2266(8)	1218(8)	9199(6)	64(3)
C19	1779(8)	3357(8)	7452(5)	50.1(19)
B1	4472(7)	3665(6)	7275(5)	32.8(14)
F1	-976(4)	7386(3)	9745(2)	44.7(10)
F2	963(4)	8803(4)	10020(2)	55.7(12)
F3	-415(4)	8952(3)	9499(2)	43.8(9)
F4	-1848(9)	7547(10)	6796(3)	148(4)
F5	-2218(6)	5934(7)	6491(4)	111(3)
F6	-753(5)	7250(5)	6082(2)	56.2(12)
F7	-680(4)	3018(4)	6234(3)	59.6(12)
F8	-647(4)	3132(4)	5059(3)	58.4(12)

F9	592(4)	2836(4)	5585(3)	53.5(11)
F10	2966(13)	6622(15)	4373(9)	78(2)
F12	3400(13)	8043(14)	5182(9)	72(2)
F13	-1256(4)	4091(4)	9076(3)	45.8(10)
F14	-962(4)	2856(4)	8541(3)	62.9(13)
F15	-522(4)	3477(4)	9748(3)	55.1(11)
F16	3718(11)	4619(9)	9767(8)	44.5(18)
F17	4945(11)	5797(12)	9114(7)	48.4(17)
F18	4670(14)	6364(12)	10213(9)	47(2)
F19	7106(6)	8894(9)	7197(4)	129(4)
F20	7223(8)	8464(8)	8158(7)	147(4)
F21	8265(5)	10120(6)	8168(5)	117(3)
F22	6617(4)	12044(4)	9561(3)	59.8(13)
F23	5150(5)	11757(4)	8780(3)	53.2(11)
F24	4711(4)	11071(3)	9765(2)	40.2(9)
F25	4009(9)	4664(8)	9453(7)	47.4(16)
F26	5258(9)	6328(10)	9314(6)	50.1(17)
F27	4384(12)	6067(11)	10337(7)	50(2)
C20	1306(5)	7303(4)	7927(3)	21.7(11)
C21	1078(5)	7669(4)	8643(3)	22.4(11)
C22	182(5)	7891(5)	8722(3)	25.2(11)
C23	-573(5)	7733(5)	8089(3)	28.1(12)
C24	-406(6)	7333(6)	7381(3)	31.3(13)
C25	525(6)	7140(5)	7300(3)	27.2(12)
C26	-47(6)	8260(5)	9496(4)	32.4(13)
C27	-1282(8)	7053(9)	6689(4)	52(2)
C28	2211(5)	6399(5)	6962(3)	25.5(12)
C29	1307(6)	5241(5)	6712(3)	28.3(12)
C30	1054(6)	4665(6)	5953(4)	36.2(15)
C31	1710(7)	5239(7)	5418(4)	42.2(16)
C32	2610(7)	6375(7)	5646(4)	42.4(16)
C33	2852(6)	6950(6)	6403(4)	32.0(13)
C34	73(7)	3425(6)	5717(4)	43.8(17)
C35	3346(10)	6993(10)	5076(6)	72.5(16)
C36	2218(5)	6254(5)	8417(3)	22.8(11)
C37	1022(5)	5422(5)	8552(3)	24.1(11)
C38	844(6)	4693(5)	9000(3)	28.0(12)
C39	1843(6)	4738(5)	9337(4)	31.7(13)
C40	3039(6)	5558(5)	9216(3)	29.3(12)
C41	3225(5)	6300(5)	8770(3)	24.9(11)

C42	-471(6)	3785(5)	9093(4)	38.0(15)
C43	4134(7)	5629(6)	9577(4)	41.3(11)
C44	3808(5)	8252(5)	8086(3)	22.9(11)
C45	4882(5)	8295(5)	7895(4)	28.1(12)
C46	6083(6)	9244(5)	8133(4)	33.1(13)
C47	6307(6)	10225(5)	8577(4)	30.0(13)
C48	5267(6)	10217(5)	8768(3)	27.7(12)
C49	4053(5)	9253(5)	8527(3)	24.6(11)
C50	7184(6)	9211(6)	7904(5)	45.9(18)
C51	5444(6)	11263(5)	9222(4)	35.3(14)
B2	2402(6)	7072(5)	7846(4)	22.3(12)
C3A	250(30)	90(30)	6617(18)	96(3)
C2A	1100(30)	430(20)	6020(20)	94.8(19)
C1A	1429(11)	-193(11)	5647(7)	95.9(16)
F11	4588(12)	7443(12)	5239(7)	79(2)
F11A	4149(11)	6744(12)	4887(7)	76(2)
F10A	2497(12)	6490(14)	4383(8)	67(2)
F12A	3790(13)	7991(15)	5193(9)	75(2)

### Bond Lengths (Å)

Atom	Atom	Length/Å	Atom	Atom	Length/Å
Pt1	N1	2.124(6)	F19	C50	1.257(10)
Pt1	N3	2.070(6)	F20	C50	1.296(11)
Pt1	C1	2.147(11)	F21	C50	1.280(9)
Pt1	C2	2.12(2)	F22	C51	1.331(8)
Pt1	C4	2.070(8)	F23	C51	1.354(8)
Pt1	C2A	2.18(4)	F24	C51	1.334(7)
N1	N2	1.379(9)	F25	C43	1.312(12)
N1	C5	1.336(10)	F26	C43	1.393(13)
N2	C7	1.360(9)	F27	C43	1.352(15)
N2	B1	1.337(10)	C20	C21	1.406(8)
N3	N4	1.367(8)	C20	C25	1.401(8)
N3	C10	1.349(9)	C20	B2	1.638(8)
N4	C12	1.365(9)	C21	C22	1.374(8)
N4	B1	1.488(8)	C22	C23	1.392(9)
N5	N6	1.366(8)	C22	C26	1.498(8)
N5	C15	1.333(9)	C23	C24	1.377(9)
N6	C17	1.349(8)	C24	C25	1.389(8)

N6	B1	1.732(9)	C24	C27	1.506(9)
C1	C2	1.300(5)	C28	C29	1.398(9)
C2	C3	1.499(5)	C28	C33	1.396(9)
C5	C6	1.384(14)	C28	B2	1.648(8)
C5	C8	1.497(15)	C29	C30	1.397(9)
C6	C7	1.351(14)	C30	C31	1.380(11)
C7	C9	1.486(14)	C30	C34	1.497(11)
C10	C11	1.368(12)	C31	C32	1.373(11)
C10	C13	1.479(12)	C32	C33	1.394(10)
C11	C12	1.367(11)	C32	C35	1.486(11)
C12	C14	1.475(12)	C35	F11	1.357(17)
C15	C16	1.371(10)	C35	F11A	1.313(16)
C15	C18	1.491(11)	C35	F10A	1.426(19)
C16	C17	1.391(10)	C35	F12A	1.21(2)
C17	C19	1.482(10)	C36	C37	1.404(8)
F1	C26	1.348(8)	C36	C41	1.406(8)
F2	C26	1.329(8)	C36	B2	1.652(8)
F3	C26	1.344(7)	C37	C38	1.384(8)
F4	C27	1.284(9)	C38	C39	1.385(9)
F5	C27	1.362(12)	C38	C42	1.507(9)
F6	C27	1.295(9)	C39	C40	1.390(9)
F7	C34	1.329(9)	C40	C41	1.394(8)
F8	C34	1.342(8)	C40	C43	1.494(8)
F9	C34	1.357(9)	C44	C45	1.409(8)
F10	C35	1.256(19)	C44	C49	1.392(8)
F12	C35	1.48(2)	C44	B2	1.643(8)
F12	F12A	0.553(19)	C45	C46	1.376(9)
F13	C42	1.324(8)	C46	C47	1.382(9)
F14	C42	1.331(9)	C46	C50	1.514(9)
F15	C42	1.336(8)	C47	C48	1.391(8)
F16	C43	1.387(14)	C48	C49	1.393(8)
F17	C43	1.295(14)	C48	C51	1.492(8)
F18	C43	1.284(16)	C3A	C2A	1.503(5)

### Bond Angles (°)

Atom	Atom	Atom	Angle/°	Atom	Atom	Atom	Angle/°
N1	Pt1	C1	102.7(5)	C32	C31	C30	118.9(6)
N1	Pt1	C2A	85.1(8)	C31	C32	C33	121.0(6)

N3	Pt1	N1	84.1(2)	C31	C32	C35	119.2(7)
N3	Pt1	C1	161.4(3)	C33	C32	C35	119.8(8)
N3	Pt1	C2	160.8(4)	C32	C33	C28	121.8(6)
N3	Pt1	C2A	163.2(5)	F7	C34	F8	108.0(6)
C2	Pt1	N1	101.1(6)	F7	C34	F9	105.8(6)
C2	Pt1	C1	35.5(2)	F7	C34	C30	113.8(5)
C4	Pt1	N1	174.0(4)	F8	C34	F9	104.7(5)
C4	Pt1	N3	90.8(4)	F8	C34	C30	112.2(6)
C4	Pt1	C1	83.2(6)	F9	C34	C30	111.7(6)
C4	Pt1	C2	82.7(7)	F10	C35	F12	98.9(13)
C4	Pt1	C2A	99.2(9)	F10	C35	C32	122.4(11)
N2	N1	Pt1	117.5(4)	F10	C35	F11	111.9(10)
C5	N1	Pt1	136.3(7)	F12	C35	C32	108.1(8)
C5	N1	N2	106.1(7)	F11	C35	F12	99.5(11)
C7	N2	N1	108.9(7)	F11	C35	C32	112.3(9)
B1	N2	N1	117.9(6)	F11A	C35	F12	133.2(11)
B1	N2	C7	130.8(8)	F11A	C35	C32	110.5(10)
N4	N3	Pt1	119.0(4)	F11A	C35	F10A	101.1(11)
C10	N3	Pt1	133.8(5)	F10A	C35	F12	92.5(11)
C10	N3	N4	107.1(6)	F10A	C35	C32	106.1(9)
N3	N4	B1	115.7(5)	F12A	C35	F12	20.7(9)
C12	N4	N3	109.2(6)	F12A	C35	C32	118.1(11)
C12	N4	B1	131.9(6)	F12A	C35	F11A	113.6(11)
C15	N5	N6	111.4(6)	F12A	C35	F10A	105.5(13)
N5	N6	B1	122.3(5)	C37	C36	C41	115.5(5)
C17	N6	N5	105.8(5)	C37	C36	B2	121.4(5)
C17	N6	B1	131.9(5)	C41	C36	B2	123.0(5)
C2	C1	Pt1	71.1(10)	C38	C37	C36	122.3(5)
C1	C2	Pt1	73.4(10)	C37	C38	C39	121.7(6)
C1	C2	C3	121.5(1 7)	C37	C38	C42	119.6(6)
C3	C2	Pt1	112.7(1 4)	C39	C38	C42	118.7(6)
N1	C5	C6	110.1(8)	C38	C39	C40	117.2(6)
N1	C5	C8	120.5(9)	C39	C40	C41	121.4(5)
C6	C5	C8	129.3(8)	C39	C40	C43	118.3(6)
C7	C6	C5	106.6(7)	C41	C40	C43	120.3(6)
N2	C7	C9	123.0(8)	C40	C41	C36	122.0(6)
C6	C7	N2	108.2(8)	F13	C42	F14	106.2(6)
C6	C7	C9	128.7(7)	F13	C42	F15	106.3(5)
N3	C10	C11	108.8(7)	F13	C42	C38	112.9(5)

N3	C10	C13	122.6(8)	F14	C42	F15	106.3(6)
C11	C10	C13	128.6(7)	F14	C42	C38	111.8(5)
C12	C11	C10	108.1(6)	F15	C42	C38	112.7(6)
N4	C12	C11	106.7(7)	F16	C43	C40	109.3(7)
N4	C12	C14	123.3(7)	F17	C43	F16	107.4(8)
C11	C12	C14	129.9(7)	F17	C43	C40	111.5(7)
N5	C15	C16	106.9(6)	F18	C43	F16	104.0(9)
N5	C15	C18	121.0(7)	F18	C43	F17	110.6(10)
C16	C15	C18	132.1(6)	F18	C43	C40	113.7(9)
C15	C16	C17	107.0(6)	F25	C43	F26	103.5(8)
N6	C17	C16	108.9(6)	F25	C43	F27	108.6(9)
N6	C17	C19	121.9(6)	F25	C43	C40	113.8(7)
C16	C17	C19	129.2(6)	F26	C43	C40	113.9(6)
N2	B1	N4	125.7(7)	F27	C43	F26	104.1(8)
N2	B1	N6	110.7(5)	F27	C43	C40	112.1(8)
N4	B1	N6	101.7(5)	C45	C44	B2	120.9(5)
F12A	F12	C35	51(3)	C49	C44	C45	114.8(5)
C21	C20	B2	121.5(5)	C49	C44	B2	124.1(5)
C25	C20	C21	115.5(5)	C46	C45	C44	122.8(6)
C25	C20	B2	123.0(5)	C45	C46	C47	121.5(6)
C22	C21	C20	122.4(5)	C45	C46	C50	119.3(6)
C21	C22	C23	121.0(5)	C47	C46	C50	119.3(6)
C21	C22	C26	120.7(5)	C46	C47	C48	117.2(6)
C23	C22	C26	118.2(5)	C47	C48	C49	121.1(5)
C24	C23	C22	118.0(5)	C47	C48	C51	119.8(5)
C23	C24	C25	121.0(6)	C49	C48	C51	119.2(5)
C23	C24	C27	119.5(6)	C44	C49	C48	122.6(5)
C25	C24	C27	119.5(6)	F19	C50	F20	102.3(9)
C24	C25	C20	122.1(5)	F19	C50	F21	110.0(8)
F1	C26	C22	112.0(5)	F19	C50	C46	113.3(7)
F2	C26	F1	107.4(5)	F20	C50	C46	111.6(7)
F2	C26	F3	106.6(5)	F21	C50	F20	103.5(9)
F2	C26	C22	113.0(5)	F21	C50	C46	115.0(6)
F3	C26	F1	105.2(5)	F22	C51	F23	105.9(5)
F3	C26	C22	112.1(5)	F22	C51	F24	106.7(5)
F4	C27	F5	105.0(9)	F22	C51	C48	113.8(5)
F4	C27	F6	108.8(7)	F23	C51	C48	111.5(5)
F4	C27	C24	113.1(7)	F24	C51	F23	105.6(5)
F5	C27	C24	111.2(7)	F24	C51	C48	112.8(5)
F6	C27	F5	103.9(7)	C20	B2	C28	108.6(4)

F6	C27	C24	114.0(6)	C20	B2	C36	108.1(4)
C29	C28	B2	121.3(5)	C20	B2	C44	111.2(4)
C33	C28	C29	115.8(5)	C28	B2	C36	108.5(4)
C33	C28	B2	122.7(5)	C44	B2	C28	111.2(5)
C30	C29	C28	122.6(6)	C44	B2	C36	109.1(4)
C29	C30	C34	120.3(6)	C3A	C2A	Pt1	115(3)
C31	C30	C29	120.0(7)	F12	F12A	C35	108(3)
C31	C30	C34	119.7(6)				

## APPENDIX 3.7

### Atomic coordinates and isotropic displacement parameters for [κ<sup>2</sup>(Tp'<sup>(NH)</sup>)Pt(O=C(H)(CH<sub>3</sub>))(Me)][B(Ar<sup>F</sup>)<sub>4</sub>] (12)

<b>Atom</b>	<b>x/a</b>	<b>y/b</b>	<b>z/c</b>	<b>U(eq)</b>
Pt1	1899.5(2)	6170.6(2)	8578.6(2)	43.31(10)
N1	2660(3)	7250(4)	8042(2)	32.0(9)
N2	2015(4)	8279(4)	7600(3)	31.4(9)
N3	835(4)	7594(4)	8946(3)	38.1(10)
N4	378(4)	8591(4)	8404(3)	38(1)
N5	1000(4)	7417(4)	6683(3)	38.4(11)
N6	338(3)	7977(3)	7169(2)	28.3(9)
C3	4654(5)	6205(7)	8465(4)	61.7(19)
C4	3715(5)	7188(6)	8033(3)	40.9(12)
C5	3750(5)	8161(6)	7585(3)	45.1(13)
C6	2689(5)	8842(5)	7311(3)	38.9(12)
C7	2248(6)	9979(6)	6784(4)	57.6(17)
C8	817(7)	6920(7)	10329(4)	71(2)
C9	466(5)	7811(6)	9610(4)	50.0(14)
C10	-229(5)	8930(6)	9500(4)	55.1(15)
C11	-270(5)	9408(6)	8746(4)	46.8(14)
C12	-907(6)	10584(6)	8317(5)	62.8(19)
C13	1041(6)	6224(7)	5794(5)	61(2)
C14	478(5)	6913(5)	6340(4)	40.3(13)
C15	-560(5)	7176(5)	6601(3)	38.3(12)
C16	-627(4)	7841(4)	7116(3)	32.2(11)
C17	-1581(5)	8364(6)	7554(4)	47.0(15)
C18	2972(8)	4886(6)	8154(6)	82(3)
B1	768(5)	8698(5)	7649(4)	36.1(13)
O1	1650(8)	4781(8)	9368(5)	142(3)
C1	140(30)	5080(30)	8245(19)	114(10)
C2	597(12)	5537(16)	8978(13)	62(5)
O1A	1650(8)	4781(8)	9368(5)	142(3)
C1A	-251(13)	5762(13)	8765(10)	81(5)
C2A	893(15)	5150(13)	8713(9)	74(4)
F1	4652(3)	-904(3)	5921(2)	42.8(8)
F2	6183(3)	-2144(3)	6458(2)	57.6(10)
F3	6003(3)	-1519(3)	5244(2)	51.1(9)
F10	4568(3)	7046(3)	5442(2)	59.3(11)
F11	3383(3)	6760(3)	6221(2)	51.7(9)

F12	3640(3)	6069(3)	5235.1(18)	39.1(7)
F13	2151(3)	3807(3)	4984.7(18)	53.1(9)
F14	626(2)	3953(3)	5509.6(18)	39.8(7)
F15	1639(3)	2390(3)	5254.7(18)	42.1(8)
F16	606(3)	2515(7)	8208(2)	119(2)
F17	2002(3)	2245(3)	8925.0(18)	50.2(9)
F18	1853(5)	927(5)	8508(3)	97.2(17)
F22	6207(3)	-1860(3)	9935(2)	54.3(9)
F23	7749(3)	-2170(3)	9414(2)	49.3(9)
F24	6293(3)	-1979(3)	8764(2)	55.1(9)
C19	5961(4)	1260(4)	6582(2)	20.6(9)
C20	5603(4)	430(4)	6450(3)	22.9(9)
C21	6154(4)	-307(4)	5998(3)	26.8(10)
C22	7104(4)	-252(4)	5661(3)	29.5(10)
C23	7482(4)	566(4)	5786(3)	26.8(10)
C24	6926(4)	1301(4)	6229(3)	23.8(9)
C25	5756(5)	-1211(5)	5906(3)	36.0(11)
C27	5553(4)	3258(4)	6919(3)	21.6(9)
C28	6588(4)	3292(4)	7115(3)	26.6(10)
C29	6833(4)	4258(4)	6874(3)	29.7(10)
C30	6076(4)	5231(4)	6430(3)	28.9(10)
C31	5046(4)	5219(4)	6237(3)	26.4(10)
C32	4802(4)	4256(4)	6480(3)	23.7(9)
C34	4178(4)	6267(4)	5784(3)	34.6(11)
C35	4002(4)	2304(4)	7077(3)	19.6(9)
C36	3412(4)	2673(4)	6361(3)	22.0(9)
C37	2283(4)	2893(4)	6283(3)	22.4(9)
C38	1695(4)	2724(4)	6915(3)	26.1(10)
C39	2264(4)	2326(4)	7623(3)	27.7(10)
C40	3393(4)	2129(4)	7706(3)	24.5(10)
C41	1685(4)	3264(4)	5508(3)	29.8(10)
C42	1674(5)	2030(6)	8313(3)	45.8(14)
C43	5812(4)	1404(4)	8037(3)	23.6(9)
C44	5904(4)	1952(5)	8600(3)	30.1(10)
C45	6235(5)	1377(5)	9357(3)	39.0(12)
C46	6476(5)	232(5)	9583(3)	39.5(12)
C47	6390(4)	-337(5)	9044(3)	31.6(11)
C48	6066(4)	241(4)	8291(3)	24.5(9)
C50	6648(5)	-1572(5)	9284(3)	41.9(13)
B2	5333(4)	2070(4)	7159(3)	20.4(10)

F4	9262(4)	-364(4)	5432(4)	76(2)
F5	8309(3)	1199(4)	4715(2)	56.8(14)
F6	9017(4)	1127(7)	5773(3)	78(2)
F7	8210(6)	3883(8)	7830(4)	79(2)
F8	8768(4)	3461(7)	6814(6)	95(3)
F9	8098(6)	5179(6)	6874(5)	81(3)
F19	5554(6)	3038(5)	9806(3)	76.9(19)
F20	6167(6)	1537(5)	10632(3)	76.7(19)
F21	7318(7)	2070(11)	9941(6)	126(4)
C26	8505(4)	629(5)	5428(3)	33.0(11)
C33	7963(5)	4214(5)	7097(4)	45.5(13)
C49	6360(7)	2004(7)	9923(4)	61.5(16)
F4A	8880(30)	-190(30)	5010(20)	38(6)
F5A	8480(30)	1620(30)	5190(20)	45(6)
F6A	9270(20)	310(30)	5867(18)	34(5)
F7A	7910(20)	4660(30)	7743(16)	68(6)
F8A	8653(17)	3268(18)	7449(17)	55(5)
F9A	8380(20)	4740(30)	6612(16)	57(6)
F19A	5730(30)	2430(40)	10270(20)	89(7)
F20A	7310(30)	1440(30)	10408(19)	80(7)
F21A	6680(30)	2940(30)	9592(14)	70(6)
C26A	8505(4)	629(5)	5428(3)	33.0(11)
C33A	7963(5)	4214(5)	7097(4)	45.5(13)
C49A	6360(7)	2004(7)	9923(4)	61.5(16)

### Bond Lengths (Å)

Atom	Atom	Length/Å	Atom	Atom	Length/Å
Pt1	N1	2.072(4)	F24	C50	1.339(7)
Pt1	N3	2.118(5)	C19	C20	1.394(6)
Pt1	C18	2.050(7)	C19	C24	1.409(6)
Pt1	O1	2.174(8)	C19	B2	1.649(7)
Pt1	C2	2.187(16)	C20	C21	1.394(7)
Pt1	C2A	2.161(13)	C21	C22	1.385(7)
N1	N2	1.372(6)	C21	C25	1.494(7)
N1	C4	1.340(7)	C22	C23	1.390(7)
N2	C6	1.366(7)	C23	C24	1.382(7)
N2	B1	1.516(7)	C23	C26	1.490(7)

N3	N4	1.381(7)	C27	C28	1.410(6)
N3	C9	1.338(7)	C27	C32	1.388(7)
N4	C11	1.365(7)	C27	B2	1.648(7)
N4	B1	1.445(8)	C28	C29	1.394(7)
N5	N6	1.362(6)	C29	C30	1.377(7)
N5	C14	1.341(7)	C29	C33	1.501(7)
N6	C16	1.334(6)	C30	C31	1.392(7)
N6	B1	1.648(7)	C31	C32	1.389(7)
C3	C4	1.481(9)	C31	C34	1.493(7)
C4	C5	1.368(9)	C35	C36	1.406(6)
C5	C6	1.366(9)	C35	C40	1.401(6)
C6	C7	1.492(9)	C35	B2	1.641(6)
C8	C9	1.489(11)	C36	C37	1.387(6)
C9	C10	1.386(10)	C37	C38	1.387(7)
C10	C11	1.361(10)	C37	C41	1.500(7)
C11	C12	1.492(10)	C38	C39	1.381(7)
C13	C14	1.489(8)	C39	C40	1.394(7)
C14	C15	1.367(8)	C39	C42	1.505(7)
C15	C16	1.392(8)	C43	C44	1.397(7)
C16	C17	1.491(8)	C43	C48	1.405(7)
O1	C2	1.441(10)	C43	B2	1.638(7)
C1	C2	1.76(4)	C44	C45	1.396(8)
C1A	C2A	1.42(3)	C45	C46	1.382(9)
F1	C25	1.341(6)	C45	C49	1.492(8)
F2	C25	1.336(7)	C46	C47	1.379(8)
F3	C25	1.343(6)	C47	C48	1.391(7)
F10	C34	1.330(6)	C47	C50	1.491(8)
F11	C34	1.351(7)	F4	C26	1.315(7)
F12	C34	1.343(6)	F5	C26	1.314(6)
F13	C41	1.329(6)	F6	C26	1.327(8)
F14	C41	1.342(6)	F7	C33	1.306(9)
F15	C41	1.346(6)	F8	C33	1.336(9)
F16	C42	1.293(7)	F9	C33	1.315(8)
F17	C42	1.312(7)	F19	C49	1.351(10)
F18	C42	1.344(9)	F20	C49	1.354(9)
F22	C50	1.340(6)	F21	C49	1.276(10)
F23	C50	1.350(7)			

### Bond Angles (°)

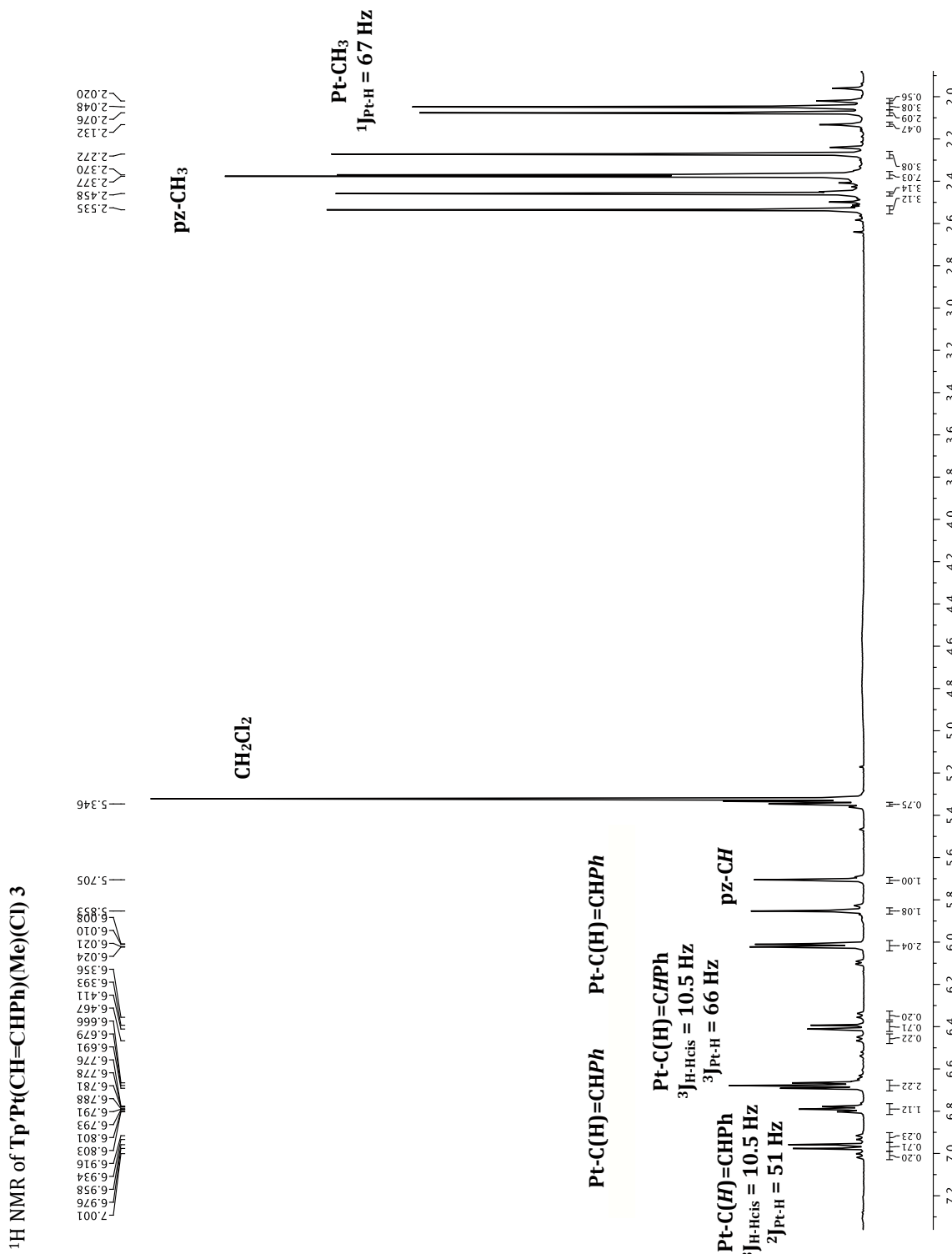
<b>Atom</b>	<b>Atom</b>	<b>Atom</b>	<b>Angle/°</b>	<b>Atom</b>	<b>Atom</b>	<b>Atom</b>	<b>Angle/°</b>
N1	Pt1	N3	84.35(17)	C28	C29	C33	118.4(5)
N1	Pt1	O1	160.2(3)	C30	C29	C28	121.6(4)
N1	Pt1	C2	160.4(4)	C30	C29	C33	119.9(5)
N1	Pt1	C2A	159.1(4)	C29	C30	C31	117.3(4)
N3	Pt1	O1	102.8(3)	C30	C31	C34	119.5(4)
N3	Pt1	C2	81.6(7)	C32	C31	C30	120.9(5)
N3	Pt1	C2A	100.9(6)	C32	C31	C34	119.6(4)
C18	Pt1	N1	90.9(3)	C27	C32	C31	123.1(4)
C18	Pt1	N3	175.0(3)	F10	C34	F11	106.4(4)
C18	Pt1	O1	82.1(4)	F10	C34	F12	106.3(4)
C18	Pt1	C2	102.7(7)	F10	C34	C31	114.0(4)
C18	Pt1	C2A	83.1(6)	F11	C34	C31	111.7(5)
O1	Pt1	C2	38.6(3)	F12	C34	F11	105.4(4)
N2	N1	Pt1	119.0(3)	F12	C34	C31	112.4(4)
C4	N1	Pt1	133.6(4)	C36	C35	B2	121.4(4)
C4	N1	N2	107.4(5)	C40	C35	C36	116.0(4)
N1	N2	B1	119.0(4)	C40	C35	B2	122.6(4)
C6	N2	N1	108.6(4)	C37	C36	C35	122.0(4)
C6	N2	B1	130.6(5)	C36	C37	C41	120.5(4)
N4	N3	Pt1	117.6(3)	C38	C37	C36	120.9(4)
C9	N3	Pt1	135.9(5)	C38	C37	C41	118.6(4)
C9	N3	N4	106.5(5)	C39	C38	C37	118.2(4)
N3	N4	B1	120.4(4)	C38	C39	C40	121.1(4)
C11	N4	N3	109.1(5)	C38	C39	C42	119.5(4)
C11	N4	B1	129.4(5)	C40	C39	C42	119.3(5)
C14	N5	N6	111.1(4)	C39	C40	C35	121.7(4)
N5	N6	B1	121.0(4)	F13	C41	F14	106.8(4)
C16	N6	N5	106.5(4)	F13	C41	F15	106.9(4)
C16	N6	B1	132.5(4)	F13	C41	C37	113.2(4)
N1	C4	C3	123.1(6)	F14	C41	F15	105.7(4)
N1	C4	C5	109.1(6)	F14	C41	C37	111.9(4)
C5	C4	C3	127.8(6)	F15	C41	C37	111.9(4)
C6	C5	C4	107.8(5)	F16	C42	F17	108.6(6)
N2	C6	C5	107.1(5)	F16	C42	F18	104.2(6)
N2	C6	C7	122.1(6)	F16	C42	C39	113.1(5)
C5	C6	C7	130.8(6)	F17	C42	F18	104.6(5)

N3	C9	C8	121.1(6)	F17	C42	C39	113.4(5)
N3	C9	C10	109.7(6)	F18	C42	C39	112.2(5)
C10	C9	C8	129.2(6)	C44	C43	C48	115.1(4)
C11	C10	C9	107.0(5)	C44	C43	B2	123.1(4)
N4	C11	C12	122.8(6)	C48	C43	B2	121.5(4)
C10	C11	N4	107.6(6)	C45	C44	C43	122.1(5)
C10	C11	C12	129.6(6)	C44	C45	C49	119.4(6)
N5	C14	C13	121.2(5)	C46	C45	C44	120.9(5)
N5	C14	C15	106.4(5)	C46	C45	C49	119.7(6)
C15	C14	C13	132.4(5)	C47	C46	C45	118.7(5)
C14	C15	C16	107.3(5)	C46	C47	C48	120.0(5)
N6	C16	C15	108.7(5)	C46	C47	C50	119.0(5)
N6	C16	C17	122.2(5)	C48	C47	C50	121.0(5)
C15	C16	C17	129.1(5)	C47	C48	C43	123.2(5)
N2	B1	N6	104.9(4)	F22	C50	F23	105.4(4)
N4	B1	N2	116.4(5)	F22	C50	C47	112.5(5)
N4	B1	N6	110.4(4)	F23	C50	C47	112.3(5)
C2	O1	Pt1	71.2(7)	F24	C50	F22	107.1(5)
O1	C2	Pt1	70.2(7)	F24	C50	F23	105.7(5)
O1	C2	C1	115(2)	F24	C50	C47	113.3(5)
C1	C2	Pt1	109.0(16)	C27	B2	C19	109.0(4)
C1A	C2A	Pt1	113.6(12)	C35	B2	C19	107.9(4)
C20	C19	C24	115.2(4)	C35	B2	C27	110.9(4)
C20	C19	B2	121.4(4)	C43	B2	C19	109.0(4)
C24	C19	B2	123.2(4)	C43	B2	C27	111.3(4)
C19	C20	C21	122.6(4)	C43	B2	C35	108.7(4)
C20	C21	C25	120.0(4)	F4	C26	C23	113.1(5)
C22	C21	C20	120.9(5)	F4	C26	F6	104.8(6)
C22	C21	C25	119.0(5)	F5	C26	C23	112.9(4)
C21	C22	C23	117.6(5)	F5	C26	F4	106.5(5)
C22	C23	C26	118.0(5)	F5	C26	F6	105.3(5)
C24	C23	C22	121.2(4)	F6	C26	C23	113.5(5)
C24	C23	C26	120.8(5)	F7	C33	C29	112.9(6)
C23	C24	C19	122.4(4)	F7	C33	F8	103.9(7)
F1	C25	F3	105.5(4)	F7	C33	F9	106.8(7)
F1	C25	C21	112.9(4)	F8	C33	C29	111.9(5)
F2	C25	F1	105.5(5)	F9	C33	C29	113.9(5)
F2	C25	F3	106.7(5)	F9	C33	F8	106.8(7)
F2	C25	C21	112.5(5)	F19	C49	C45	111.9(6)
F3	C25	C21	113.2(5)	F19	C49	F20	100.6(6)

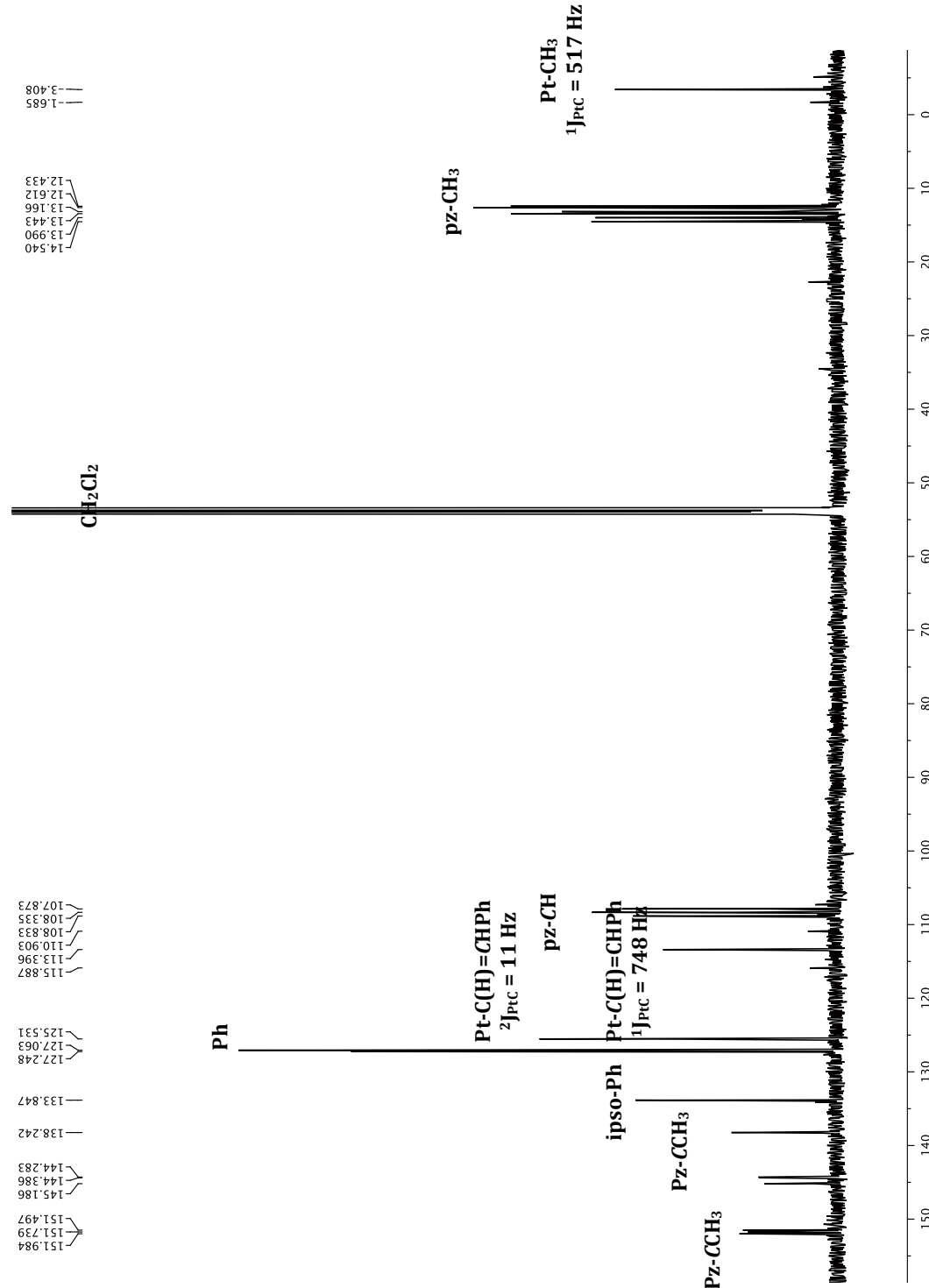
C28	C27	B2	120.2(4)	F20	C49	C45	111.8(6)
C32	C27	C28	115.1(4)	F21	C49	C45	112.3(7)
C32	C27	B2	124.5(4)	F21	C49	F19	110.6(8)
C29	C28	C27	121.9(5)	F21	C49	F20	109.1(8)

## APPENDIX 4.1

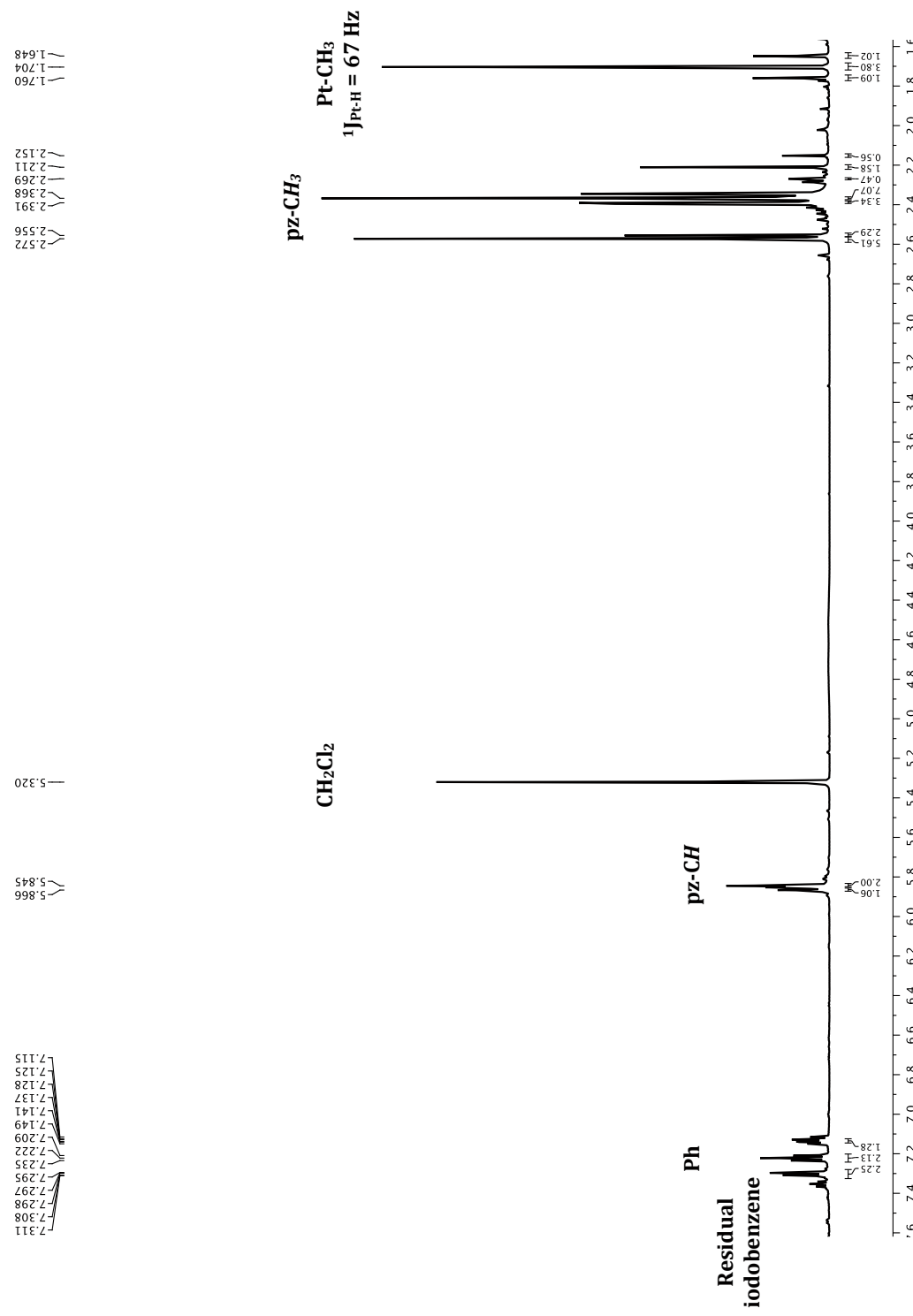
### Representative NMR Data for Chapter 4



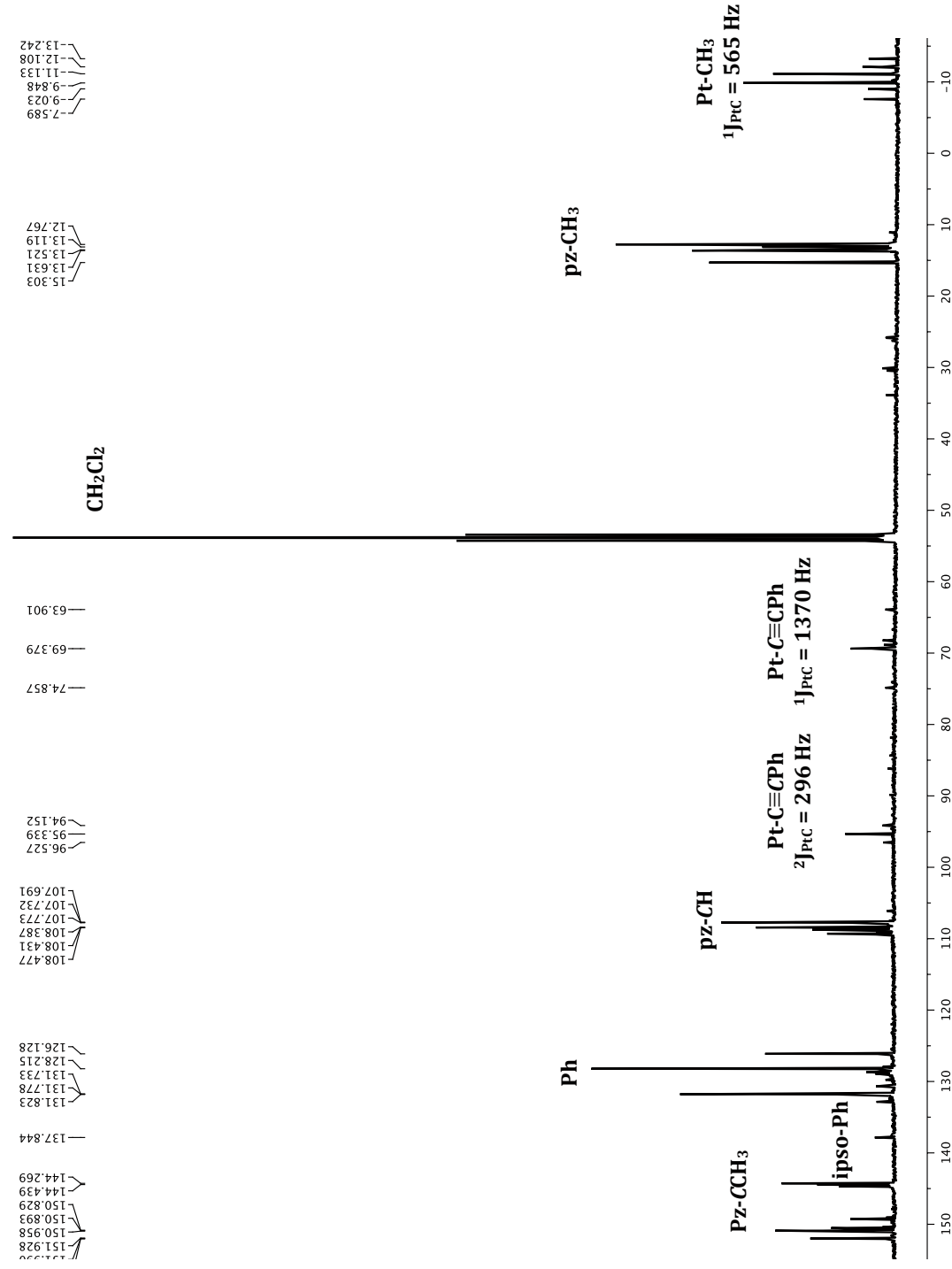
$^{13}\text{C}$  NMR of  $\text{Tp}'\text{Pt}(\text{CH}=\text{CHPh})(\text{Me})(\text{Cl})$  3

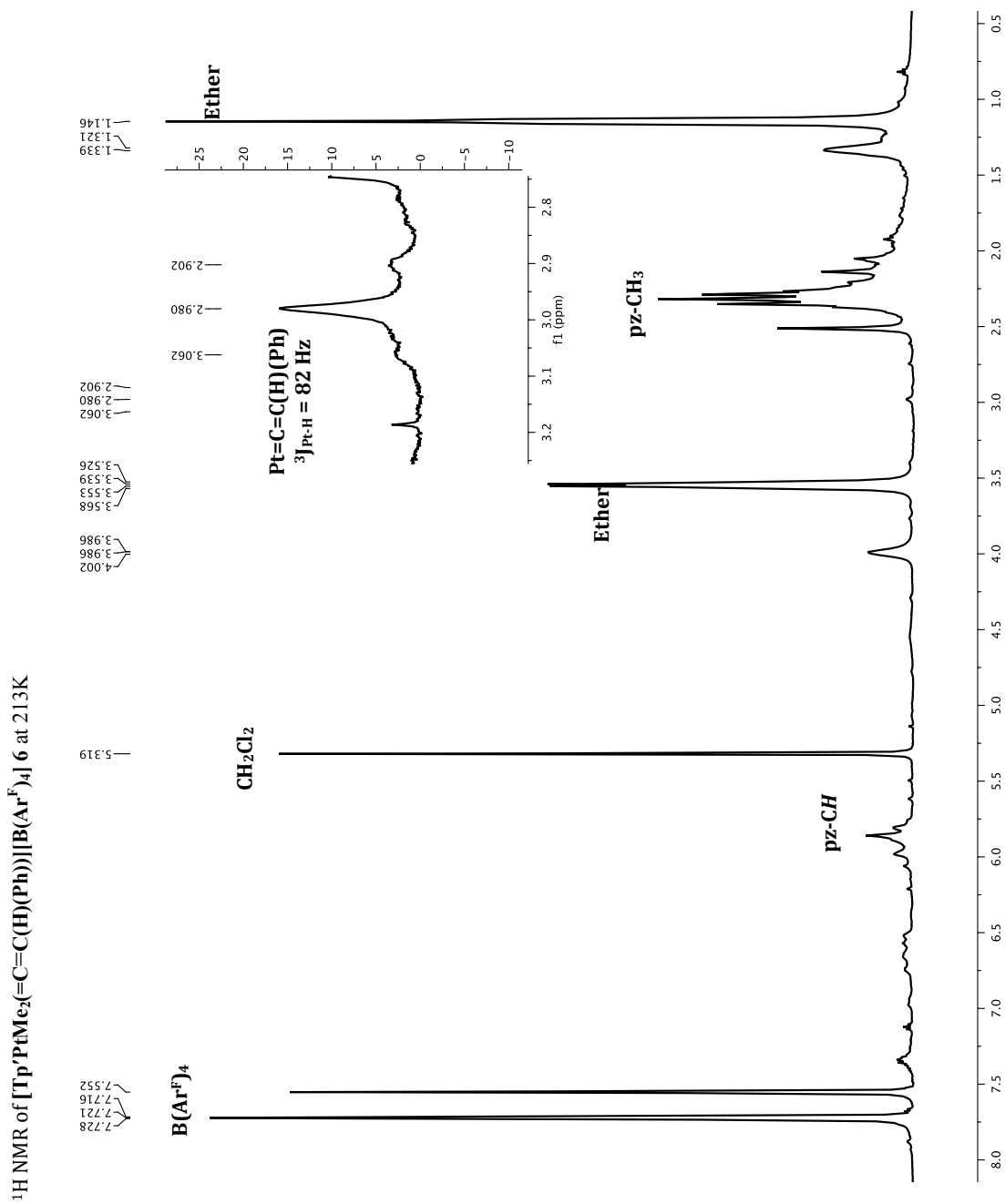


<sup>1</sup>H NMR of  $\text{Tp}'\text{PtMe}_2(\text{C}\equiv\text{CPH})$  5

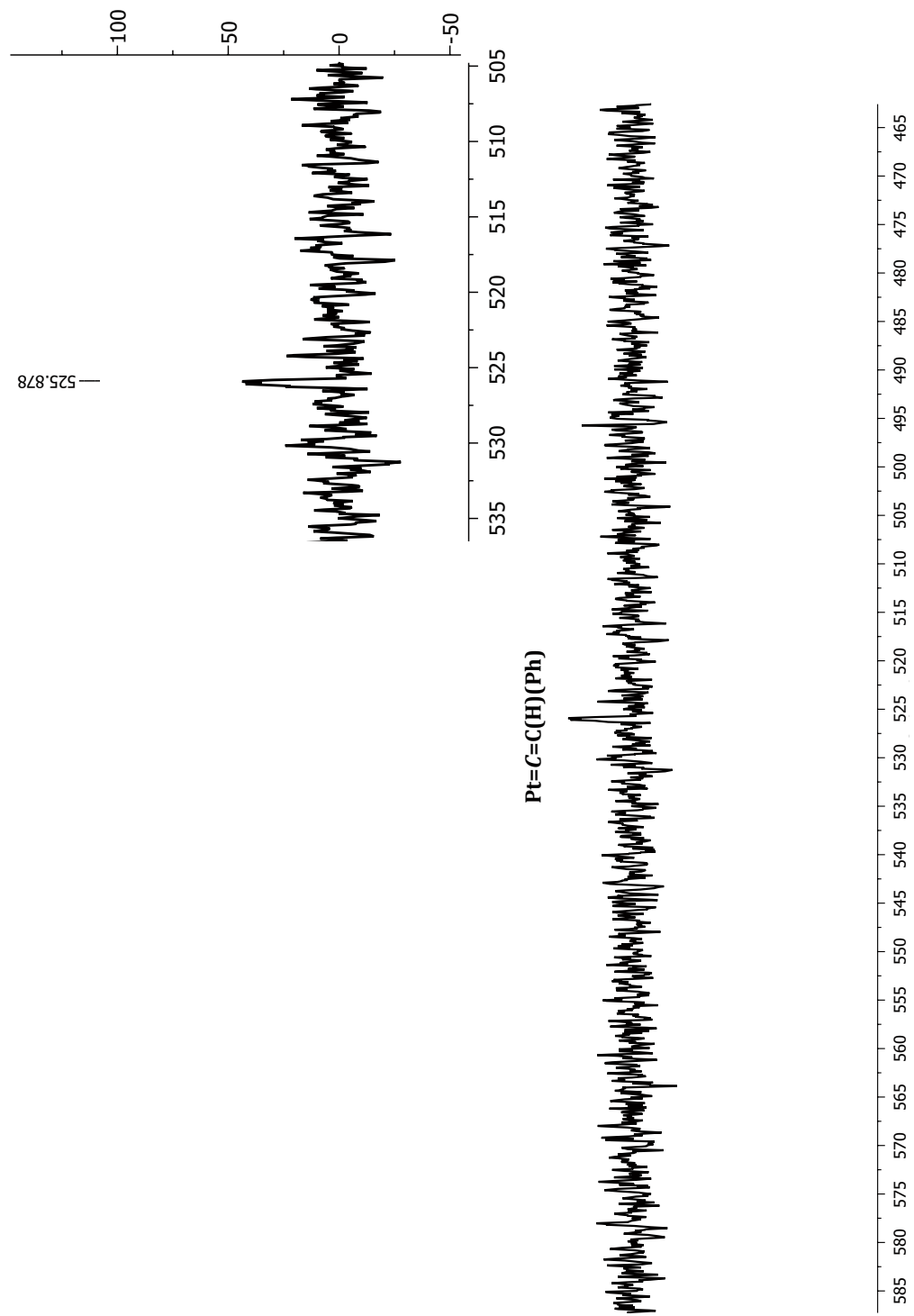


$^{13}\text{C}$  NMR of  $\text{Tp}^{\bullet}\text{PtMe}_2(\text{C}\equiv\text{CPh})$  5



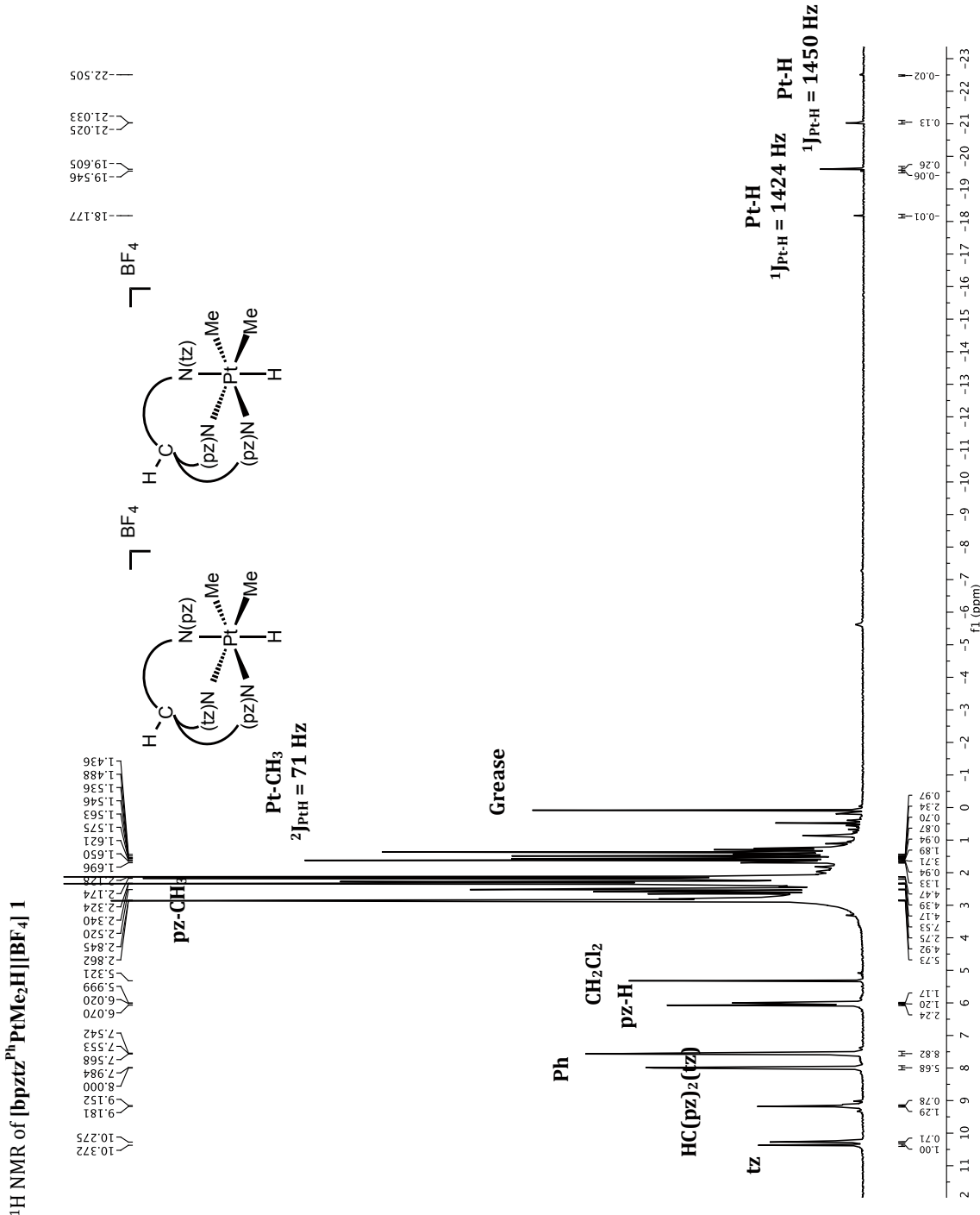


$^{13}\text{C}$  NMR of  $[\text{Tp}'\text{PtMe}_2(\text{=C}(\text{H})(\text{Ph}))\text{B}(\text{Ar}^{\text{F}})_4]$  6 at 213K

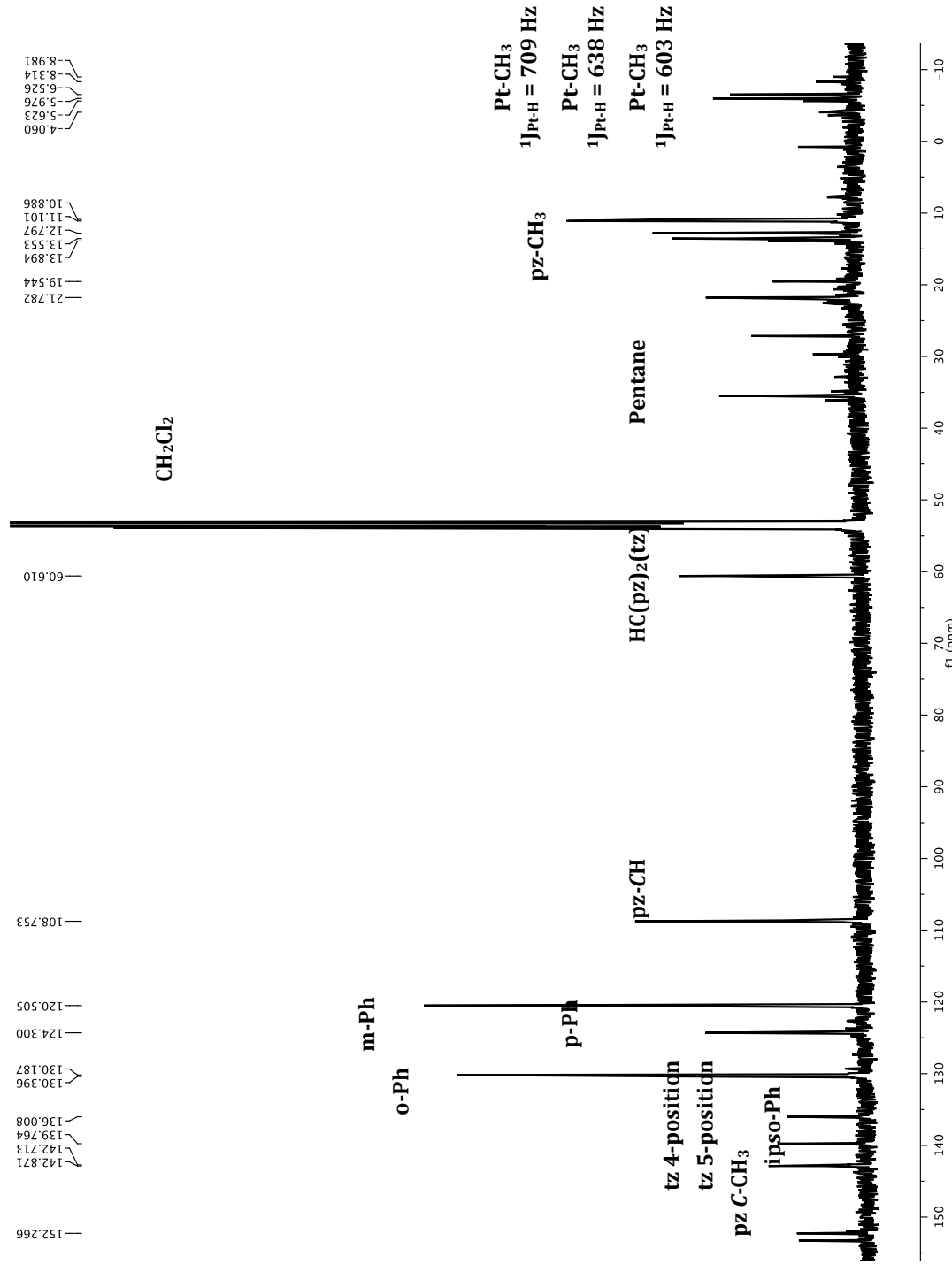


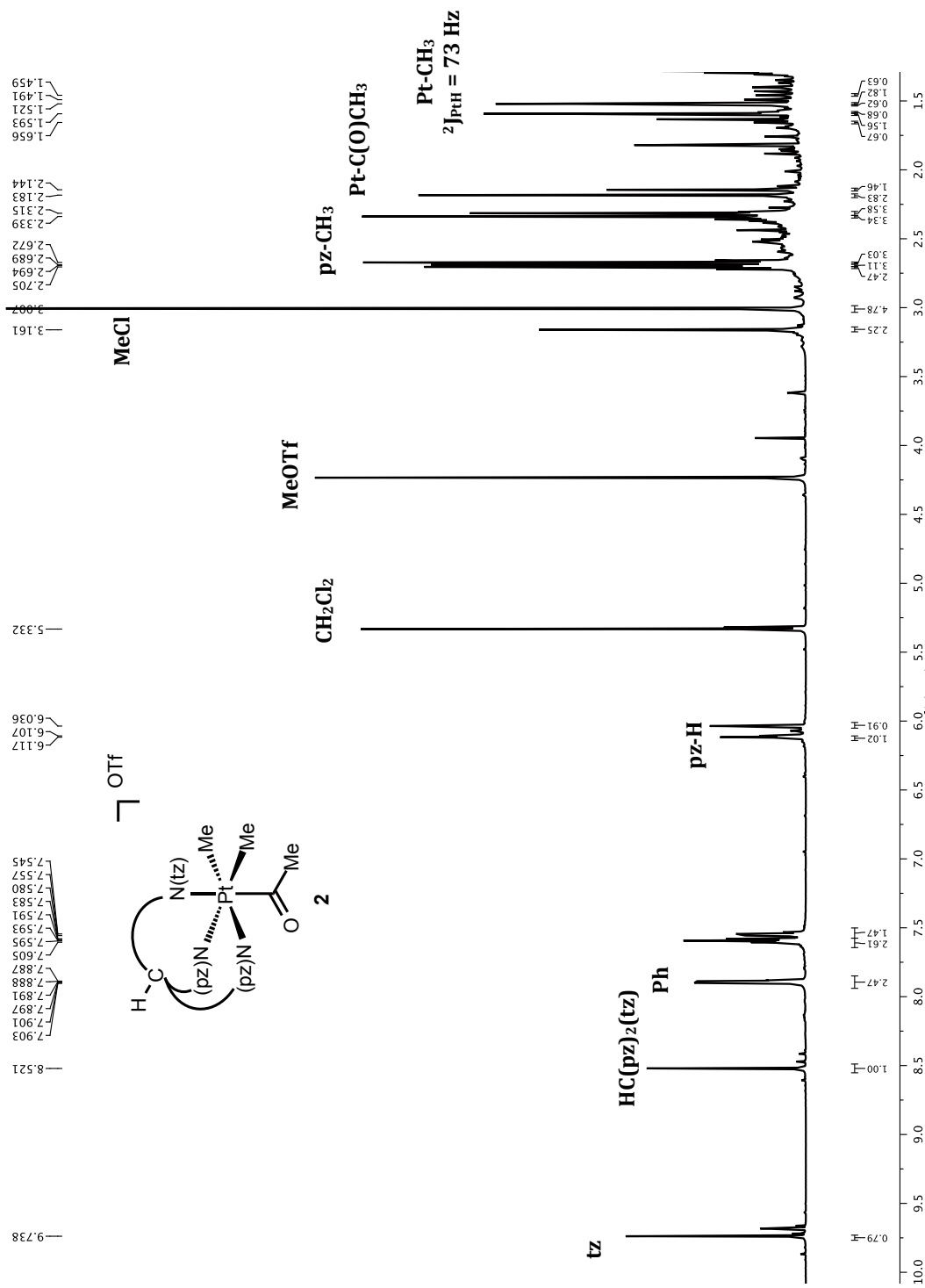
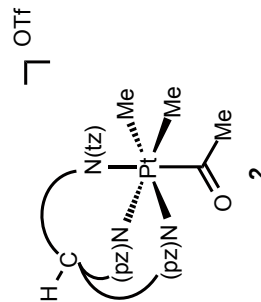
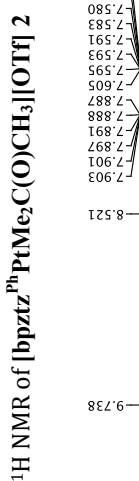
## APPENDIX 5.1

### Representative NMR Data for Chapter 5

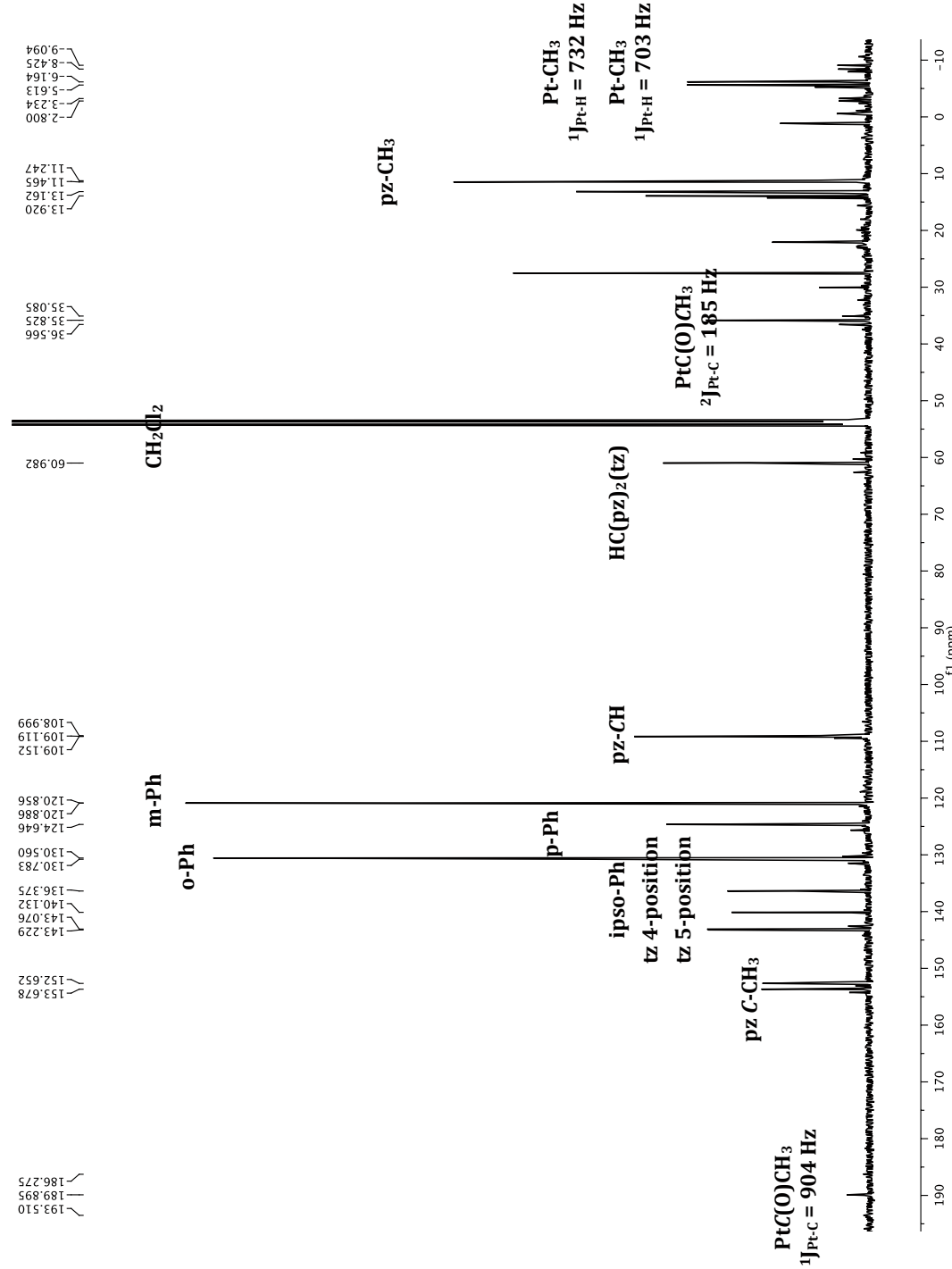


$^{13}\text{C}$  NMR of [bpz<sub>2</sub><sup>Ph</sup>PtMe<sub>2</sub>H][BF<sub>4</sub>] 1

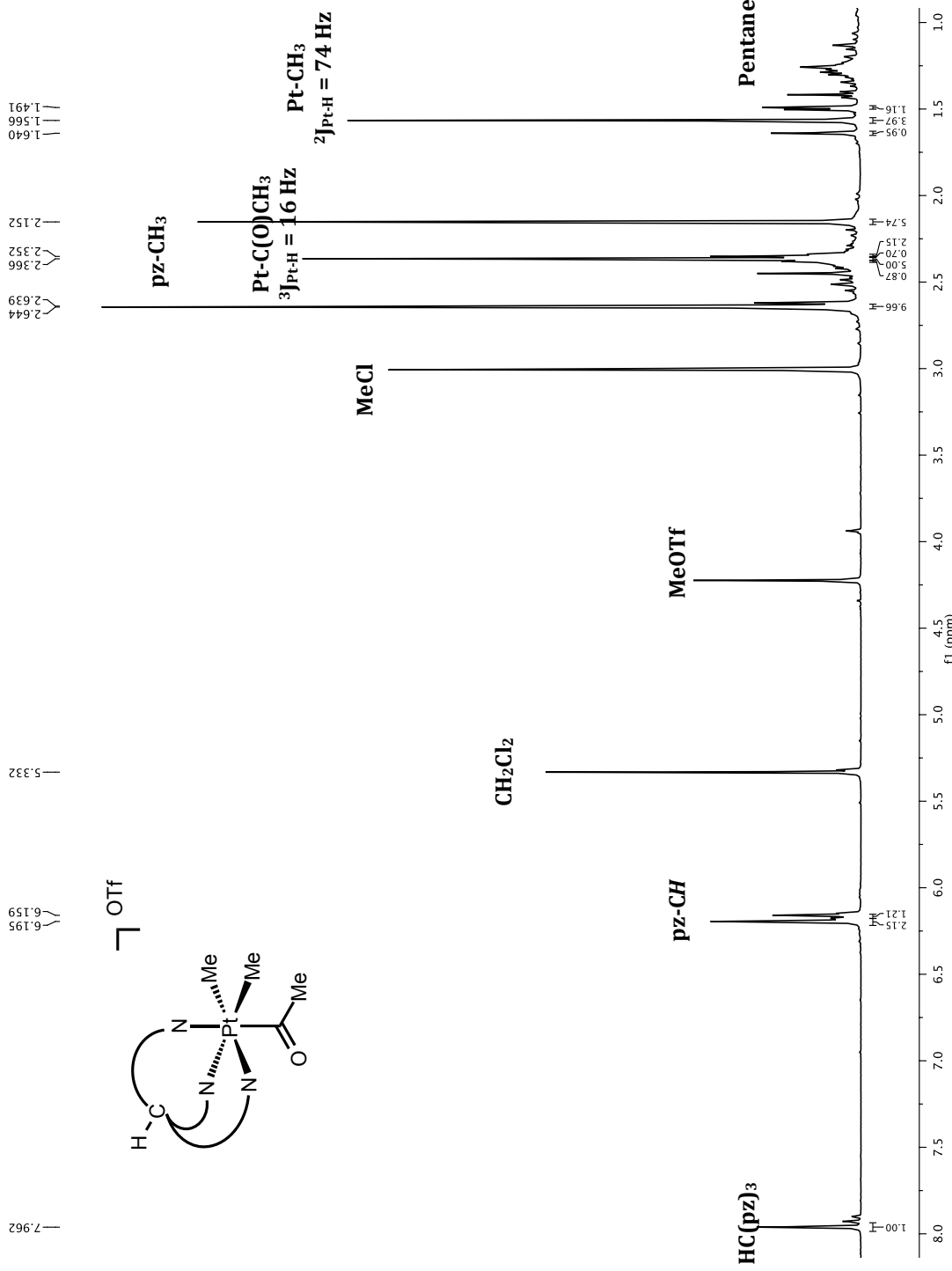




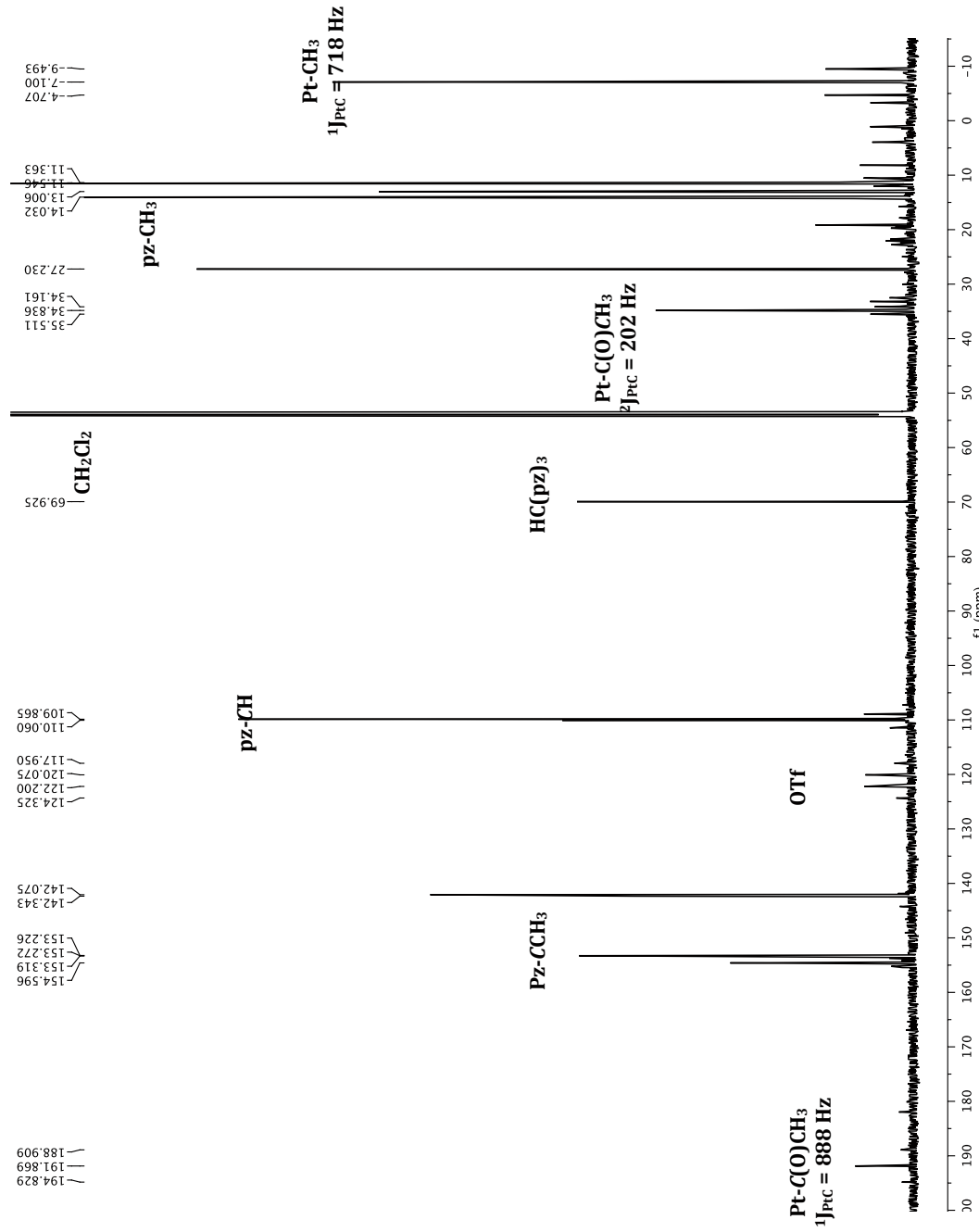
<sup>13</sup>C NMR of [bpz<sub>2</sub><sup>Ph</sup>PtMe<sub>2</sub>C(O)CH<sub>3</sub>]OTf 2



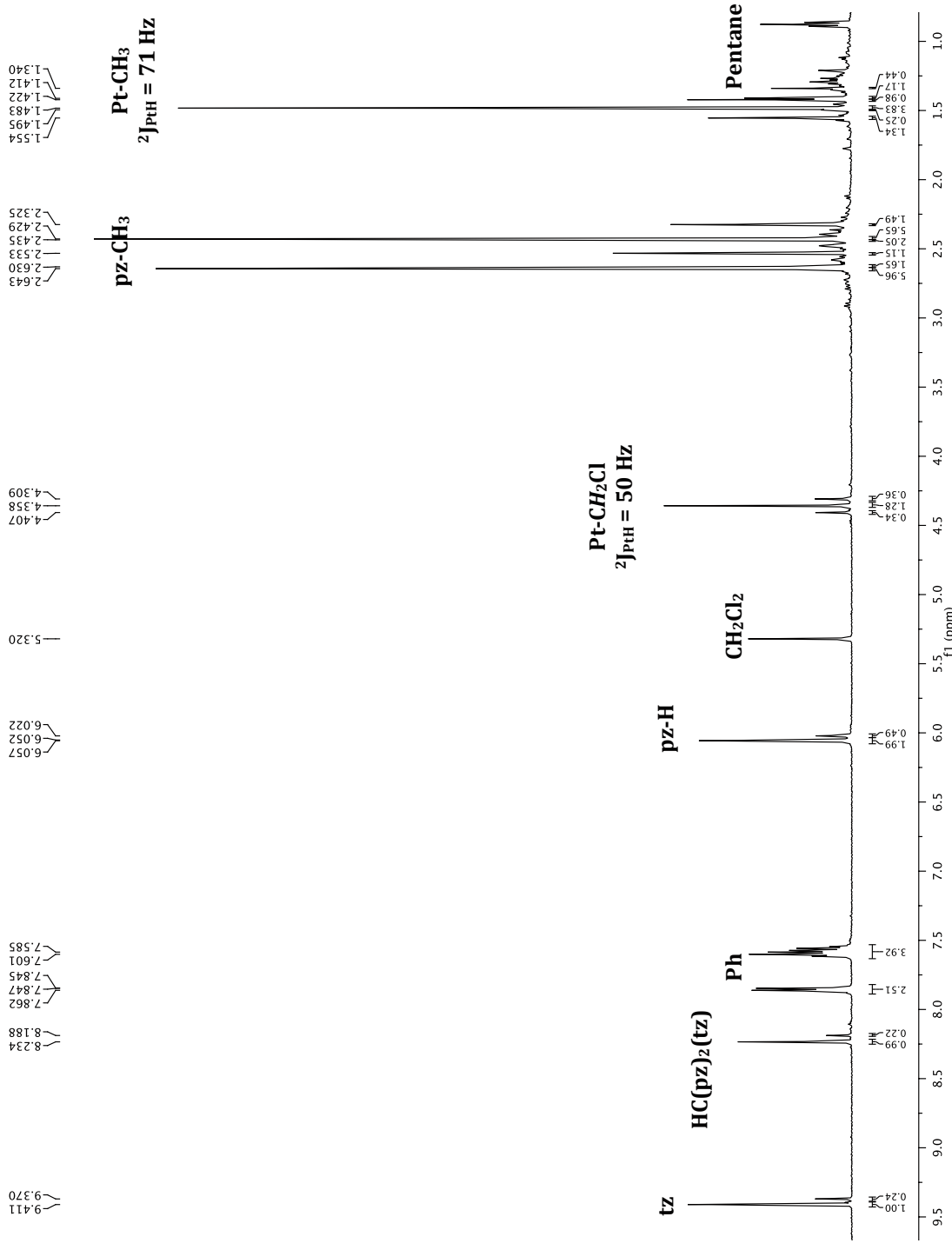
<sup>1</sup>H NMR of [Tp<sup>m</sup>PtMe<sub>2</sub>C(O)CH<sub>3</sub>]OTf 3



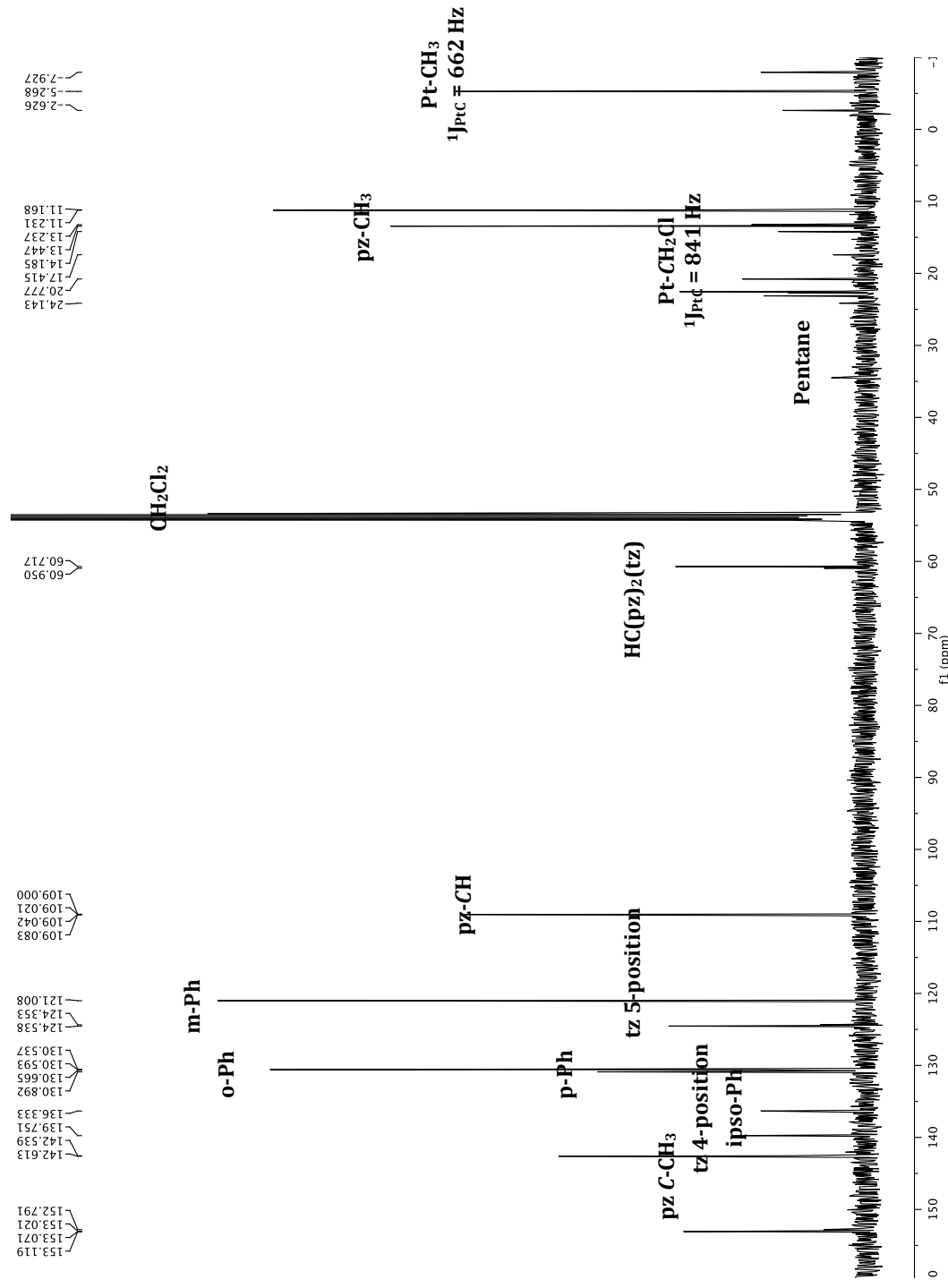
$^{13}\text{C}$  NMR of [Tp<sup>m</sup>PtMe<sub>2</sub>C(O)CH<sub>3</sub>][OTf]<sup>3</sup>

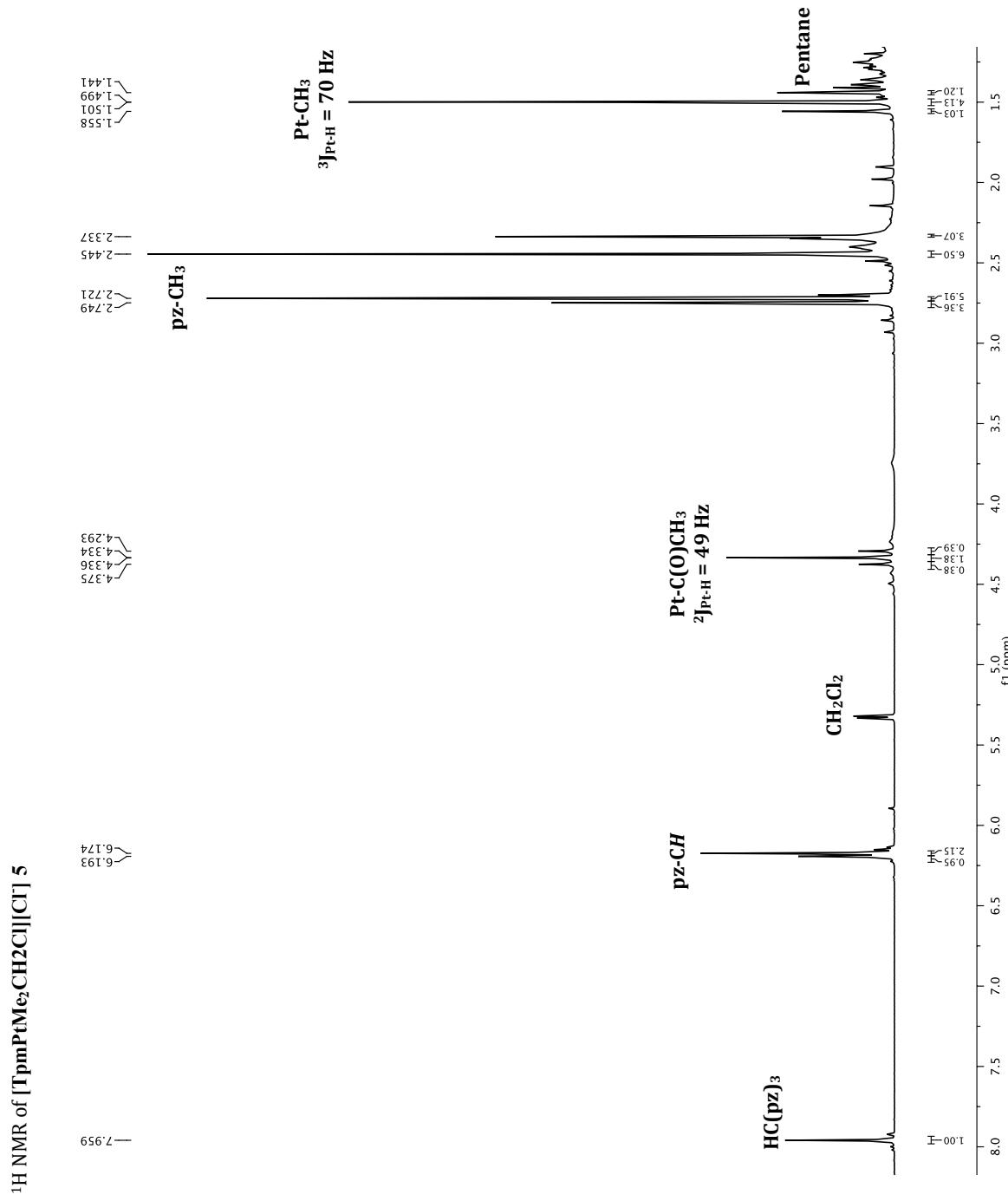


<sup>1</sup>H NMR of [bpz<sub>2</sub>]<sup>Ph</sup>PtMe<sub>2</sub>CH<sub>2</sub>Cl][BF<sub>4</sub>]<sub>4</sub>

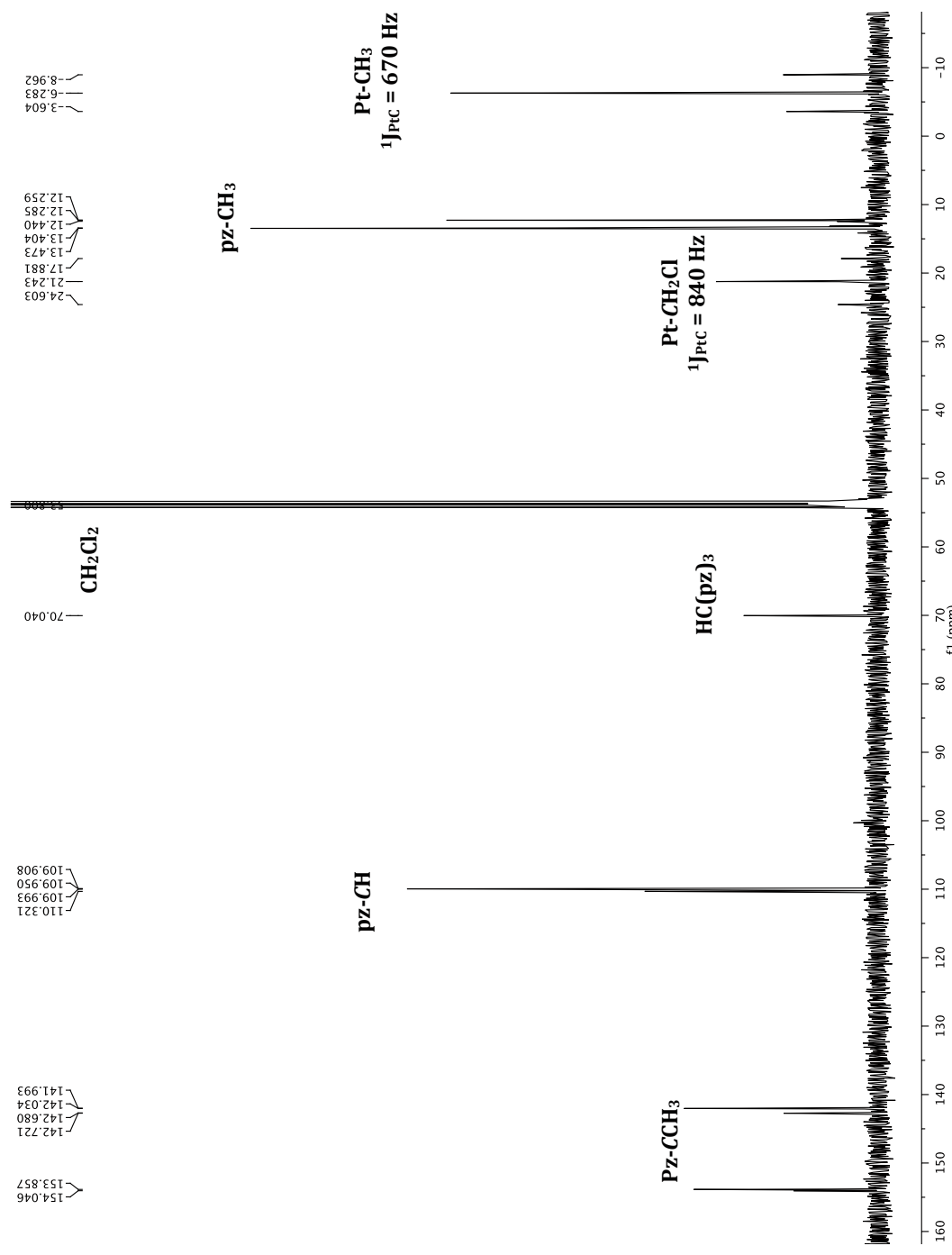


$^{13}\text{C}$  NMR of [bp<sup>Ph</sup>tz<sup>Ph</sup>PtMe<sub>2</sub>CH<sub>2</sub>Cl] $[\text{BF}_4^-]$  4

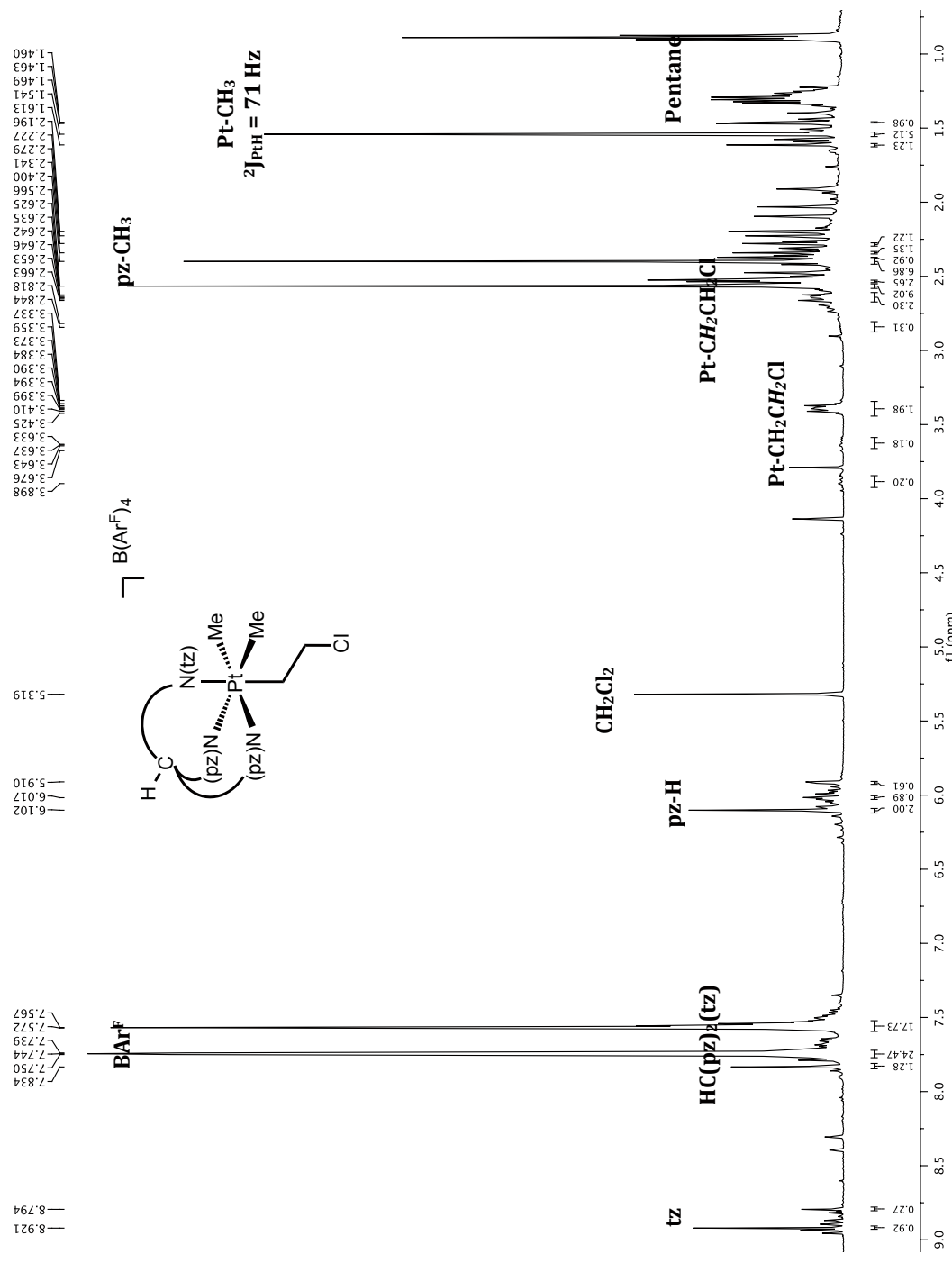




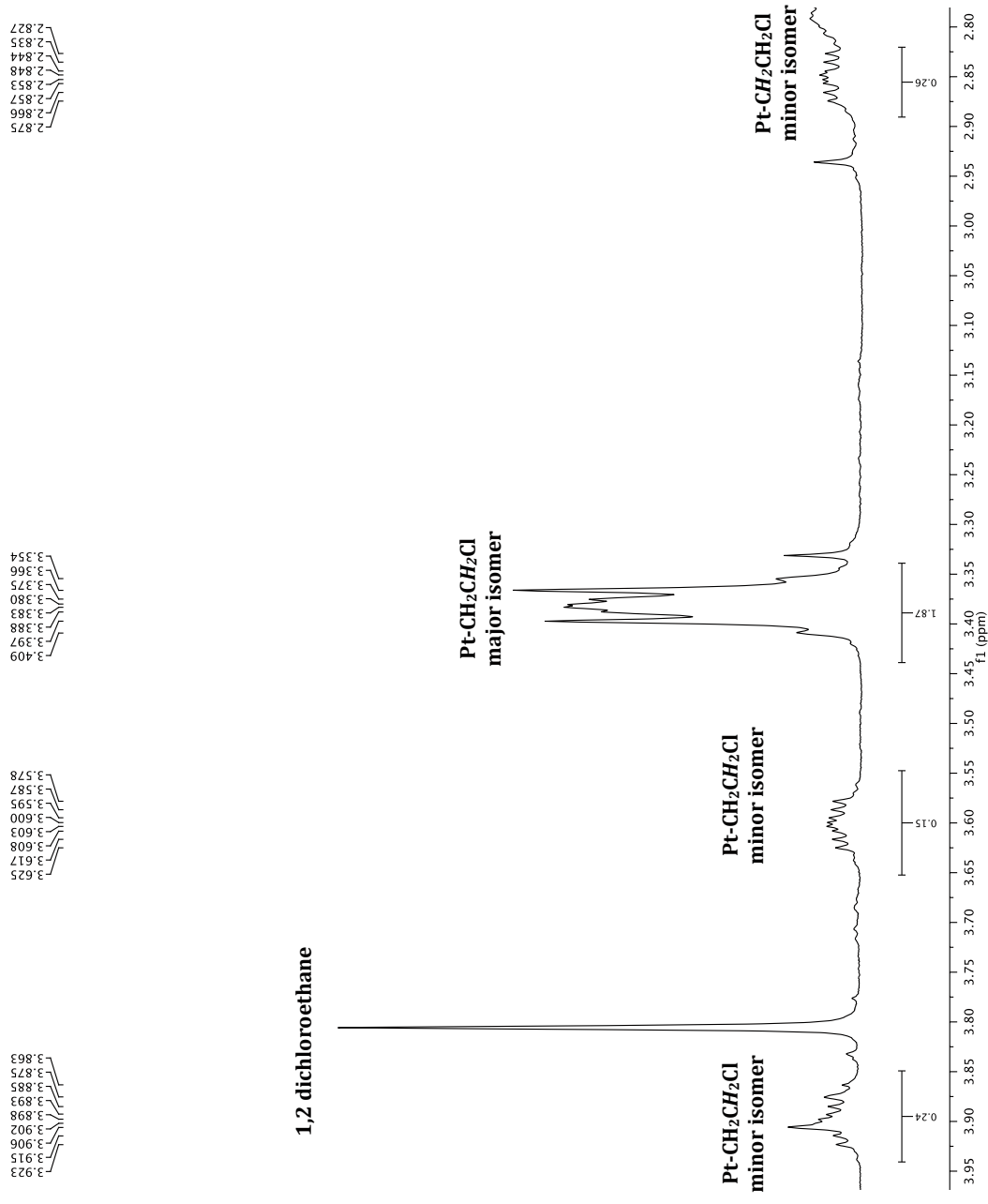
<sup>13</sup>C NMR of [Tp<sup>m</sup>PtMe<sub>2</sub>CH<sub>2</sub>Cl]<sub>2</sub>Cl] 5



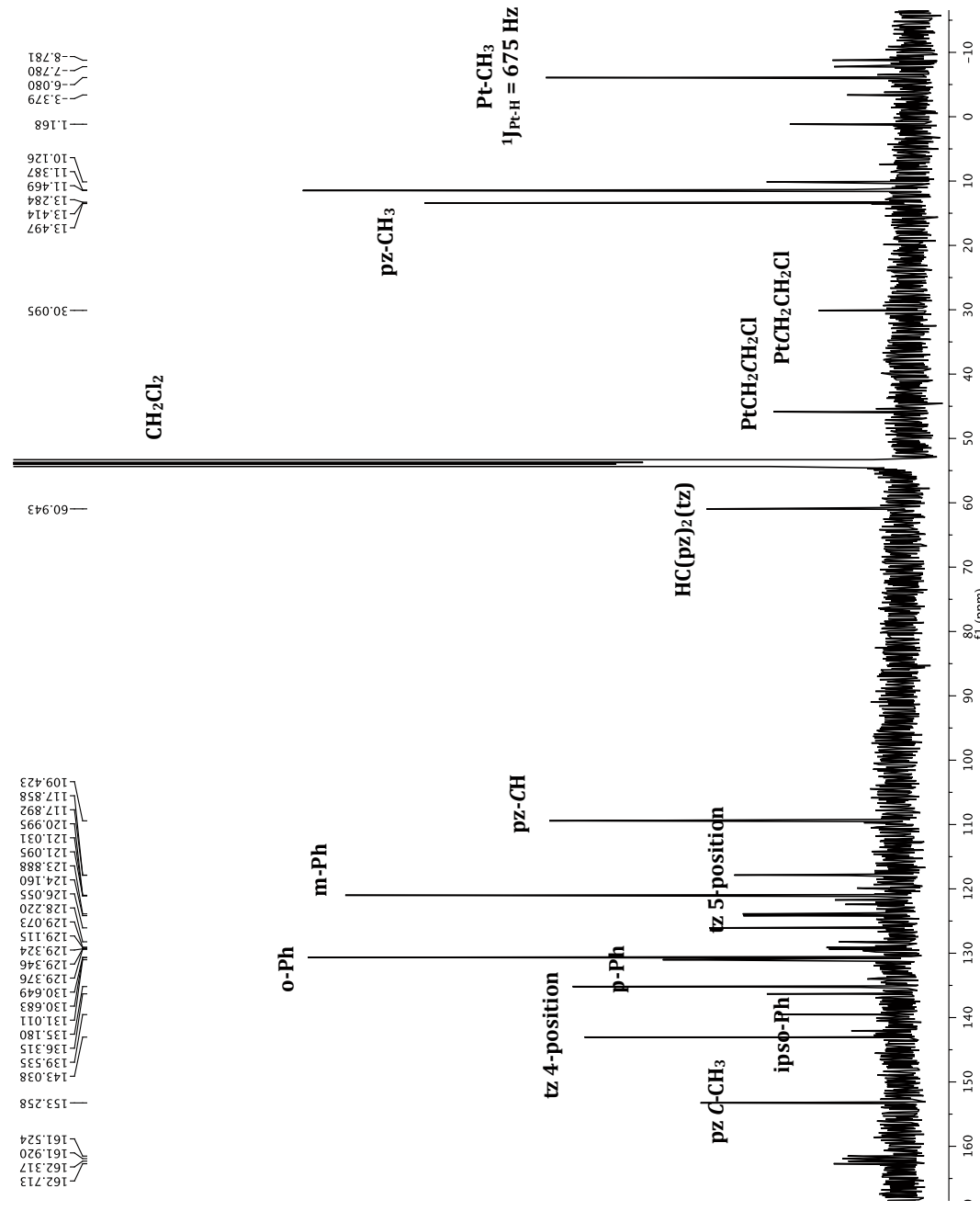
<sup>1</sup>H NMR of [bp<sub>2</sub>tz <sup>Ph</sup>PtMe<sub>2</sub>(CH<sub>2</sub>CH<sub>2</sub>Cl)]|[BAr<sup>F</sup>] 6

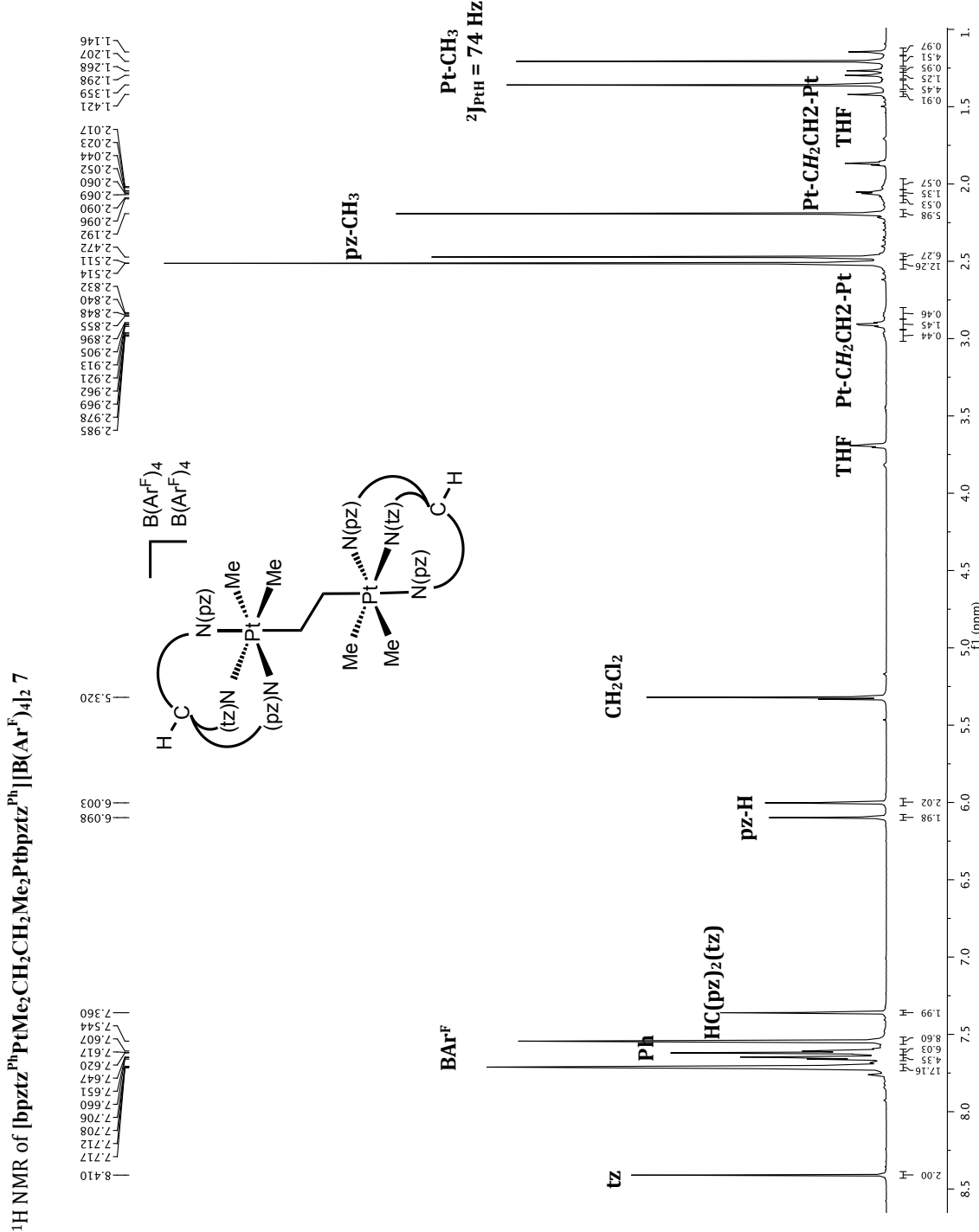


$^1\text{H}$  NMR of [bpz<sub>2</sub><sup>Ph</sup>PtMe<sub>2</sub>(CH<sub>2</sub>CH<sub>2</sub>Cl)][BAr<sup>F</sup>] **6** close up of ethyl chloride protons

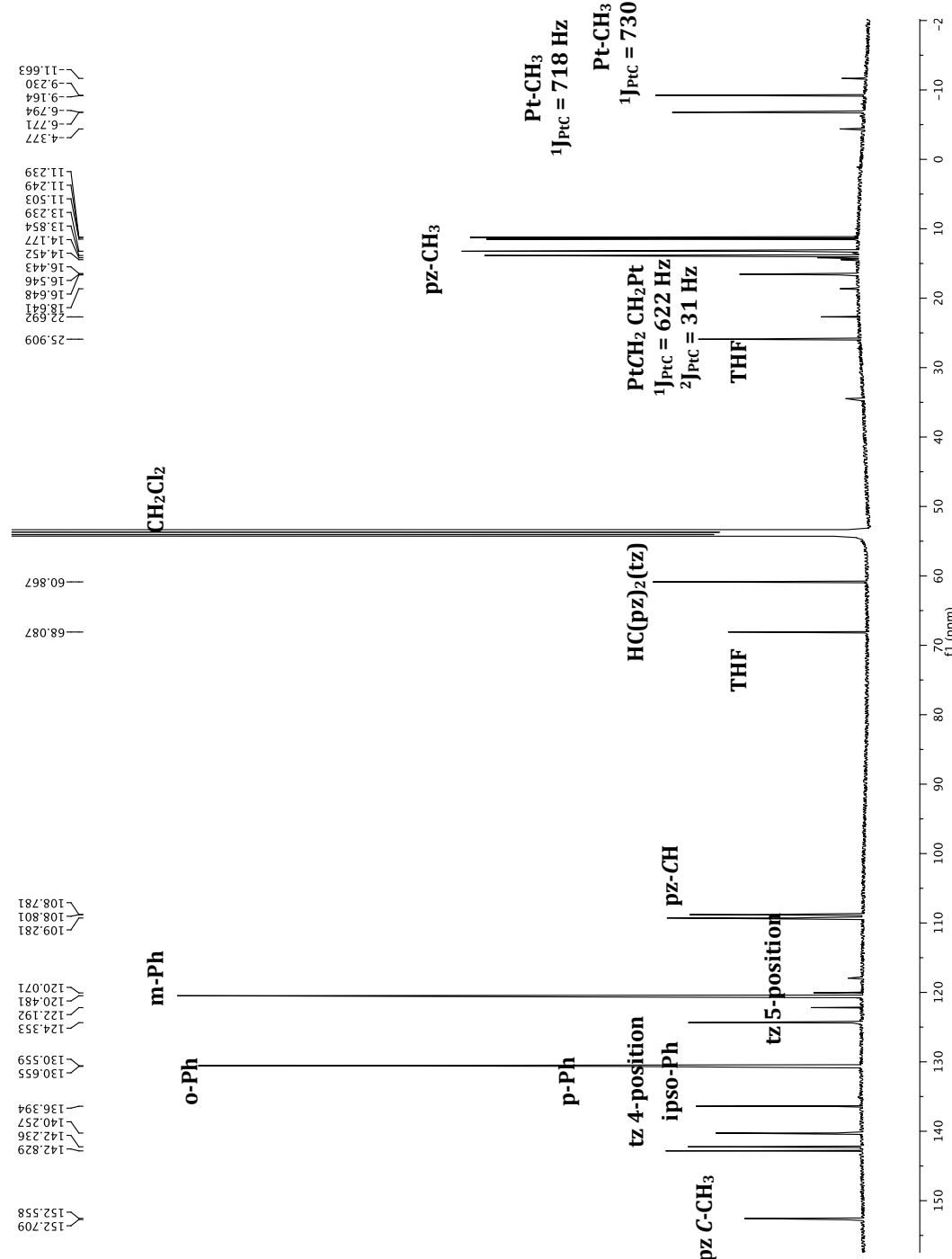


$^{13}\text{C}$  NMR of [bpptz $^{\text{Pn}}$ PtMe<sub>2</sub>CH<sub>2</sub>CH<sub>2</sub>Cl][B(Ar $^{\text{F}}$ )<sub>4</sub>] 6





<sup>13</sup>C NMR of [bpz<sub>2</sub>PtMe<sub>2</sub>CH<sub>2</sub>CH<sub>2</sub>Me<sub>2</sub>Ptbpz<sub>2</sub>]<sub>n</sub>]Cl<sub>2</sub> 7



## APPENDIX 5.2

### Atomic coordinates and isotropic displacement parameters for [bpztz<sup>Ph</sup>PtMe<sub>2</sub>C(O)CH<sub>3</sub>]|OTf] (2)

U(eq) is defines as one third of the trace of the orthogonalized U<sub>ij</sub> tensor.

<b>Atom</b>	<b>x/a</b>	<b>y/b</b>	<b>z/c</b>	<b>U(eq)</b>
Pt1	2473.9(3)	1966.0(2)	6312.1(2)	37.08(10)
C2	2615(8)	59(5)	6665(5)	50.0(16)
C3	3916(7)	1901(5)	4898(4)	40.5(14)
C4	746(9)	1774(6)	5727(6)	52.3(17)
C6	880(20)	877(15)	5101(11)	187(9)
N7	1163(5)	2101(4)	7741(4)	36.9(11)
N8	39(6)	1481(4)	8240(4)	40.5(11)
N9	-416(5)	1976(4)	9079(4)	38.0(11)
C10	414(6)	2905(5)	9101(4)	36.6(12)
C11	1424(6)	2985(5)	8236(4)	34.4(12)
C12	-1717(7)	1537(6)	9773(5)	42.5(14)
C13	-2044(8)	304(6)	9873(5)	49.4(16)
C14	-3351(9)	-76(7)	10485(5)	59(2)
C15	-4284(9)	745(8)	10965(5)	63(2)
C16	-3919(8)	1957(8)	10878(5)	59.1(19)
C17	-2627(7)	2359(7)	10275(5)	49.8(16)
C18	2651(6)	3820(5)	7780(4)	35.5(12)
N19	2298(6)	3996(4)	6047(4)	43.7(12)
N20	2507(5)	4568(4)	6805(4)	37.3(11)
C21	2639(8)	5807(5)	6461(5)	46.8(15)
C22	2460(10)	6022(6)	5484(6)	63(2)
C23	2258(9)	4899(6)	5243(5)	58.5(19)
C24	2964(9)	6660(6)	7099(6)	54.3(18)
C25	2012(12)	4661(7)	4268(6)	78(3)
N26	4245(6)	2230(4)	7065(4)	39.4(11)
N27	4016(5)	3118(4)	7660(4)	36.3(10)
C28	5201(7)	3276(6)	8002(5)	45.1(14)
C29	6237(8)	2443(7)	7622(5)	56.4(18)
C30	5610(7)	1817(6)	7047(5)	48.3(15)
C31	5246(8)	4208(7)	8642(6)	57.3(18)
C32	6300(9)	824(7)	6478(6)	63(2)
S33	1245.5(18)	4107.2(17)	1307.6(12)	50.7(4)

O34	-177(5)	4006(4)	1147(3)	49.7(11)
O35	2343(6)	4121(7)	435(4)	87(2)
O36	1347(6)	5027(5)	1911(5)	66.8(14)
C37	1547(9)	2664(7)	2146(6)	62(2)
F38	2832(5)	2603(5)	2388(4)	81.8(15)
F39	583(6)	2522(6)	3000(4)	93.6(17)
F40	1510(10)	1711(5)	1704(6)	141(3)
O5	-280(10)	2397(9)	5973(7)	123(3)

### Bond Lengths (Å)

Atom	Atom	Length/Å	Atom	Atom	Length/Å
Pt1	C2	2.057(5)	C18	N27	1.452(7)
Pt1	C3	2.133(5)	N19	N20	1.377(7)
Pt1	C4	2.030(7)	N19	C23	1.337(8)
Pt1	N7	2.111(5)	N20	C21	1.357(7)
Pt1	N19	2.188(5)	C21	C22	1.364(10)
Pt1	N26	2.234(5)	C21	C24	1.499(9)
C4	C6	1.415(15)	C22	C23	1.380(10)
C4	O5	1.173(11)	C23	C25	1.487(10)
N7	N8	1.304(7)	N26	N27	1.369(7)
N7	C11	1.361(7)	N26	C30	1.339(8)
N8	N9	1.345(7)	N27	C28	1.353(8)
N9	C10	1.354(7)	C28	C29	1.379(10)
N9	C12	1.444(8)	C28	C31	1.487(9)
C10	C11	1.350(8)	C29	C30	1.398(11)
C11	C18	1.496(8)	C30	C32	1.494(10)
C12	C13	1.391(9)	S33	O34	1.440(5)
C12	C17	1.378(10)	S33	O35	1.408(6)
C13	C14	1.388(10)	S33	O36	1.453(5)
C14	C15	1.374(12)	S33	C37	1.809(8)
C15	C16	1.382(11)	C37	F38	1.332(9)
C16	C17	1.378(9)	C37	F39	1.315(10)
C18	N20	1.455(7)	C37	F40	1.320(9)

### Bond Angles (°)

Atom	Atom	Atom	Angle/°	Atom	Atom	Atom	Angle/°
C2	Pt1	C3	89.5(2)	N27	C18	N20	109.1(5)

C2	Pt1	N7	92.4(2)		N20	N19	Pt1	117.3(3)
C2	Pt1	N19	176.1(2)		C23	N19	Pt1	135.5(4)
C2	Pt1	N26	94.6(2)		C23	N19	N20	106.2(5)
C3	Pt1	N19	93.9(2)		N19	N20	C18	119.6(4)
C3	Pt1	N26	92.7(2)		C21	N20	C18	129.9(5)
C4	Pt1	C2	86.7(3)		C21	N20	N19	110.3(5)
C4	Pt1	C3	92.0(3)		N20	C21	C22	106.1(6)
C4	Pt1	N7	92.0(3)		N20	C21	C24	122.4(6)
C4	Pt1	N19	95.1(2)		C22	C21	C24	131.4(6)
C4	Pt1	N26	175.2(3)		C21	C22	C23	108.1(6)
N7	Pt1	C3	175.7(2)		N19	C23	C22	109.2(6)
N7	Pt1	N19	84.07(18)		N19	C23	C25	122.8(6)
N7	Pt1	N26	83.37(18)		C22	C23	C25	128.0(6)
N19	Pt1	N26	83.31(19)		N27	N26	Pt1	117.2(4)
C6	C4	Pt1	117.3(9)		C30	N26	Pt1	137.4(4)
O5	C4	Pt1	116.0(6)		C30	N26	N27	105.1(5)
O5	C4	C6	126.6(11)		N26	N27	C18	119.2(5)
N8	N7	Pt1	129.5(4)		C28	N27	C18	128.4(5)
N8	N7	C11	111.3(5)		C28	N27	N26	112.2(5)
C11	N7	Pt1	119.0(4)		N27	C28	C29	105.8(6)
N7	N8	N9	104.7(4)		N27	C28	C31	122.8(6)
N8	N9	C10	112.0(5)		C29	C28	C31	131.4(7)
N8	N9	C12	118.5(5)		C28	C29	C30	106.8(6)
C10	N9	C12	129.3(5)		N26	C30	C29	110.2(6)
C11	C10	N9	104.7(5)		N26	C30	C32	122.5(7)
N7	C11	C18	120.0(5)		C29	C30	C32	127.2(7)
C10	C11	N7	107.3(5)		O34	S33	O36	114.3(3)
C10	C11	C18	132.8(5)		O34	S33	C37	103.4(3)
C13	C12	N9	118.4(6)		O35	S33	O34	114.4(3)
C17	C12	N9	119.4(5)		O35	S33	O36	115.0(4)
C17	C12	C13	122.1(6)		O35	S33	C37	105.4(4)
C14	C13	C12	117.5(7)		O36	S33	C37	102.3(3)
C15	C14	C13	120.8(7)		F38	C37	S33	111.6(6)
C14	C15	C16	120.7(7)		F39	C37	S33	112.0(5)
C17	C16	C15	119.7(7)		F39	C37	F38	107.1(6)
C16	C17	C12	119.2(7)		F39	C37	F40	108.5(8)
N20	C18	C11	112.5(5)		F40	C37	S33	110.5(6)
N27	C18	C11	111.3(4)		F40	C37	F38	107.0(7)

### APPENDIX 5.3

#### Atomic coordinates and isotropic displacement parameters for [TpmpMe<sub>2</sub>C(O)CH<sub>3</sub>][OTf] (3)

U(eq) is defines as one third of the trace of the orthogonalized U<sub>ij</sub> tensor.

<b>Atom</b>	<b>x/a</b>	<b>y/b</b>	<b>z/c</b>	<b>U(eq)</b>
Pt1	1879.4(2)	5594.2(2)	4236.3(2)	29.35(8)
C1	2427(4)	4505(4)	3774(3)	42.9(13)
C2	1790(20)	4590(30)	4822(16)	46(2)
C2A	3036(6)	5816(6)	4602(4)	30.2(16)
C3	3130(13)	6128(9)	4525(12)	30.2(16)
C3A	1548(6)	4661(10)	4886(6)	46(2)
O4	3373(6)	6939(6)	4608(5)	25(3)
O4A	810(4)	4592(6)	5041(3)	64(2)
C5	3592(13)	5214(9)	4662(11)	55(5)
C5A	2236(7)	3948(10)	5029(6)	96(4)
N6	2037(2)	6646(3)	3554.0(17)	26.4(8)
N7	1340(2)	7228(3)	3443.2(16)	22.7(8)
C8	1492(3)	7841(3)	3002(2)	25.5(9)
C9	2311(3)	7640(4)	2825(2)	30.5(10)
C10	2624(3)	6900(4)	3168(2)	28.5(10)
C11	851(3)	8545(4)	2790(2)	32.1(11)
C12	3478(3)	6411(4)	3140(3)	39.3(13)
N13	1284(3)	6811(3)	4676.4(17)	29.9(9)
N14	747(2)	7384(3)	4366.6(16)	24.8(8)
C15	453(3)	8153(4)	4662(2)	32.1(11)
C16	820(4)	8079(5)	5186(2)	45.0(15)
C17	1330(4)	7237(5)	5178(2)	41.0(13)
C18	-124(3)	8902(4)	4417(2)	36.0(12)
C19	1864(5)	6844(6)	5647(2)	58.1(19)
N20	638(3)	5379(3)	3840.7(19)	31.4(9)
N21	182(2)	6202(3)	3731.3(16)	24.1(8)
C22	-625(3)	5994(4)	3545(2)	27.4(10)
C23	-683(3)	5001(4)	3532(2)	34.2(11)
C24	118(4)	4652(4)	3715(2)	39.6(13)
C25	-1277(3)	6742(4)	3410(2)	36.2(12)
C26	374(5)	3609(4)	3764(4)	69(2)
C27	573(3)	7143(3)	3782.2(18)	22.0(9)

S1	3298.0(8)	5245.5(10)	6790.7(8)	43.2(4)
C28	4012(3)	4233(4)	6912(2)	28.3(10)
F29	4264(2)	4148(3)	7436.4(15)	57.8(10)
F30	4714.0(19)	4321(3)	6588.7(16)	48.4(9)
F31	3645(2)	3396(2)	6772.9(15)	47.5(8)
O32	3815(3)	6051(3)	6938(3)	90(2)
O33	3112(3)	5136(6)	6194(2)	85(2)
O34	2584(2)	5053(3)	7162(2)	46(1)

### Bond Lengths (Å)

Atom	Atom	Length/Å	Atom	Atom	Length/Å
Pt1	C1	2.047(5)	N14	C15	1.352(6)
Pt1	C2	1.97(3)	N14	C27	1.453(5)
Pt1	C2A	2.024(8)	C15	C16	1.373(7)
Pt1	C3	2.192(17)	C15	C18	1.488(7)
Pt1	C3A	2.075(12)	C16	C17	1.406(8)
Pt1	N6	2.188(4)	C17	C19	1.492(8)
Pt1	N13	2.184(4)	N20	N21	1.364(5)
Pt1	N20	2.170(4)	N20	C24	1.323(7)
C3	O4	1.197(10)	N21	C22	1.362(6)
C3	C5	1.488(10)	N21	C27	1.438(6)
C3A	O4A	1.211(8)	C22	C23	1.374(7)
C3A	C5A	1.492(9)	C22	C25	1.482(7)
N6	N7	1.375(5)	C23	C24	1.406(8)
N6	C10	1.341(6)	C24	C26	1.497(8)
N7	C8	1.366(6)	S1	C28	1.807(5)
N7	C27	1.446(6)	S1	O32	1.416(5)
C8	C9	1.372(7)	S1	O33	1.454(6)
C8	C11	1.481(7)	S1	O34	1.444(4)
C9	C10	1.394(7)	C28	F29	1.312(6)
C10	C12	1.493(7)	C28	F30	1.342(6)
N13	N14	1.365(5)	C28	F31	1.330(6)
N13	C17	1.331(7)			

### Bond Angles (°)

Atom	Atom	Atom	Angle/°	Atom	Atom	Atom	Angle/°
C1	Pt1	C3	92.5(6)	C9	C10	C12	128.0(5)

C1	Pt1	C3A	92.7(4)	N14	N13	Pt1	116.5(3)
C1	Pt1	N6	92.4(2)	C17	N13	Pt1	138.1(4)
C1	Pt1	N13	176.1(2)	C17	N13	N14	105.1(4)
C1	Pt1	N20	92.2(2)	N13	N14	C27	119.8(4)
C2	Pt1	C1	83.7(11)	C15	N14	N13	112.4(4)
C2	Pt1	C3	94.4(12)	C15	N14	C27	127.8(4)
C2	Pt1	N6	176.0(10)	N14	C15	C16	105.7(4)
C2	Pt1	N13	100.1(11)	N14	C15	C18	123.0(4)
C2	Pt1	N20	98.5(10)	C16	C15	C18	131.2(5)
C2A	Pt1	C1	88.3(3)	C15	C16	C17	106.5(5)
C2A	Pt1	C3A	89.7(4)	N13	C17	C16	110.2(5)
C2A	Pt1	N6	96.8(3)	N13	C17	C19	122.6(5)
C2A	Pt1	N13	93.2(3)	C16	C17	C19	127.2(5)
C2A	Pt1	N20	179.1(3)	N21	N20	Pt1	115.6(3)
C3A	Pt1	N6	171.8(3)	C24	N20	Pt1	138.3(4)
C3A	Pt1	N13	90.9(4)	C24	N20	N21	105.6(4)
C3A	Pt1	N20	90.9(4)	N20	N21	C27	120.9(4)
N6	Pt1	C3	84.8(6)	C22	N21	N20	111.5(4)
N13	Pt1	C3	88.3(6)	C22	N21	C27	127.4(4)
N13	Pt1	N6	83.84(15)	N21	C22	C23	106.1(4)
N20	Pt1	C3	166.6(5)	N21	C22	C25	123.8(4)
N20	Pt1	N6	82.52(15)	C23	C22	C25	130.1(5)
N20	Pt1	N13	86.21(15)	C22	C23	C24	106.0(5)
O4	C3	Pt1	130.3(12)	N20	C24	C23	110.7(5)
O4	C3	C5	127.0(13)	N20	C24	C26	123.2(5)
C5	C3	Pt1	102.3(10)	C23	C24	C26	126.1(5)
O4A	C3A	Pt1	120.6(8)	N7	C27	N14	111.0(4)
O4A	C3A	C5A	124.2(10)	N21	C27	N7	112.1(4)
C5A	C3A	Pt1	113.5(7)	N21	C27	N14	111.5(4)
N7	N6	Pt1	116.1(3)	O32	S1	C28	102.5(3)
C10	N6	Pt1	139.1(3)	O32	S1	O33	115.8(4)
C10	N6	N7	104.8(4)	O32	S1	O34	115.5(3)
N6	N7	C27	119.9(4)	O33	S1	C28	101.4(3)
C8	N7	N6	111.8(4)	O34	S1	C28	103.5(2)
C8	N7	C27	128.3(4)	O34	S1	O33	115.0(3)
N7	C8	C9	105.7(4)	F29	C28	S1	113.9(4)
N7	C8	C11	123.4(4)	F29	C28	F30	107.9(4)
C9	C8	C11	130.9(5)	F29	C28	F31	106.6(4)
C8	C9	C10	107.0(4)	F30	C28	S1	109.9(3)
N6	C10	C9	110.6(4)	F31	C28	S1	111.6(3)

N6      C10      C12      121.4(5)      F31      C28      F30      106.6(4)

## APPENDIX 5.4

### Atomic coordinates and isotropic displacement parameters for [bpztz<sup>Ph</sup>PtMe<sub>2</sub>CH<sub>2</sub>Cl][BF<sub>4</sub>] (4)

U(eq) is defines as one third of the trace of the orthogonalized U<sub>ij</sub> tensor.

<b>Atom</b>	<b>x/a</b>	<b>y/b</b>	<b>z/c</b>	<b>U(eq)</b>
Pt1	5318.9(2)	2521.2(2)	3315.3(2)	21.01(7)
Cl1	4420.4(8)	1668.0(16)	4242.0(6)	51.7(4)
C1	4697(3)	1237(6)	3590(3)	42.9(14)
C2	4881(2)	2274(5)	2514(2)	31.7(12)
C3	5847(2)	938(5)	3118(2)	34.7(12)
C4	5822.7(19)	5214(4)	3873.5(18)	20.3(9)
N5	5954.0(16)	3878(4)	3021.5(15)	19.8(8)
N6	6233.9(17)	3864(4)	2558.0(16)	22.8(8)
N7	6570.3(16)	4994(4)	2577.5(15)	21.0(8)
C8	6503.6(19)	5700(5)	3048.0(18)	21.6(9)
C9	6104.6(19)	4974(4)	3330.3(18)	18.8(9)
C10	6916(2)	5336(5)	2116(2)	25.5(10)
C11	6845(2)	4607(6)	1624(2)	36.8(12)
C12	7151(3)	4990(6)	1173(2)	42.6(14)
C13	7524(2)	6100(6)	1206(2)	41.8(14)
C14	7600(2)	6813(6)	1706(2)	37.8(13)
C15	7302(2)	6431(5)	2165(2)	29.6(11)
N16	4808.7(17)	4318(4)	3505.6(15)	21.9(8)
N17	5150.9(16)	5337(4)	3771.4(15)	19.6(8)
C18	4782(2)	6358(5)	3891.3(19)	22.7(10)
C19	4185(2)	6006(5)	3695.1(19)	24.7(10)
C20	4218(2)	4731(5)	3462.3(18)	24.3(10)
C21	5032(2)	7590(5)	4179(2)	30.4(11)
C22	3686(2)	3928(5)	3206(2)	33.8(12)
N23	5835.8(17)	2882(4)	4140.2(16)	22.0(8)
N24	5989.6(17)	4168(4)	4277.7(15)	20.9(8)
C25	6304(2)	4258(5)	4803.1(19)	25.2(10)
C26	6356(2)	3000(5)	5005.6(19)	27.3(10)
C27	6062(2)	2163(5)	4594(2)	25.8(10)
C28	6522(2)	5557(5)	5058(2)	33.7(12)
C29	5978(3)	696(5)	4621(2)	34.8(12)
Pt2	9689.1(2)	8443.5(2)	6686.4(2)	23.89(7)

Cl2	10506.0(9)	7635(2)	5703.7(8)	69.3(5)
C30	10307(3)	7219(6)	6366(3)	48.9(16)
C31	9209(3)	6809(5)	6916(3)	39.8(13)
C32	10190(2)	8216(6)	7463(2)	38.2(13)
C33	9095(2)	11089(5)	6163.1(18)	22.7(9)
N34	9059.8(16)	9746(4)	7028.0(15)	21.3(8)
N35	8817.1(17)	9713(4)	7511.9(16)	24.4(8)
N36	8444.5(16)	10781(4)	7503.9(16)	22.1(8)
C37	8110(2)	11067(5)	7982.0(19)	24.7(10)
C38	8136(2)	10194(6)	8428(2)	35.7(12)
C39	7828(3)	10509(6)	8893(2)	43.6(14)
C40	7497(2)	11661(6)	8906(2)	41.5(15)
C41	7466(2)	12524(6)	8457(3)	41.3(15)
C42	7774(2)	12230(5)	7987(2)	31.7(11)
C43	8458(2)	11506(4)	7022.7(19)	23.3(10)
C44	8861.0(19)	10822(4)	6721.9(18)	19.4(9)
N45	10142.7(17)	10279(4)	6460.8(16)	25.7(9)
N46	9764.9(17)	11268(4)	6222.0(16)	22.2(8)
C47	10099(2)	12317(5)	6067(2)	27.2(11)
C48	10712(2)	11992(5)	6208(2)	32.7(12)
C49	10726(2)	10731(5)	6445(2)	32.1(11)
C50	9806(3)	13544(5)	5807(2)	34.4(12)
C51	11282(2)	9959(6)	6665(3)	43.0(14)
N52	9111.0(18)	8778(4)	5886.2(16)	24.4(8)
N53	8912.2(16)	10035(4)	5766.6(15)	21.4(8)
C54	8547(2)	10109(5)	5264.8(19)	26.5(10)
C55	8515(2)	8848(5)	5052(2)	29.1(11)
C56	8870(2)	8042(5)	5444(2)	26.5(10)
C57	8244(3)	11359(5)	5045(2)	36.8(12)
C58	8973(3)	6575(5)	5402(2)	36.5(13)
B1	2174(3)	5734(6)	3723(3)	32.3(13)
F1	2282.1(14)	4509(3)	3966.5(13)	41.2(7)
F2	2649.9(16)	6601(3)	3874.8(17)	55.5(9)
F3	1621.1(14)	6254(3)	3883.2(15)	46.7(8)
F4	2106.5(18)	5612(4)	3138.0(14)	59.7(10)
B2	2855(3)	1567(6)	6166(3)	32.2(13)
F7	3402.2(16)	2115(3)	6008.2(14)	48.4(8)
F5	2369.0(18)	2423(3)	6024.0(18)	65.3(12)
F6	2742.5(14)	363(3)	5904.5(13)	38.3(7)
F8	2920.9(17)	1417(3)	6747.5(14)	54.3(9)

### Bond Lengths (Å)

<b>Atom</b>	<b>Atom</b>	<b>Length/Å</b>	<b>Atom</b>	<b>Atom</b>	<b>Length/Å</b>
Pt1	C1	2.026(5)	Pt2	N45	2.190(4)
Pt1	C2	2.056(5)	Pt2	N52	2.194(4)
Pt1	C3	2.048(5)	Cl2	C30	1.729(7)
Pt1	N5	2.110(4)	C33	C44	1.495(6)
Pt1	N16	2.196(4)	C33	N46	1.453(6)
Pt1	N23	2.187(4)	C33	N53	1.450(6)
Cl1	C1	1.775(6)	N34	N35	1.315(5)
C4	C9	1.505(6)	N34	C44	1.354(6)
C4	N17	1.454(5)	N35	N36	1.346(5)
C4	N24	1.450(6)	N36	C37	1.439(6)
N5	N6	1.312(5)	N36	C43	1.362(6)
N5	C9	1.351(6)	C37	C38	1.376(7)
N6	N7	1.353(5)	C37	C42	1.382(7)
N7	C8	1.348(6)	C38	C39	1.386(7)
N7	C10	1.435(6)	C39	C40	1.370(9)
C8	C9	1.361(6)	C40	C41	1.377(9)
C10	C11	1.377(7)	C41	C42	1.391(7)
C10	C15	1.383(7)	C43	C44	1.371(6)
C11	C12	1.373(7)	N45	N46	1.377(5)
C12	C13	1.380(9)	N45	C49	1.346(6)
C13	C14	1.385(8)	N46	C47	1.355(6)
C14	C15	1.380(7)	C47	C48	1.374(7)
N16	N17	1.382(5)	C47	C50	1.496(7)
N16	C20	1.338(6)	C48	C49	1.391(8)
N17	C18	1.354(6)	C49	C51	1.485(7)
C18	C19	1.374(6)	N52	N53	1.362(5)
C18	C21	1.495(6)	N52	C56	1.349(6)
C19	C20	1.407(7)	N53	C54	1.364(6)
C20	C22	1.487(6)	C54	C55	1.371(7)
N23	N24	1.372(5)	C54	C57	1.492(7)
N23	C27	1.351(6)	C55	C56	1.406(7)
N24	C25	1.363(6)	C56	C58	1.503(7)
C25	C26	1.360(7)	B1	F1	1.376(7)
C25	C28	1.501(7)	B1	F2	1.372(7)
C26	C27	1.396(7)	B1	F3	1.395(6)

C27	C29	1.496(7)	B1	F4	1.390(7)
Pt2	C30	2.027(5)	B2	F7	1.394(6)
Pt2	C31	2.055(5)	B2	F5	1.376(7)
Pt2	C32	2.055(5)	B2	F6	1.377(6)
Pt2	N34	2.115(4)	B2	F8	1.384(7)

### Bond Angles (°)

Atom	Atom	Atom	Angle/°	Atom	Atom	Atom	Angle/°
C1	Pt1	C2	87.9(2)	C31	Pt2	N34	92.02(19)
C1	Pt1	C3	88.8(2)	C31	Pt2	N45	175.65(19)
C1	Pt1	N5	179.0(2)	C31	Pt2	N52	95.5(2)
C1	Pt1	N16	95.64(19)	C32	Pt2	N34	91.40(19)
C1	Pt1	N23	96.5(2)	C32	Pt2	N45	96.2(2)
C2	Pt1	N5	91.43(18)	C32	Pt2	N52	176.01(18)
C2	Pt1	N16	95.67(18)	N34	Pt2	N45	83.68(14)
C2	Pt1	N23	175.63(18)	N34	Pt2	N52	84.61(14)
C3	Pt1	C2	84.6(2)	N45	Pt2	N52	83.49(14)
C3	Pt1	N5	91.93(18)	Cl2	C30	Pt2	115.5(3)
C3	Pt1	N16	175.59(18)	N46	C33	C44	111.2(4)
C3	Pt1	N23	95.22(19)	N53	C33	C44	110.6(4)
N5	Pt1	N16	83.67(14)	N53	C33	N46	110.9(4)
N5	Pt1	N23	84.21(14)	N35	N34	Pt2	130.7(3)
N23	Pt1	N16	84.16(14)	N35	N34	C44	111.0(4)
Cl1	C1	Pt1	114.8(3)	C44	N34	Pt2	118.3(3)
N17	C4	C9	110.9(3)	N34	N35	N36	105.1(4)
N24	C4	C9	110.9(4)	N35	N36	C37	119.9(4)
N24	C4	N17	110.4(3)	N35	N36	C43	112.2(4)
N6	N5	Pt1	130.1(3)	C43	N36	C37	127.8(4)
N6	N5	C9	111.1(4)	C38	C37	N36	119.8(4)
C9	N5	Pt1	118.8(3)	C38	C37	C42	121.2(5)
N5	N6	N7	104.8(3)	C42	C37	N36	119.0(4)
N6	N7	C10	119.9(4)	C37	C38	C39	118.9(5)
C8	N7	N6	111.8(4)	C40	C39	C38	120.7(6)
C8	N7	C10	128.2(4)	C39	C40	C41	120.2(5)
N7	C8	C9	104.6(4)	C40	C41	C42	120.1(5)
N5	C9	C4	120.2(4)	C37	C42	C41	119.0(5)
N5	C9	C8	107.6(4)	N36	C43	C44	103.8(4)
C8	C9	C4	132.1(4)	N34	C44	C33	120.4(4)

C11	C10	N7	120.0(4)	N34	C44	C43	107.9(4)
C11	C10	C15	120.9(5)	C43	C44	C33	131.7(4)
C15	C10	N7	119.0(4)	N46	N45	Pt2	117.0(3)
C12	C11	C10	119.5(5)	C49	N45	Pt2	137.7(3)
C11	C12	C13	120.7(6)	C49	N45	N46	105.0(4)
C12	C13	C14	119.2(5)	N45	N46	C33	119.5(4)
C15	C14	C13	120.7(5)	C47	N46	C33	128.7(4)
C14	C15	C10	118.9(5)	C47	N46	N45	111.8(4)
N17	N16	Pt1	117.0(3)	N46	C47	C48	105.9(4)
C20	N16	Pt1	137.6(3)	N46	C47	C50	123.1(4)
C20	N16	N17	105.3(4)	C48	C47	C50	131.0(5)
N16	N17	C4	119.5(3)	C47	C48	C49	107.4(4)
C18	N17	C4	129.1(4)	N45	C49	C48	110.0(4)
C18	N17	N16	111.4(3)	N45	C49	C51	122.6(5)
N17	C18	C19	106.5(4)	C48	C49	C51	127.4(5)
N17	C18	C21	122.5(4)	N53	N52	Pt2	117.7(3)
C19	C18	C21	130.9(4)	C56	N52	Pt2	137.1(3)
C18	C19	C20	106.7(4)	C56	N52	N53	105.2(4)
N16	C20	C19	110.1(4)	N52	N53	C33	119.4(3)
N16	C20	C22	123.6(4)	N52	N53	C54	112.1(4)
C19	C20	C22	126.3(4)	C54	N53	C33	128.6(4)
N24	N23	Pt1	117.4(3)	N53	C54	C55	106.0(4)
C27	N23	Pt1	137.5(3)	N53	C54	C57	123.1(4)
C27	N23	N24	105.0(4)	C55	C54	C57	130.8(4)
N23	N24	C4	119.7(3)	C54	C55	C56	106.8(4)
C25	N24	C4	128.7(4)	N52	C56	C55	109.9(4)
C25	N24	N23	111.6(4)	N52	C56	C58	123.1(4)
N24	C25	C28	122.4(4)	C55	C56	C58	127.0(4)
C26	C25	N24	106.1(4)	F1	B1	F3	109.7(5)
C26	C25	C28	131.5(4)	F1	B1	F4	109.7(5)
C25	C26	C27	107.6(4)	F2	B1	F1	111.9(5)
N23	C27	C26	109.7(4)	F2	B1	F3	109.1(5)
N23	C27	C29	122.1(4)	F2	B1	F4	108.6(5)
C26	C27	C29	128.2(4)	F4	B1	F3	107.7(5)
C30	Pt2	C31	88.8(3)	F5	B2	F7	109.4(5)
C30	Pt2	C32	87.9(2)	F5	B2	F6	110.4(4)
C30	Pt2	N34	178.8(2)	F5	B2	F8	108.2(5)
C30	Pt2	N45	95.5(2)	F6	B2	F7	110.1(5)
C30	Pt2	N52	96.1(2)	F6	B2	F8	110.5(5)
C31	Pt2	C32	84.5(2)	F8	B2	F7	108.1(4)

## APPENDIX 5.5

### Atomic coordinates and isotropic displacement parameters for [TpmpMe<sub>2</sub>CH<sub>2</sub>Cl][Cl] (5)

U(eq) is defines as one third of the trace of the orthogonalized U<sub>ij</sub> tensor.

<b>Atom</b>	<b>x/a</b>	<b>y/b</b>	<b>z/c</b>	<b>U(eq)</b>
Pt1	2171.7(4)	6429.3(5)	8479.4(7)	19.99(13)
Pt1A	2260.5(16)	6264.9(14)	8246(2)	19.99(13)
C11	4268.2(15)	5752.4(13)	8111(2)	53.6(5)
Cl1A	2329(5)	8131(4)	9273(7)	43.4(16)
N1	3512(3)	6407(2)	10346(3)	25.4(7)
C1	3148(6)	6457(5)	7467(6)	35.3(15)
C1A	3290(30)	6126(19)	7270(30)	35.3(15)
N2	3439(3)	5854(2)	11242(3)	18.8(7)
C2	2139(5)	7712(4)	8441(6)	29.2(13)
C2A	2260(20)	7532(16)	7980(20)	29.2(13)
N3	1193(3)	6322(2)	9558(4)	25.7(8)
C3	843(6)	6437(5)	6728(7)	29.7(15)
C3A	1000(30)	6190(20)	6500(30)	29.7(15)
N4	1512(3)	5743(2)	10546(3)	19.5(7)
C4	4433(3)	6833(3)	10971(4)	26.7(9)
N5	2206(3)	5046(2)	8602(3)	26.5(8)
C5	4939(3)	6548(3)	12254(4)	23.9(9)
N6	2484(3)	4734(2)	9830(3)	18.8(7)
C6	4295(3)	5929(3)	12406(4)	20.0(8)
C7	4820(4)	7517(3)	10345(5)	39.9(12)
C8	4426(3)	5411(3)	13574(4)	26.6(9)
C9	277(3)	6662(3)	9551(5)	29.5(10)
C10	21(3)	6296(3)	10535(5)	29.6(10)
C11	814(3)	5717(3)	11159(4)	22.8(8)
C12	-359(4)	7318(3)	8607(6)	43.8(14)
C13	971(3)	5185(3)	12311(4)	26.7(9)
C14	2196(3)	4392(3)	7851(4)	27.5(9)
C15	2477(3)	3660(3)	8607(4)	25.7(9)
C16	2665(3)	3889(3)	9867(4)	20.1(8)
C17	1908(5)	4464(4)	6412(5)	45.0(13)
C18	2993(4)	3373(3)	11070(4)	25.8(9)
C19	2526(3)	5284(2)	10876(4)	16.6(7)

Cl2	7230.1(8)	6361.8(7)	5909.8(10)	28.5(2)
-----	-----------	-----------	------------	---------

### Bond Lengths (Å)

<b>Atom</b>	<b>Atom</b>	<b>Length/Å</b>	<b>Atom</b>	<b>Atom</b>	<b>Length/Å</b>
Pt1	N1	2.147(3)	N3	C9	1.340(6)
Pt1	C1	2.039(7)	N4	C11	1.362(5)
Pt1	C2	2.046(6)	N4	C19	1.456(5)
Pt1	N3	2.109(4)	C4	C5	1.396(6)
Pt1	C3	2.060(7)	C4	C7	1.494(6)
Pt1	N5	2.208(4)	N5	N6	1.364(5)
Pt1A	N1	2.292(4)	N5	C14	1.335(6)
Pt1A	C1A	2.08(3)	C5	C6	1.365(6)
Pt1A	C2A	2.04(3)	N6	C16	1.368(5)
Pt1A	N3	2.420(5)	N6	C19	1.443(5)
Pt1A	C3A	2.01(3)	C6	C8	1.494(6)
Pt1A	N5	1.990(4)	C9	C10	1.401(7)
Cl1	C1	1.783(8)	C9	C12	1.489(6)
Cl1A	C2A	1.70(3)	C10	C11	1.372(6)
N1	N2	1.365(5)	C11	C13	1.484(6)
N1	C4	1.338(5)	C14	C15	1.402(7)
N2	C6	1.357(5)	C14	C17	1.500(6)
N2	C19	1.448(5)	C15	C16	1.376(6)
N3	N4	1.370(5)	C16	C18	1.486(6)

### Bond Angles (°)

<b>Atom</b>	<b>Atom</b>	<b>Atom</b>	<b>Angle/°</b>	<b>Atom</b>	<b>Atom</b>	<b>Atom</b>	<b>Angle/°</b>
N1	Pt1	N5	86.23(14)	N4	N3	Pt1	116.6(3)
C1	Pt1	N1	93.7(2)	N4	N3	Pt1A	113.0(3)
C1	Pt1	C2	88.9(3)	C9	N3	Pt1	137.6(3)
C1	Pt1	N3	176.4(2)	C9	N3	Pt1A	140.4(3)
C1	Pt1	C3	88.7(3)	C9	N3	N4	105.8(4)
C1	Pt1	N5	93.1(2)	N3	N4	C19	120.4(3)
C2	Pt1	N1	92.30(19)	C11	N4	N3	111.5(3)
C2	Pt1	N3	94.6(2)	C11	N4	C19	127.9(3)
C2	Pt1	C3	88.3(3)	N1	C4	C5	110.2(4)
C2	Pt1	N5	177.6(2)	N1	C4	C7	123.1(4)
N3	Pt1	N1	85.13(14)	C5	C4	C7	126.8(4)

N3	Pt1	N5	83.44(14)		N6	N5	Pt1	114.6(3)
C3	Pt1	N1	177.5(3)		N6	N5	Pt1A	122.7(3)
C3	Pt1	N3	92.5(2)		C14	N5	Pt1	138.3(3)
C3	Pt1	N5	93.1(2)		C14	N5	Pt1A	129.0(3)
N1	Pt1A	N3	75.27(14)		C14	N5	N6	106.1(4)
C1A	Pt1A	N1	100.3(9)		C6	C5	C4	106.7(4)
C1A	Pt1A	N3	173.8(9)		N5	N6	C16	111.4(3)
C2A	Pt1A	N1	90.4(7)		N5	N6	C19	120.0(3)
C2A	Pt1A	C1A	89.4(12)		C16	N6	C19	128.6(3)
C2A	Pt1A	N3	94.9(9)		N2	C6	C5	106.3(4)
C3A	Pt1A	N1	171.5(10)		N2	C6	C8	123.4(4)
C3A	Pt1A	C1A	88.1(14)		C5	C6	C8	130.3(4)
C3A	Pt1A	C2A	88.0(12)		N3	C9	C10	109.5(4)
C3A	Pt1A	N3	96.6(11)		N3	C9	C12	123.7(5)
N5	Pt1A	N1	87.81(15)		C10	C9	C12	126.8(5)
N5	Pt1A	C1A	94.9(9)		C11	C10	C9	107.4(4)
N5	Pt1A	C2A	175.5(8)		N4	C11	C10	105.8(4)
N5	Pt1A	N3	80.70(15)		N4	C11	C13	124.3(4)
N5	Pt1A	C3A	93.2(10)		C10	C11	C13	129.8(4)
N2	N1	Pt1	116.6(2)		N5	C14	C15	109.8(4)
N2	N1	Pt1A	116.8(2)		N5	C14	C17	123.2(5)
C4	N1	Pt1	138.0(3)		C15	C14	C17	127.1(4)
C4	N1	Pt1A	137.3(3)		C16	C15	C14	107.0(4)
C4	N1	N2	105.3(3)		N6	C16	C15	105.8(4)
C11	C1	Pt1	112.7(3)		N6	C16	C18	124.0(4)
N1	N2	C19	119.7(3)		C15	C16	C18	130.3(4)
C6	N2	N1	111.5(3)		N2	C19	N4	110.8(3)
C6	N2	C19	128.8(3)		N6	C19	N2	111.6(3)
Cl1A	C2A	Pt1A	115.9(14)		N6	C19	N4	111.5(3)